An Investigation of Organomagnesium Bi/Tridentate Nitrogen Ligand Complexes as Ziegler-Natta Polymerisation Catalysts

Caroline Dick

PhD

The University of Edinburgh

2002

Confidential

Declaration

I declare that this thesis has been entirely composed by myself and that the work described herein is my own except where clearly mentioned either in acknowledgement, reference or text. It has not been submitted in whole or in part, for any other degree.

CONTENTS

Abstract

The main objective of this research was to produce magnesium alkyl complexes which are active catalysts or procatalysts in the polymerisation of ethene. The nitrogen based ligands in the magnesium complexes were chosen because of the reported activity of similar transition metal diimine and aluminium alkyl amidinate catalysts. Three classes of compounds were investigated: 1) magnesium di-/tri-amine dialkyl complexes, 2) magnesium alkyl α-diimine complexes, and 3) magnesium alkyl bis(iminophosphorano)methanide complexes.

Preparation of the magnesium diamine dialkyl complexes

$[Mg(\eta^2-R_2NCH_2CH_2NR_2)R'_2]$ (R=Me, or Et; R'= Me, or CH_2Ph)
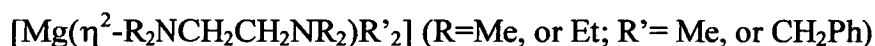
(and also $[Mg(\eta^3-PMDETA)Me_2]$ (PMDETA= pentamethyldiethylenetriamine)) was trivial once a method for preparing the $MgMe_2$ was perfected. However, following the activation of the compounds by boron based activators such as $B(C_6F_5)_3$, $[CPh_3][B(C_6F_5)_4]$ and $[NHMe_2Ph][B(C_6F_5)_4]$ was not easy due to the sensitivity of the products to, and insolubility in, many solvents.

The reaction of $[Mg(\eta^2-R_2NCH_2CH_2NR_2)R'_2]$ and $[Mg(\eta^3-PMDETA)Me_2]$ with $B(C_6F_5)_3$ produces ion-pairs, e.g. $[Mg(\eta^2-R_2NCH_2CH_2NR_2)R'\{R'B(C_6F_5)_4\}]$ which are prone to deactivation *via* C_6F_5 transfer to produce
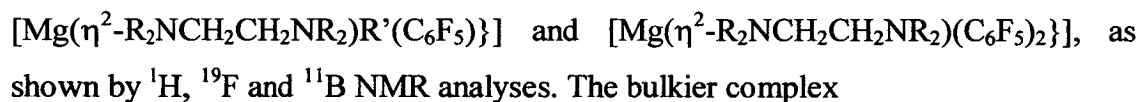
$[Mg(\eta^2-R_2NCH_2CH_2NR_2)R'(C_6F_5)\}]$ and $[Mg(\eta^2-R_2NCH_2CH_2NR_2)(C_6F_5)_2\}]$, as shown by ^1H, ^{19}F and ^{11}B NMR analyses. The bulkier complex $[Mg(\eta^3-PMDETA)Me_2]$ produces the salt $[Mg(\eta^3-PMDETA)Me][MeB(C_6F_5)_4]$ which also is prone to C_6F_5 transfer but at a much slower rate.

Reaction of $[Mg(\eta^2-R_2NCH_2CH_2NR_2)Me_2]$ and $[Mg(\eta^3-PMDETA)Me_2]$ with $[CPh_3][B(C_6F_5)_4]$ and $[NHMe_2Ph][B(C_6F_5)_4]$ produces the products

$[Mg(\eta^2-R_2NCH_2CH_2NR_2)Me][B(C_6F_5)_4]$ and $[Mg(\eta^3-PMDETA)Me][B(C_6F_5)_4]$ which in the presence of THF remain unsolvated. However, reaction of
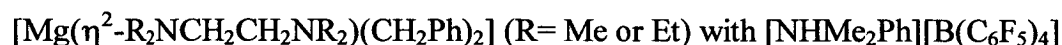
$[Mg(\eta^2-R_2NCH_2CH_2NR_2)(CH_2Ph)_2]$ (R= Me or Et) with $[NHMe_2Ph][B(C_6F_5)_4]$ produces $[Mg(\eta^2-R_2NCH_2CH_2NR_2)(NMe_2Ph)(CH_2Ph)]$ $[B(C_6F_5)_4]$ and addition of THF results in the exchange of the NMe_2Ph to produce

$[Mg(\eta^2-R_2NCH_2CH_2NR_2)(THF)(CH_2Ph)]$ $[B(C_6F_5)_4]$.
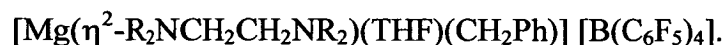
Reaction of $[Mg(\eta^2\text{-}R_2NCH_2CH_2NR_2)R_2]$ and $[CPh_3][B(C_6F_5)_4]$ produces complexes of type $[Mg(\eta^2\text{-}R_2NCH_2CH_2NR_2)(CH_2Ph)][B(C_6F_5)_4]$ which complex THF in its presence.

The complexes $[Mg(\eta^2\text{-}R_2NCH_2CH_2NR_2)R_2]$ and $[Mg(\eta^3\text{-PMDETA})Me_2]$ when activated with $B(C_6F_5)_3$, $[CPh_3][B(C_6F_5)_4]$ or $[NHMe_2Ph][B(C_6F_5)_4]$, in the presence or absence of trisobutyl aluminium, at $70°C/6$ bar or $80°C/30$ bar, are inactive for ethene polymerisation. This is thought to be due to the unstable nature of these compounds.

Complexation of α–diimines with magnesium alkyls results in the formation of several reaction products, which are in equilibrium with one another, *via* complex radical mechanisms. It has been proven that several species can be produced from dimeric radicals e.g. $[Mg^+(\mu_2\text{-Me})(\eta^2\text{-L})^\bullet]_2$, to doubly reduced monomeric species e.g. $[Mg^{2+}(\eta^2\text{-L})^{2-}(THF)_3]$. It is also observed that the ligand is prone to methylation to become an iminoamide ligand on complexation e.g. $[Mg(\mu_2\text{-Me})\{\eta^2\text{-L(Me)}\}]_2$, thus rendering the complex neutral. Ethene polymerisation studies of these products were implemented and revealed that these compounds are inactive under both mild and forcing conditions.

Treatment of $CH_2(Ph_2PNSiMe_3)_2$ with $MgMe_2$, in the presence of THF, results in the reduction of the ligand *via* the formation of methane producing the complex $[Mg(Me)\{CH(PPh_2NSiMe_3)_2\}(THF)]$. The THF can be removed by heating in vacuum producing the dimeric species $[Mg(\mu_2\text{-Me})\{CH(PPh_2NSiMe_3)_2\}]_2$. The THF adduct is shown to be inactive for alkene polymerisation. The molecular structure of the dimer suggests that coordination of an ethene molecule would be very difficult, and although not tested, it is expected that the THF dimeric species will also be inactive for alkene polymerisation.

Acknowledgements

The whole embodiment of PhD research relies on an individual obtaining support, guidance and encouragement from others as they branch out to find themselves and develop as a professional. I have learned a lot about respect in the last few years, especially for colleagues expertise, patience, understanding and general helpfulness.

I have several people I would like to thank.

Firstly I would like to thank Dr Philip Bailey, without whom I would not have the opportunity to be a part of an industrial linked PhD. I thank you Phil for your friendly approachable manner, your guidance, feedback and patience (especially for the wait for the thesis).

I would also like to thank Dr Sylvie Fabre for training me in the arts of air sensitive techniques. I am greatly indebted to Sylvie for her help, advice, discussions and friendship.

A big thank you must also go to the technical staff, without which I would not have been able to function! A special thanks to the NMR staff, i.e. John Millar and Wesley Kerr for allowing me to use their facilities, and for encouraging me to train on their equipment. Also a big thanks to Dr David Reed for interesting discussions, and for training and allowing me to use the 360 MHz NMR machine. I would also like to thank Alan Taylor for mass spectrometry, Lorna Eades for Elemental analysis and Dr Lesley Yellowlees for allowing me to use her EPR machine for analysis. I owe a great debt of gratitude to Donald Robertson and Patrick Hencher for their assistance and use of their facilities. A special thanks must go to the Crystallographic service, especially to Dr Simon Parsons, Dr Andrew Parkin and Dr Bob Coxall. It is thanks to their skills that I have so many quality crystal structures to report.

It goes without saying that I am grateful to (the then) catalysis group of Shell Research and Technology Centre in Amsterdam, for allowing me the opportunity to carry out this research and for making me feel so welcome whilst I worked in Amsterdam. I wish to especially thank Dr Andrew Horton and Hans Stapersma for their hospitality, helpfulness and discussions. I would like to thank Andrew for making sure my stay in Amsterdam was comfortable, enjoyable and fruitful. I would also like to thank Klaas Von Hebel for his support, friendship and the work he

implemented for me whilst I was based in Amsterdam. Bart Van Oort was an invaluable acquaintance, many thanks for the NMR advice, analyses and the CD.

I would like to thank the Bailey group, and the Tasker group who latterly I maintained a lot of contact with, for their day to day support, discussions and company. I would like to personally thank Dr Clare Squires for keeping me sane, Sarah Resouly for her bubbly air and Dr Timothy Higgs for his guidance and thought provoking conversations! Also a personal thanks to Drs Karen Curley and Jenny Pringle for their unwavering friendship and personal support.

My biggest thank you goes to my family, my friends from home (and at university), and to Barry. Thanks for putting up with my roller coaster ride and for being there every step of the way. More personally I would like to dedicate this achievement to my late grandfather Mr James Dawson whom I miss very much. I'm sure his comment on seeing this thesis would have been "Its just as good as I could have done myself!".

Abbreviations

α	alpha
Å	angstrom
Ar	aromatic
ATI	aminotroponiminate
atm.	atmosphere
β	beta
BIAN	bis(imino)acenaphthene
Bipy	2,2-bipyridine
br	broad
Bz	benzyl
^{t}Bu	tertiary butyl
c.f.	compared with
CHN	elemental analysis
cm	centimetre
cm^{-1}	reciprocal centimetre
Cp	cyclopentadienyl
Cp*	pentamethylcyclopentadienyl
Cy	cyclohexyl
°	degree
°C	degrees Celsius
δ	chemical shift
d	doublet
Δ	delta (difference of)
DME	dimethoxyethane
E	exponential (to the power of 10)
EPR	Electron Paramagnetic Resonance Spectroscopy
ES	Electrospray
et al	Et alli (and others)
FAB	fast atom bombardment
g	gram

γ	gamma
GC	gas chromatography
h	hour
Hz	Hertz
IR	Infra-Red spectroscopy
J	spin-spin coupling constant
K	degrees Kelvin
Kg	kilogram
L	Ligand
m	multiplet
m	meta
M	molar
MAO	methyl aluminium oxide
Me	methyl
mm	millimetre
MMA	methyl methacrylate
mmoles	millimoles
NMR	Nuclear Magnetic Resonance Spectroscopy
MS	Mass Spectrometry
o	ortho
p	para
%	percent
Phen	1, 10-phenanthroline
Ph	phenyl
PE	polyethene
PMDETA	pentamethyldiethylenetriamine
ppm	parts per million
^{i}Pr	isopropyl
p.s.i.	
pyca	^{t}Bu-NCH-2-C_5H_4N
q	quartet
R	alkyl

R_{int}	independent reflections
s	singlet
t	triplet
T	tesla
TIBA	triisobutyl aluminium
THF	tetrahydrofuran
TEEDA	tetraethylethylenediamine
θ	theta (angle)
TIPEDA	tetraisopropylethylenediamine
TMEDA	tetramethylethylenediamine
UV	Ultra Violet
UV-Vis	Ultra Violet-Visible

R_{int}	independent reflections

CHAPTER ONE INTRODUCTION

This introductory chapter will explain the history of Ziegler-Natta catalysis and the extensively reported transition metal catalysts that developed as a result of Ziegler and Natta's initial findings. Similarly there will be some discussion on rare earth metal catalysts, before going on to discuss the reported activity of main group metal (Al and Mg) catalysts.

An introduction to the chemistry of magnesium akyls will be given as well as an overview of some relevant results obtained by group colleagues with reference to the synthesis of β-diketiminate and troponiminate ligated magnesium alkyl complexes.

1.1 The History of Ziegler–Natta Ethene Polymerisation

Today's chemical industry is mainly based on oil and natural gas. Crude oil represents the major primary feedstock for plastics, fibres and colours. Fossil resources (i.e. oil and natural gas) are converted into key chemicals like ethene, propene, etc.[1] Of these commodities produced world wide ethene is in highest demand. The total volume of ethene based chemicals and polymers produced amounted to 79 million tonnes in 1995.[1] The polymerisation of alkenes in the absence of a catalyst requires very forcing conditions, about 200°C and 2000 atmospheres of pressure with a small impurity of oxygen as an initiator, which produces highly branched polymer *via* a free radical addition polymerisation mechanism.[2] Studies have elucidated that alkenes may be polymerised *via* a number of processes, of which the most important are free-radical polymerisation, anionic polymerisation, Ziegler-Natta polymerisation and cationic polymerisation.[3] Ziegler-Natta polymerisation differs from cationic polymerisation in that it is necessary for the initiators to contain alkyl or hydrido ligands. Karl Ziegler discovered that heterogeneous suspensions of hydrocarbon solutions containing $TiCl_4$ in the presence of $AlEt_3$ produced polyethylene at pressures as low as 1 bar (Figure 1.01).[4] The polymerisation is thought to take place at the dislocations and edges of $TiCl_3$ crystals. As a result there are many different active sites, and the resulting polymer has a very broad molecular weight distribution.

$$CH_2{=}CH_2 \xrightarrow[25^{\circ}C, 1\ bar]{TiCl_4/AlEt_3} Polyethene$$

Molecular weight 10^4-10^5
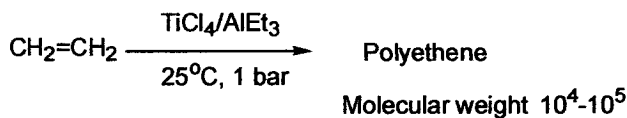
Figure 1.01

The link between the stereochemical structure and the bulk properties of the polymer, was elucidated by G.Natta in 1955, by studying the reactions of Ziegler-Natta type catalysts with propene (Figures 1.02 and 1.03). Isotactic polymer is produced from propene by the Ziegler-Natta catalyst.[4]

$$CH_2{=}CH{-}CH_3 \xrightarrow[25^{\circ}C, 1\ bar]{TiCl_4/AlEt_3} Polypropene$$

Molecular weight 10^5-10^6
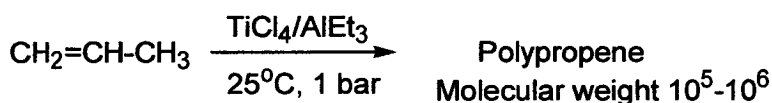
Figure 1.02
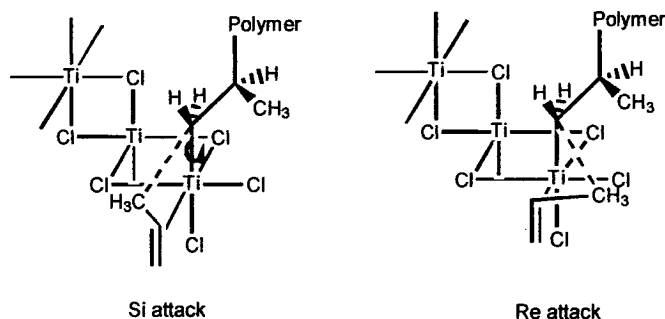
Si attack   Re attack

Figure 1.03 Illustration of Re and Si attack of a propene molecule at the edge of a TiCl₃ crystal.

The mechanism for the reaction of alkenes with TiCl$_4$/AlEt$_3$ was proposed by Cossee in 1960, and involves the insertion of C$_2$H$_4$ into a titanium-alkyl group, initially formed by the aluminium alkyl, on the surface (Figure 1.04).[5]
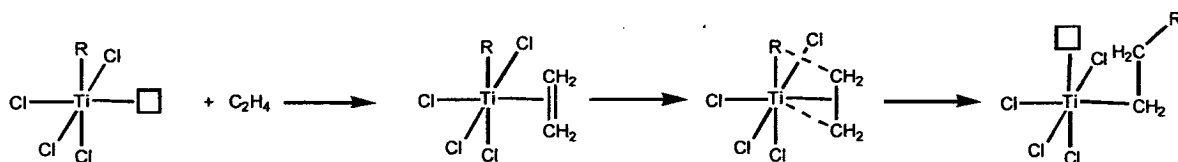
Figure 1.04

The metal is electronically unsaturated and contains a vacant co-ordination site. The alkene is inserted into a metal-carbon σ-bond via a four centred transition state.[6] This mechanism is also generally accepted as that for metallocene type catalysts e.g. $[Cp*_2ZrMe]^+$.

1.2 Activation

Activators are used in conjunction with procatalysts to generate the catalytically active species, which in Ziegler-Natta ethene polymerisations is accepted as being an electronically unsaturated cationic metal alkyl species. Activators generally abstract ligands from the metal to make the metal coordinatively unsaturated, and some also act as alkylating agents.[7]

There is an economic incentive for industry to develop new high performance and low-cost cocatalysts, due to the fact that the cost of the cocatalysts is typically more than that of the precatalyst. Currently there is a large choice of activators, although herein we are only interested in trialkylaluminium compounds namely trimethyl aluminium ($AlMe_3$) (1) and tri-iso-butylaluminium (Al^iBu_3) (2); both the Lewis acids triphenylcarbenium tetrakis(pentafluorphenyl)borate $[CPh_3][B(C_6F_5)_4]$ (3) and tris(perfluorphenyl)borane $B(C_6F_5)_3$ (4); and the Brønsted acid dimethylanilinium tetrakis(pentafluorphenyl) borate $[NHMe_2Ph][B(C_6F_5)_4]$(5) (Figure 1.05).
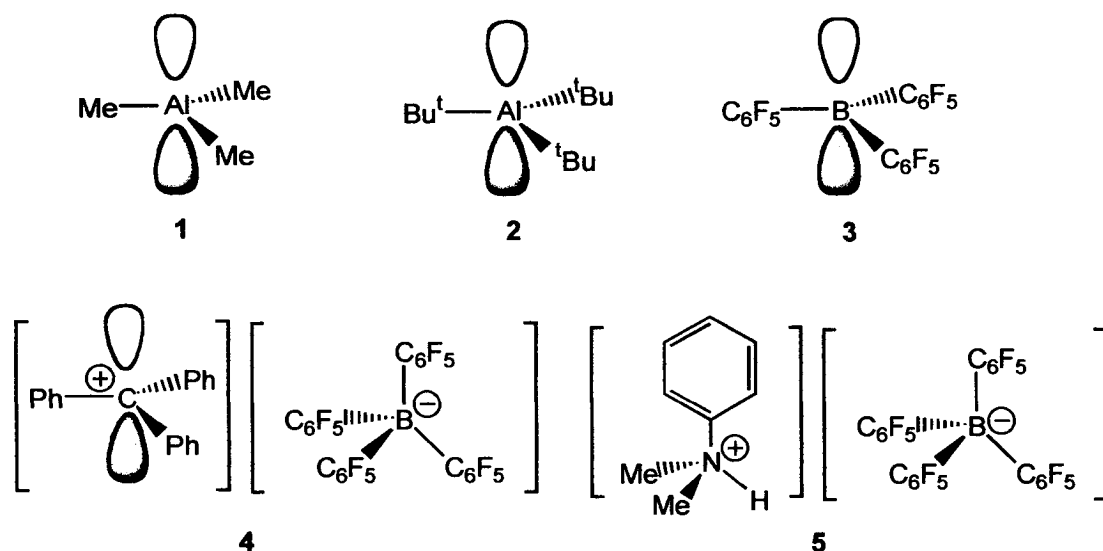
Figure 1.05

1.21 Activation with Aluminium Alkyls

Alkyl aluminium activators are classed as the "classic" activators, and can act as both alkylating and abstracting agents. Aluminium alkyls such as (AlMe$_3$) (**1**), triethyl aluminium (AlEt$_3$), (Al(^{i}Bu)$_3$) (**2**) and dimethyl aluminium chloride (AlMe$_2$Cl) are commonly used co-catalysts. Aluminium alkyls act as water scavengers as well as activators, and have also been shown to act as catalysts for alkene oligomerisation or polymerisation (Chapter 1.3.2).[2,7]

1.22 Activation with Boron Based Activators

Minimal interactions between the cation-anion pair, produced from the activation reaction of a procatalyst with either **3**, **4** or **5**, produce more active alkene polymerisation catalyst species. For example, the [Cp$_2$ThCH$_3$]$^+$ cation is deactivated by the weak interaction of the fluorine atoms on the [B(C$_6$F$_5$)$_4$]$^-$ anion with the metal centre (Figure 1.06).[7]
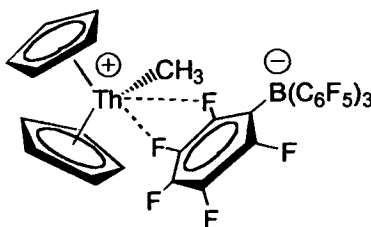
Figure 1.06

1.2.2.1 Activation with [CPh$_3$][B(C$_6$F$_5$)$_4$]

Triphenylcarbenium tetrakis(pentafluorphenyl)borate [CPh$_3$][B(C$_6$F$_5$)$_4$] activates a procatalyst by the removal of an alkyl group by the electronically unsaturated cation (Figure 1.07).[8] The reaction produces the active catalyst, the triphenylcarbenium tetrakis (pentafluorphenyl) borate counter anion and a soluble inert organic biproduct CPh$_3$R. The anion is usually non-coordinating, which is a very important as the Lewis acidity of the metal cation would be quenched through significant intramolecular interactions or ion-ion contacts with the counter ion.[7] In the development of new catalyst systems it is imperative that these interactions are minimised by the use of weakly co-ordinating counter ions whilst maintaining a

stable catalyst species. The disadvantages of working with these compounds as activators are: their poor solubility in non-polar solvents (hydrocarbons), their poor thermal stability and the formation of liquid clatherates by the salts they produce.[7] Such behaviour leads to both short catalytic lifetimes and limits the techniques by which the reactive species can be analysed and thus characterised.

Activator **3** can be prepared by mixing Li[B(C$_6$F$_5$)$_4$] with triphenylmethyl chloride in n-hexane with refluxing overnight. The product is extracted from LiCl into CH$_2$Cl$_2$ and crystallised from CH$_2$Cl$_2$/hexane.[9]
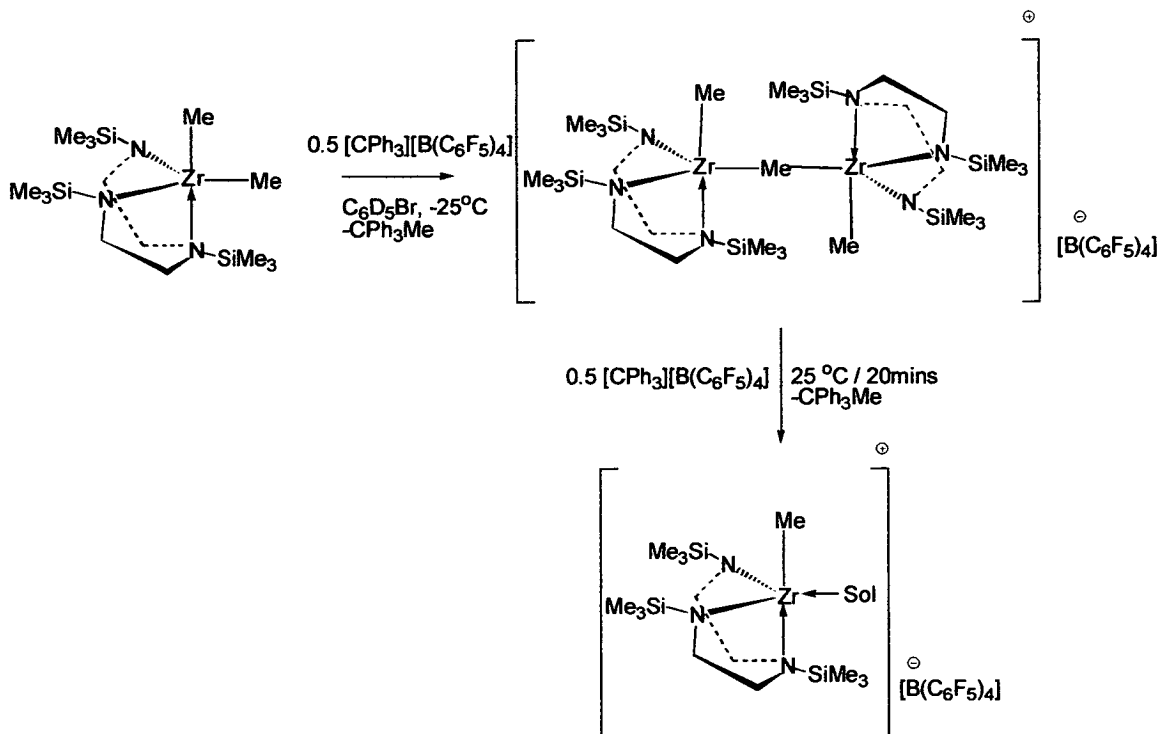
Figure 1.07

1.2.2.2 Activation with B(C$_6$F$_5$)$_3$

Being a strong Lewis acid, B(C$_6$F$_5$)$_3$ activates saturated metal complexes by alkyl/hydride extraction to produce a [RB(C$_6$F$_5$)$_3$]⁻ or [HB(C$_6$F$_5$)$_3$]⁻ counterion.[10] Preparation of an active cationic catalyst by reaction with B(C$_6$F$_5$)$_3$ can be quite complex producing several different products depending on the metal, ligands and reaction conditions. The methyl tris(pentaflurophenyl)borate anion [MeB(C$_6$F$_5$)$_3$]⁻ has a tendency to weakly co-ordinate to the metal centre *via* the methyl group, either through the carbon atom or the hydrogen atoms (Figure 1.08).[8] The interaction of the

metal centre with $[Me(C_6F_5)_3]^-$ acts to improve solubility in non-polar hydrocarbons, it increases the stability of the cation and lifetime substantially. However this interaction deactivates the catalyst to alkene polymerisation as the anion satisfies some of the electronic requirements of the metal, and sterically hinders the approach of an alkene molecule.
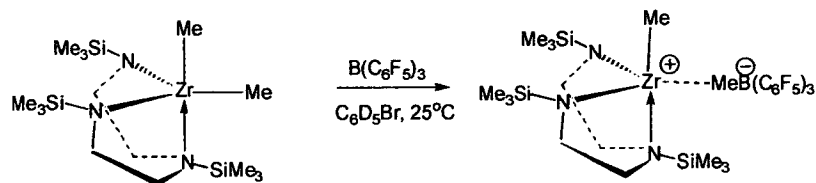
Figure 1.08

The co-ordinating nature of the $[MeB(C_6F_5)_3]^-$ anion with the catalyst cation complex can easily be established in solution from the ^{19}F NMR spectrum. If the anion is co-ordinating then there is a large $\Delta\delta$ (*m, p*-F) of approximately 3.9 ppm, whereas a non co-ordinating anion has a small $\Delta\delta$ (*m, p*-F) of approximately 2.7 ppm.[8]

The counter anion $[B(CH_2Ph)(C_6F_5)_3]^-$ can either produce discrete ion pairs with negligible cation-anion association, or can produce cation-anion pairs that have η^n-arene co-ordination interactions (Figure 1.09).[11,12]
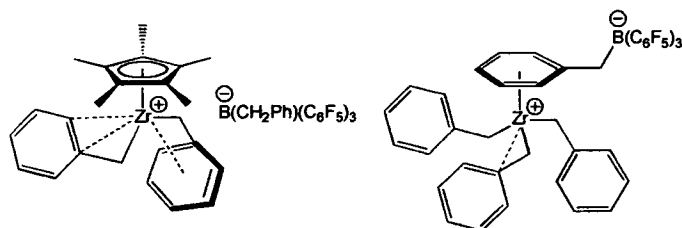
Figure 1.09

Tris(pentafluorophenyl)borane (FABA) can be prepared by reaction of pentafluorophenyllithium and boron trichloride in pentane at low temperature (Figure 1.10),[13] or is commercially available and can be purchased from Aldrich.

$$BCl_3 + 3\,C_6F_5Li \longrightarrow B(C_6F_5)_3 + 3\,LiCl$$
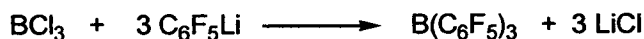
Figure 1.10

Tris(pentafluorophenyl)boron is surprisingly thermally stable.[13] Typically the ortho and meta resonances in $B(C_6F_5)_3$ are shifted by about 20 ppm to high frequency in the ^{19}F NMR spectrum in comparison to those observed for tetrahedral borates. It is suggested that this effect is indicative of an interaction of the aromatic system of the phenyl rings with the vacant boron p_z orbital, resulting in a greater deshielding of the *para* fluorine only. This interaction acts to stabilise the molecule to oxidative decomposition.[13]

1.2.2.2a C₆F₅ Transfer Reactions

There is a precedent for $B(C_6F_5)_3$ to occasionally form incompatible anions on reaction with a procatalyst.[13-15, 17, 19-20] The ions within the resulting salt react with each other *via* C_6F_5 anion transfer, to produce species which are inactive to alkene polymerisation. An example of C_6F_5 transfer includes the treatment of $[ZrMe_2(\eta\text{-}C_5H_5)\{\eta^2\text{-}PhC\{N(SiMe_3)_2\}\}]$ with $B(C_6F_5)_3$ in benzene to produce the neutral inactive species$[\{(\eta\text{-}C_5H_5)\{\eta^2\text{-}PhC(NSiMe_3)_2\}(C_6F_5)\}Zr\{\eta\text{-}B(C_6F_5)_3Me\}]$ (Figure 1.11).[14]
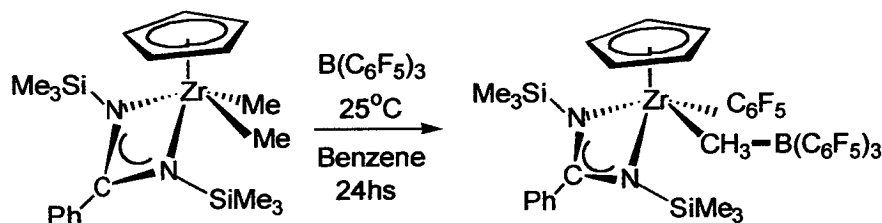
Figure 1.11

A summary of the ^{19}F NMR *o/p/m*-F positions for the (C_6F_5) groups in various compounds is given in Table 1.01 and all the structures of the complexes are shown in Figure 1.12. Comparison of the *o/p/m*-F peaks for the activator $B(C_6F_5)_3$ with complexes containing $M(C_6F_5)$(where M= Al, Zr, Pd, Li, or Ti) indicate the *o*-F peak is shifted to a higher frequency during C_6F_5 transfer from $B(C_6F_5)_3$ to the metal. There is also a shift in the *p/m*-F peaks to a lower frequency by several ppm.

Compound	Solvent	^{19}F NMR ppm (J_{FF},Hz)		
		o-F	*p*-F	*m*-F
B(C$_6$F$_5$)$_3$[13]	C$_6$D$_6$	-129.2	-142.1	-160.4
[Cp$_2$ZrMe(μ-Me)Al(C$_6$F$_5$)$_3$]15	Tol-*d$_8$*	-124.0 (16.9 Hz)	-155.2 (19.8 Hz)	-162.6
[Cp$_2$ZrMe(C$_6$F$_5$)][15]	Tol-*d$_8$*	-115.2 (25.4 Hz)	-156.7 (19.8 Hz)	-162.2
[Al(C$_6$F$_5$)$_3$.THF][16]	C$_6$D$_6$	-120.1	-153.8	-160.1
[PdBr(C$_6$F$_5$)][17]	CD$_2$Cl$_2$	-115.6, -116.5,	-163.1, -164.0	-165.83
[PdI(C$_6$F$_5$)][17]	CD$_2$Cl$_2$	-113.5, -115.4	-163.1, -164.2	-165.2
[(TTP)AlMe(C$_6$F$_5$)][18]	C$_6$D$_6$	-121.7	-154.9	-162.4
[Li{Ga(C$_6$F$_5$)$_4$}][19]	THF-*d$_8$*	-123.1	-160.5	-165.4
[Li{Ga(C$_6$F$_5$)$_4$}].2Et$_2$O [19]	C$_6$D$_6$(1mL) +THF(0.3mL)	-123.0	-159.3	-164.6
[Zr(C$_6$F$_5$){η^5-C$_4$H$_3$MeB(C$_6$F$_5$)}Cp"][20]	Tol-*d$_8$*	-122.9, -136.1	-155.6	-149.5, -150.9
[Zr(C$_6$F$_5$)(OEt$_2$){η^5-C$_4$H$_3$MeB(C$_6$F$_5$)}Cp"][20]	Tol-*d$_8$*	-123.7, -130.6	-156.7, -158.1	-162.1, -163.0
[{η^2-NAr(CH$_2$)$_3$NAr}Ti{CH$_2$B(C$_6$F$_5$)$_2$](C$_6$F$_5$)][21]	Tol-*d$_8$*	-119.4, -132.3	-154.0, -163.2	-164.2

Table 1.01 Summary of ^{19}F NMR information for M (C$_6$F$_5$) moieties
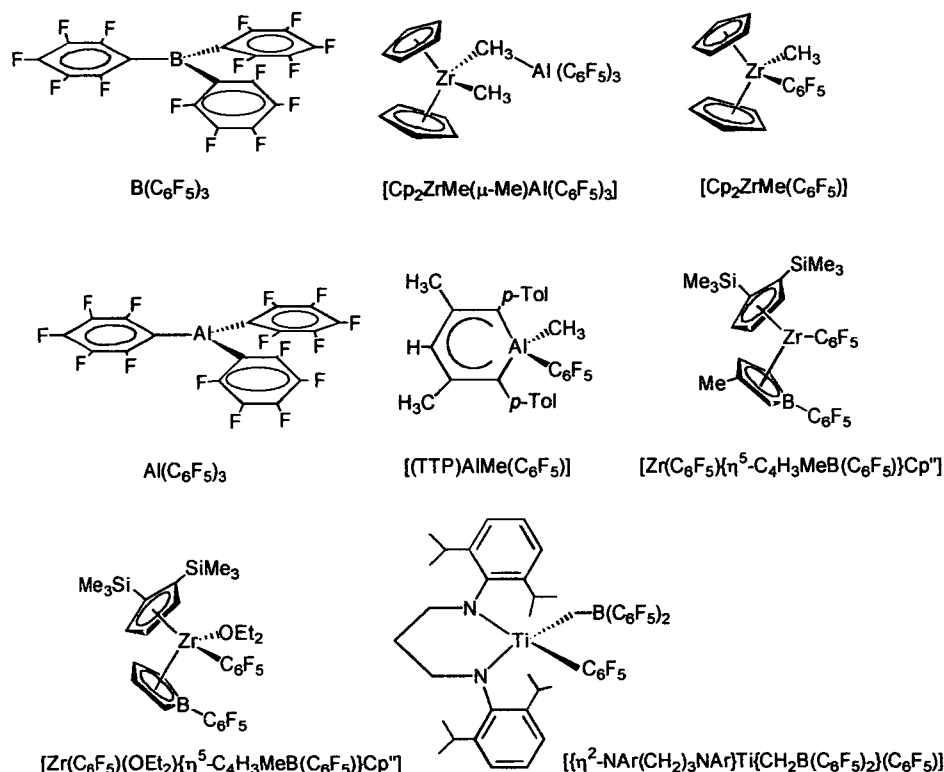
Figure 1.12

1.2.2.3 Activation with [NHMe₂Ph][B(C₆F₅)₄]

Activators such as dimethyl anilinium tetrakis(pentafluorphenyl)borate [NHMe₂Ph][B(C₆F₅)₄] **(5)** cause the protonolysis of M-R bonds to produce the activated catalyst, [22] as well as the byproducts RH and NMe₂Ph (Figure 1.13).[8] Co-ordination of the neutral amine produced during activation commonly occurs.[7] Amine coordination results in a stabilising effect on the cation which, although it may make the cation less active to polymerisation due to the reduced electronic unsaturation and more steric crowding of the system, has the advantage of making the cation more easy to characterise and possibly crystallise.
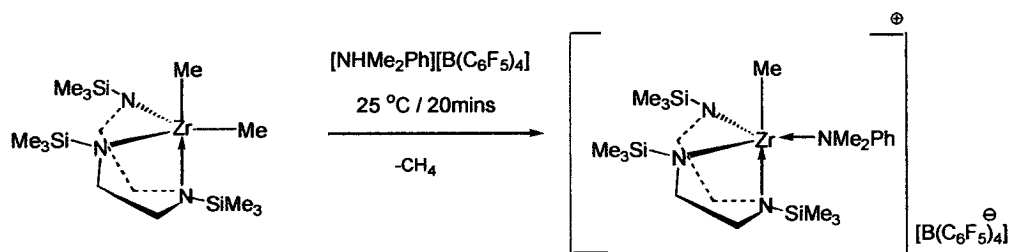
Figure 1.13

1.3 Active Alkene Polymerisation Catalysts

The majority of the research into Ziegler-Natta type catalysis has revolved around the preparation, activation and polymerisation testing of transition metal complexes. Zirconocene (group 4) (e.g. [(η⁵-C₅H₅)₂ZrMe] [MeB(C₆F₅)₃]), [15] chromium (group 6) (e.g.[Cp*Cr(OEt₂)₂CH₂SiMe₃][BAr'₄] (Ar'= 3,5-bis(trifluormethyl)phenyl),[23] and Ni/Pd (group 10) based catalysts systems (e.g. (α-diimine)NiBr₂, Chapter 3.11.) have been thoroughly investigated.[24] Other element blocks have been investigated, such as lanthanide metal based complexes (e.g. Cp*LnCH₃) which have also been proven to be active. [25] Similarly, but more recently, main group metal based complexes (e.g. [{ᵗBuC(NR')₂}AlMe][MeB(C₆F₅)₃]) have reported activity to ethene and methyl methacrylate (MMA) polymerisation.[26] It is clear then that a transition metal centre is not a prerequisite for an active Ziegler-Natta catalyst. There have been extensive studies on the development of activators too, these will not be discussed but are addressed in a recent review.[7]

1.3.1 Transition Metal and Lanthanide Based Alkene Polymerisation Catalysts

1.3.1.1 Group 4 Catalysts

In 1957, Berslow and Natta first produced the soluble catalyst Cp_2TiCl_2 which polymerised ethene under mild conditions, when activated by Et_3Al or Et_2AlCl but with lower activities than the heterogeneous systems. [27, 28] This system was inactive for propene polymerisation. Coupled with the fact that these systems were inclined to be readily reduced to inactive titanium(III) species, they could not compete with their heterogeneous counter parts.

Inevitably Ziegler catalysts are susceptible to hydrolysis, however it was observed that traces of water improved the rate of polymerisation in zirconocene systems by the formation of aluminoxanes by partial hydrolysis of the aluminium alkyl component present.[29] Sinn and co-workers made a profound discovery in 1980 that the partially hydrolysed Me_3Al [Methylaluminoxane (MAO)] was potentially a more effective activator that aluminuim alkyls alone.[30] A highly reactive catalyst was produced from an inactive system $[ZrCp_2Me_2]$-$AlMe_3$, simply by the addition of water. The activity was maintained when the $AlMe_3$ was partially hydrolysed before being added to the group 4 metallocene complex. Since the discovery of the improved activity obtained from MAO, the development of a new type of catalyst e.g. metallocene Ziegler-Natta catalysts, in particular zirconocene catalysts, and polyolefin materials emerged. Industry aspires to obtain maximum control over the properties of the polymers they can produce, and to enhance and improve their product range to new polymer combinations, by searching for new highly selective catalyst families that tolerate a variety of functional groups. There is a strong incentive for companies to own the intellectual properties for catalyst systems and there has been an explosion of innovation in the development of homogenous Ziegler-Natta type catalysts. The major drawback of heterogeneous titanium-based catalysts is the diversity of the actives sites on the catalyst surface.[31] Further studies into developing Ziegler-Natta type catalysts resulted in the search to produce more highly selective and efficient catalysts. There was a big driving force to produce

homogeous Ziegler-Natta catalysts which could provide advantages such as: (1) allowing more control over the catalysts molecular nature, producing identical catalytic centres which increase the selectivity and reduces the molecular weight distribution; (2) improved economy (reacting at low temperatures, facile heat transfer and all the catalyst is active (not just the surface), 3) the easy modification of the catalysts activity, and the polymer properties, by variation of parameters; (4) the ease of kinetic and mechanistic studies by in situ methods such as high pressure IR or NMR (Table 1.02). The main disadvantages of homogenous catalysts are that product separation is problematic and catalyst recycling can be expensive.[31]

	Heterogeneous	*Homogeneous*
Catalyst	Metal or	Metal/ ligand
	Metal support	
Pressure	1-300 bar	1-300 bar
Temperature	25-400 °C	<200
pH	Acidic and basic	
Solvent	Gas phase preferred	Liquid phase
Selectivity	Various	High
Activity	Various	Various
Diffusion	Difficult	Easy

Table 1.02 Comparison of Heterogeneous and Homogeneous catalysts

Variation of either the ligand system/functionality, or the transition metal used, may affect a number of variables: 1) the activity of the catalyst, 2) the charge and 3) the total valence electron count of the active species.[7,10,32-35] Unsurprisingly, the most active systems are the most electronically unsaturated and have 14 or fewer valence electrons and therefore a highly Lewis acidic centre and a high electrophilicity. The first proposal for such an active species was by Shilov in 1960, who identified $[Cp_2MR]^+$ a metallocene-based catalyst containing a 14-electron cationic metal alkyl.[36]

There has been substantial investigation into preparing new zirconium based catalyst systems by varying the ligand: e.g.monocyclopentadienyl ligands, non-

cyclopentadienyl ligands, ancilary ligands isolobal to cyclopentadienide, and neutral ancillary ligands (Figure 1.14).[33]
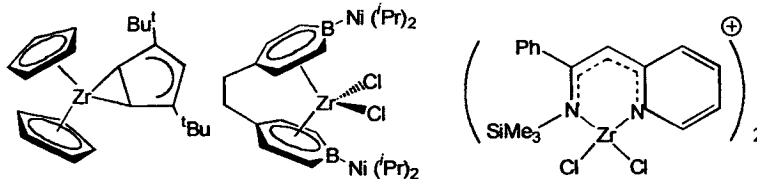
Figure 1.14

1.3.1.2 Group 3 Metal Catalysts

As mentioned in a recent review, neutral alkyl complexes of scandium and yttrium are isoelectronic with group 4 cationic alkyl complexes: c.f. $[Cp_2ScR]$ and $[Cp_2ZrR]^+$.[32] There has been interest in developing Group 3 olefin polymerisation catalysts as monomeric complexes can be afforded using bulky ligands and the complexes are single-component catalysts that do not require a cocatalyst. There have been different ligand systems studied for scandium which have reported ethene activity (Figure 1.15). Exemplary scandium complexes include $[(\eta^5-C_5H_5)_2ScR]$ (where R = H, alkyl) with low activity, and $[Sc\{N(SiMe_2CH_2P^iPr_2)_2\}R_2]$ (where R = Me, Et, or CH_2SiMe_3) which polymerises ethene (no activity figures are given).[37, 38] Exemplary yttrium complexes include the dimers $[rac-Me_2Si(2-SiMe_3-4-CMe_3C_5H_2)_2Y(\mu-H)]_2$ and $[Me_2Si(2-SiMe_3-4-^tBuMe_2SiC_5H_2)_2Y(\mu-H)]_2$.[39-41] The former polymerises propylene, 1-butene, 1-pentene and 1-hexene slowly over several days at 25°C, to produce modest molecular weight polymers. The latter displays high activity for olefin polymerisation reactions, e.g. 5.84×10^5 g/molh, 25°C, C_2H_4. Polystyrene can be polymerised using both complexes $Cp'_2YbAlH_3.L$ ($Cp'= {}^tBuCp$, Cp^*; $L=NEt_3$, THF, Et_2O) and $[(^tBuCp)_2Yb(THF)_2][BPh_4].THF$.[42]
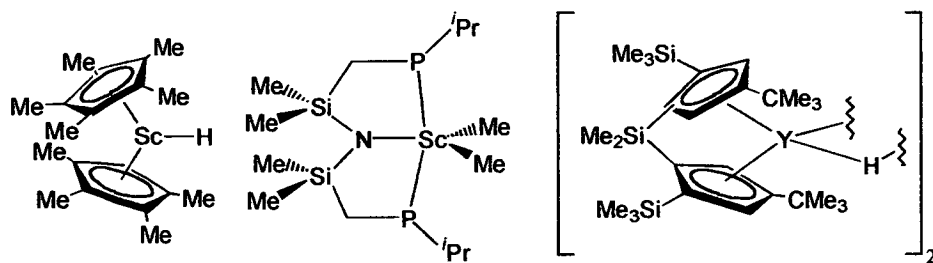
Figure 1.15

1.3.1.3 Lanthanide Metal Catalysts

As early as 1978, it was reported that certain f-block metal complexes are active homogeous alkene polymerisation catalysts, e.g. certain $(Cp'_2UH)_2$ and $[Cp'_2U\{CH_2Si(CH_3)_3\}_2]$.[43] Complexes of $[(Cp'_2MH)_2]$ (M=La, Nd and Lu) undergo extremely rapid reaction with ethene to immediately produce large quantities of polyethene.[44] The complex $[(\eta^5-Cp^*)_3Sm]$ reacts with ethene to form polyethene (Figure 1.16).[45] Similarly the complex $[Cp_2^*NdCH(SiMe_3)_2]$ reacts with BuMgEt and $MgCl_2$ to produce a solid ethene polymerisation catalyst.[46] The methylutetium compound Cp_2^*LuMe polymerises both ethene and propene to produce high density polyethene and a mixture of oligomers respectively.[25]
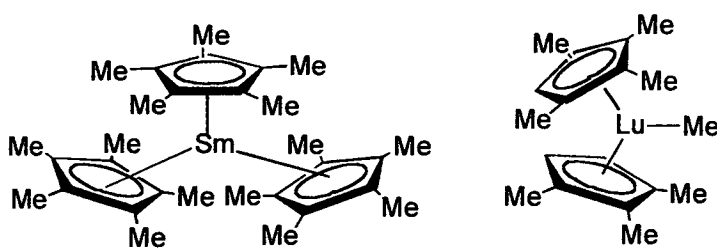
Figure 1.16

1.3.1.4 Group 6 Metal Based Catalysts

There have been two significant Group 6 metal based ethene polymerisation catalyst system discoveries:

1) the single-component catalyst of activated chromium oxides suspended in inert hydrocarbons and supported on Silica (Philips catalyst)

2) the gas phase reaction of C_2H_4 with alumina treated with $[Cr(\eta-C_6H_6)_2]$ (Union carbide catalyst).[6]

Both these systems are highly active heterogeneous catalysts and play a major part in the commercial production of polyethene. However, the precise nature of the active sites in these systems is not fully understood, and homogeneous analogues of the group 6 metal catalyst have been developed and recently reviewed.[23, 32, 33]

A couple of examples of active homogeneous chromium catalysts are shown in Figure 1.17. The Cp-amide chromium complex, displays high activities with ethene e.g. 16 Kg PE/mmolCrh^{-1} when activated with MAO at ambient temperature and 2 bar.[47] The bis-imido complex produces a high-valent chromium (VI) species which has moderate ethene polymerisation activity e.g. 25 Kgmmol^{-1}h^{-1}bar^{-1} 10 bar (information on temperature not given).[48]
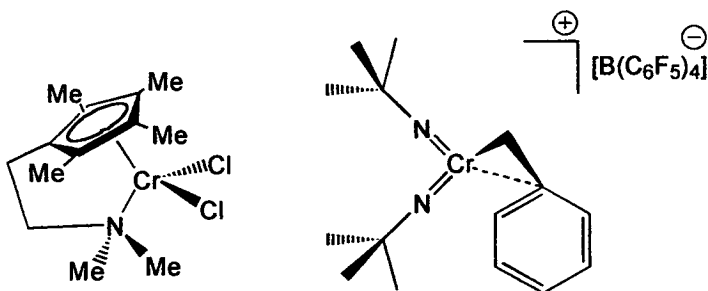
Figure 1.17

1.3.2 Main Group Metal Based Alkene Polymerisation Catalysts

1.3.2.1 Evidence for the Alkene Polymerisation Activity of Aluminium

Alkyls

Monomeric AlR_3 species catalyse chain growth by repetitive insertion of ethene into the Al-C bond to produce 1-alkenes following β-hydride elimination (Figure 1.18). Low molecular weight polymers are produced because the rate of the β-hydride elimination step is competitive with the ethene insertion step.[2]

$$Et_3Al \xrightarrow[\text{Growth}]{\substack{CH_2=CH_2 \\ 110^\circ C/\, 100bar}} Al \begin{array}{l} (C_2H_4)_mEt \\ (C_2H_4)_nEt \\ (C_2H_4)_oEt \end{array}$$

$CH_2=CH_2$ (upward arrow to Et_3Al)

β-H elimination $\mid$ 200-300°C (downward arrow)

$$AlH_3 \ + \ 3CH_2=CH-(CH_2CH_2)\underset{m,n,o}{\quad}H$$
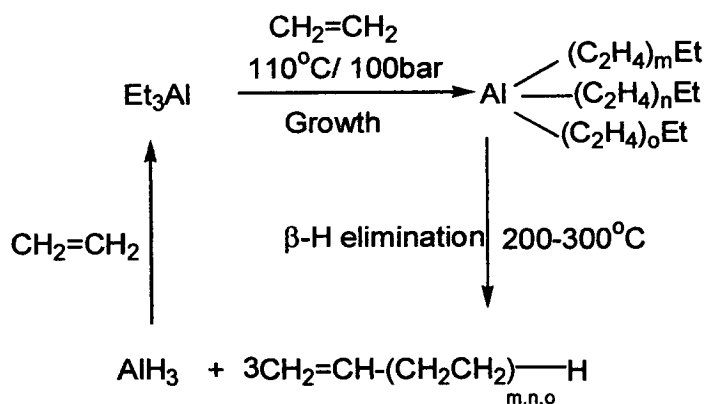
Figure 1.18

In 1971 a patent was submitted describing the reactions of tri[n]hexyl aluminum and di[n]pentyl magnesium with ethene in benzene at high temperature and pressure.[49] The results of the reaction with di[n]pentyl magnesium will be discussed in Chapter 1.3.2.4. The rate of alkene insertion into M-C bonds determines the activity of the catalyst complex, but it is the rate of chain termination which determines the chain length of the products. To obtain a high molecular weight polymer, the rate of alkene insertion must be significantly greater than the rate of chain termination, due to the competitive nature of these processes. The patent states that in the reaction of the Al system an alkane/alkene ratio of 1.8 is obtained following the hydrolysis of the reaction mixture. The presence of C_2 and C_4 alkanes in the product mixture could only be due to a fast β-H elimination (chain termination) reaction in comparison to the rate of alkene insertion, followed by, in the case of alkanes, subsequent ethene hydroalumination by the resulting Al-H species and chain growth (Figure 1.19).

[(C$_6$H$_{13}$)$_3$Al] $\xrightarrow[\text{2500 psi C}_2\text{H}_4]{\text{Benzene, 423K, 1h}}$

Chain growth Reaction

	Mol% n-alkane	Mol% n-alkene
C$_2$	2.6	0
C$_4$	4.3	0
C$_6$	9.5	6.4
C$_8$	10.0	6.9
C$_{10}$	7.6	8.1
C$_{12}$	7.4	4.5
C$_{14}$	6.0	3.2
C$_{16}$	4.8	2.7
C$_{18}$	3.9	2.0
C$_{20}$	2.9	1.4
C$_{22}$	2.4	0.7
C$_{24}$	1.7	0
C$_{26}$	1.0	0
	64.1	35.9

Figure 1.19 Oligomerisation of ethene in the presence of [Al(C$_6$H$_{13}$)$_3$]$_2$

Similarly, an ethene oligomerisation reaction in the presence of alkyl aluminium chlorides produces linear aliphatics with a maximum chain length of about C$_{200}$, due to the competing dehydroalumination reaction (Figure 1.20).[4]

$$R_2AlC_2H_5 \ + \ (n\text{-}1)\ CH_2{=}CH_2 \ \xrightarrow[\text{100 bar}]{90\text{-}120^{\circ}C} \ R_2Al(CH_2CH_2)_nH \qquad (1)$$

$$R_2AlCH_2CH_2R' \ \xrightarrow{\text{Dehydroalumination}} \ R_2AlH \ + \ CH_2{=}CHR' \qquad (2)$$
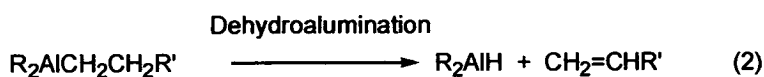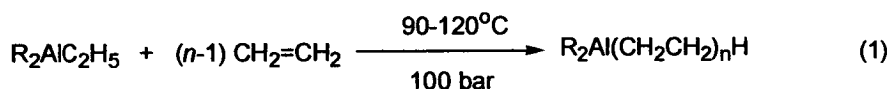
Figure 1.20

Sen et al, report the preparation of high molecular weight, linear homo- and copolymers of ethene and propene *via* a catalyst system consisting of alkyl aluminium compounds activated by Lewis acids (Table 1.3).[50] This is the first known example of the polymerisation of higher alkenes by an aluminium-based system. They observed an increase in molecular weight with increasing reaction lifetime in

the polymerisation of ethene, and narrow polydispersities for the polyethene and polypropene formed, suggesting a single-site catalyst. It was noted that certain combinations, e.g. AlEt$_3$ and BEt$_3$ did not catalyse the polymerisation of ethene. Thus Lewis acid activation influences the rate of insertion or elimination, or both in the polymerisation of alkenes by methyl aluminiums.

Starting material	Activator	Solvent	Monomer	Reported Activity (Kg/mol.h)
AlEt$_3$	MAO	C$_6$H$_5$Cl	Ethene	3.25
AlEt$_3$	B(C$_6$F$_5$)$_3$	C$_6$H$_5$Cl	Ethene	0.85
AlEt$_3$	[CPh$_3$][B(C$_6$F$_5$)$_4$]	C$_6$H$_5$Cl	Ethene	2.33
AlEt$_3$	[NMe$_2$HPh][B(C$_6$F$_5$)$_4$]	C$_6$H$_5$Cl	Ethene	13.75
AlEt$_3$	B(C$_6$F$_5$)$_3$	C$_6$H$_5$Cl	Propene	0.12
AMe$_3$	B(C$_6$F$_5$)$_3$	C$_6$H$_5$Cl	Propene	0.03

Table 1.3 Polymerisation activities for the reaction of ethene or propene with activated AlR$_3$

1.3.2.2 Initial Evidence of the Alkene Polymerisation Activity of Chelated Aluminium Alkyls

Before commencing our studies into magnesium alkyl catalysts there was at that time a strong background presented in the literature that aluminium alkyl or hydride complexes supported by nitrogen donor ligands were active to ethene and methyl methacrylate (MMA) polymerisation (Figure 1.21, Table 1.4).[51-55] These include neutral and cationic complexes containing bi- or tridentate N-donor ligands including amidinates (1-3),[51-53] pyridyliminoamides (4-6),[54] and aminotroponiminates (7-10).[55] Three structural types of catalyst were characterised:

1) Base free three co-ordinate species

2) Base stabilised four co-ordinate cations

3) Dinuclear methyl bridged cations.

Complex	Monomer	Pressure	Temperature	Reported Activity
1	C_2H_4	4 atm	40 °C	-
2	C_2H_4	2 atm	60 °C	700 gPE/mol.h.atm
3	C_2H_4	< 1 atm	50 °C	Trace
4	C_2H_4	5 bar	40 °C	80 gPE/mol.h.bar
5	C_2H_4	5 bar	40 °C	60 gPE/mol.h.bar
6	C_2H_4	5 bar	40 °C	120 gPE/mol.h.bar
7	C_2H_4	1 atm	80 °C	2600 gPE/mol.h.atm
8	C_2H_4	1 atm	80 °C	900 gPE/mol.h.atm
9	C_2H_4	Not given	Not given	Trace
9	MMA	-	23 °C	None
10	C_2H_4	Not given	Not given	Trace
10	MMA	-	23 °C	100% yield Syndiotactic poly(MMA)

Table 1.4 Some reported details of the activities of the aluminium alkyl/hydride complexes given in figure 1.21.

4 R=H, R^1=^{i}Pr,R^2=^{i}Pr,R^3=H   **7** R=Et   **9** R=Me

5 R=H, R^1= Me, R^2=Me, R^3=Me   **8** R=^{i}Bu   **10** R=H

6 R=Me, R^1=^{i}Pr, R^2=^{i}Pr, R^3=H
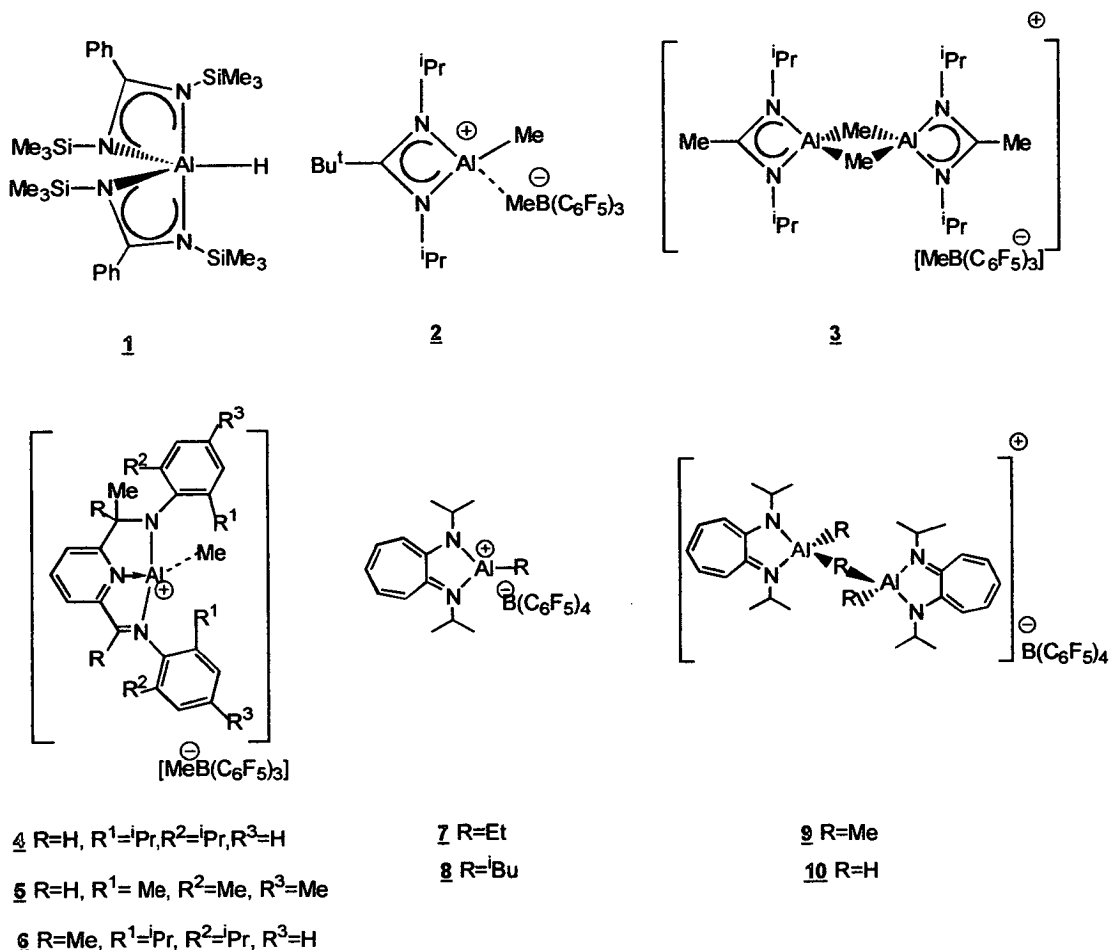
Figure 1.21 Aluminium alkyl and hydride complexes that are reportedly active for ethene and/or MMA polymerisation.

18

The activities for these systems are not particularly high but were an indication that, as a main group metal, magnesium may also be active in a similar way. An important observation can be made from the activity results, namely that monomeric species give much greater activities in comparison to the corresponding alkyl bridged dimeric species, for obvious steric reasons during the attack of an ethene molecule.

The base free [('Pr$_2$-ATI)AlR]$^+$ species (Where ATI = aminotroponiminate) polymerise ethene, whereas the base free [(diketiminate)AlR]$^+$ species undergo a cycloaddition reaction with ethene to produce unusual bicyclic complexes 14 and 15, as shown by COSY NMR (Figure 1.22).
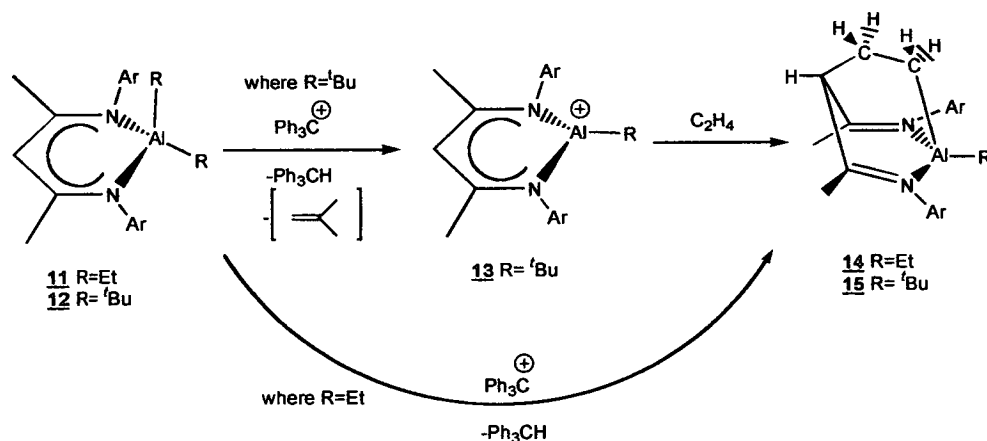
Figure 1.22 Cycloaddition reaction of a cationic aluminium β-diketiminate complex with ethylene

1.3.2.3 Discussion of the Literature Published About Ethene Polymerisation by Aluminium Alkyl Complexes (1999-2001)

During our research, there have been several papers published about the alkene polymerisation activity of aluminium alkyl complexes which have created some controversy, particularly about the work described by Jordan et al.[56, 59-61] Some theoretical studies indicated the favourability of the reaction path for the addition of simple alkenes and alkynes into Al-C bonds.[57]

1.3.2.3a Diketiminate Aluminium Alkyl Complexes

Although Jordan published the impressive crystal structures of both [{diketiminate}AlMe][B(C_6F_5)$_4$] (<u>17</u>) and [{diketiminate}AlMe] [MeB(C_6F_5)$_3$] (<u>18</u>) in 1999, their activities as ethene polymerisation catalysts were not discussed (Figure 1.23).[59]
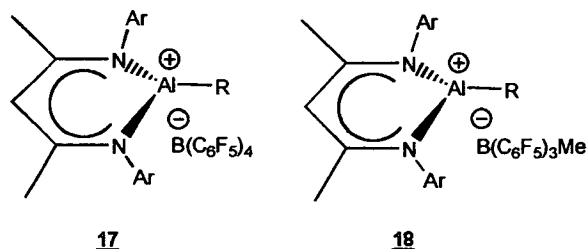
Figure 1.23 Structures of <u>17</u> and <u>18</u>.

1.3.2.3b Amidinate Aluminium Alkyls

In contrast to the earlier theoretical studies mentioned above, on the basis of *ab initio* calculations evidence was provided that an [(Amidinate)AlR]$^+$ species (<u>2</u>) (Figure 1.21) would not be active for ethene polymerisation, not because the insertion barrier is too high, but because of the fast rate of chain transfer, and it was suggested that the catalyst would at best be a dimerisation catalyst.[58] Talarico and Budzelaar report that the positive charge and geometric constraints in <u>2</u> contribute to the preference for chain transfer. In comparison, monomeric aluminium alkyls that are both neutral and unstrained would be expected to have noticable preference for oligomerisation/polymerisation and an insertion barrier lower than that of <u>2</u>.

In 2000, after further examination of the amidinate aluminium alkyl complexes Jordan describes the discovery of the variable solution structures of the cationic complexes [{RC(NR')$_2$}AlMe$_2$] (R=Me or ^{t}Bu, R'=^{i}Pr or Cy) on activation with [CPh$_3$][B(C_6F_5)$_4$] or B(C_6F_5)$_3$ and proposed several types of chelating and bridging bonding modes adopted by the amidinate ligands (Figure 1.24).[60] The stability and structure of the cations depend primarily on the reactivity of the anion [B(C_6F_5)$_4$$^-$ < RB(C_6F_5)$_3$$^-$] and the steric properties of the amidinate substituents. Isolation of the monomeric [{RC(NR')$_2$}AlR]$^+$ species is problematic as the small

bite angle of the amidinate ligand (N-Al-N *ca* 70°C) produces a sterically open, highly reactive Al centre, which reacts with a [RC(NR')$_2$AlMe$_2$] complex to become a dinuclear species. Interestingly, it was discovered that in the presence of a Lewis base such as NMe$_2$Ph, the base stabilised 4-coordinate cations were obtained via reaction of 19 directly with one equivalent of [HNMe$_2$Ph][B(C$_6$F$_5$)$_4$], or 19 and 21 with 0.5 equivalents of [CPh$_3$][B(C$_6$F$_5$)$_4$] followed by the reaction of NMe$_2$Ph (Figure 1.25).
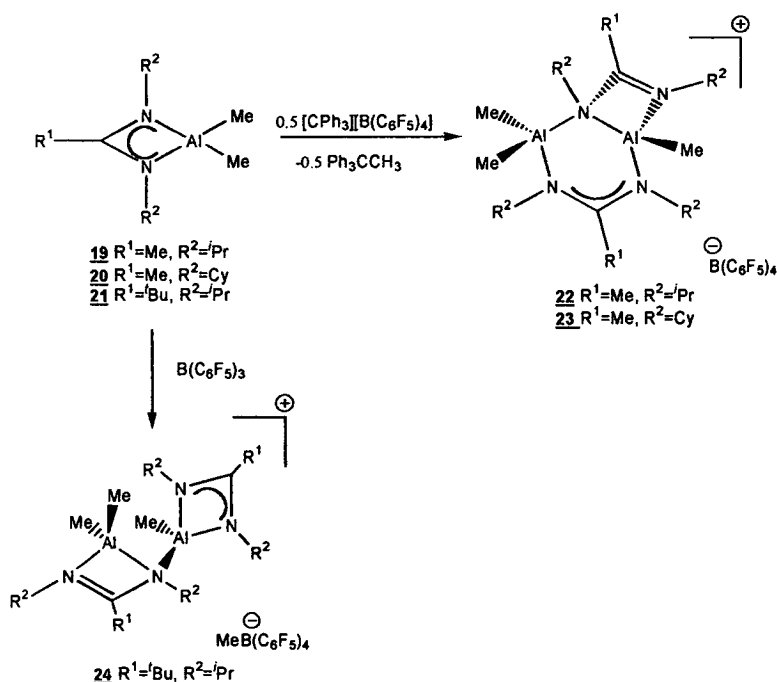
Figure 1.24 Variable solution structures of aluminium alkyl complexes 19 and 21.
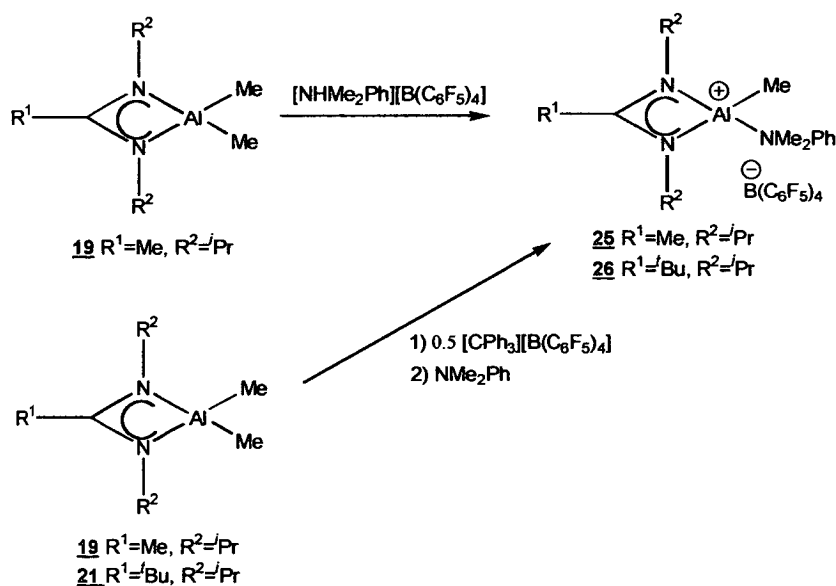
Figure 1.25 Preparation of NMe$_2$Ph stabilised four co-ordinate aluminium alkyl complexes

1.3.2.3c Aminotroponiminate Aluminium Alkyl Complexes

Jordan reported that $[(^iPr_2ATI)Al(alkyl)]^+$ and $[(^iPr_2ATI)Al(alkenyl)]^+$ cations may adopt dinuclear structures following the reporting of the crystal structures of $[(^iPr_2\text{-}ATI)Al(\mu\text{-}O^iPr)]_2{}^{2+}$ (**27**) and $[(^iPr_2\text{-}ATI)Al(\mu\text{-}C\equiv C^tBu)]_2{}^{2+}$ (**28**).[56] It is also mentioned that $[(^iPr_2ATI)AlR]^+$ complexes containing β-hydrogens, such as $[(^iPr_2ATI)AlEt]^+$, react with unsaturated substrates (Figure 1.26). Initially β-H transfer occurs, followed by an insertion/σ-bond metathesis which causes terminal alkyne dimerisation.
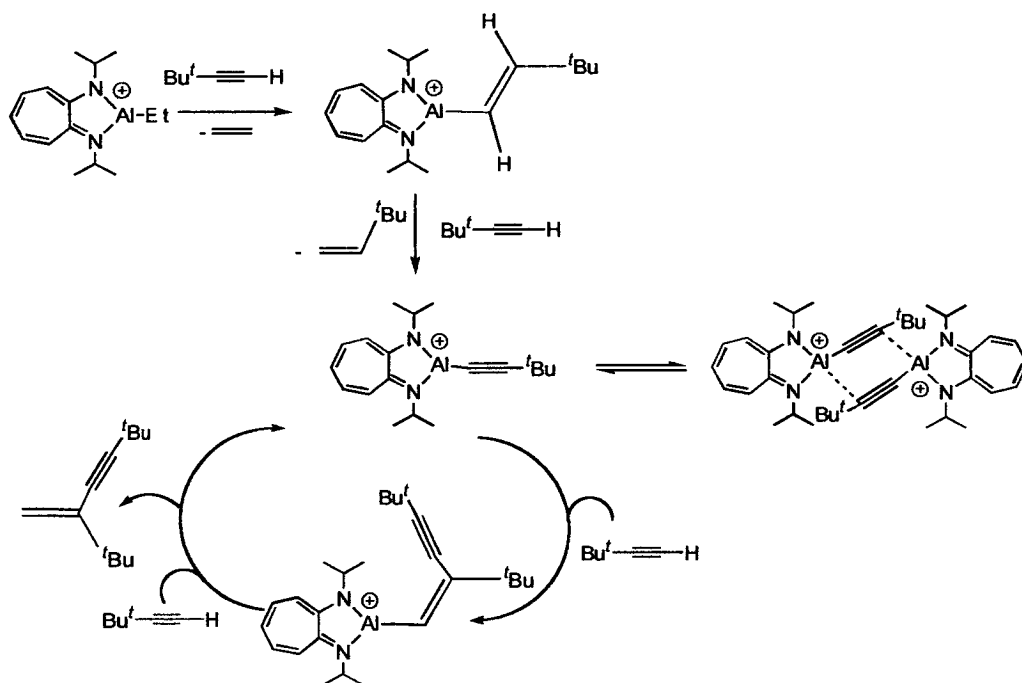
Figure 1.26 Reaction of (ATI)AlEt⁺ with *tert*-butylacetylene

In a paper published in 2001 Jordan confirmed that an equilibrium reaction of $[(^iPr_2\text{-}ATI)AlR]^+$ cations with the starting material $[(^iPr_2\text{-}ATI)AlR_2]$ produces a dinuclear species in CD_2Cl_2 (Figure 1.27).[61] Complexes **35-37** have a lower stability when R is a higher alkyl than methyl, consequently washing with hexanes to extract the neutral dialkyl complex results in the selective yield of the monomeric cation. However, when R is methyl a mixture of both the monomeric and dimeric cations are obtained.
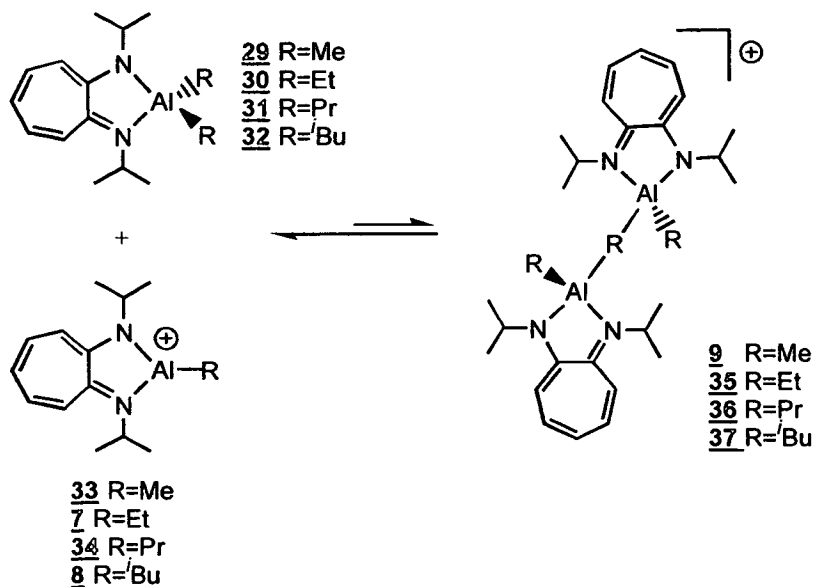
Figure 1.27 Reaction of [(ATI)AlR]⁺ with [(ATI)AlR₂] to produce R-bridged dimer

Complex **8** polymerises a 500-fold excess of propylene oxide to yield atactic poly(propylene oxide) with an activity of 240 t.o/h. The dinuclear cationic aluminium hydride complex [{^{i}Pr₂-ATIAl}₂H₃][B(C₆F₅)₄] polymerises a 450-fold excess of MMA to produce moderately syndiotactic poly(MMA). Only the base free monomeric [(^{i}Pr₂-ATI)AlR]⁺ cations produced polyethene on reaction with ethene, as shown in Table 1.4. Jordan monitored the reaction of **7** and **8** with ethene-d_4. The results indicated the reaction proceeds *via* β-H transfer to yield ethene or isobutene. Jordan conceded that this result, coupled with the theoretical results obtained for the amidinate ligands, suggests that the [(^{i}Pr₂-ATI)AlR]⁺ cations are not active to ethene polymerisation, and that it is at this time an unidentified species in solution that is the active species.[61]

1.3.2.3d Transfer of C_6F_5 in Chelated Aluminium Alkyl/Hydride Complexes

Of the most commonly used activators, e.g. $[CPh_3][B(C_6F_5)_4]$ (**3**), $B(C_6F_5)_3$ (**4**) and $[NHMe_2Ph][B(C_6F_5)_4]$(**5**), Jordan found **3** to be the most effective due to the stability of the $[B(C_6F_5)]^-$ anion, the chemical inertness of the organic biproducts (Ph_3CR or Ph_3CH), and the production of the base free **3** co-ordinate cation. The ammonium salts produce much more stable inactive aluminium alkyl cations which are 4 co-ordinate and the borane **4** produces an incompatible $[RB(C_6F_5)_3]^-$ anion which reacts with the $[(L-X)AlR]^+$ cation *via* $[R]^-$ or $[C_6F_5]^-$ transfer to produce neutral products (Figures 1.28 and 1.29).[60,61]

30 R=Et
38 R=CH$_2$Ph

39 R=Et
40 R=CH$_2$Ph

41 R=Et
42 R=CH$_2$Ph
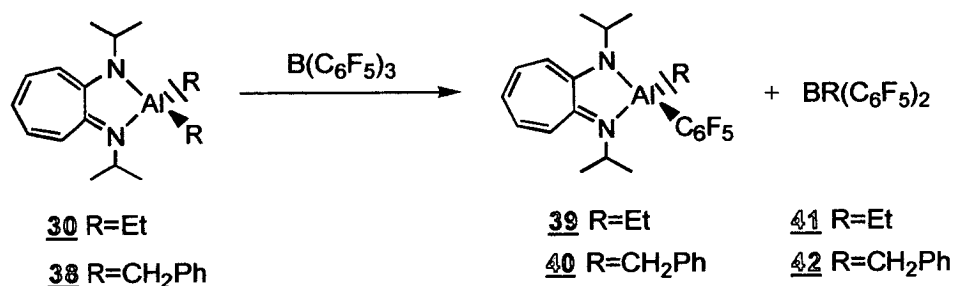
Figure 1.28 Reaction of [(ATI)AlR$_2$] with B(C$_6$F$_5$)$_3$ showing [C$_6$F$_5$]⁻ transfer

43 R^1=^{t}Bu
44 R^2=^{i}Pr

45 R^1=^{t}Bu
46 R^2=^{i}Pr

47 R^1=^{t}Bu
48 R^2=^{i}Pr
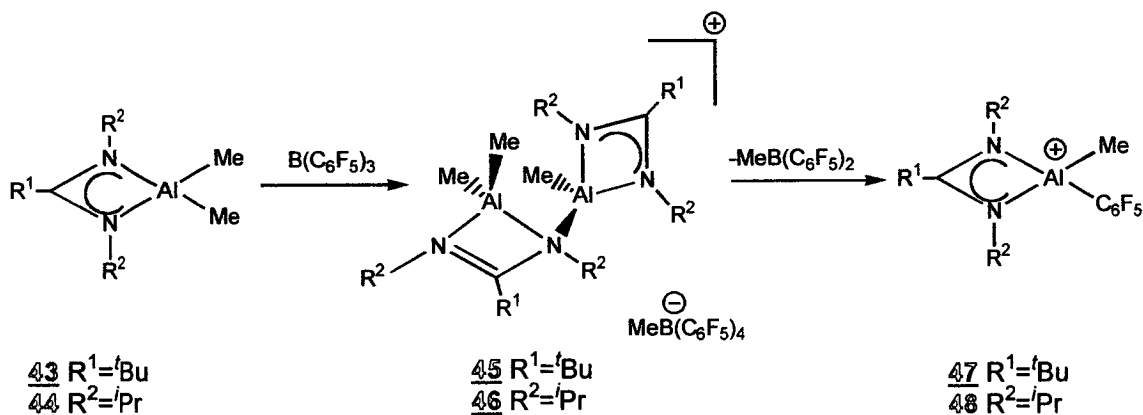
Figure 1.29 Reaction of [(amidinate)AlR$_2$] with B(C$_6$F$_5$)$_3$ showing [C$_6$F$_5$]⁻ transfer

Similarly the reaction of the β-diketiminate complex [(TTP)AlMe$_2$] [TTPH=2-(p-tolylamino)-4-(p-tolylimino)-2-pentene] with **4** at low temperature in CD$_2$Cl$_2$ produces [MeB(C$_6$F$_5$)$_3$]⁻ as shown by ^{11}B NMR; however the identity of the cationic species could not be readily interpreted. Degradation was observed to occur (as

judged by ^{19}F and ^{11}B NMR) to the proposed products [(TTP)Al(CH$_3$)(C$_6$F$_5$)] and MeB(C$_6$F$_5$)$_2$ (Figure 1.30).[18]
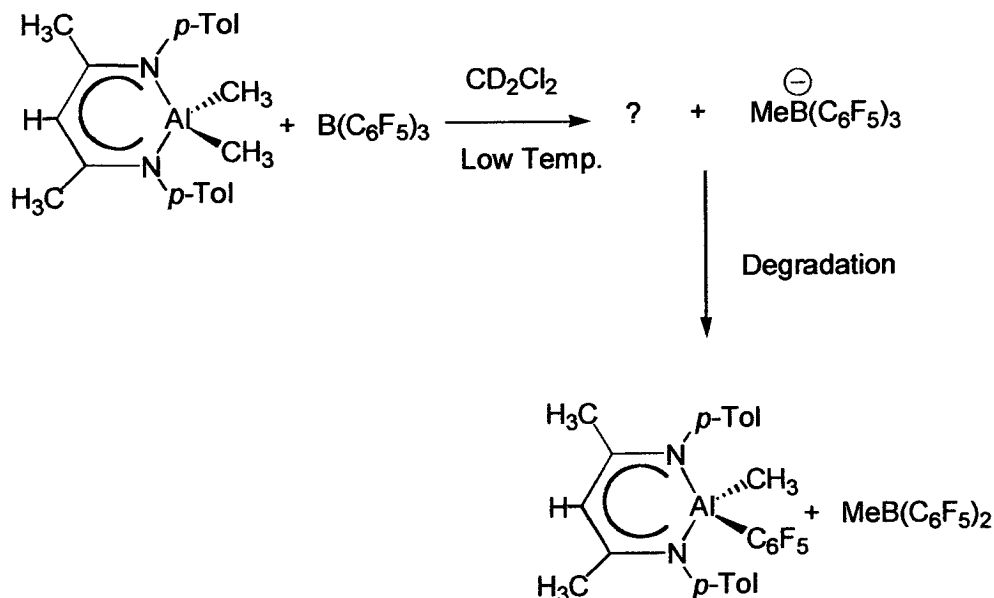
Figure 1.30 Reaction of [(diketiminate)AlMe$_2$] and B(C$_6$F$_5$)$_3$

1.3.2.3e Reactions of Aluminium Alkyls with (Perfluroaryl)boranes /Borates

Bochmann reported that the reaction of the AlMe$_3$ co-catalyst with the catalyst activator [CPh$_3$][B(C$_6$F$_5$)$_4$] at elevated temperatures produces a mixture of [AlMe$_{3-x}$(C$_6$F$_5$)$_x$] compounds, depending on the Al/B ratio.[62] These compounds in turn can react with the catalyst *via* C$_6$F$_5$ transfer and deactivate the catalyst to alkene polymerisation, as shown in the reaction of [Cp$_2$ZrMe(C$_6$F$_5$)] with Al(C$_6$F$_5$)$_3$ or [AlMe$_2$(C$_6$F$_5$)] (Figure 1.31).[62]
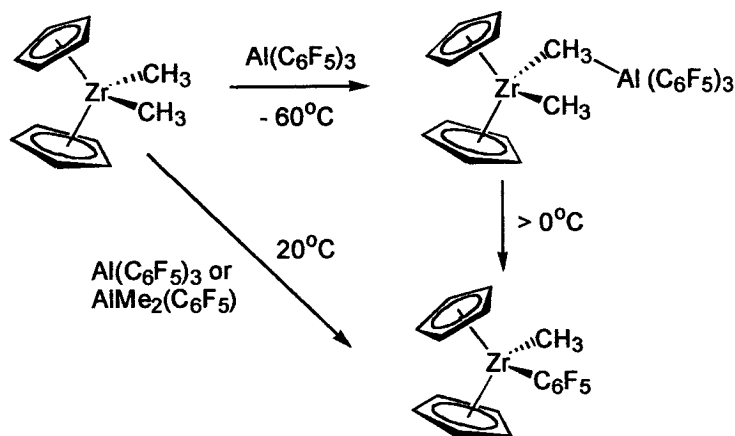
Figure 1.31 Reaction of Al(C$_6$F$_5$)$_3$ with [ZrCp$_2$Me$_2$]

Klosin and Chen report the effect of changing of the reaction solvent during the reaction of $B(C_6F_5)_3$ with AlR_3.[63] They discovered that in apolar hydrocarbon solvents, facile aryl/alkyl group exchange occurs and the preparative-scale reaction can produce quantitative amounts of $Al(C_6F_5)_3$ by precipitation of the product with aliphatic solvents or by vacuum removal of BMe_3 (Figure 1.32).

$$B(C_6F_5)_3 \;+\; AlMe_3 \xrightarrow{\;fast\;} MeB(C_6F_5)_2 \;+\; 0.5\,[(C_6F_5)_2Al_2Me_4]$$

$$\Updownarrow$$

$$BMe_3 \;+\; Al(C_6F_5)_3 \rightleftharpoons Me_2B(C_6F_5) + 0.5\,[(C_6F_5)_4Al_2Me_2]$$
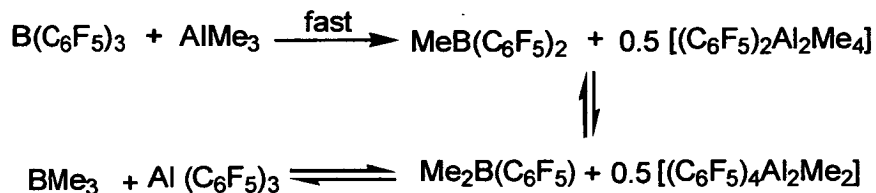
Figure 1.32 Reaction of $B(C_6F_5)_3$ with $AlMe_3$ in hydrocarbons

When the $AlMe_3$ is in excess the ligand exchange increases considerably, and the final exchange products are dimeric aluminium species such as: $[(C_6F_5)_3Al_2Me_3]$, $[(C_6F_5)_4Al_2Me_2]$ and $[(C_6F_5)_5Al_2Me]$. However, reaction of $B(C_6F_5)_3$ with AlR_3 in the presence of a co-ordinating solvent such as diethylether or tetrahydrofuran produces a single stable product (Figure 1.33).[63]

$$B(C_6F_5)_3 \;+\; AlR_3 \xrightarrow{\;Et_2O\;} [R_2Al\,(OEt_2)_2]^{\oplus} [RB(C_6F_5)_3]^{\ominus}$$

$$R=Me, Et, Octyl$$
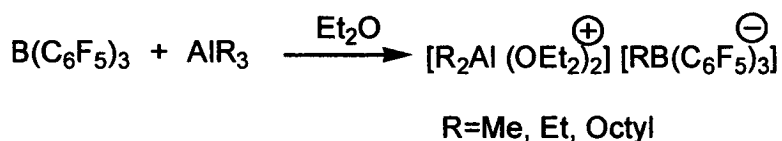
Figure 1.33 Reaction of $B(C_6F_5)_3$ with AlR_3 in Et_2O

1.3.2.4 Reported Reactivity of Magnesium Alkyls with Alkenes

There are only a handful of papers that provide evidence that magnesium dialkyls react with alkenes.[49, 64, 65] Some of the reaction conditions and products produced by a study are described in Table 1.5 below.

Mg Catalyst	Solvent	Alkene	Reaction Conditions	Products
Et_2Mg[64]	Et_2O	ethene	100°C, 740p.s.i.g., 43h	45% Et_2Mg, 2.8% n-hexylmagnesium, 2.5%vinylmagnesium, 2.5% MgH_2, 13% ethynyl magnesium complexes
Et_2Mg[64]	n-hexane or n-heptane	ethene	100°C, 600-900p.s.i.g	Liquid hydrocarbon ranging from C_{10} and a small amount of solid polymer
Et_2Mg[64]	Et_2O	BDPE	-	1-ethyl-2-benzylbidiphenyleneethane

Table 1.5 Reactions of Et_2Mg and $(^nC_5H_{11})_2Mg$ with some alkenes, (BDPE= Bidiphenyleneethylene)

The reaction of di^{n}pentyl magnesium with ethene in benzene at high temperature and pressure produces a mixture of n-alkanes and n-alkenes from C_7-C_{23} (Figure 1.34).[49] The alkane/alkene ratio is given as 4.3. The absence of C_2, C_4 and C_6 alkanes in the product mixture and the lower alkane/alkene ratio of 1.8 obtained in comparison to tri^{n}hexyl aluminium (Chapter 1.3.2.1) under the same conditions, suggests that there is less β-H elimination (chain termination) for magnesium alkyls. Therefore an organomagnesium polymerisation catalyst would be expected to produce substantially increased molecular weight polymers than the better known aluminium based oligomerisation reaction.

$[(C_5H_{11})_2Mg]_2$ $\xrightarrow[\text{2500 psi } C_2H_4]{\text{Benzene, 423K, 1h}}$

Chain growth Reaction

	Mol% n-alkane	Mol% n-alkene
C_7	8.1	5.8
C_9	11.7	4.8
C_{11}	14.4	3.2
C_{13}	15.2	3.0
C_{15}	12.5	1.2
C_{17}	9.1	0.7
C_{19}	5.6	0.4
C_{21}	3.1	0
C_{23}	1.3	0
	81.0	19.1

Figure 1.34 Polymerisation of ethene in the presence of $[Mg(C_5H_{11})]_2$

An international patent published by Sen and Kim in 2000 describes the invention of active ethene and/or α-olefin polymerisation/ oligomerisation catalyst systems comprising of both an alkyl magnesium component and a Lewis acid component.[65] At high pressures of between 700-900 psi of ethene, using either $B(C_6F_5)_3$ or $AlCl_3$, activators they report the activity of $Mg(C_4H_9)_2$ and $Mg(Np)_2$ in producing both solid and liquid branched polymers.

MgR$_2$ (µmol)	Activator	Solvent	Temp °C	Pressure psi	Productivity Kg/mol.h	Polymer
$Mg(C_4H_9)_2$	$B(C_6F_5)_3$	C_6H_5Cl	60	700	112.0	solid
$Mg(C_4H_9)_2$	$B(C_6F_5)_3$	Toulene	60	700	11.1	solid
$Mg(Np)_2$	$B(C_6F_5)_3$	Toulene	60	700	7.2	solid
$Mg(C_4H_9)_2$	$AlCl_3$	C_6H_5Cl	60	700	14.4	solid
$Mg(C_4H_9)_2$	$AlCl_3$	C_6H_5Cl	150	700	56.6	liquid
$Mg(Np)_2$	$AlCl_3$	C_6H_5Cl	60	700	23.8	liquid

Table 1.6 A selection of results published on the activity of $Mg(C_4H_9)_2$ and $Mg(Np)_2$ with ethene using $B(C_6F_5)_3$ or $AlCl_3$ activators

There appears to be scope for the modification of magnesium alkyls to produce viable polymerisation catalysts.

1.4 Background to Magnesium Alkyls

1.4.1 Aspects of Bonding in Organomagnesium Complexes

Magnesium atoms have the electronic structure: $1s^2 2s^2 2p^6 3s^2$. Magnesium exhibits a covalent bonding character with carbon, but due to the electropositive nature of magnesium the bond formed is strongly polarized ($Mg^{\delta+}-C^{\delta-}$). Organomagnesium compounds are useful in synthetic chemistry as they provide a source of $C^{\delta-}$.

1.4.2 Solvent Effects

In the absence of donor solvent, solid Grignard reagents and dialkyl magnesium species have polymeric structures,[66] e.g. MgMeCl, or MgMe$_2$ (Figure 1.35).
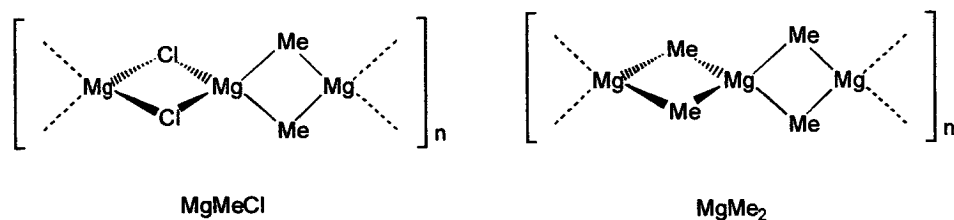
MgMeCl   MgMe$_2$

Figure 1.35 Polymeric structures of MgMeCl and MgMe$_2$

The organomagnesium acts as a Lewis acid and tries to obtain co-ordinative saturation by binding with a Lewis base. The central magnesium atom normally achieves (pseudo) tetrahedral co-ordination which is dictated by steric hinderance. The nature of Grignard reagents in solution is complex and depends on the solvent, concentration, temperature and on the specific organomagnesium compound.[67] In general the equilibria involved are of the Schlenk type:
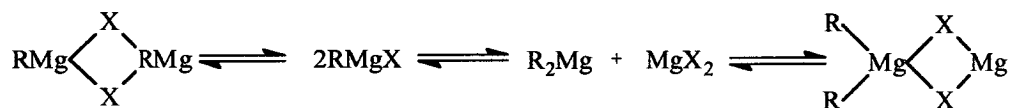
Figure 1.36

Solvation occurs and association is commonly *via* the better bridging candidate i.e. the halide, except for halide free compounds, where bridging by alkyl groups may occur. In non-polar solvents (e.g. petroleum-ether, benzene, or toluene) Grignard reagents are essentially insoluble and as a result remain polymeric. However, in the presence of donor solvents (e.g. Ethers, THF, tertiary amines) organomagnesium compounds tend to form complexes with the solvent (Figure 1.37). The co-ordination, be it monomeric, dimeric, etc., seems very dependent on the type of solvent used: e.g. monomeric complexes are obtained when using donor solvents such as THF.[66b,67]
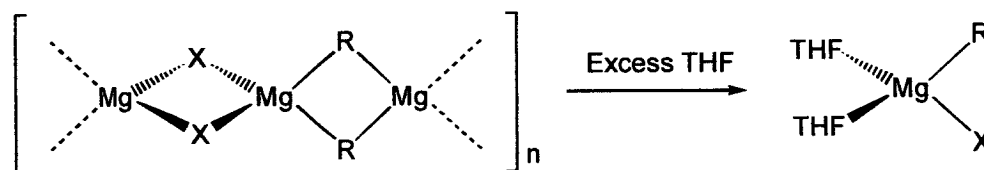
Figure 1.37

Aggregates (dimers) are afforded when Grignard reagents are crystallised from weakly co-ordinating solvents, indicating that the co-ordinating power of the solvent is too poor to break the organomagnesium complexes into monomers.

1.4.3 Relevant Organomagnesium compounds

Grignard reagents that have β-hydrogen atoms tend to convert to alkenes on thermolysis *via* β-hydride transfer (Figure 1.38).[68]
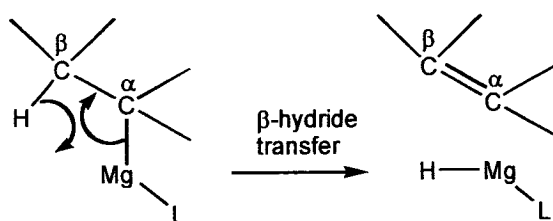
Figure 1.38

This tendency has led our work to concentrate on preparing our Mg complexes with MgMeCl, MgMe$_2$ and Mg(CH$_2$Ph)$_2$ which have no β-hydrogens present.

1.4.3.1 Preparation of MgMeCl (6)

MgRX type Grignard reagents are made by the direct reaction of Magnesium with an organic halide RX in a suitable solvent, usually an ether such as diethyl ether or THF.[69] The reaction is normally most rapid with iodides RI, and iodine may be used as an initiator. For most purposes RMgX reagents are used in situ. However, initially we bought in our supply of MgMeCl which was a 3M solution in THF.

1.4.3.2 Preparation of MgMe₂ (7)

The literature contains various reaction methods for the preparation of MgMe$_2$. [66, 70] According to a review, solvent-free dimethyl magnesium was reported to have been prepared as early as the 1920s. There are essentially three major routes to dimethyl magnesium: 1) transmetallation of magnesium with diorganomercury compounds, 2) the dioxane precipitation method, and 3) the reaction of dimethyl magnesium with methyl lithium (Figure 1.39). Methods 1) and 2) have problems associated with them so we preferentially used method 3). The transmetallation reaction is undesirable due to the toxicity of mercury, and the dioxane method can prove synthetically challenging without a centrifuge, and remaining traces of dioxane could prove problematic in the subsequent chemistry envisaged.

1 Mg   +   HgMe$_2$ ⟶ MgMe$_2$ + Hg ↓

2 MgMeCl + 2 dioxane ⇌ MgMe$_2$ + MgCl$_2$(dioxane)$_2$ ↓

3 MgMeCl   LiMe   ⟶ MgMe$_2$ + LiCl ↓

Figure 1.39

1.4.3.3 Preparation of Mg(CH₂Ph)₂(THF)₂ (8)

Similarly, Mg(CH$_2$Ph)$_2$ can be made by both the dioxane and transmetallation methods with the same synthetic draw backs.[71] The preferred method used is that reported by Schlosser and Hartmann,[71] which initially involves the preparation of the reaction precursor benzylpotassium, *via* the reaction of toluene, ⁿBuLi and KO^{t}Bu (Figure 1.40). The second step of the synthesis is the reaction of the K(CH$_2$Ph) with benzylmagnesiumchloride in THF to produce a yellow/clear solution. The product is

extracted from KCl with ether and worked up to produce $[Mg(CH_2Ph)_2(THF)_2]$(**8**) (Figure 1.40).
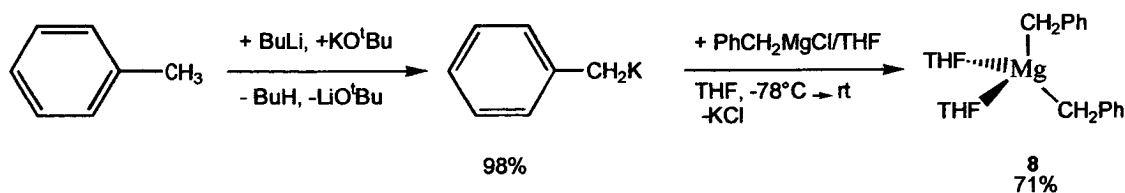
Figure 1.40

1.4.4 The Preparation of Neutral Magnesium Alkyls Supported by {η²-(ⁱPr)₂ATI} and β-dikiminate Bidentate Nitrogen Donor Ligands

It is appropriate to discuss the chemistry that colleagues within our research group have discovered since some reference will be given to their polymerisation activities in Chapter 5 (Figure 1.41). Dr Sylvie Fabre prepared complexes of N-isopropyl-2-(isopropylamino)troponiminate and β-diketiminate ligated methylmagnesium complexes: $[MgMe\{η^2-(^iPr)_2ATI\}_2(THF)]$(**9**),[72] $[Mg(μ-Me)\{η^2-(^iPr)_2ATI\}]_2$ (**10**),[72] $[Mg(μ-OMe)\{η^2-(^iPr)_2ATI\}]_2$ (**11**),[72] $[MgMe\{HC[C(Me)NAr']_2\}(THF)]$ (**12**),[72] $[Mg(μ-Me)\{HC[C(Me)NAr']_2\}]_2$ (**13**),[72] $[MgMe\{HC[C(^tBu)NAr']_2\}(THF)]$(**14**) and $[MgMe\{HC[C(^tBu)NAr']_2\}]$(**15**) (Ar'=2,6-Diisopropylphenyl).[73] Christian Herber prepared the β-diketiminate ligated benzylmagnesium complex: $[Mg(CH_2Ph)\{HC[C(Me)NAr']_2\}(THF)]$(**16**) (Ar'=2,6-Diisopropylphenyl).[74]

Dr Steve Liddle followed on the work started by Christian by synthesising the β-diketiminate ligated benzylmagnesium complexes: $[Mg(CH_2Ph)\{HC[C(Me)NAr']_2\}]$ (**17**), $[Mg(CH_2Ph)\{HC[C(^tBu)NAr']_2\}(THF)]$ (**18**) and $[Mg(CH_2Ph)\{HC[C(^tBu)NAr']_2\}]$ (**19**) (Ar'=2,6-Diisopropylphenyl).[75]
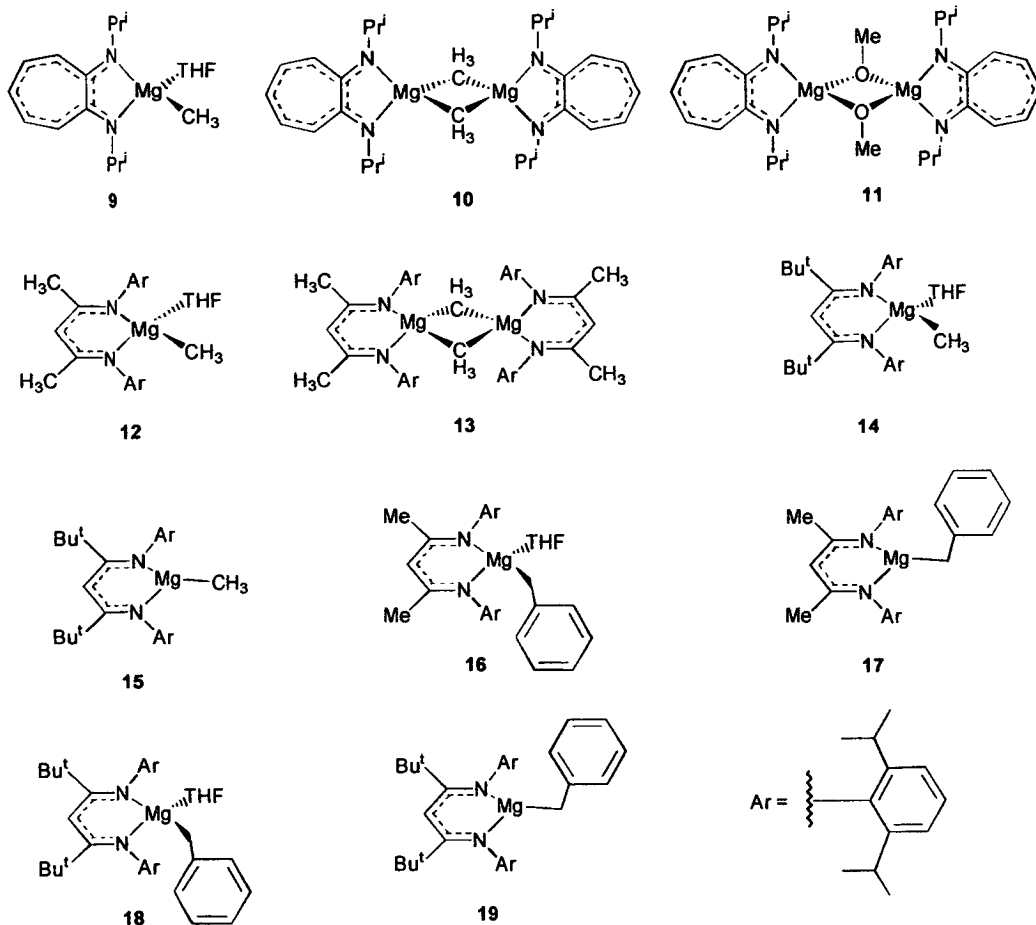
Figure 1.41 Structural formulae of organomagnesium complexes 9-19

1.4.4.1 Preparation of [Mg(η₂-L-X)Me(THF)] Complexes

The chelated methylmagnesium THF solvate complexes **9**, **12** and **14** were prepared by the same reaction method.[72, 73] The corresponding ligand H{(ⁱPr)₂-ATI} or Ar'N=C(R)C(R)=C(Me)NHAr' (Ar'=2,6-Diisopropylphenyl, R= Me or ᵗBu)} was reacted with one equivalent of ⁿBuLi in THF at low temperature with stirring. The reaction mixture was allowed to warm to room temperature and MgMeCl added in a THF solution. The volatiles are removed in vacuum and the product extracted from LiCl into hexane (Figure 1.42).
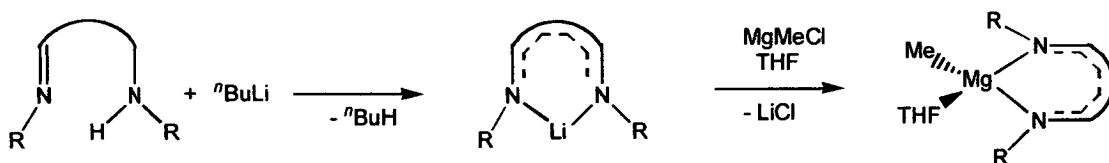
Figure 1.42 Preparation of 9, 12, 14.

Complexes **12**, and **14** can be crystallised from hexane (Figure 1.43). Complex **9** forms an orange oil which cannot be crystallised.
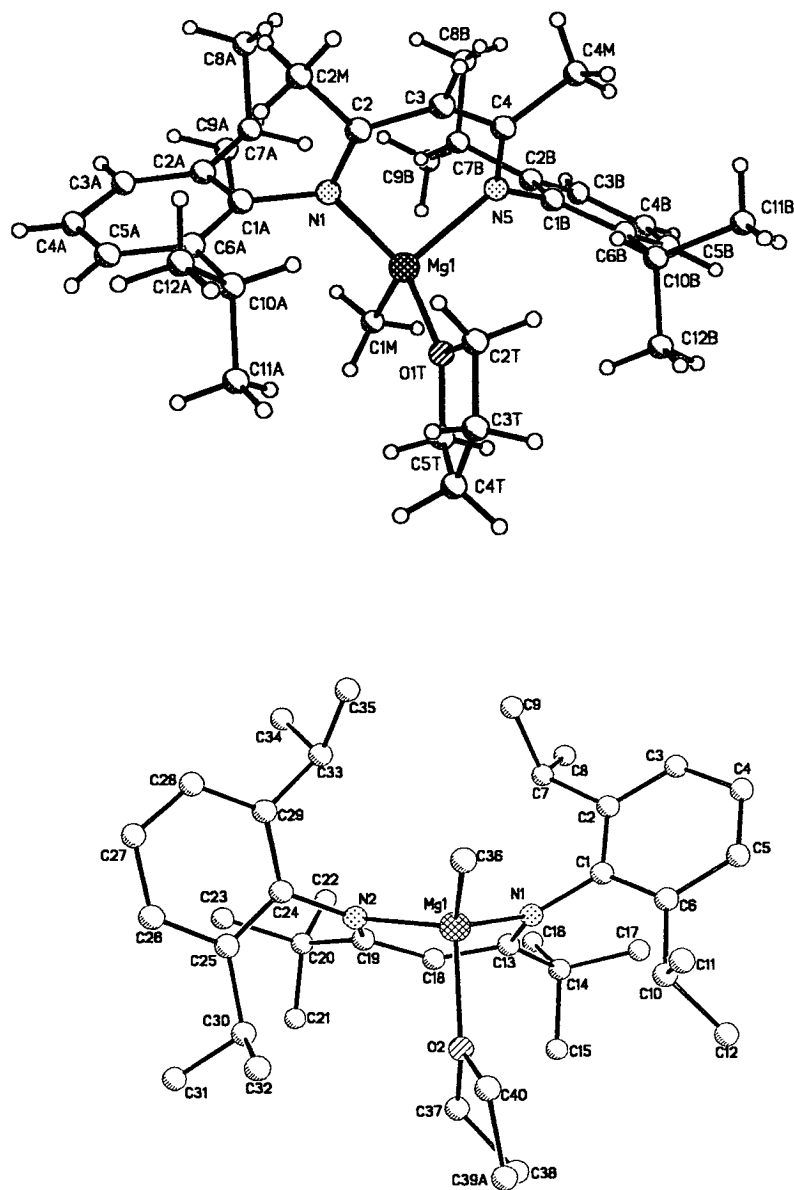
Figure 1.43 Molecular structures of 12 and 14, with atom labelling

Both organomagnesium complexes **12** and **14** are crystallised as 4-coordinate, distorted tetrahedral, THF solvate monomers.

1.4.4.2 Preparation of [Mg(η₂-L-X)(CH₂Ph)(THF)] Complexes

There are two reaction methods to prepare complexes **16** and **18**.

Method 1:

Reaction of Ar′N=C(R)C(H)=C(R)NHAr′ in THF with [Mg(CH₂Ph)₂ (THF)₂] (when R=^{t}Bu reflux is required). Volatiles are removed in vacuum to produce the yellow solid products of complexes [Mg (CH₂Ph){HC[C(R)NAr′]}(THF)] {Ar′=2,6-Diisopropylphenyl, R= Me (**16**) or ^{t}Bu (**18**)}, which can be crystallised in toluene.
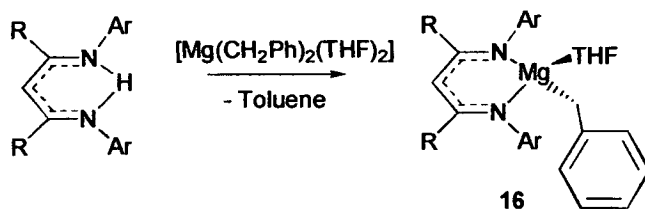
Figure 1.44 Preparation of 16 *via* [Mg (CH₂Ph)₂(THF)₂]
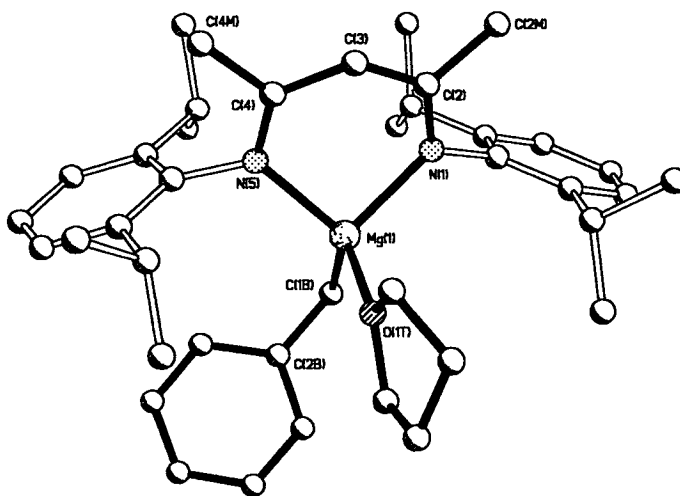
Figure 1.45 Molecular structure of 16.
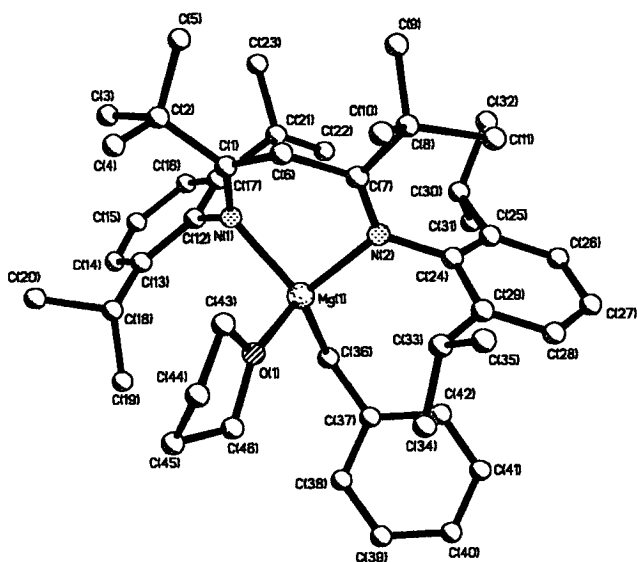
Figure 1.46 Molecular structure of 18.

Method 2:

The corresponding ligand Ar'N=C(R)C(R)=C(Me)NHAr'

(Ar'=2,6-Diisopropylphenyl, R= Me} is reacted with one equivalent of ^{n}BuLi in THF at low temperature with stirring. The reaction mixture is allowed to warm to room temperature and [Mg(CH$_2$Ph)Cl] added in a THF solution. The volatiles are removed in vacuum, and the product extracted from LiCl into toluene. Crystals suitable for X-ray analysis were obtained crystallised from the toluene solution.
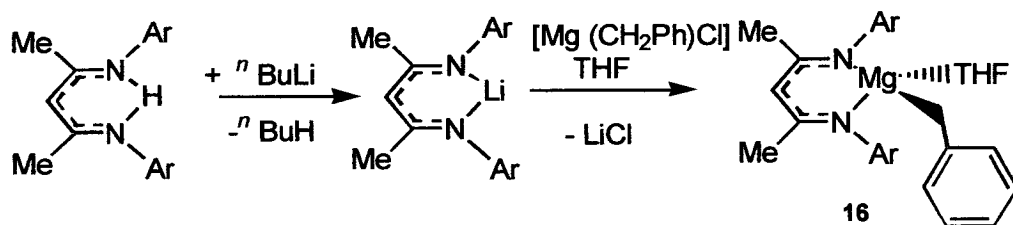
Figure 1.47 Preparation of 16 *via* 1) ^{n}BuLi and 2) [Mg(CH$_2$Ph)Cl].

1.4.4.3 Preparation of Solvent Free Neutral Magnesium Alkyls Supported by {η²-('Pr)₂ATI} and β-dikiminate Bidentate Nitrogen Donor Ligands

In general the solvent free complexes were prepared by heating the corresponding THF solvated complex under vacuum at high temperatures (110-150°C) (Figure 1.48).[73] Both the steric bulk of the ligand and the R' group, contribute to the production of either an alkyl bridged dimeric species or a 3 co-ordinate monomeric species.
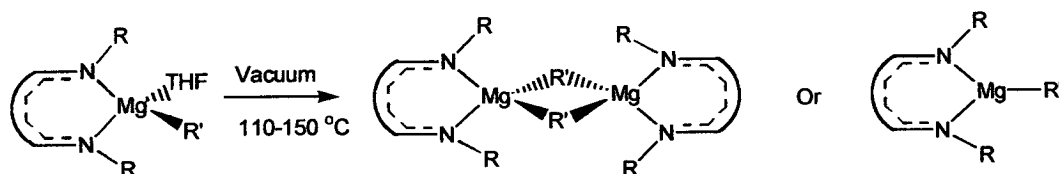
Figure 1.48 Preparation of solvent free neutral magensium alkyl complexes

1.4.4.3a Dimeric Neutral Magnesium Alkyls Supported by {η²-('Pr)₂ATI} and β-dikiminate Bidentate Nitrogen Donor Ligands

Complex **12** produces the dimeric species [Mg(μ-Me)[HC{C(Me)NAr'}₂]]₂ (Ar'=2,6-Diisopropylphenyl) (**13**) in the absence of THF (Figure 1.49).[72] Complex **13** was crystallised in a toluene suspension at room temperature, as **13** is essentially insoluble in most solvents.

Gibson and Segal published a paper in 2000, at the same time as ourselves, on the same work.[76] They prepared the same dimeric species **13** by reacting MgMe₂ with Ar'N=C(R)C(R)=C(Me)NHAr' (Ar'=2,6-Diisopropylphenyl, R= Me) in toluene (i.e. in the absence of a donor ligand). They do not discuss any solubility problems. It may be that with in the baking step, of the synthesis carried out by Dr Fabre, a polymeric product has been produced, and on adding toluene some dimeric species have dissolved to allow crystal formation.
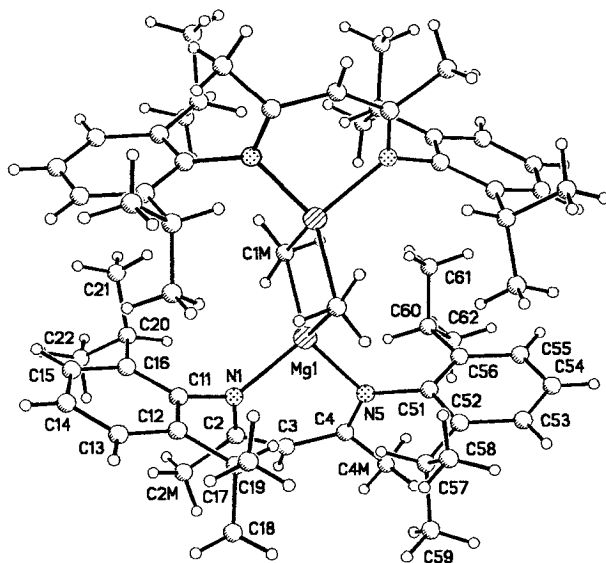
Figure 1.49 Molecular structures of 13 with atom labelling

1.4.4.3b Undetermined Neutral Magnesium Alkyls Supported by {η²-(*i*Pr)₂ATI} and β-diketiminate Bidentate Nitrogen Donor Ligands

Removal of THF from **9** produced an orange powder. Crystals could not be grown, and the compound was presumed to be dimeric (i.e.complex **10**) due to the dimeric nature of the complex **13**. The diketiminate ligand in **13** should provide more steric bulk around the magnesium than the troponiminate and the diketiminate complex is dimeric. Also the corresponding methoxy magnesium complex

[Mg(μ-OMe){η²-(*i*Pr)₂ATI}]₂ (**13**) is dimeric, bridged by two μ-OMe groups.[73]

The product produced from heating the orange oil **16** in vacuum has only been characterised *via* NMR spectroscopy. The NMR spectra indicate the total removal of THF, and a lack of asymmetry of the benzyl aryl signals. Therefore there are no hapto interactions occurring between the magnesium and the aromatic ring. There is no evidence, in the absence of a crystal structure or low temperature NMR, to suggest whether the complex is dimeric or monomeric (**15**).

1.4.4.3c Monomeric Neutral Magnesium Alkyls Supported by {η²-(ⁱPr)₂ATI} and β-dikiminate Bidentate Nitrogen Donor Ligands

Both complexes **14** and **18** produce the monomeric species

[MgR{HC[C(ᵗBu) NAr']₂}] (Ar'=2,6-Diisopropylphenyl, R= Me (**15**), R=ᵗBu (**19**))

respectively, in the absence of THF. Crystals suitable for X-ray study were grown by

sublimation at 150°C (10⁻² Torr) (Figures 1.50 and 1.51).
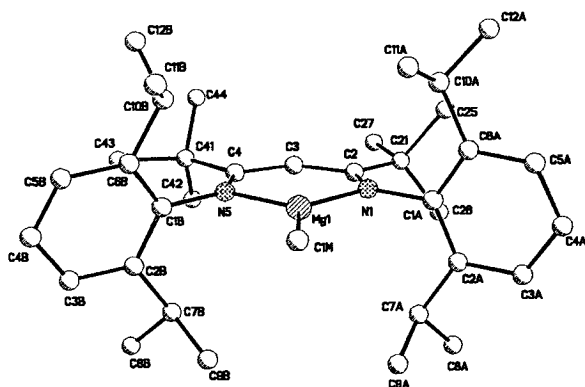
Figure 1.50 Molecular structure of 15 with atom labelling; hydrogen atoms are omitted for clarity.
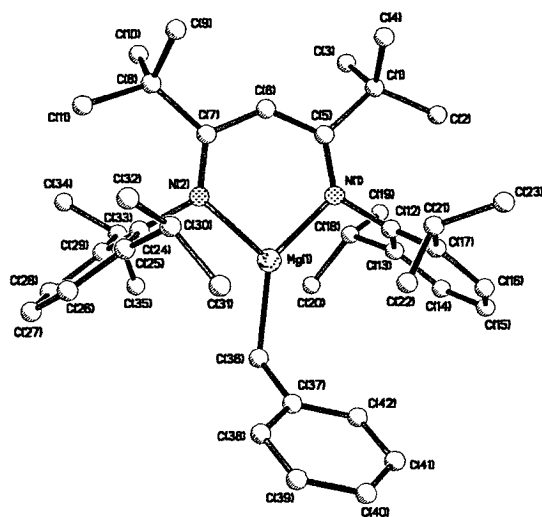
Figure 1.51 Molecular structure of 19 with atom labelling; hydrogen atoms are omitted for clarity.

Clearly the steric bulk of the ^{t}Bu groups (c.f. Me) in the 1,3 position on the ligand backbone is sufficient to produce the desired 3-coordinate monomeric species. In the case of the benzyl species, it was expected that removal of the THF molecule may result in η^2 or η^3 co-ordination of the benzyl ring to the magnesium. However, a space filling model of the complex clearly illustrates that the bulkyl iso-propyl groups prevent the close approach of the benzyl groups, so such interactions cannot exist.

Comparison of the crystal structure data for the magnesium complexes (Table 1.7) where R=Me and ^{t}Bu groups in the 1, 3-positions on the ligand backbone clearly displays:

1) Larger C(5)-N(1)-C(1) and C(6)—N(2)-C(3) angles (Figure 1.52) when R = ^{t}Bu in comparison to Me, indicating the forcing of the aromatic groups toward the magnesium by the backbone ^{t}Bu groups.

2) Larger Mg-O bond lengths in the THF adduct complexes (**14** and **18**) where R= ^{t}Bu (c.f. **12** and **16**) due to the increased congestion of the active site.

3) Shorter Mg-C and Mg-N bond lengths in the THF free complexes **15** and **19**, due to the increase in electronic unsaturation at Mg, and the increased donation of the β-diketiminate ligand.

4) Shorter ipso-carbon-N-Mg angles [e.g.C(6)-N(2)-Mg(1) and C(5)-N(1)-Mg(1)] in the THF free complexes **15** and **19**, indicating the increase in the steric shielding of the Mg-R unit by the nitrogen substituent groups.
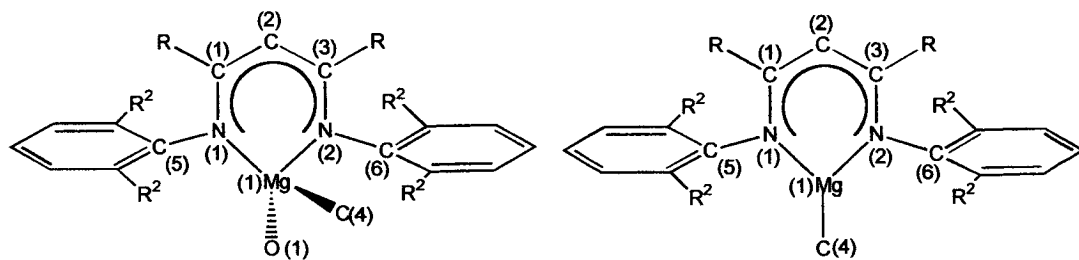
Figure 1.52 Selected atom labelling key for table 1.7

Coordination	4 co-ord	4 co-ord	4 co-ord	4 co-ord	3 co-ord	3 co-ord
R	Me	^{t}Bu	Me	^{t}Bu	^{t}Bu	^{t}Bu
Complex	**12**	**14**	**16**	**18**	**15**	**19**
Mg(1)-C(4)	2.107 (6)	2.189 (4)	2.1325 (18)	2.149 (3)	2.077 (2)	2.122 (4)
Mg(1)-O(1)	2.066 (4)	2.097 (3)	2.0333 (13)	2.068 (2)	-	-
Mg(1)-N(2)	2.061 (5)	2.083 (3)	2.0484 (15)	2.062 (3)	2.0163 (18)	2.017 (3)
Mg(1)-N(1)	2.063 (5)	2.063 (3)	2.0575 (15)	2.070 (3)	2.0137 (17)	2.015 (3)
C(6)-N(2)-C(3)	117.7 (4)	122.8 (3)	119.45 (14)	124.7 (3)	125.92 (16)	108.09 (19)
C(5)-N(1)-C(1)	119.6 (4)	125.9 (3)	118.71 (13)	124.3 (3)	125.44 (15)	129.1 (3)
N(1)-Mg(1)-N(2)	93.09 (18)	94.51 (12)	93.29 (6)	95.03 (11)	95.68 (8)	93.91 (11)
N(1)-Mg(1)-C(4)	119.5 (2)	121.05 (13)	117.35 (7)	120.06 (13)	129.68 (8)	137.84 (16)
N(2)-Mg(1)-O(1)	105.12 (16)	103.93 (11)	105.43 (6)	103.89 (11)	-	-
C*5)-N(1)-Mg(1)	118.6 (3)	115.1 (2)	120.57 (10)	117.6 (2)	110.91(11)	105.89 (19)
C(6)-N(2)-Mg(1)	121.1 (3)	122.8 (3)	119.45 (10)	119.0 (2)	110.02 (11)	108.09 (19)
N(2)-Mg(1)-C(4)	124.7 (2)	125.11 (4)	121.78 (7)	119.75 (12)	129.68 (8)	127.84 (16)

Table 1.7 Selected bond lengths and angles for 12-16, 18 and 19.

From the paper published by Gibson and Segal, it is also clear that the steric bulk of the R group, bonded to the magnesium centre, also affects the coordination mode produced i.e.monomeric, dimeric, etc. They prepared the coordinatively unsaturated monomeric complex [Mg(^{t}Bu){HC[C(Me) NAr']$_2$}] (Ar'=2,6-Diisopropylphenyl) (**20**), by the reaction of Ar'N=C(Me)C(H)=C(Me)NHAr' (Ar'=2,6-Diisopropylphenyl) with Mg^{t}Bu$_2$ etherate in toluene. Crystals suitable for X-Ray analysis were crystallised from pentane. Clearly the adoption of the monomeric geometry is due to the change in R from Me to ^{t}Bu, and is a steric effect in the absence of a coordinating solvent. They observed no significant perturbation of either the bond lengths or bite angles within the six-membered C$_3$N$_2$Mg chelate ring on comparison of **20** with **13** and the 4-coordinate etherate solvate complex of **20**.

1.4.5 The Oxygenation of Organomagnesium Compounds

When exposed to oxygen organomagnesium (Grignard) compounds are thought to undergo a two stage process 1) oxidation followed by 2) metathesis (Figure 1.53).[77]

$$RMgX + O_2 \longrightarrow ROOMgX \qquad \text{Oxidation}$$

$$ROOMgX + RMgX \longrightarrow 2\,ROMgX \qquad \text{Metathesis}$$
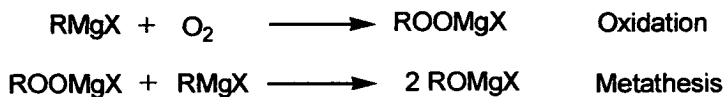
Figure 1.53

The initial oxidation step is thought to be radical in nature, in comparison the metathesis stage is not. The generation of the peroxide species may result from a radical chain reaction similar to that of the autoxidation of a hydrocarbon (Figure 1.54).[77]

$$\dot{R} + O_2 \longrightarrow ROO^{\bullet} \xrightarrow{\ RMgX\ } ROOMgX + \dot{R}$$
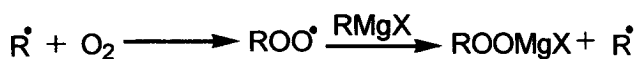
Figure 1.54

Bailey et al report NMR evidence of the initial formation of a methyl peroxide species[(^{i}Pr$_2$-ATI)Mg(THF)(OOMe)] on treatment of **9** with oxygen under controlled conditions, before decomposition to the methoxy bridged dimer **11** (Figure 1.55).[72]
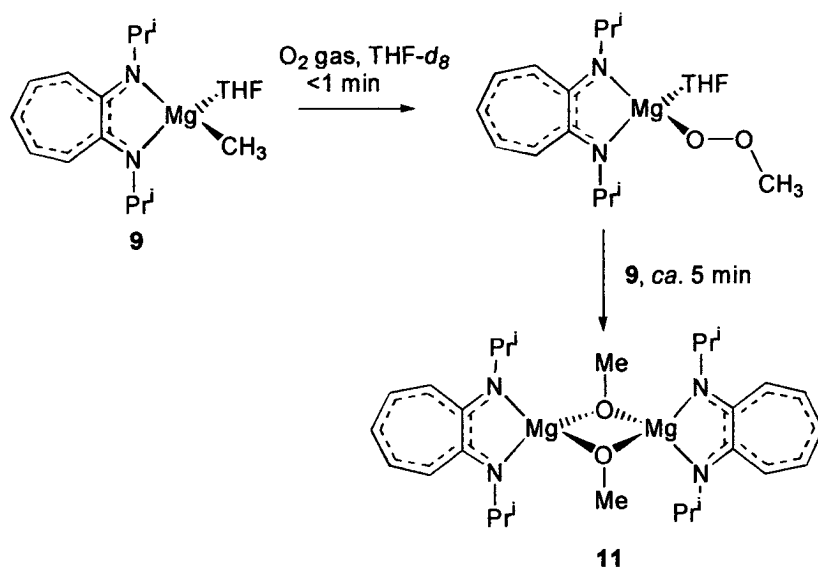
Figure 1.55

Since then Herber and Liddle, from the Bailey group, have provided the first structural characterisation of an alkyl peroxide complex of magnesium.[78] Reaction of **16** with pre-dried oxygen, in toluene, afforded an off-white precipitate. The volatiles were removed in vacuum and the resulting orange oil extracted into n-hexane, on concentration, colourless crystals of co-crystallised $[HC\{C(CH_3)NAr'\}_2Mg(\mu\text{-}\eta^2\text{:}\eta^1\text{-}OOBz)]_2$ (**21**) and $[HC\{C(CH_3)NAr'\}_2Mg(\mu\text{-}OBz)]_2$ (**22**) were produced (Figure 1.56).
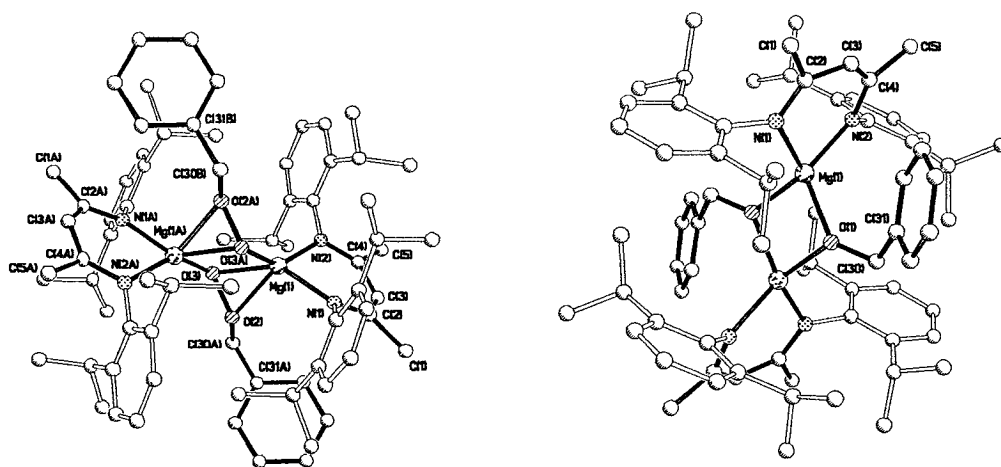
Figure 1. 56 Structures of $[HC\{C(CH_3)NAr'\}_2Mg(\mu\text{-}\eta^2\text{:}\eta^1\text{-}OOBz)]_2$ **(21) and** $[HC\{C(CH_3)NAr'\}_2Mg(\mu\text{-}OBz)]_2$ **(22) with selected atom labelling; hydrogen atoms are omitted for clarity.**

The two step mechanism suggested by Garst was confirmed by the addition of the appropriate amount of **16** to the mixture of **21** and **22**, with the clean and total conversion to **22**.

1.5 Project Aim

The aim of our research was to prepare neutral alkyl magnesium complexes chelated by nitrogen donor ligands (e.g. amines or diimines). These neutral complexes could then be activated to produce cationic magnesium alkyl complexes, and the polymerisation activity of these cationic complexes investigated. We were interested in the preparation of:

1) neutral amine magnesium alkyl complexes and their activation with **3**, **4** and **5**; Chapter 2 (Figure 1.57).

$$\text{Amine} + \text{MgXR} \longrightarrow \text{AmineMgXR} \xrightarrow[-X]{\text{Activator}} [\text{AmineMgR}]^{\oplus}$$

Figure 1.57

2) neutral magnesium alkyl diimine complexes; Chapter 3 (Figure 1.58)
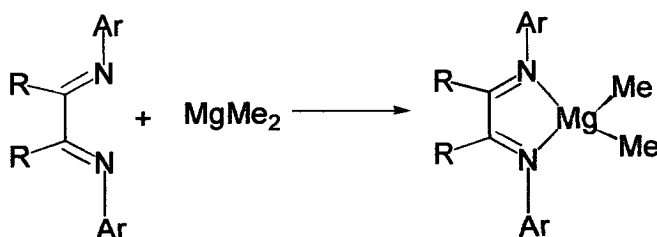
Figure 1.58

3) neutral magnesium alkyl bis(iminodiphenylphosphorano)methane complexes Chapter 4; (Figure 1.59)
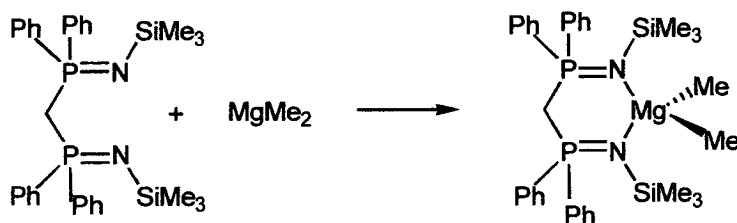
Figure 1.59

Some ethene polymer studies of the compounds produced by these studies, and some colleagues compounds discussed in this chapter, are addressed in chapter 5.

1.6 References

1   Danner, H.; Braun, R., *Chem.Soc.Rev.*, 1999, **28**, 395-405.

2   Elschenbroich, C.; Salzer, A., Organometallics, **1989**, 77,VCH publishers.

3   Baird, M.C., *Chem.Rev.*, **2000**, *100*, 1471-1478.

4   Elschenbroich, C.; Salzer, A., Organometallics, **1989**, 423-424,VCH publishers.

5   Cossee, P., *Tetrahedron Lett.*, **1960**, *17*, 12-16.

6   Cotton and Wilkinson, Advanced Inorganic Chemistry, **1980**, 4th Ed, 1280-1281, Wiley and Sons Inc.

7   Chen; E.Y.X; Marks, T.J., *Chem.Rev.*, **2000**; *100*; 1391-1434.

8   Horton, A.D.; De With, J.; Van der Linden, A.J.; Van de Weg, H., *Organomet.*, **1996**; *15*; 2672-2674.

9   Chien, J.C.W.; Tsai, W.M.; Raush, M.D., *J.Am.Chem.Soc.*, **1991**, *113*, 8570.

10 Bochmann, M., *J.*Chem.Soc., *Dalton Trans.*, **1996**, 255-270.

11 Pellechia, C.; Immirzi, A.; Pappalardo, D.; Peluso, A., *Organometallics*, **1994**, *13*, 3773-3775.

12 Pellechia, C.; Grassi, A.; Immirzi, A., *J.Am.Chem.Soc.*, **1993**, *115*, 1160-1162.

13 a) Massey, A.G.; Park, A.J., *J.Organomet.Chem.*, **1966**; *5*; 218-225; b) Massey, A.G.; Park, A.J., *J.Organomet.Chem.*, **1964**; *2*; 245-250.

14 Gomez, R.; Green, M.L.H.; Haggit, J.L, *J.Chem.Soc., Chem.Comm*, 1994; 2607.

15 Bochmann, M.; Sarsfield, M.J, *Organomet.*, **1998**; *17*; 5908-5912.

16 Belgardt, T.; Storre, J.; Roesky, H.W.; Noltemeyer,M.; Schmidt, H., *Inorg.Chem.*, **1995**, *34*, 3821-3822.

17 Tschoerner, M.; Pregosin, P.S., *Organomet.*, **1999**; *18*; 670-678.

18 Qian, B.; Ward, D.L.; Smith, M.R., *Organomet.*, **1998**; *17*; 3070.

19 King, W.A.; Scott, B.L., Eckert, J.; Kubas, G.J., *Inorg.Chem.*, **1999**; *38*; 1069.

20 Pindado, G.J, Lancaster, S.J.; Thornton-Pett, M.; Bochmann, M., *J.Am.Chem.Soc.*, **1998**, 120, 6816-6817.

21 Scollard, J.D.; McConville, D.H.; Rettig, S.J., *Organomet.*, **1997**, *16*, 1810-1812.

22 Uhrhammer,R.; Black, D.G.; Gardner,T.G.; Olsen, G.D.; Jordan, R.F., *J.Am.Chem.Soc.*, **1993**, 115, 8493-8494.

23 Theopold, K.H., *Eur.J.Inorg.Chem.*, **1998**, 15-24.

24 Johnson, L.K.; Killian, C.M., Brookhart, M., *J.Am.Chem.Soc.*, **1995**, 117,6414-6415.

25 Watson,P.L.; Parshall, G.W., Acc.Chem.Res., **1985**, *107*, 8091-8103

26 Coles, M.P.; Jordan, R.F., *J.Am.Chem.Soc.*, **1997**, *119*,8125-8126.

27 Breslow, D.S; Newberg, N.R., *J.Am.Chem.Soc.*, **1957**, *79*, 5072-5073.

28 Natta, G.; Pino, P.; Mazzaanti, G.; Giannini, U., *J.Am.Chem.Soc.*, **1957**, 79, 2975-2976.

29 a) Reichert, K.H.; Meyer, K.R., *Makromol. Chem.*, **1973**, *169*, 163; b) long, W.P.; Breslow, D.S., Liebigs.Ann.Chem., **1975**, 463.

30 Andersen, A.A.; Cordes, H.G.; Herwig, J.; Kaminsky, W.; Merck, A.; Mottweiler, R.; Pein, J.; Sinn, H.; Vollmer, J., *Angew.Chem.*, **1976**, *88*, 698; Angew.Chem.Ed.Engl., **1976**, *15*, 630.

31 Whyman, R.; Iggo, J., Catalysis Fundamentals and Practice Course, Leverhulme Centre, University of Liverpool, **2001**.

32 Britovsek, G.P.; Gibson, V.C.; Wass, D.F., *Angew.Chem.Int.Ed.*, **1999**, *38*, 429-447

33 Hlatky, G.G., *Coordn.Chem.Rev.*, **2000**, *199*, 235-329.

34 McKnight, A.L.; Waymouth, R.M., *Chem.Rev.*, **1998**, *98*, 2587-2598.

35 Britvsek, G.J.P.; Mastroianni, S.; Solan, G.A.; Baugh, S.P.D.; Redshaw, C.; Gibson, V.C.; White, A.J.P.; Williams, D.J.; Elsegood, M.R.J., *Chem.Eur.J.*, **2000**, *6*, 2221-2231.

36 Zefirova, A.K.; Shilov, A.E., *Dokl.Akad.Nauk.SSSR*, **1961**, *136*, 599-602.

37 Shapiro, P.J.; Cotter, W.D.; Schaefer, W.P.; Labinger, J.A.; Bercaw, J.E., *J.Am.Chem.Soc.*, **1994**, *116*, 4623-4640.

38 Fryzuk, M.D.; Giesbrecht, G.; Rettig, S.J., *Organometallics*, **1996**, *15*, 3329-3336.

39 Mitchell, J.P.; Hajela, S.; Brookhart, S.K.; Hardcastle, K.I.; Henling, L.M.; Bercaw, J.E., *J.Am.Chem.Soc.*, **1996**, *118*, 1045-1053.

40 Coughlin, E.B.; Bercaw, J.E., *J.Am.Chem.Soc.*, **1992**, *114*, 7606-7607.

41 Yasuda, H.; Ihara, E., *Tetrahedron*, **1995**, *51*, 4563-4570.

42 Yuan, F.; Shen, Q.; Sun, J., *J.Organomet.Chem.*, **1997**, *538*, 241.

43 Jeske, G.; Lauke, H.; Mauermann, H.; Swepston, P.N.; Schumann, H.; Marks, T.J., *J.Am.Chem.Soc.*, **1985**, *107*, 8091-9103.

44 Watson, P.L.; Parshall, G.W., *Acc.Chem.Res.*, **1985**, *18*, 51.

45 Evans, W.J.; Forrestal, K.J.; Ziller, J.W., *Angew.Chem.Int.Ed.Engl.*, **1997**, *36*, 774.

46 Soga, K.; Yamamoto, S; Inematsu, K., *Jpn.Laid-Open Appl.*, 09/272710, **1997**, Chem.Abstr.127: 331944.

47 Tinkler, S.; Deeth, R.J.; Duncalf, D.J.; McCamley, A., *Chem.Commun.*, **1996**, 2623.

48 Cloke, F.G.N.; Geldbach, T.J.; Hitchcock, P.B.; Love, J.B., *J.Organomet.Chem.*, **1996**, *506*, 343-345.

49 Sheppard Jr., L.H., *Ger.Offen.*, 2008602, **1970**, [Chem.Abstr., 1971, 74, 13256]

50 Kim, J.S.; Wojcinski, L.M.; Liu, S.; Sworen, J.C.; Sen, A., *J.Am.Chem.Soc.*, **2000**, *122*, 5668-5669

51 Duchateau, R.; Meetsma, A.; Teuben, J.H., *Chem.Commun.*, **1996**, 223-224.

52 Coles, M.P.; Jordan, R.F., *J.Am.Chem.Soc.*, **1997**, *119*, 8125-8126.

53 Bruce, M.; Gibson, V.C.; Redshaw, C.; Solan, G.A.; White, A.J.P.; Williams, D.J., *Chem.Commun.*, **1998**, 2523-2524.

54 Ihara, E.; Young, V.G.; Jordan, R.F., *J.Am.Chem.Soc.*, **1998**, *120*, 8277-8278

55 Radzewich, C.E.; Coles, M.P.; Jordan, R.F., *J.Am.Chem.Soc.*, **1998**, *120*, 9384-9385.

56 Krolev, A.V.; Guzei, I.A.; Jordan, R.F., *J.Am.Chem.Soc.*, **1999**, *121*, 11605-11606.

57 Bundens, J.W.; Yudenfreund, J.; Francl, M.M., *Organometallics*, **1999**, 18, 3913-3920.

58 Talarico, G.; Budzelaar, P.H.M., *Organometallics*, **2000**, *19*, 5691-5695.

59 Radzewich, C.E.; Guzei, I.A; Jordan, R.F., *J.Am.Chem.Soc.*, **1999**, *121*, 8673-8674.

60 Dagorne, S.; Guzei, I.A.; Coles, M.P.; Jordan, R.F.; *J.Am.Chem.Soc.*, **2000**, *122*, 274-289.

61 Korolev, A.V.; Ihara.E, Guzei, I.A., Young, V.G, Jr.; Jordan, R.F., *J.Am.Chem.Soc.*, **2001**, *123*, 8291-8309.

62 Bochman, M.; Sarsfield, M.J., *Organometallics*, **1998**, *17*, 5908-5912.

63 Klosin, J.; Roof, G.R.; Chen, E.Y.X., *Organometallics*, **2000**, *19*, 4684-4686.

64 H.E.Podall, W.E.Foster, *J.Org Chem*, 1958, **23**, 1848.

65 Sen, A.; Kim, J.S., *International publication.*, WO0073359, **2000**, [Application Number: WO2000US15117 2000602]

66 a) Weiss, E., *J. Organomet. Chem.*, **1964**, *2*, 314-321.b) Pinkus, A.G., *Coordn.Chem.Rev.*, **1978**, *25*, 173-197.

67 Cotton and Wilkinson, Advanced Inorganic Chemistry, **1980**, 4th Ed, 286, Wiley and Sons Inc.

68 Elschenbroich, C.; Salzer, A., Organometallics, **1989**, 198,VCH pubishers;

69 a) Ramsden, H.E.; Balint, A.E, Whitford, W.R.; Walburn, J.J.; Cserr, R., *J.Org.Chem.*, **1957**, *22*, 1202; b) Gilman,; Heck, *J. Am. Chem. Soc.*, **1930**, *52*, 4949; c) Johnson, G.; Adkins, *J. Am. Chem. Soc.*, **1931**, *51*, 1520-1523.

70 a) Ashby, E.C.; Arnott, R.C., *J. Organomet. Chem.*, **1968**, *14*, 1-11; b) Kamienski, C.W.; Eastham, J.F., *J. Org. Chem.*, **1969**, *34*, 1116-1121; c) Ziegler, V.K.; Nagel, K.; Patheiger, M., *Z.Anorg.Allg.Chemie.Bd.* , **1955**, *282*, 345-351; d) Kamienski, C.W. ; Eastham, J.F., *J.Organomet. Chem.*, **1967**, *8*, 542-546.

71 a) Pocker, Y.; Exner, J.H., *J. Am. Chem. Soc.*, **1968**, *90*, 6764-6765; b) Schrock, R.R., *J.Organomet. Chem.*, **1976**, *122*, 209-225; c) Baker, K.V.; Brown, J. M.; Hughes, N.; Shamulis, A.J.; Sexton, A., *J. Org. Chem.*, **1991**, *56*, 698-705.

72 Bailey, P.J.; Dick, C.M.E.; Fabre, S.; Parsons, S., *J.Chem.Soc., Dalton Trans.*, **2000**, 1655.

73 Bailey, P.J.; Coxall, R.A.; Dick, C.M.E.; Fabre, S.; Parsons, S., *Organometallics.*, **2001**, 20, 798.

74 Herber, C.; *Project report*, C.O. Bailey, P.J.; Department of Chemistry, University of Edinburgh, July *2000*.

75 Liddle, S.; *End of grant report*, C.O. Bailey, P.J.; Department of Chemistry, University of Edinburgh, Sept **2001**.

76 Gibson, V.C.; Segal, J.A.; White, A.J.P.; Williams, D.J., *J. Am. Chem. Soc.*, **2000**, *122*, 7120-7121.

77 a) Davies, A.G., *J.Organomet.Chem.*, **1980**, *200*, 87-99; b) Garst, J.F.; Smith, C.D.; Farrar, A.C., *J.Am.Chem.Soc.*, **1972**, 7707-7710; c) Walling, C.; Cioffari, A., *J.Am.Chem.Soc.*, **1970**, 6609-6611; d) Lamb, R.C.; Ayres, P.W.; Toney, M.K.; Garst, J.F., *J.Am.Chem.Soc.*, **1966**, 4261-4262.

78 Bailey, P.J.; Herber, C.; Liddle, S.; Parsons, S.; *in press*.

CHAPTER TWO COMPLEXATION AND ACTIVATION OF MAGNESIUM ALKYLS WITH SIMPLE AMINES

2.1 Active Amine/Amide Based Transition Metal Catalyst Systems

As discussed in Chapter one there are several reviews that describe the progress of developing families of transition metal based alkene polymerisation catalysts. Amine and amide based systems have been moderately studied in comparison to other ligand based systems (e.g. Cp and diimine). Examples of some pro-catalyst systems studied are given in Figure 2.01. These include mixed amine/amide systems (**1-2**), amide ligand systems (**3-6**) and amide ligands containing Cp groups (**7-8**).[1,2]
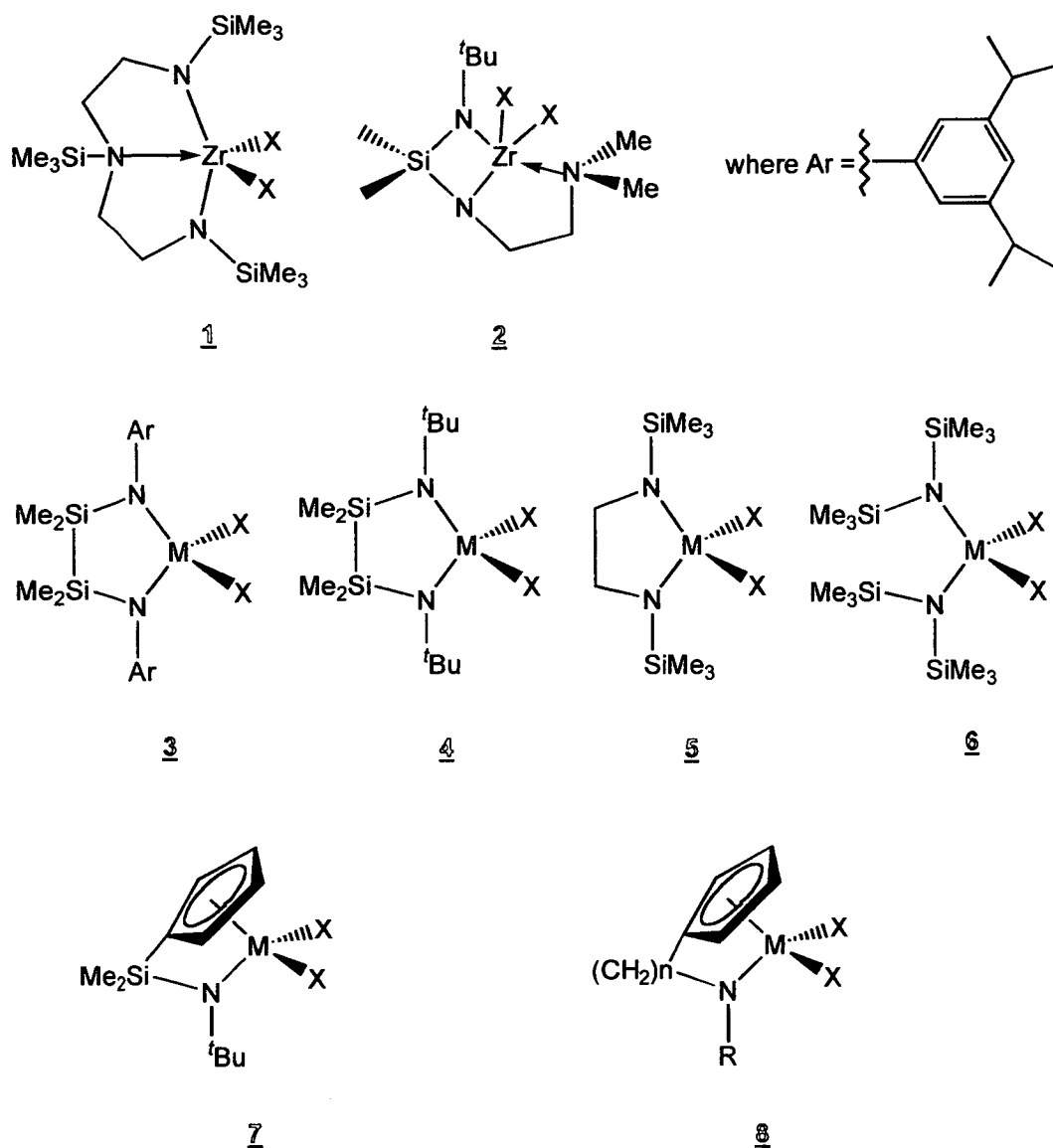
Figure 2.01 Examples of some amine/amide based transition metal alkene polymerisation pro-catalysts discussed in the literature

Mixed amine/amide ligated complexes 1 and 2 have significantly different activities for alkene polymerisation.[1] Complexes of type 1 where X= Me or CH_2Ph when activated with $B(C_6F_5)_3$ rapidly polymerise a 20-fold excess of ethene in less than 5 mins at 20°C. However reaction of 20 equiv. of propene is much slower under the same conditions. Complex 2 is inactive in the polymerisation of 1-hexene.

The use of monodentate amide ligands has also been reported, e.g as in 3 and 6.[1, 3] The zirconium complex of 3 (Figure 2.01), in the presence of MAO cocatalyst, has a moderate activity of 13 g mmol^{-1}h^{-1}bar^{-1}. Complexes of 6 (where X=CH_2Ph) activated by either $B(C_6F_5)_3$ or $[NHMe_2Ph][B(C_6F_5)_4]$ produce catalysts that are highly active for both ethene and propene polymerisation, e.g 6 activated with $[NHMe_2Ph][B(C_6F_5)_4]$ affords polyethene at a rate of 34 000 g mol^{-1}bar^{-1}h^{-1}.[16] The use of bidentate bis-amide ligands has also been reported, e.g as in 4 and 5.[1, 3]

Complex 4 contains a di-silicon backbone, the silicon removes electron density from the metal centre in comparison to the carbon back-boned ligand in 5, and it is observed that complex 4 is considerably more active i.e. 100 g mmol^{-1}bar^{-1}h^{-1}.

The incorporation of ligands containing both amide and Cp functionalities were developed to form hybrid "half metallocene, constrained geometry" catalysts. These systems are highly active e.g. Complexes of type 7, where M=Ti and X=CH_2Ph) typical activities include 1500 gmmol^{-1}bar^{-1}h^{-1}.

2.2 Reported Amine Complexed Organomagnesium Complexes

During a review of the crystal structures reported for amine complexed organomagnesium complexes it was observed that in general the complexes are monomeric, unless in the presence of a good bridging group (e.g. Cl).[4-13] The products were prepared in the presence of potential co-ordinating solvents, such as THF or diethyl ether, however the complexes produced are solvent free. Several four co-ordinate complexes of the type $[Mg(\eta^2$-TMEDA)R_2]$ [R= ^sBu (9),[14] Ph (10),[15] Me (23),[4,12] Et (11),[4] and C_7H_{11}[5] (13)) have been reported, which were prepared from the reaction of TMEDA with MgR_2 (Figure 2.02). The five co-ordinate complex $[Mg(\eta^3$-PMDETA)Me_2]$ (24) is formed by the complexation of $MgMe_2$ (7) with the tridentate ligand pentamethyldiethylenetriamine (PMDETA).[4] The dimeric mono(amido) μ-NR_2 bridged species $[Mg\{N(CH_2Ph)_2\}_2]$ (20) has been prepared by

reaction of MgBu$_2$ with two equivalents of dibenzylamine in toluene.[9] The mono(amido)magnesium complex [Mg(^{n}Bu)(CH$_2$CH$_2$NMe$_2$)(CH$_2$Ph)]$_2$ (21) can be prepared from the reaction of a 1:1 molar ratio of ^{n}BuMgCl with [{PhCH$_2$(Me$_2$NCH$_2$CH$_2$)N}Li]$_n$ in a hexane THF mixture.[10] Reaction of a Grignard (containing Cl) e.g. allylmagnesium chloride, with TMEDA produced a five co-ordinate chloride bridged dimer [Mg(η^2-TMEDA)(μ-Cl)(η^1-CH$_2$=CHCH$_2$)]$_2$ (14).[6] A selection of crystal data obtained for the complexes shown in Figure 2.02 can be observed in Table 2.01.
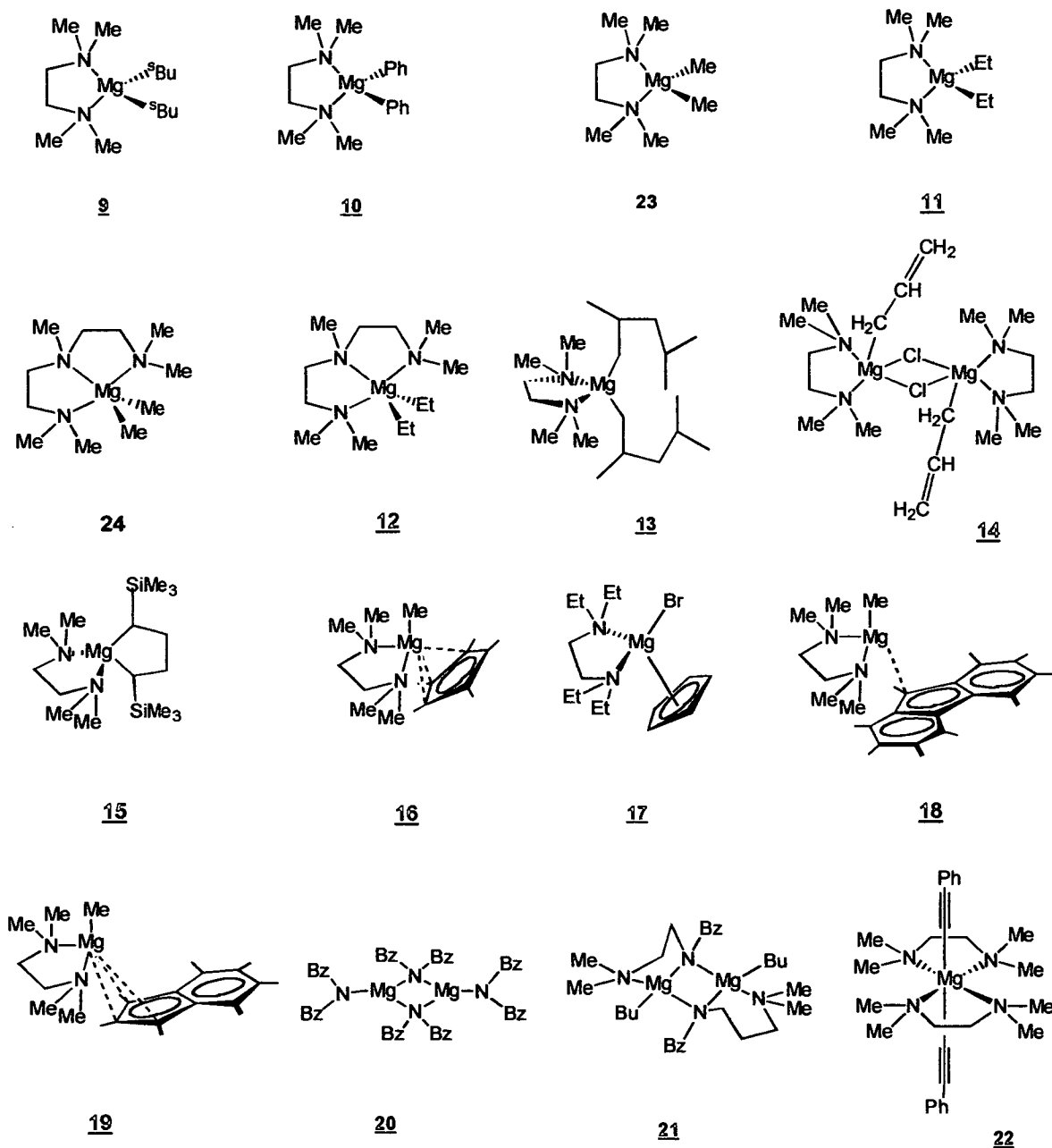
Figure 2.02 Reported amine complexed organomagnesium complexes

Complex	Ref	Mg-N	Mg-C	N-C	C-C
9	14	2.252 (3)	2.181 (3)	1.470 (5)	1.505 (9)
10	15	2.205 (3) 2.199 (3)	2.167 (3) 2.167 (3)	1.458 (6) 1.463 (6)	1.365 (9)
11	4	2.236 (5)	216.3 (6)	.	1.538 (10)
12	4	2.371 (6) 2.365 (6) 2.362 (6)	2.223 (9) 2.174 (7)		1.412 (14) 1.517 (11)
13	5	2.202 (12)	2.179 (15)	1.475 (20)	1.48 (5)
14	6	2.285 (2) 2.211 (2)	2.179 (3)		
15	7	2.17 (1) 2.213 (7)	2.200 (9) 2.191 (9)		
16	8	2.256 (2) 2.290 (2)	2.130 (3)		
17	16	2.269 (5) 2.230 (5) 2.259 (5) 2.218 (5)		1.501 (8) 1.462 (8) 1.480 (9) 1.478 (9)	1.48 (1) 1.46 (1)
18	17	2.1806 (19)	2.120 (2)		
19	17	2.2415 (16) 2.2008 (18)	2.115 (3)		
20	9	2.077 (2) 1.935 (2)			
21	10	2.113 (2)	2.135 (2)	1.502 (3) 1.463 (3)	1.507 (4)
22	11	2.375 (3)	2.176 (6) 2.220 (6)	1.519 (10) 1.492 (11)	1.492 (11)
23	4, 12	2.257 (6) 2.227 (6)	2.166 (6) 2.166 (6)	1.488 (7) 1.480 (11)	1.570 (14)
24	4	2.346 (3) 2.381 (3) 2.351 (3)	2.191 (4) 2.173 (4)		

Table 2.01 A selection of bond lengths for the amine based organomagnesium complexes given in figure 2.02.

2.3 Preparation of Amine Magnesium Dimethyl Complexes

2.3.1 Synthesis of Dimethyl Magnesium Amine Complexes

The preparation of complexes $[Mg(\eta^2\text{-TMEDA})R_2]$ (**23**), $[Mg(\eta^3\text{-PMDETA})Me_2]$

(**24**) and $[Mg(\eta^2\text{-TEEDA})Me_2]$ (**25**) is trivial (Figure 2.03). They are synthesised by

direct complexation of the commercially available amine with $MgMe_2$ (**7**), in either

Et_2O or THF at ambient temperature. Subsequent removal of the solvent in vacuum

leaves the product, in good yield (77-87%) in the form of a white powder which can

be crystallised from either hexane, Et_2O, etc., depending on the particular complex.

The crystal structures of $[Mg(\eta^2\text{-TMEDA})R_2]$(**23**),[12] and $[Mg(\eta^3\text{-PMDETA})Me_2]$

(**24**) have previously been reported in the literature.[4] Crystals of

$[Mg(\eta^2\text{-TEEDA})Me_2]$(**25**) were grown from a hexane solution at 5°C.

23 R=Me
25 R=Et
26 R=^{i}Pr

24
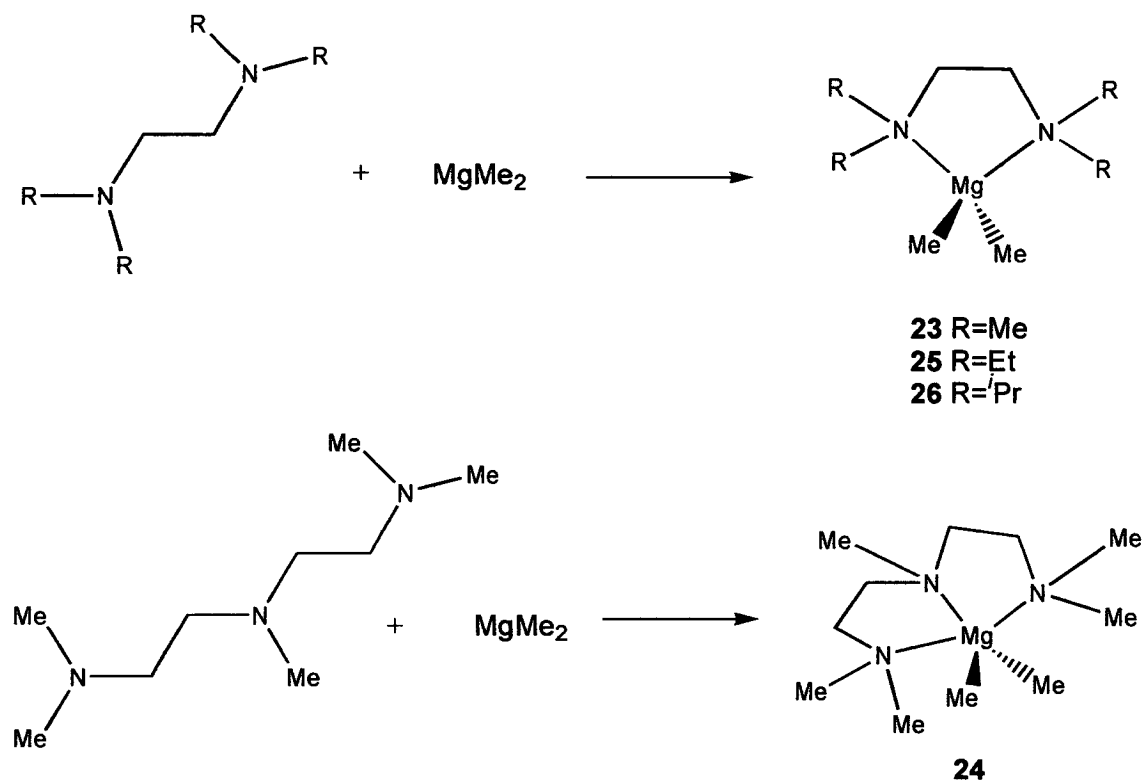
Figure 2.03 Synthesis of [Mg(η²-TMEDA)R₂] (23), [Mg(η³-PMDETA)Me₂] (24), [Mg(η²-TEEDA)Me₂] (25) and [Mg(η²-TIPEDA)Me₂] (26).

The ^{1}H NMR spectrum of [Mg(η^2-TEEDA)Me$_2$] (**25**) in benzene-d_6 displays asymmetry within the molecule, with the presence of two (NCH_2CH$_3$) environments at 2.18 ppm (m, 4H, NCH_2CH$_3$) and 2.62 ppm (m, 4H, NCH_2CH$_3$). Further investigation, by means of a COSY NMR experiment, revealed that the protons assigned at 2.62 ppm couple to the protons at 2.18 ppm and 0.67 ppm (Figure 2.04). Therefore the H atoms on the CH$_2$ group in (NCH_2CH$_3$) are inequivalent. This inequivalence may be due to limited rotation caused by steric hinderence.
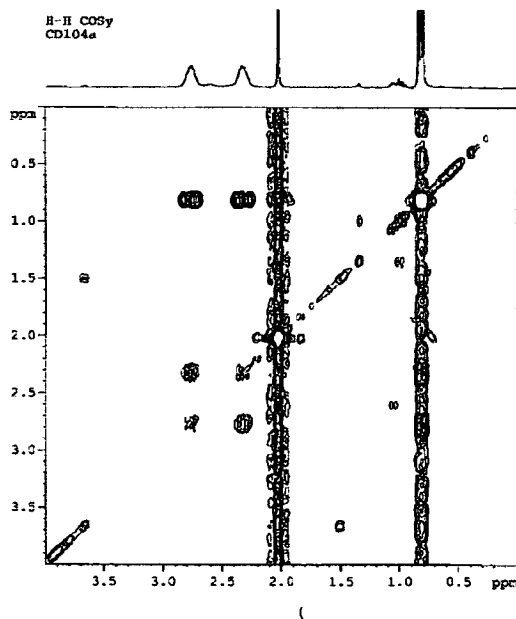
Figure 2.04 ^{1}H COSY NMR of [Mg(η^2-TEEDA)Me$_2$] (25) in benzene-d_6

The crystal structure of **25** has been refined to a good R$_1$ factor of 0.0615. The molecular structure shows the magnesium to be four co-ordinate (Figure 2.05, Table 2.02), tetrahedral distorted [N(1)-Mg(1)-N(4)= 82.64(8)°, C(2M)-Mg(1)-C(1M)= 127.28(11)°, N(1)-Mg(1)-C(2M)= 105.55(9)°, N(4)-Mg(1)-C(1M)= 108.47 (10)°]. The Mg-CH$_3$ bond lengths 2.157(2) Å and 2.173(3) Å, are comparable to those reported in the structures of [Mg(η^2-TMEDA)Me$_2$] (**23**) (2.166(6) Å) and [Mg(η^3-PMDETA)Me$_2$] (**24**) [2.191(4) Å and 2.173(4) Å].
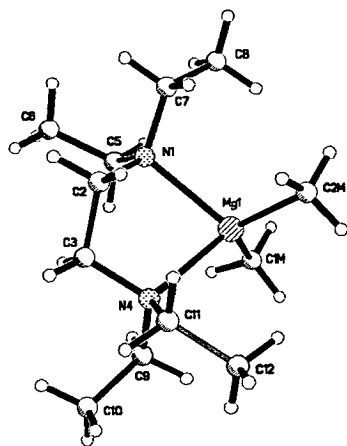
Figure 2.05 Molecular structure of [Mg(η^2-TEEDA)Me$_2$] (25), with selected atom labelling.

Mg(1)-C(2M)	2.157 (2)	C(1M)-Mg(1)-N(4)	108.47 (10)
Mg(1)-C(1M)	2.173 (3)	N(1)-Mg(1)-N(4)	82.64 (8)
Mg(1)-N(1)	2.223 (2)	C(2)-Mg(1)-C(7)	108.76 (18)
Mg(1)-N(4)	2.256 (2)	C(2)-Mg(1)-C(5)	112.45 (19)
N(1)-C(2)	1.478 (3)	C(7)-Mg(1)-C(5)	112.56 (19)
N(1)-C(7)	1.482 (3)	C(2)-N(1)-Mg(1)	100.93 (14)
N(1)-C(5)	1.491 (3)	C(7)-N(1)-Mg(1)	112.69 (14)
C(2)-C(3)	1.515 (3)	C(5)-N(1)-Mg(1)	108.91 (14)
C(3)-N(4)	1.486 (3)	N(1)-C(2)-C(3)	112.0 (2)
N(4)-C(11)	1.481 (3)	N(4)-C(3)-C(2)	111.41 (19)
N(4)-C(9)	1.486 (3)	C(11)-N(4)-C(3)	109.08 (18)
C(5)-C(6)	1.519 (4)	C(11)-N(4)-C(9)	112.37 (19)
C(7)-C(8)	1.511 (4)	C(3)-N(4)-C(9)	110.25 (18)
C(9)-C(10)	1.521 (4)	C(11)-N(4)-Mg(1)	109.69 (14)
C(11)-C(12)	1.516 (4)	C(3)-N(4)-Mg(1)	105.05 (14)
C(2M)-Mg(1)-C(1M)	127.28 (11)	C(9)-N(4)-Mg(1)	110.14 (15)
C(2M)-Mg(1)-N(1)	105.55 (9)	N(1)-C(5)-C(6)	116.6 (2)
C(1M)-Mg(1)-N(1)	112.01 (9)	N(1)-C(7)-C(8)	113.5 (2)
C(2M)-Mg(1)-N(4)	111.89 (9)	N(4)-C(9)-C(10)	116.0 (2)
		N(4)-C(11)-C(12)	114.0 (2)

Table 2.02 Selected bond lengths (Å) and angles (°) for [Mg(η^2-TEEDA)Me$_2$] (25)

Synthesis of the complex [Mg(η^2-TIPEDA)Me$_2$] (**26**) [TIPEDA= tetraisopropylethylenediamine (**27**)] was not very successful. The ligand was generated, in poor yield, by the reaction of 1,2-dibromoethane with diisopropylamine

at 80°C in an EtOH/water mixture for 42h, followed by the work up with KOH (Figure 2.06).[13]
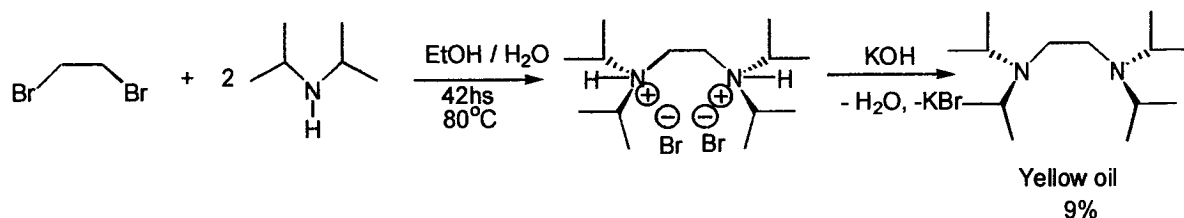
Figure 2.06 Preparation of TIPEDA (27)

The reaction of TIPEDA (**27**) with MgMe$_2$(**7**) using different reaction conditions, i.e. stirring times, solvents, reaction temperatures always produced only a trace of the complex [Mg(η^2-TIPEDA)Me$_2$] (**26**) as a yellow oil as shown by ^{1}H NMR (figure 2.07).
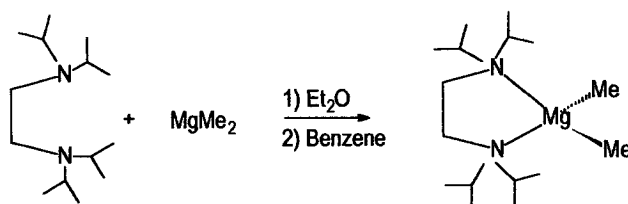
Figure 2.07 Preparation of [Mg(η^2-TIPEDA)Me$_2$] (26)

The signal assigned to the Mg-CH$_3$ protons is very broad spanning 0.3ppm at −0.87ppm in benzene-d_6 (Figure 2.08). Due to the synthetic difficulties associated with the preparation of **26** it was decided not to pursue this complex any further as a potential catalyst. Comparison of rough energetic calculations completed on the optimised geometry of [Mg(η^2-TEEDA)Me$_2$] (**25**) and [Mg(η^2-TIPEDA)Me$_2$] (**26**) using the CACHE program, indicated that complex **26** had twice the final structure energy (80 kcal/mol) of the less sterically challenged **25** (40 kcal/mol).
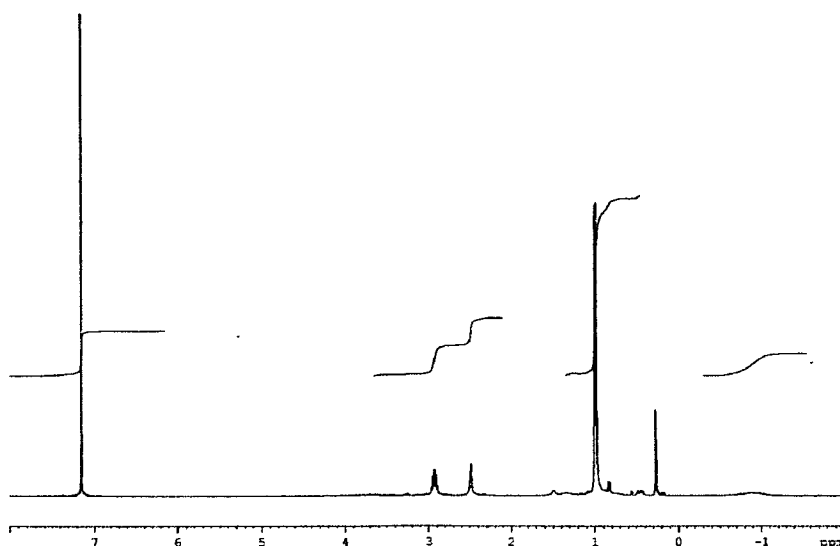
Figure 2.08 ^{1}H NMR of [Mg(η^2-TIPEDA)Me$_2$] (26) in benzene-d_6

2.3.2 Synthesis of Methyl Magnesium Chloride Amine Complexes

Due to the availability of Grignards, we initially investigated the preparation of [Mg(η^2-TMEDA)MeCl]. Reaction of the dried, degassed TMEDA with MgMeCl in THF at ambient temperature with stirring, produces a green coloured solution. Removal of the solvent in vacuum afforded the crude white powder product in quantitative yield. Crystals suitable for X-ray analysis were grown from a toluene solution at -20°C (Figure 2.08). The crystal structure reveals the co-crystallisation of the two products [Mg(μ-Cl)(η^2-TMEDA)Me]$_2$(**28**) and [Mg(μ-Cl)(η^2-TMEDA)Cl]$_2$ (**29**) in a 80:20 % ratio. The formation of the dichloro species has obviously been a result of the Schlenk equilibrium (Figures 2.09, 2.10 and 2.11).
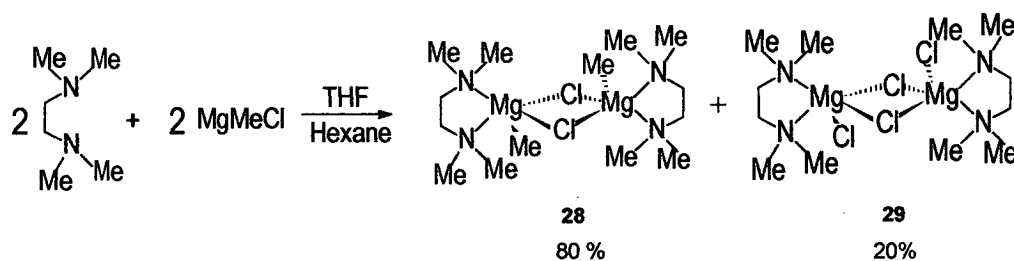
Figure 2.09 Preparation of [Mg(μ-Cl)(η^2-TMEDA)Me]$_2$(28) and [Mg(μ-Cl)(η^2-TMEDA)Cl]$_2$ (29)

$$MgMeCl \rightleftharpoons MgMe_2 + MgCl_2$$

Figure 2.10 The Schlenk equilibrium
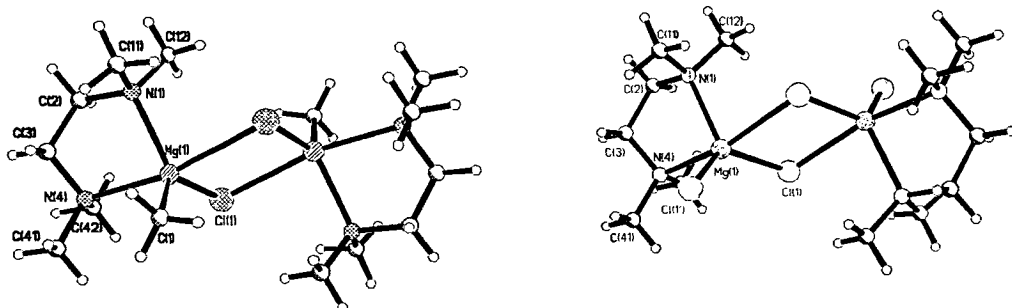
Figure 2.11 Molecular structures of [Mg(μ-Cl)(η^2-TMEDA)Me$_2$]Me]$_2$(28) and [Mg(μ-Cl)(η^2-TMEDA)Me$_2$]Cl]$_2$(29), with selected atom labelling.

Cl(1)-Mg(1)	2.3812 (6)	N(4)-Mg(1)-Cl(1)	94.49 (4)
Cl(1)-Mg(1)#1	2.6891 (6)	Cl(1')-Mg(1)-Cl(1)#1	91.54 (4)
Mg(1)-Cl(1') /C(1)	2.2010 (12)	N(1)-Mg(1)-Cl(1)#1	87.75 (4)
Mg(1)-N(1)	2.2162 (13)	N(4)-Mg(1)-Cl(1)#1	166.48 (4)
Mg(1)-N(4)	2.3106 (13)	Cl(1)-Mg(1)-Cl(1)#1	83.955 (19)
Mg(1)-Cl(1)#1	2.6891 (6)	C(11)-N(1)-C(12)	108.45 (13)
N(1)-C(11)	1.476 (2)	C(11)-N(1)-C(2)	110.33 (13)
N(1)-C(12)	1.4788 (19)	C(12)-N(1)-C(2)	108.42 (12)
N(1)-C(2)	1.4831 (19)	C(11)-N(1)-Mg(1)	106.18 (10)
C(2)-C(3)	1.511 (2)	C(12)-N(1)-Mg(1)	115.15 (10)
C(3)-N(4)	1.4768 (19)	C(2)-N(1)-Mg(1)	108.29 (9)
N(4)-C(41)	1.472 (2)	N(1)-C(2)-C(3)	111.64 (13)
N(4)-C(42)	1.473 (2)	N(4)-C(3)-C(2)	110.91 (13)
Mg(1)-Cl(1)-Mg(1)#1	96.045 (19)	C(41)-N(4)-C(42)	107. 82 (13)
Cl(1')-Mg(1)-N(1)	118.42 (5)	C(41)-N(4)-C(3)	108.78 (13)
Cl(1')-Mg(1)-N(4)	99.69 (5)	C(42)-N(4)-C(3)	109.77 (13)
N(1)-Mg(1)-N(4)	80.33 (5)	C(41)-N(4)-Mg(1)	112.75 (10)
Cl(1')-Mg(1)-Cl(1)	129.51 (4)	C(42)-N(4)-Mg(1)	114.77 (10)
N(1)-Mg(1)-Cl(1)	111.63 (4)	C(3)-N(4)-Mg(1)	102.73 (9)

Table 2.03 Selected bond lengths (Å) and angles (°) for Mg$_2$C$_{13.60}$H$_{36.80}$Cl$_{2.40}$N$_4$

The magnesium centre is 5 co-ordinate distorted trigonal bipyramidal. The bond lengths and angles are all within normal expectations (Table 2.03). The chloride bridging is asymmetric: Cl(1)-Mg(1): 2.312(6) Å and Cl(1)-Mg(1)#1: 2.6891 (6) Å. Therefore the dimer seems to be held together by a weak association between the two monomer complexes and it seems feasible that the two Cl bridges could be cleaved to form the monomer complexes.

2.3.3 Synthesis of Dibenzyl Magnesium Amine Complexes

Complexes such as $[Mg(\eta^2\text{-TMEDA})(CH_2Ph)_2]$ (**30**) and $[Mg(\eta^2\text{-TEEDA})(CH_2Ph)_2]$ (**31**) can be prepared by the direct complexation reaction of $[(PhCH_2)_2Mg(THF)_2]$, dissolved in Et_2O, with the corresponding ligand at room temperature (Figure 2.12). Each product can be precipitated as a white powder by the addition of *n*-hexane after 24h of stirring. $[Mg(\eta^2\text{-TMEDA})(CH_2Ph)_2]$ (**30**) can be crystallised from a toluene and THF mixture at -20°C, as shown by a colleague C.Herber (Figure 2.13, Table 2.04).[18] Where as $[Mg(\eta^2\text{-TEEDA})(CH_2Ph)_2]$ (**31**) can be crystallised from an Et_2O, THF and n-hexane mixture at 5°C (Figure 2.13, Table 2.05).
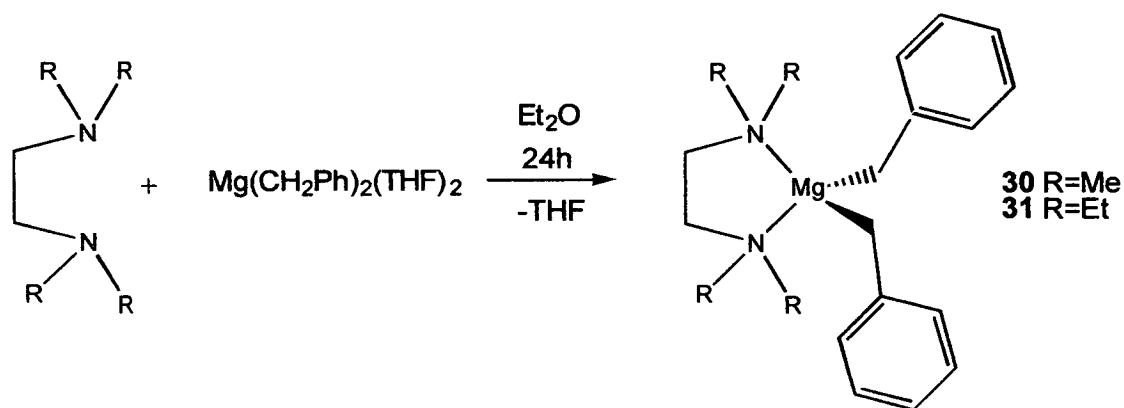
Figure 2.12 Synthesis of $[Mg(\eta^2\text{-TMEDA})(CH_2Ph)_2]$ (30) & $[Mg(\eta^2\text{-TEEDA})(CH_2Ph)_2]$ (31)
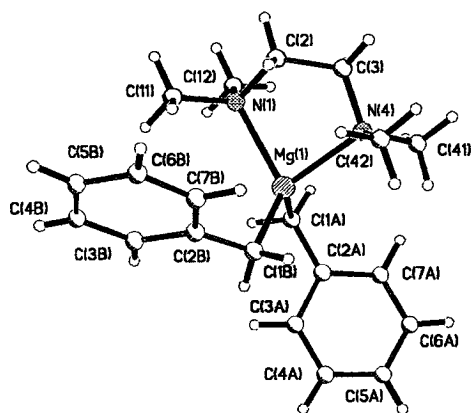
30
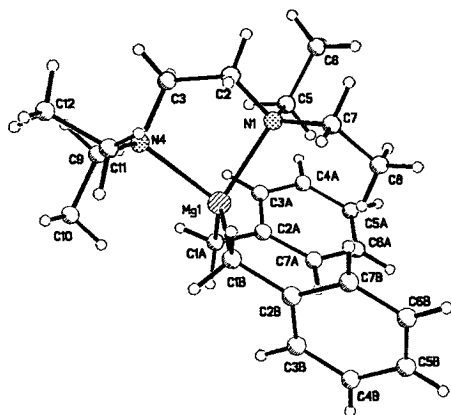
31

Figure 2.13 Molecular structure of [Mg(η^2-TMEDA)(CH$_2$Ph)$_2$] (30) and [Mg(η^2-TEEDA)(CH$_2$Ph)$_2$] (31), with selected atom labelling.

Mg(1)-C(1B)	2.1697 (17)	C(1B)-Mg(1)-C(1A)	117.12 (7)	C(5)-C(4)-C(3A)	120.6 (2)
Mg(1)-C(1A)	2.1697 (17)	C(1B)-Mg(1)-N(4)	113.63 (7)	C(6A)-C(5A)-C(4A)	118.83 (19)
Mg(1)-N(4)	2.1929 (13)	C(1A)-Mg(1)-N(4)	112. 81(6)	C(5A)-C(6A)-C(7A)	121.1 (2)
Mg(1)-N(1)	2.2073 (12)	C(1B)-Mg(1)-N(1)	115.38 (6)	C(6A)-C(7A)-C(2A)	121.92 (19)
N(1)-C(12)	1.474 (2)	C(1A)-Mg(1)-N(1)	109.87 (6)	C(2B)-C(1B)-Mg(1)	113.95 (10)
N(1)-C(11)	1.480 (2)	N(4)-Mg(1)-N(1)	83.36 (5)	C(7B)-C(2B)-C(3B)	115.38 (15)
N(1)-C(2)	1.4890 (19)	C(12)-N(1)-C(11)	108.03 (14)	C(7B)-C(2B)-C(1B)	121.98 (15)
C(2)-C(3)	1.505 (2)	C(13)-N(1)-C(2)	110.53 (12)	C(3B)-C(2B)-C(1B)	122.55 (16)
C(3)-N(4)	1.4859 (19)	C(11)-N(1)-C(2)	108.24 (13)	C(4B)-C(3B)-(C2B)	121.26 (19)
N(4)-C(41)	1.481 (2)	C(12)-N(1)-Mg(1)	108.28 (10)	C(5B)-C(4B)-C(3B)	120.71 (19)
N(4)-C(42)	1.482 (2)	C(11)-N(1)-Mg(1)	117.95 (10)	C(6B)-C(5B)-C(4B)	118.85 (19)
C(1A)-C(2A)	1.470 (2)	C(2)-N(1)-Mg(1)	103.71 (8)	C(5B)-C(6B)-C(7B)	120.7 (2)
C(2A)-C(7A)	1.401 (2)	N(1)-C(2)-C(3)	111.74 (12)	C(6B)-C(7B)-C(2B)	123.08 (18)
C(2A)-C(3A)	1.403 (2)	N(4)-C(3)-C(2)	111.72 (12)		
C(3A)-C(4A)	1.390 (3)	C(41)-N(4)-C(42)	108.44 (13)		
C(4A)-C(5A)	1.374 (3)	C(41)-N(4)-C(3)	109.55 (12)		
C(5A)-C(6A)	1.370 (3)	C(42)-N(4)-C(3)	109. 60 (12)		
C(6A)-C(7A)	1.379 (3)	C(41)-N(4)-Mg(1)	114.72 (10)		
C(1B)-C(2B)	1.465 (2)	C(42)-N(4)-Mg(1)	108. 90 (9)		
C(2B)-C(7B)	1.396 (2)	C(3)-N(4)-Mg(1)	105.53 (9)		
C(2B)-C(3B)	1.410 (2)	C(2A)-C(1A)-Mg(1)	109.76 (11)		
C(3B)-C(4B)	1.402 (3)	C(7A)-C(2A)-C(3A)	115.82 (15)		
C(4B)-C(5B)	1.376 (3)	C(7A)-C(2A)-C(1A)	121.75 (15)		
C(5B)-C(6B)	1.372 (3)	C(3A)-C(2A)-C(1A)	122.41 (15)		
C(6B)-C(7B)	1.375 (2)	C(4A)-C(3A)-C(2A)	121.71 (19)		

Table 2.04 Selected bond lengths (Å) and angles (°) for [Mg(η^2-TMEDA)(CH$_2$Ph)$_2$] (30)

Mg(1)-C(1B)	2.1749 (14)	C(2B)-C(7B)	1.406 (2)	C(11)-N(4)-Mg(1)	111.23 (8)
Mg(1)-C(1A)	2.1834 (15)	C(3B)-C(4B)	1.377 (2)	N(1)-C(5)-C(6)	116.13 (12)
Mg(1)-N(1)	2.1847 (12)	C(4B)-C(5B)	1.377 (3)	N(1)-C(7)-C(8)	113.81 (13)
Mg(1)-N(4)	2.2085 (12)	C(5B)-C(6B)	1.377 (3)	N(4)-C(9)-C(10)	112.50 (12)
N(1)-C(2)	1.4823 (18)	C(6B)-C(7B)	1.395 (2)	N(4)-C(11)-C(12)	116.24 (12)
N(1)-C(7)	1.4882 (17)	C(1B)-Mg(1)-C(1A)	121.63 (6)	C(2A)-C(1A)-Mg(1)	116.83 (10)
N(1)-C(5)	1.4929 (17)	C(1B)-Mg(1)-N(1)	111.07 (5)	C(3A)-C(2A)-C(7A)	116.02 (13)
C(2)-C(3)	1.514 (2)	C(1A)-Mg(1)-N(1)	114.99 (5)	C(3A)-C(2A)-C(1A)	122.14 (13)
C(3)-N(4)	1.4915 (18)	C(1B)-Mg(1)-N(4)	107.71 (5)	C(7A)-C(2A)-C(1A)	121.77 (13)
N(4)-C(9)	1.4899 (18)	C(1A)-Mg(1)-N(4)	110.11(5)	C(4A)-C(3A)-C(2A)	121.73 (15)
N(4)-C(11)	1.4941 (17)	N(4)-Mg(1)-N(1)	84.94 (5)	C(3A)-C(4A)-C(5A)	120.44 (16)
C(5)-C(6)	1.518 (2)	C(2)-N(1)-C(7)	108.56 (11)	C(6A)-C(5A)-C(4A)	118.96 (16)
C(7)-C(8)	1.513 (2)	C(2)-N(1)-C(5)	111.93 (11)	C(5A)-C(6A)-C(5A)	120.29 (16)
C(9)-C(10)	1.513 (2)	C(7)-N(1)-C(5)	111.76 (10)	C(6A)-C(7A)-C(2A)	122.54 (15)
C(11)-C(12)	1.524 (2)	C(2)-N(1)-Mg(1)	101.69 (8)	C(2B)-C(1B)-Mg(1)	112.69 (9)
C(1A)-C(2A)	1.470 (2)	C(7)-N(1)-Mg(1)	112.58 (8)	C(3B)-C(2B)-C(7B)	115.92 (14)
C(2A)-C(3A)	1.400 (2)	C(5)-N(1)-Mg(1)	109.2 (8)	C(3B)-C(2B)-C(1B)	120.96 (13)
C(2A)-C(7A)	1.400 (2)	N(1)-C(2)-C(3)	112.43 (12)	C(7B)-C(2B)-C(1B)	123.09 (14)
C(3A)-C(4A)	1.382 (2)	C(9)-N(4)-C(3)	109.74 (10)	C(4B)-C(3B)-C(2B)	122.81 (15)
C(4A)-C(5A)	1.386 (2)	C(9)-N(4)-C(11)	111.57 (11)	C(5B)-C(4B)-C(3B)	119.89 (16)
C(5A)-C(6A)	1.379 (3)	C(3)-N(4)-C(11)	110.11 (11)	C(6B)-C(5B)-C(4B)	119.58 (16)
C(6A)-C(7A)	1.372 (2)	C(9)-N(4)-Mg(1)	110.37 (9)	C(5B)-C(6B)-C(7B)	120.54 (16)
C(1B)-C(2B)	1.471 (2)	C(3)-N(4)-Mg(1)	103.53 (8)	C(6B)-C(7B)-C(2B)	121.26 (16)
C(2B)-C(3B)	1.402 (2)				

Table 2.05 Selected bond lengths (Å) and angles (°) for [Mg(η^2-TEEDA)(CH$_2$Ph)$_2$] (31)

2.4 Activation of Diamine MgR₂ Complexes with B(C₆F₅)₃

In general we expected the Lewis acid activator $B(C_6F_5)_3$ (**4**) to react with the magnesium methyl complexes to produce the activated cation $[Mg(Amine)Me]^+$ and the anion $[BMe(C_6F_5)_3]^-$, which would be either co-ordinating or non-coordinating (Figure 2.14).
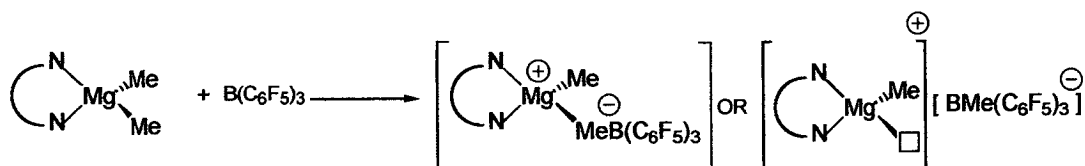
Figure 2.14 Activation of [Mg(η²-amine)Me₂] with B(C₆F₅)₃

Similarly we expected **4** to react with the magnesium benzyl complexes to produce the activated cation $[Mg(Amine)(CH_2Ph)]^+$ which may or may not be stabilised by hapto interactions between the benzyl ring and the electronically unsaturated magnesium centre. The counter anion $[B(CH_2Ph)(C_6F_5)_3]^-$ produced could either be co-ordinating through the CH_2 group (C) or Ph ring(D) or non-coordinating (A or B) (Figure 2.15).
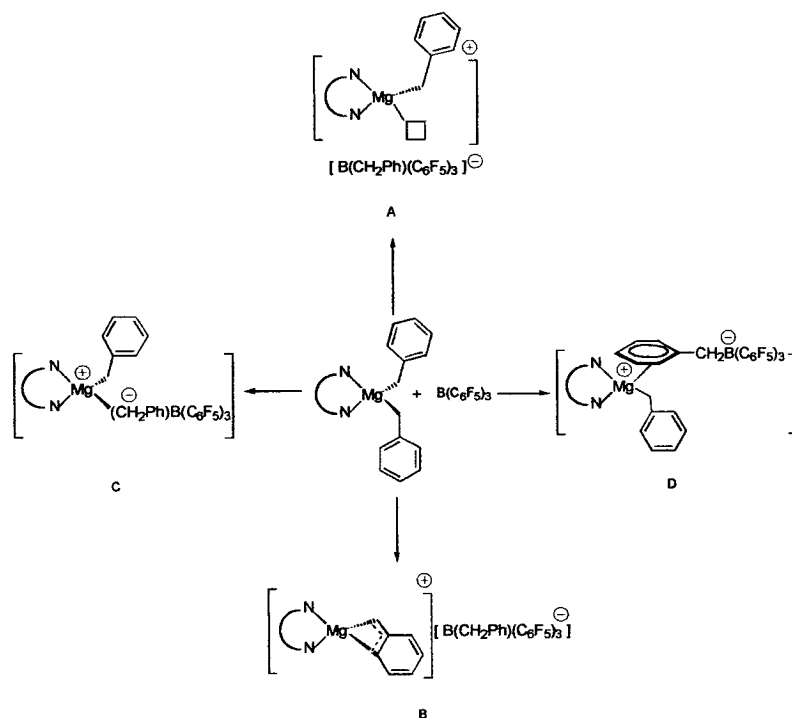
Figure 2.15 Activation of [Mg(η²-amine)(CH₂Ph)₂] with B(C₆F₅)₃

It has been reported that the η^n interaction of benzyl ligands with the metal can be determined *via* several analytical techniques. [3, 19-20] The easiest characterisation is obviously *via* solid state structure determination. In solution, NMR plays an important role. η^n interactions can be identified by an upfield shift of the *o*-Ph resonances in the ^{1}H and ^{13}C NMR, upfield resonances of the ipso carbon and large J_{CH} couplings (137 Hz) in the ^{13}C NMR. Co-ordination of the anion *via* the CH_2 group in $[(CH_2Ph)B(C_6F_5)_3]^-$ can be determined from $\Delta\delta$ (*m, p*-F) in the ^{19}F NMR (uncoordinated $\Delta\delta$ (*m, p*-F)= ~2.8ppm, coordinated $\Delta\delta$ (*m, p*-F)~ 4ppm).[3, 19-20]

The ^{19}F, ^{13}C and ^{11}B NMR spectra of $B(C_6F_5)_3$ were recorded in several NMR solvents. The reactions were initially carried out on NMR scale due to the expensive nature of the activator. The reactions were investigated by varying the molar ratio of activator to the procatalyst. In some cases, where deactivation was being observed, it was necessary to monitor the reaction products by NMR over several hours to determine the stability of the products forming. To obtain solid evidence of the reaction products forming crystallisation attempts were implemented for all combinations of the amine magnesium alkyls with the Lewis acid activator $B(C_6F_5)_3$.

2.4.1 Activation of [Mg(η²-TMEDA)Me₂] with B(C₆F₅)₃

The addition of [Mg(η²-TMEDA)Me₂] to B(C₆F₅)₃ (1:1 equivalent) in C₆D₅Br produces a colourless clear solution at room temperature, in which all the products are soluble. All the ¹H, ¹⁹F and ¹¹B NMR spectra were recorded within the hour of the reactants being added to one another. The ¹H and ¹⁹F NMR spectra are very complex. The ¹⁹F NMR spectrum is the key in this reaction, and contains 15 signals which is indicative of 5 very different C₆F₅ environments. There is a noted absence of a signal at -142.18ppm which is characteristic of the *para*-F of B(C₆F₅)₃, therefore all the B(C₆F₅)₃ has reacted. It is obvious that some kind of (C₆F₅) transfer has occurred at this point. As discussed in Section 1.2.2.2a C₆F₅ transfer to a metal centre from B(C₆F₅)₃ can be identified by a higher frequency chemical shift of the *ortho*-F in the ¹⁹F NMR spectrum. In this case signals are observed at −112.70 ppm and

−114.76 ppm in C₆D₅Br [c.f. −127.68 ppm for B(C₆F₅)₃] (Figure 2.17). We propose the two species responsible for these signals to be [Mg(η²-TMEDA)(C₆F₅)Me] (**33**) and [Mg(η²-TMEDA)(C₆F₅)₂] (**35**) respectively. The reaction pathway that lead to the production of (**33**) and (**35**) must initially involve the preparation of the "salt"

[Mg(η²-TMEDA)Me{BMe(C₆F₅)₃}](**32**) (Figure 2.16) where the anion is co-ordinated to the cation (as shown by the large Δδ (*m, p*-F) of 4.58ppm). The cation, being in close proximity to the anion, and having a higher Lewis acidity than the [MeB(C₆F₅)₄]⁻ anion, abstracts a (C₆F₅) group to produce the neutral species

[Mg(η²-TMEDA)(C₆F₅)Me] (**33**) and BMe(C₆F₅)₂ (**34**). It is also feasible that two C₆F₅ transfers can occur thus producing (**35**) and BMe₂(C₆F₅) (**36**). The presence of **32, 33, 34, 35** and **36** in solution accounts for the 5 different C₆F₅ environments observed in the ¹⁹F NMR spectrum (Figure 2.17). Similarly, this reaction scheme (Figure 2.16) is substantiated by the ¹¹B and ¹H NMR spectra. There are 3 notable types of B environment as shown by the ¹¹B NMR spectrum, with broad singlets at δ −13.15 ppm, -11.85 ppm and 89.47 ppm (Figure 2.18). There are three boron containing reaction products (Figure 2.18): [Mg(η²-TMEDA)Me{MeB(C₆F₅)₃}] (**32**), BMe(C₆F₅)₂ (**34**) and BMe₂(C₆F₅) (**36**). It is therefore reasonable to assign the signal at 89.42 ppm to **32** and those at lower frequency to **34** and **36**.
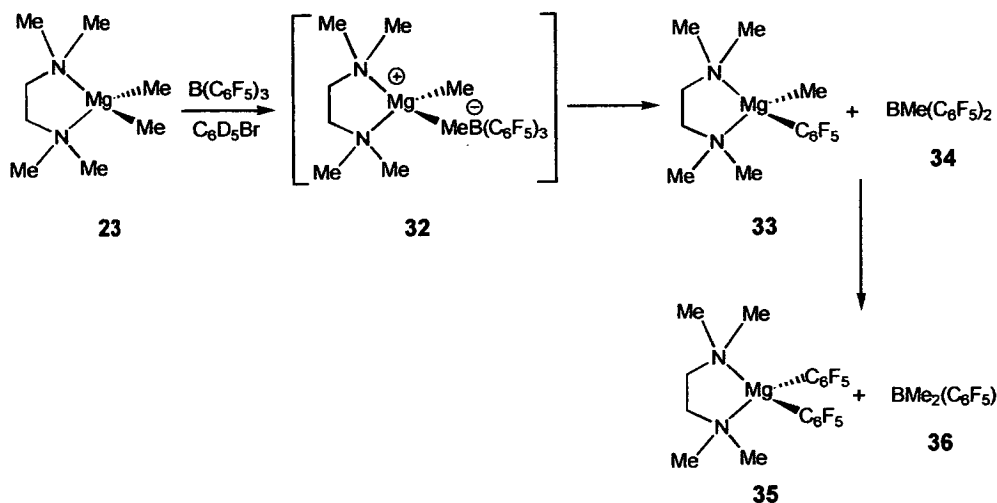
Figure 2.16 Activation of [Mg(η^2-TMEDA)Me$_2$] with B(C$_6$F$_5$)$_3$
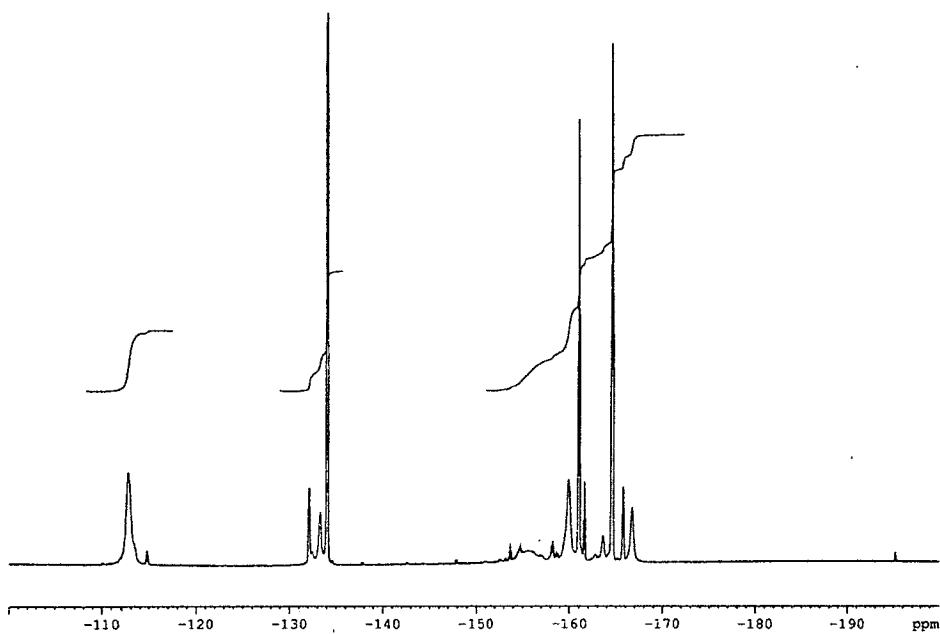
Figure 2.17 ^{19}F NMR spectrum in C$_6$D$_5$Br of [Mg(η^2-TMEDA)Me$_2$] with B(C$_6$F$_5$)$_3$
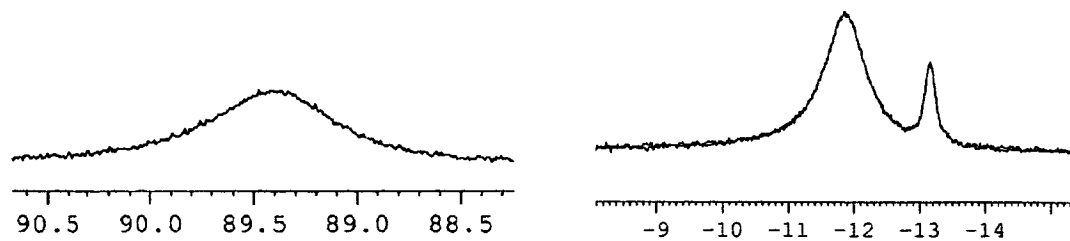
Figure 2.18 ^{11}B NMR spectrum in C$_6$D$_5$Br of [Mg(η^2-TMEDA)Me$_2$] with B(C$_6$F$_5$)$_3$ (1:1)

There are 2 B(CH_3) environments in the ^{1}H NMR spectrum at δ 0.72 and 0.88 ppm, the latter signal is very broad and half the height of the first but has the same integral, therefore the signal at 0.72 ppm can be assigned to BMe$_2$(C$_6$F$_5$) (36) and the signal at 0.88 ppm is due to (32) and BMe(C$_6$F$_5$)$_2$ (34). The two signals at δ −1.24 ppm and -1.10 ppm can be assigned to [Mg(η^2-TMEDA)(C$_6$F$_5$) Me] (33) and [Mg(η^2-TMEDA)Me{MeB(C$_6$F$_5$)$_3$}] (32) respectively.

The products identified in the ^{19}F NMR spectrum therefore have the following information: [Mg(η^2-TMEDA)(C$_6$F$_5$) Me] (33): -112.70 ppm (*o*-F, 64F), -156.10 ppm (*p*-F, 32F), -159.93 ppm (*m*-F, 64F); [Mg(η^2-TMEDA)(C$_6$F$_5$)$_2$] (35): -114.76 ppm (*o*-F, 2F), -153.69 ppm (*p*-F, 1F), -158.22 ppm (*m*-F, 2F); [Mg(η^2-TMEDA)Me{MeB(C$_6$F$_5$)$_3$}] (32): -134.04 ppm (*o*-F, 90F), -160.95 ppm (*p*-F, 45F), -164.53 ppm (*m*-F, 90F); BMe$_2$(C$_6$F$_5$) (36): -132.11 ppm(*o*-F, 24F), -163.56 ppm (*p*-F, 12F), -166.69 ppm (*m*-F, 24F); BMe(C$_6$F$_5$)$_2$ (34): -133.29 ppm (*o*-F, 24F), -161.55 ppm (*p*-F, 12F), -165.72 ppm (*m*-F, 24F) (Figure 2.17).

Elucidation of compounds 32-36 from the ^{19}F NMR suggests that the product ratios are: 15: 32: 6: 1: 12 for 32: 33: 34: 35: 36. Obviously this ratio does not completely correspond with the ratios displayed in Figure 2.16. Looking at the ^{19}F NMR spectrum it is clear that there are still trace products that have not been identified. There must be other decomposition reactions occurring which are unidentified at this stage.

To test the stability of the reaction products, the sample was re-analysed after 20 hours by ^{1}H and ^{19}F NMR. The ^{1}H NMR spectrum no longer contained any signals for magnesium bonded methyl groups. There are 3 distinct B(CH_3) environments at 0.72 ppm, 0.98 ppm and 1.08 ppm. The ^{19}F NMR spectrum shows [Mg(η^2-TMEDA)(C$_6$F$_5$)Me] (33) has been consumed and [Mg(η^2-TMEDA)(C$_6$F$_5$)$_2$] (35) produced, as shown by the diminished signals at −112.70 ppm, -156.10 ppm, and −159.93 ppm the increased intensities at −114.76 ppm, -153.73 ppm and -158.25 ppm (Figure 2.19). All the [BMe(C$_6$F$_5$)$_3$]⁻ has been consumed (signals at −134.04 ppm, -160.95 ppm and -164.53 ppm disappeared). Similarly BMe(C$_6$F$_5$)$_2$ has been consumed (-133.29 ppm, -161.55 ppm and -165.72 ppm have diminished). The

signals at −132.08 ppm, -163.38 ppm, and 166.16 ppm have grown which corresponds to the production of $BMe_2(C_6F_5)$ **(36)**.
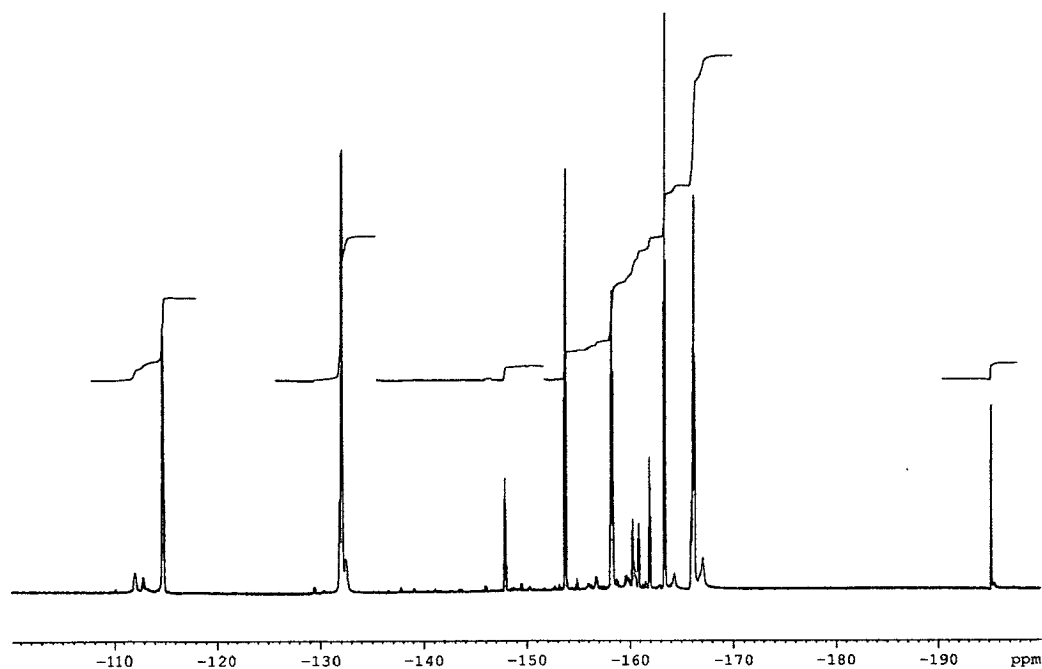
Figure 2.19 ^{19}F **NMR spectrum in** C_6F_5Br **of** $[Mg(\eta^2\text{-TMEDA})Me_2]$ **with** $B(C_6F_5)_3$ **after 20hs.**
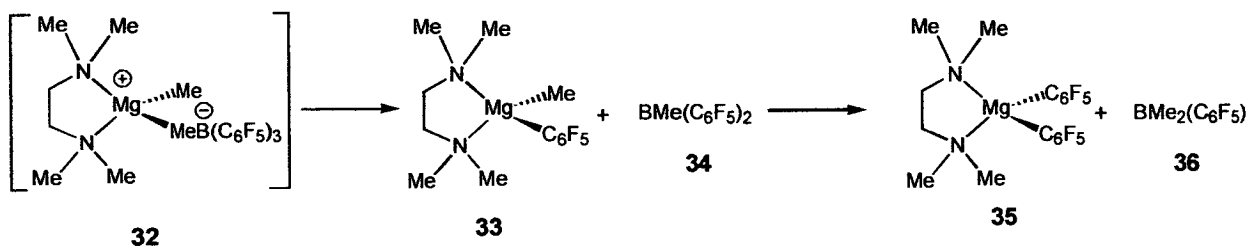
Figure 2.20 Reaction of $[Mg(\eta^2\text{-TMEDA})Me_2]$ **with** $B(C_6F_5)_3$ **(1:1) in** C_6F_5Br **after 20hs.**

To clarify that the signals at −112.70 ppm, -156.10 ppm, and −159.93 ppm correspond to the complex $[Mg(\eta^2\text{-TMEDA})(C_6F_5) Me]$ **(33)**, an independent synthesis of this compound was developed.

2.4.2 Preparation of [Mg(η^2-TMEDA)(C$_6$F$_5$)Me] (33)

Initial attempts at preparing the Grignard Mg(C$_6$F$_5$)Cl *via* reaction of C$_6$F$_5$Cl and Mg in THF, as reported in the literature, were not successful.[21a] However, the reaction of Mg(C$_2$H$_5$)Br with C$_6$F$_5$Br at low temp in THF successfully produced Mg(C$_6$F$_5$)Br (37) in quantitative yield.[21b] Reaction of Mg(C$_6$F$_5$)Br with TMEDA, followed by reaction with MeLi, produced the desired complex [Mg(η^2-TMEDA)(C$_6$F$_5$)Me] (33) as a purple solid in 89% yield (Figure 2.21).

$$\text{TMEDA} \xrightarrow[\text{THF}]{\text{Mg(C}_6\text{F}_5\text{)Br}} [\text{Mg}(\eta^2\text{-TMEDA})(\text{C}_6\text{F}_5)\text{Br}] \xrightarrow[\text{-LiCl}]{\text{MeLi}} [\text{Mg}(\eta^2\text{-TMEDA})(\text{C}_6\text{F}_5)\text{Me}]$$

33
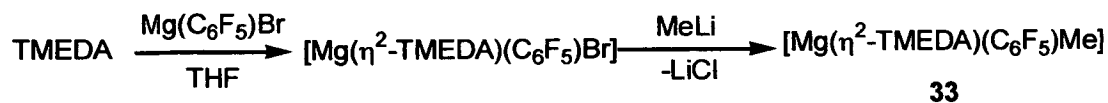
Figure 2.21 Synthesis of [Mg(η^2-TMEDA)(C$_6$F$_5$)Me]

The product was identified by ^{1}H, ^{13}C and ^{19}F NMR spectroscopy in C$_6$D$_5$Br. The ^{1}H NMR spectrum places the Mg-Me singlet at δ -1.28 ppm, and the NMe and NCH$_2$ singlets at δ 2.02 ppm and 2.17 ppm (Figure 2.22). The ^{13}C NMR spectrum shows the presence of the C$_6$F$_5$ group by the doublets at 122.65 ppm and 129.05ppm (*C*-F), there is also a peak at 125.77 ppm (*C*-F) which is part of a doublet signal but the other peak is obscured by the solvent, and the *C*-ipso singlet at 137.87ppm. The magnesium methyl at −14.68 ppm and the TMEDA signals of NMe at 46.66 ppm and NCH$_2$ at 56.65 ppm. The ^{19}F NMR spectrum shows a doublet at δ −111.66 ppm (*o*-F), a triplet at −158.28 ppm (*p*-F) and a multiplet at −161.04 ppm (*m*-F) (Figure 2.23). Thus confirming that the reaction of [Mg(η^2-TMEDA)Me$_2$] with B(C$_6$F$_5$)$_3$ (1:1 equivalent) does produce [Mg(η^2-TMEDA)(C$_6$F$_5$)Me] (33).
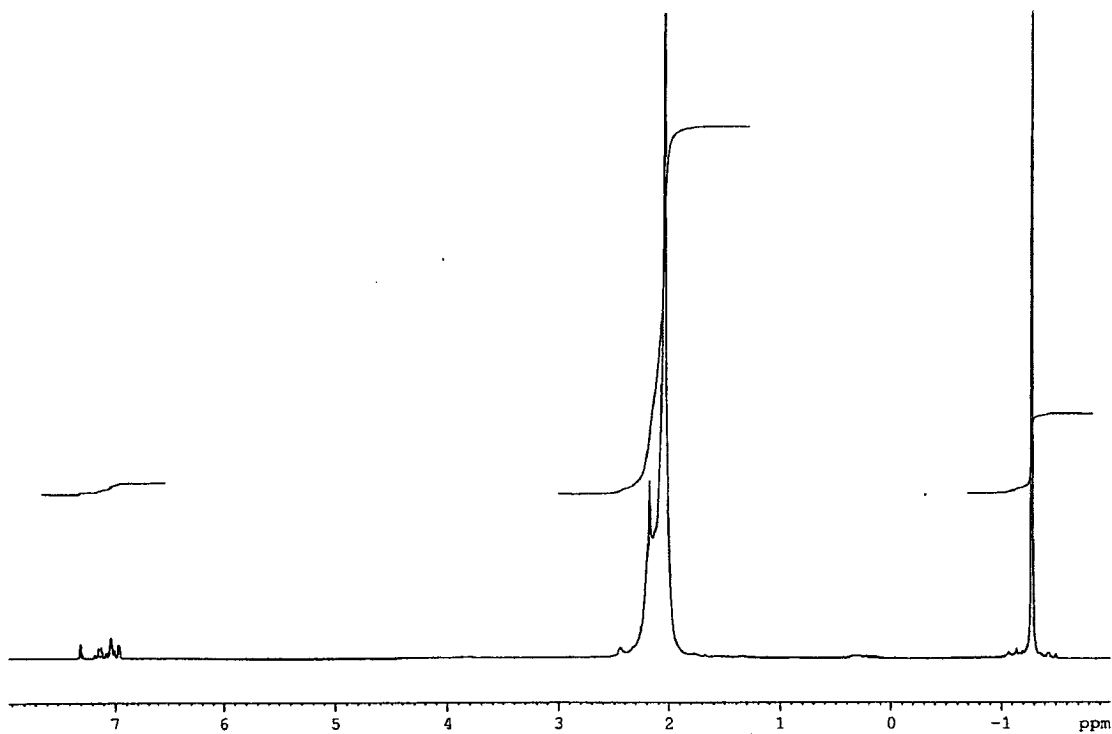
Figure 2.22 ^{1}H NMR spectrum in C$_6$D$_5$Br of [Mg(η^2-TMEDA)(C$_6$F$_5$)Me] (33)
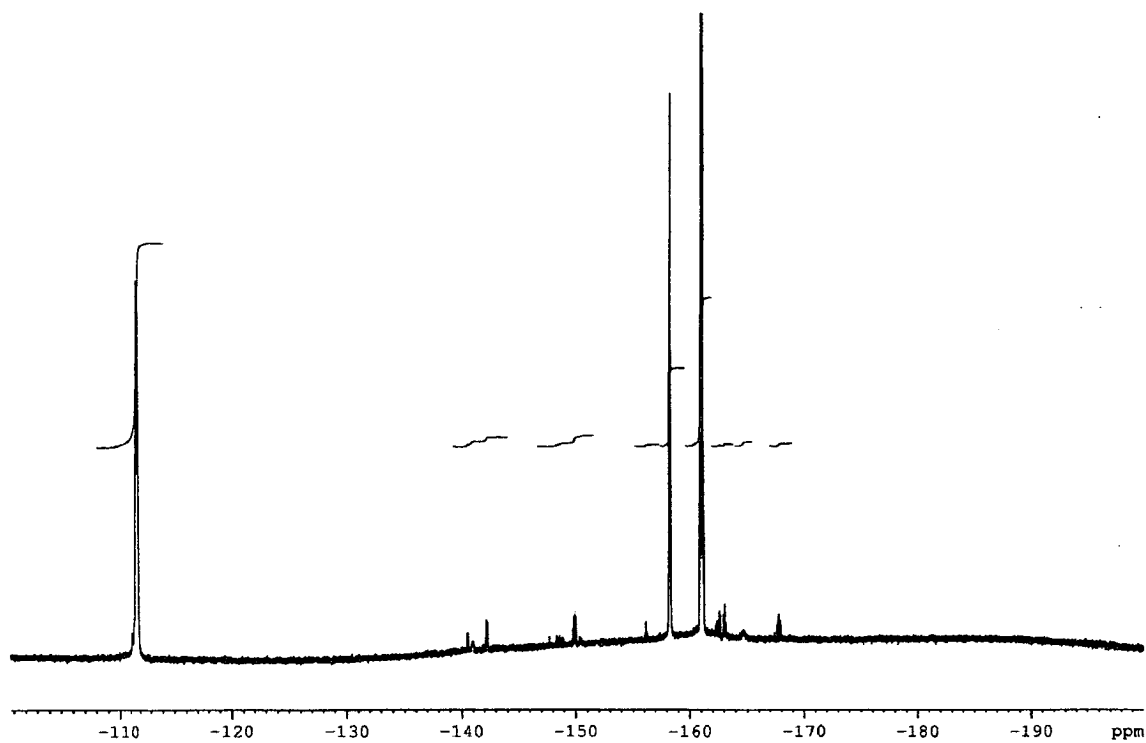
Figure 2.23 ^{11}F NMR spectrum in C$_6$D$_5$Br of [Mg(η^2-TMEDA)(C$_6$F$_5$)Me]

2.4.3 Activation of [Mg(η^2-TEEDA)Me$_2$] and [Mg(η^3-PMDETA)Me$_2$] with B(C$_6$F$_5$)$_3$

To ascertain whether increasing the steric bulk round the Mg centre, *via* the ligand, affected the reaction products produced, the reaction of [Mg(η^2-TEEDA)Me$_2$] and [Mg(η^3-PMDETA)Me$_2$] with B(C$_6$F$_5$)$_3$ (1:1) in C$_6$D$_5$Br were investigated. Complexes [Mg(η^2-TEEDA)Me$_2$] and [Mg(η^3-PMDETA)Me$_2$] were reacted with B(C$_6$F$_5$)$_3$ (1:1) in C$_6$D$_5$Br, and similarly produce C$_6$F$_5$ transfer products. However, it is initially apparent that [Mg(η^3-PMDETA)Me$_2$] is less susceptible to C$_6$F$_5$ transfer than [Mg(η^2-TMEDA)Me$_2$] and [Mg(η^2-TEEDA)Me$_2$], on comparing ^{19}F NMR spectra (Figure 2.24).

The reaction of [Mg(η^2-TEEDA)Me$_2$] with B(C$_6$F$_5$)$_3$ (1:1) produces a ^{19}F NMR spectrum which displays three easily identifiable products: [Mg(η^2-TEEDA)Me{BMe(C$_6$F$_5$)$_3$}] (**38**): (-133.25 ppm (*o*-F, 60F), -161.33 ppm (*p*-F, 30F), -165.10 ppm (*m*-F, 60F), [Mg(η^2-TEEDA)Me(C$_6$F$_5$)] (**39**): -111.74 ppm (*o*-F, 20F), -157.12 ppm (*p*-F, 10F), -160.67 ppm (*m*-F, 20F), and [Mg(η^2-TEEDA)(C$_6$F$_5$)$_2$] (**40**): -113.19 ppm (*o*-F, 18F), -153.30 ppm (*p*-F, 9F) ,-158.94 ppm (*m*-F, 18F). The [BMe(C$_6$F$_5$)$_3$]$^-$ counter ion is identified as being co-ordinated (as shown by the large $\Delta\delta$ (*m*, *p*-F) of 3.77 ppm). There are no peaks in the ^{19}F NMR spectrum that are equivalent to BMe$_2$(C$_6$F$_5$) and BMe(C$_6$F$_5$)$_2$ as identified in the reaction of [Mg(η^2-TMEDA)Me$_2$] and B(C$_6$F$_5$)$_3$. However, there are several unassigned signals: e.g. −147.93 ppm, -153.78 ppm, -158.48 ppm, -193.19 ppm. The ^{11}B NMR spectrum displays a signal at −11.80ppm, but the spectrum range was not large enough to observe any signals at approximately 90ppm, where **38** would produce a signal.

In the ^{1}H NMR spectrum there are 2 Mg-Me environments observed, and one obvious B(CH$_3$) environment. There are three NCH$_3$, NCH$_2$ (ligand back bone) and NCH$_2$ (ligand arm) environments and therefore a mixture of several products.

The ^{19}F NMR spectrum recorded the next day does not differ significantly, with only a small consumption of [Mg(η^2-TEEDA)Me(C$_6$F$_5$)].

(A)

(B)
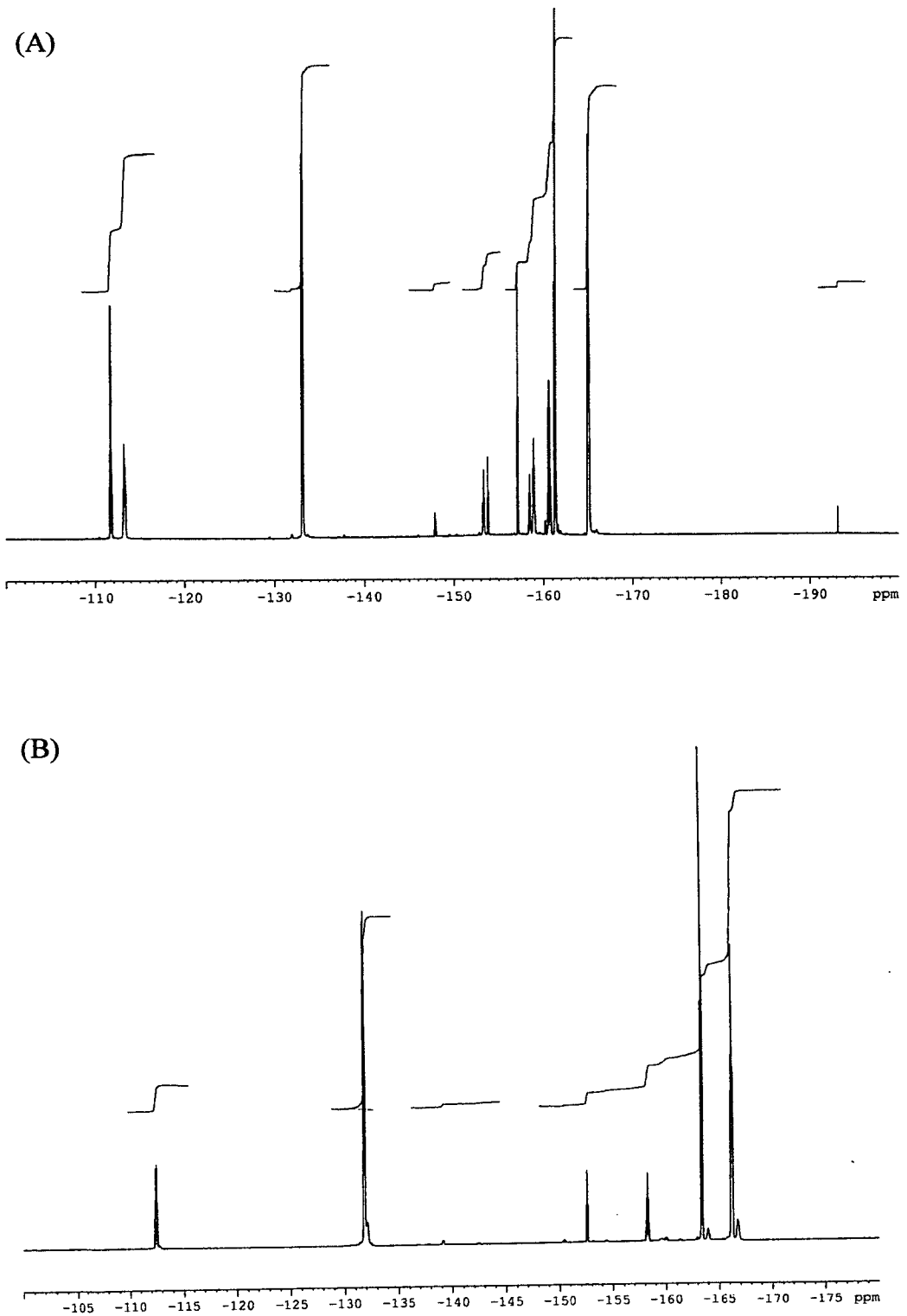
Figure 2.24 ^{19}F NMR spectrum in C$_6$D$_5$Br of (A) [Mg(η^2-TEEDA)Me$_2$] with B(C$_6$F$_5$)$_3$ and (B) [Mg(η^3-PMDETA)Me$_2$] with B(C$_6$F$_5$)$_3$
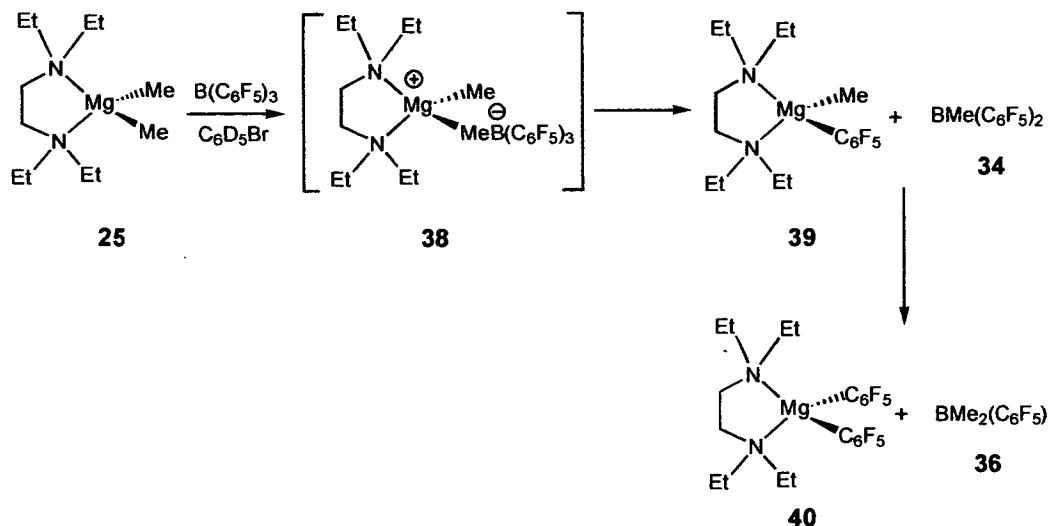
Figure 2.25 Reaction of [Mg(η²-TEEDA)Me₂] with B(C₆F₅)₃ (1:1) in C₆D₅Br

The reaction of [Mg(η³-PMDETA)Me₂] with B(C₆F₅)₃ (1:1) produces a mixture whose ¹⁹F NMR spectrum identifies three compounds: [Mg(η³-PMDETA)Me] [B(C₆F₅)₃Me]⁻ (41), [Mg(η³-PMDETA)(Me)(C₆F₅)] (42) and BMe(C₆F₅)₂ (34). The extra bulk and electronic donation of PMDETA prevents co-ordination of the anion [B(C₆F₅)₃Me]⁻ (as shown by the small Δδ (*m, p*-F) of 2.81 ppm in the ¹⁹F NMR). The sole formation of [Mg(η³-PMDETA)(Me)(C₆F₅)] (42), suggests the tridentate and more bulky ligand PMDETA provides a more stable environment at the magnesium centre (c.f. to TMEDA and TEEDA). The ¹H NMR spectrum in the reaction of [Mg(η³-PMDETA)(Me)₂] with B(C₆F₅)₃ confirms the presence of methyl groups bonded to the magnesium -1.42 ppm (s, MgCH₃). There are 2 BMe environments at 0.90 and 1.02 ppm in 1:6 ratio. Corresponding to BMe(C₆F₅)₂ and [BMe(C₆F₅)₃]⁻. The ¹¹B NMR has two peaks which correspond to 34 (-11.36 ppm) and 41 (89.14 ppm).
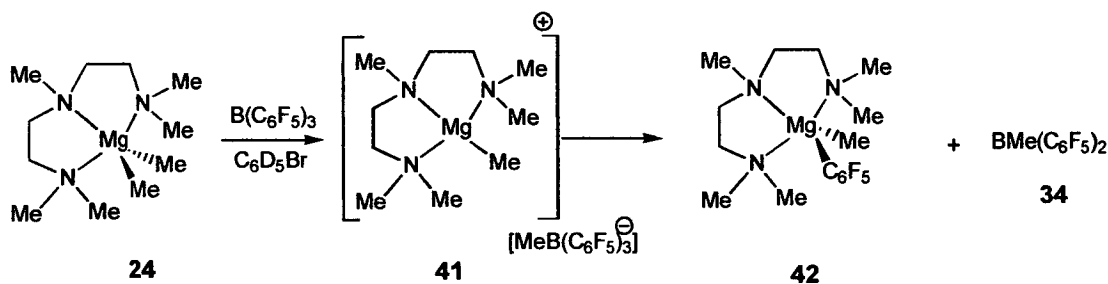
Figure 2.26 Reaction of [Mg(η³-PMDETA)Me₂] with B(C₆F₅)₃ (1:1) in C₆D₅Br

2.4.4 Activation of [Mg(η^2-TMEDA)(CH$_2$Ph)$_2$] & [Mg(η^2-TEEDA)(CH$_2$Ph)$_2$] with B(C$_6$F$_5$)$_3$

Activation of the amine benzyl magnesium complexes were investigated to determine whether increasing the steric bulk of the R substituent has a stabilising ability and investigate the possibility of η^3-benzyl coordination. Both reactions of [Mg(η^2-TMEDA)(CH$_2$Ph)$_2$] and [Mg(η^2-TEEDA)(CH$_2$Ph)$_2$] with B(C$_6$F$_5$)$_3$ in C$_6$D$_5$Br show that C$_6$F$_5$ transfer still occurs even with bulky benzyl substituents.

In the reaction of [Mg(η^2-TMEDA)(CH$_2$Ph)$_2$] with B(C$_6$F$_5$)$_3$ the ^{19}F NMR spectrum indicates the formation of 3 major products: [Mg(η^2-TMEDA)(C$_6$F$_5$)(CH$_2$Ph)] (**43**): -112.49 (*o-F*, 2F), -153.99 (*p-F*, 1F), -159.92 (m-F, 2F); [B(CH$_2$Ph)(C$_6$F$_5$)$_3$]$^-$ (**44**): -131.94 (s(br), *o-F*, 2F); -161.65 (m, *p-F*, 1F), -164.91 (t, J=21 89 Hz, *m-F*, 2F); and [B(CH$_2$Ph)(C$_6$F$_5$)$_2$] (**45**) -132.04 (s(br), *o-F*, 2F), -161.69 (m, *p-F*, 1F), -165.81 (t, J=18.84, *m-F*, 2F) (Figure 2.27).
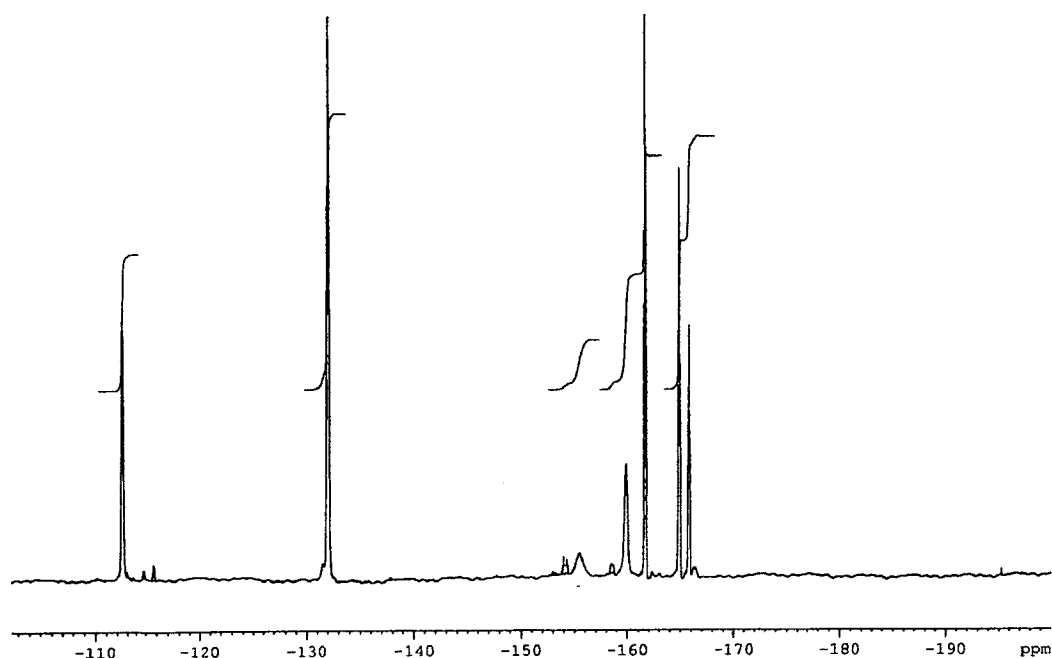
Figure 2.27 ^{19}F NMR spectrum in C$_6$D$_5$Br of [Mg(η^2-TMEDA)(CH$_2$Ph)$_2$] with B(C$_6$F$_5$)$_3$

Stability studies again confirm the degradation of the reaction mixture to further C$_6$F$_5$ transfer as shown by the consumption of [B(CH$_2$Ph)(C$_6$F$_5$)$_3$]$^-$ (**44**) and [Mg(η^2-TMEDA)(C$_6$F$_5$)(CH$_2$Ph)] (**43**), concomitant with the growth of peaks corresponding to [Mg(η^2-TMEDA)(C$_6$F$_5$)$_2$] (**46**) in the ^{19}F NMR spectrum:

-114.81 ppm (*o*-F, 4F), -153.98 ppm (*p*-F, 2F), -158.33 ppm (m-F, 4F), and [B(CH$_2$Ph)$_2$(C$_6$F$_5$)] (**47**): -130.66 (d, J= 23.39 Hz, *o*-F, 4F), -162.02 (t, J= 21.00 Hz, *p*-F, 2F),-166.00 (t, J= 21.05 Hz, *m*-F, 4F) (Figure 2.28).
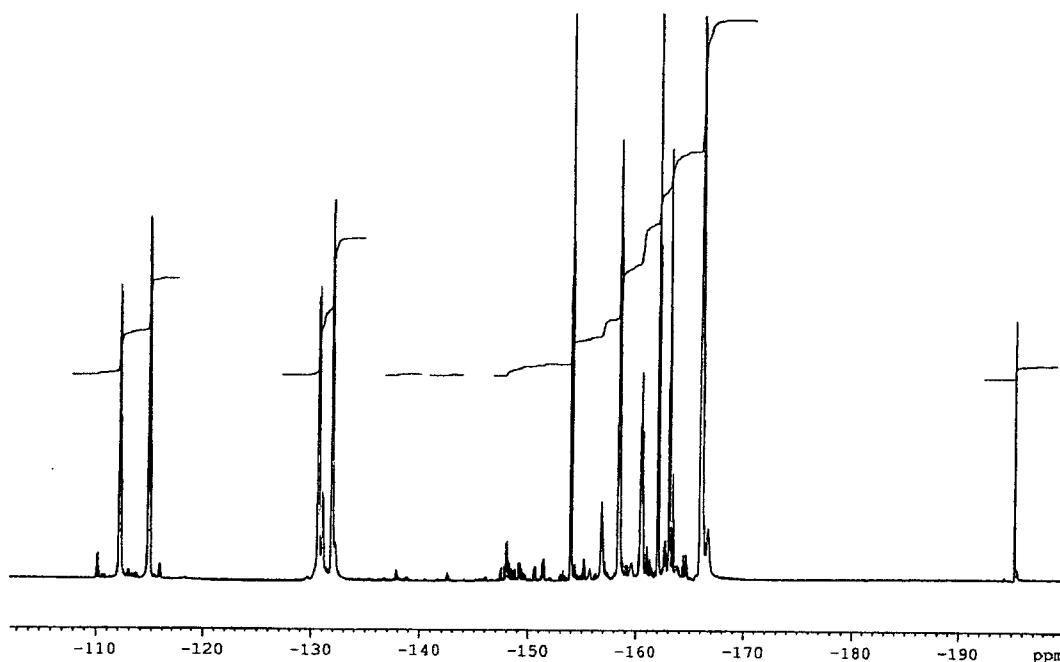
Figure 2.28 ^{19}F NMR spectrum of [Mg(η^2-TMEDA)(CH$_2$Ph)$_2$] with B(C$_6$F$_5$)$_3$ 20hs later.

The ^{11}B NMR spectrum recorded in C$_6$D$_5$Br displays 3 types of B environments –13.14, -9.26 and 85.15 ppm. The presence of [B(CH$_2$Ph)(C$_6$F$_5$)$_3$] (**44**) is observed at 2.6 ppm in the ^{1}H NMR spectrum, where as [B(CH$_2$Ph)(C$_6$F$_5$)$_2$] (**45**) is observed at 3.18 ppm. Note, the $\Delta\delta$ (*m, p*-F) of 3.26 ppm for [B(CH$_2$Ph)(C$_6$F$_5$)$_3$] (**44**), in the ^{19}F NMR spectrum, is not large enough to suggest co-ordination of the anion *via* the CH$_2$ group.

The ^{1}H NMR spectrum shows the Ar*H* region to fall within the range 6.68-7.16 ppm {c.f. to 6.63-7.06 ppm for unreacted [Mg(η^2-TMEDA)(CH$_2$Ph)$_2$] (**30**). In the ^{13}C NMR there is a significant down field shift in the Ph-*C*H resonances 125.22 ppm, 127.86 ppm, 128.76 ppm, 128.88 ppm, 129.35 ppm, 129.54 ppm (c.f. to 117.09 ppm, 124.51 ppm, and 128.97 ppm for unreacted (**30**). The Ph*C*H$_2$ enivronment has shifted down field (as shown by 135 Dept ^{13}C NMR) to 37.52 ppm (c.f. to 23.78 ppm for unreacted (**30**). The down field shifts of the aromatic groups in the ^{1}H and ^{13}C NMR suggest that the [B(PhCH$_2$)(C$_6$F$_5$)$_3$]$^-$ counter ion may be co-ordinated through the phenyl group (Figure 2.29).
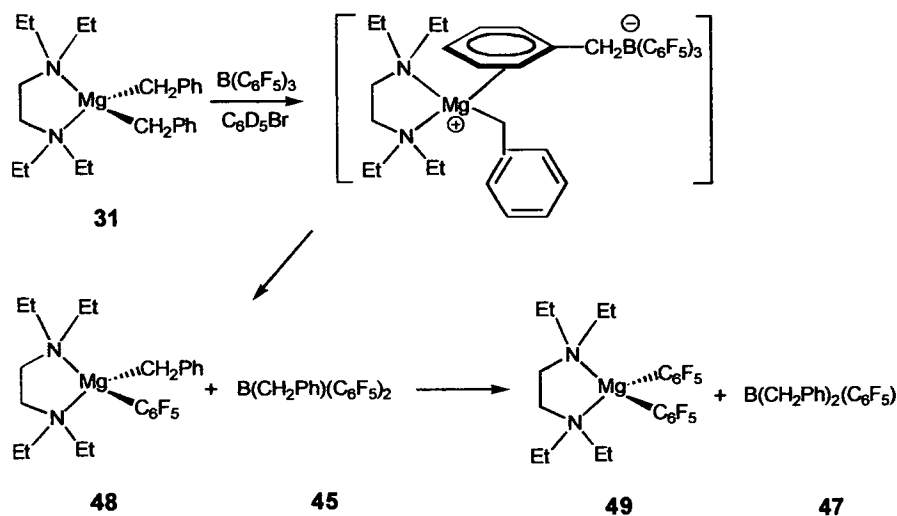
Figure 2.29 Reaction of [Mg(η^2-TEEDA)(CH$_2$Ph)$_2$] with B(C$_6$F$_5$)$_3$ in C$_6$D$_5$Br

In the reaction of [Mg(η^2-TEEDA)(CH$_2$Ph)$_2$] (**31**) with B(C$_6$F$_5$)$_3$ (**4**) the ^{19}F NMR shows indicates the formation of 4 major products. [Mg(η^2-TEEDA)(C$_6$F$_5$)(CH$_2$Ph)] (**48**): -111.64 ppm (o-F), -156.95 ppm (*p*-F), -161.29 ppm (*m*-F) ;

[Mg(η^2-TEEDA)(C$_6$F$_5$)$_2$] (**49**): -113.46 ppm (*o*-F), -153.35 ppm (p-F), -158.77 ppm (*m*-F); [B(CH$_2$Ph)(C$_6$F$_5$)$_3$]$^-$ (**44**) : -131.01 ppm (*o*-F), -161.73 ppm (*p*-F), -165.57 ppm (*m*-F).[B(CH$_2$Ph)(C$_6$F$_5$)$_2$] (**45**): -131.85 ppm (*o*-F), -160.66 ppm (*p*-F), -166.68 ppm (*m*-F) (Figure 2.30).
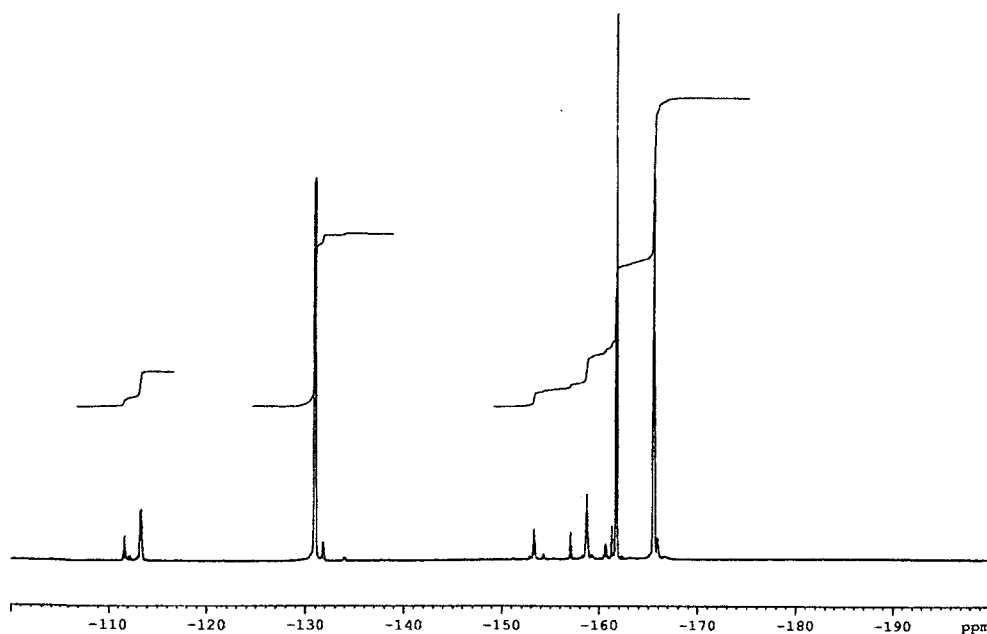
Figure 2.30 ^{19}F NMR spectrum in C$_6$D$_5$Br of [Mg(η^2-TEEDA)(CH$_2$Ph)$_2$] with B(C$_6$F$_5$)$_3$

Similarly there are 3 boron environments in the ^{11}B NMR spectrum: δ –9.20, -13.15 and 85.10 ppm. The presence of $[B(CH_2Ph)(C_6F_5)_3]^-$ is observed at 2.61 ppm in the ^{1}H NMR spectrum, where as $B(CH_2Ph)(C_6F_5)_2$ is observed at 3.19 ppm.

Note, the large $\Delta\delta$ (m, p-F) of 3.84 ppm for $[B(CH_2Ph)(C_6F_5)_3]^-$, in the ^{19}F NMR spectrum, suggests co-ordination of the anion via the CH_2 group. However, the Ar-H environments range from slightly higher resonances of 6.71-7.16 ppm (c.f. 6.65-7.08 ppm for unreacted $[Mg(\eta^2\text{-TEEDA})(CH_2Ph)_2]$ (31). The ^{13}C NMR shows a shift of the Ar-H resonances to higher frequency 123.90, 125.56, 128.08, 129.22, 129.72 and 132.19 ppm (c.f. to 116.65 ppm (p-ArCH), 124.26 ppm (m-ArCH), 128.44 ppm (o-ArCH), 156.62 ppm (C_{ipso}) for unreacted (31), The peak at 24.19 ppm (CH_2Ph in unreacted (31) is absent, however this may be due to the minimum number of scans being used to collect the data due to time constraints. It is not entirely clear what is happening in this system, except that C_6F_5 transfer is occuring.

2.5. Activation of Diamine and Triamine MgR_2 Complexes with $[NHMe_2Ph][B(C_6F_5)_4]$

In general we expected the activator $[NHMe_2Ph][B(C_6F_5)_4]$ (5) to react with the magnesium methyl complexes to produce the activated cation $[Mg(\eta^2\text{-diamine})(NMe_2Ph)Me]^+$ and the anion $[MeB(C_6F_5)_4]^-$ which is non-coordinating (Figure 2.31). Both the ^{1}H and ^{13}C NMR spectra of $[NHMe_2Ph][B(C_6F_5)_4]$ (5) and NMe_2Ph were recorded in C_6D_5Br and CD_2Cl_2 for use in interpreting the reaction spectra.
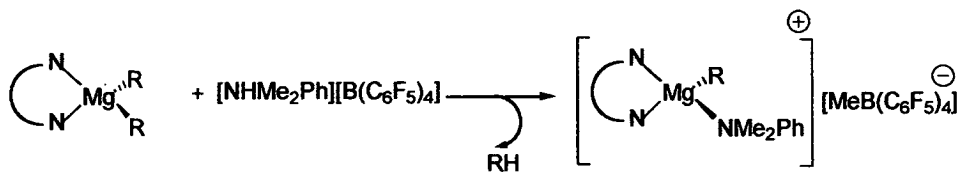
Figure 2.31 Activation of $[Mg(\eta^2\text{-amine})Me_2]$ with $[NHMe_2Ph][B(C_6F_5)_4]$

The reactions were initially carried out on NMR scale due to the expensive nature of the activator. The reactions were investigated by varying the equivalents of activator to the procatalyst.

2.5.1 Activation of [Mg(η^2-TMEDA)Me$_2$] with [NHMe$_2$Ph][B(C$_6$F$_5$)$_4$]

The NMR scale reaction of [Mg(η^2-TMEDA)Me$_2$] (**23**) with [NHMe$_2$Ph][B(C$_6$F$_5$)$_4$] (**5**) (1:1 equivalent) in CD$_2$Cl$_2$ was investigated. The reaction product was analysed by ^{1}H , ^{19}F, ^{11}B and ^{13}C NMR spectroscopies. The ^{19}F NMR spectrum shows the presence of one product with signals at δ -133.50 (m, *o*-F), -163.95 (*p*-F), -167.88 (*m*-F). Therefore, the reaction product of [Mg(η^2-TMEDA)Me$_2$] with [NHMe$_2$Ph][B(C$_6$F$_5$)$_4$] gives a stable product that is not susceptible to C$_6$F$_5$ transfer. The ^{1}H NMR spectrum (Figure 2.33) displays two NMe$_2$ environments (2.91 ppm and 3.61 ppm) and 5 Ar-H signals (6.66, 6.72, 7.20, 7.52 and 7.68 ppm). In free NMe$_2$Ph a singlet for the NMe$_2$ group occurs at 2.93 ppm, and for [NHMe$_2$Ph][B(C$_6$F$_5$)$_4$] the NMe$_2$ singlet occurs at 3.42 ppm. Looking at the reaction ^{1}H NMR spectrum, it appears that the NMe$_2$Ph biproduct must be uncoordinated. However there are 5 Ar-H environments observed, and the two NMe$_2$ peaks integrate to 3H each, thus suggesting the co-ordination of NMe$_2$Ph to the magnesium centre in such a sterically hindered fashion that there is no rotation about the Mg-N bond rendering the two N-methyl groups inequivalent.
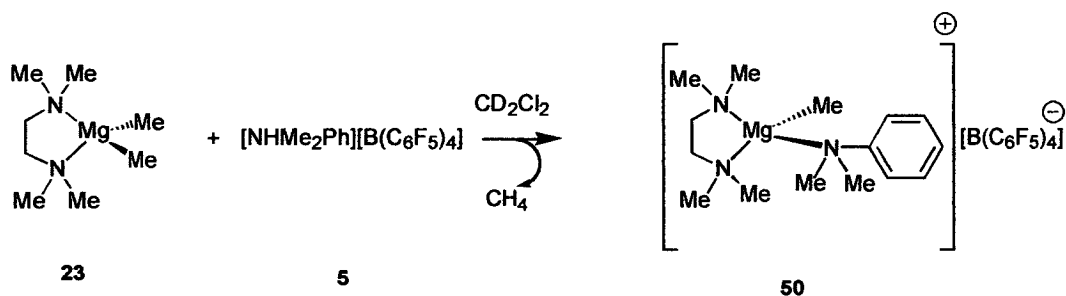
Figure 2.32 Activation of [Mg(η^2-TMEDA)Me$_2$] with [NHMe$_2$Ph][B(C$_6$F$_5$)$_4$]

To investigate the situation further a ^{1}H-^{1}H COSY experiment was implemented (Figure 2.34). The COSY suggests that the NMe groups at 2.91 ppm and 3.63 ppm couple to one another, and are in close proximity but inequivalent. It also indicates that the Ar-H signals at 6.66 ppm, 6.72 ppm and 7.20 ppm couple to one another, and that those at 7.52 ppm and 7.68 ppm couple separately to one another. Further

characterisation of the reaction product is required to determine the nature of the reaction product, e.g. elucidation of a X-Ray structure or low temperature NMR.
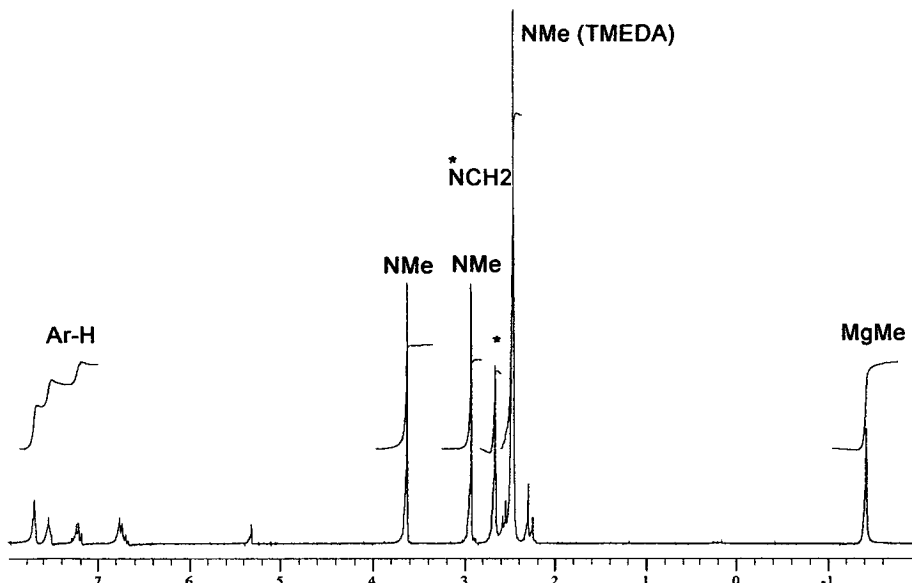
Figure 2.33 ^{1}H NMR spectrum of [Mg(η^2-TMEDA)(Me)(NMe$_2$Ph)][B(C$_6$F$_5$)$_4$] (50) in CD$_2$Cl$_2$
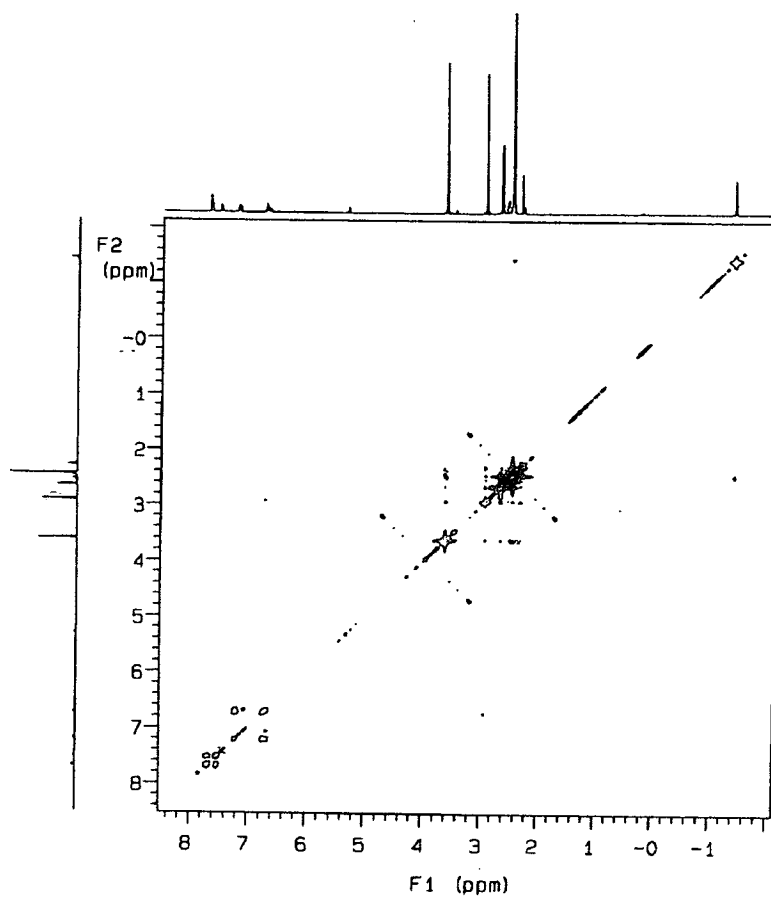
Figure 2.34 ^{1}H-^{1}H COSY spectrum of [Mg(η^2-TMEDA)(Me)(NMe$_2$Ph)][B(C$_6$F$_5$)$_4$] (50) in CD$_2$Cl$_2$

2.5.2 Activation of [Mg(η^2-TEEDA)Me₂] and [Mg(η^3-PMDETA)Me₂] with [NHMe₂Ph][B(C₆F₅)₄]

Reaction of both [Mg(η^2-TEEDA)Me₂] (**25**) and [Mg(η^2-PMDETA)Me₂] (**24**) with [NHMe₂Ph][B(C₆F₅)₄] (**5**) in a variety of solvents (C₆D₆, Tol-d_8, CD₂Cl₂ and C₆D₅Br) produces partially soluble products that can not be clearly identified by NMR. However, addition of an equivalent of THF produces spectra that are characterisable (Figure 2.35).

For comparison NMe₂Ph and THF were analysed by ¹H NMR in C₆D₅Br.

A singlet for free NMe₂Ph is clearly identifiable at 2.66 ppm, whereas free THF displays signals at 1.55 ppm (m, 4H, CH₂) and 3.57 ppm (m, 4H, CH₂O).

Comparing the NMe₂Ph signals in the ¹H NMR spectra obtained for the TEEDA reaction i.e. spectra A and B in Figure 2.35 (2.64 ppm and 2.66 ppm respectively), it is clear that the NMe₂Ph byproduct is uncoordinated. Possibly, because of the increased bulk of the ligand around the metal centre (Figure 2.36). Comparison of the THF signal positions reveals that the THF is also non co-ordinating (1.57 ppm and 3.50 ppm).
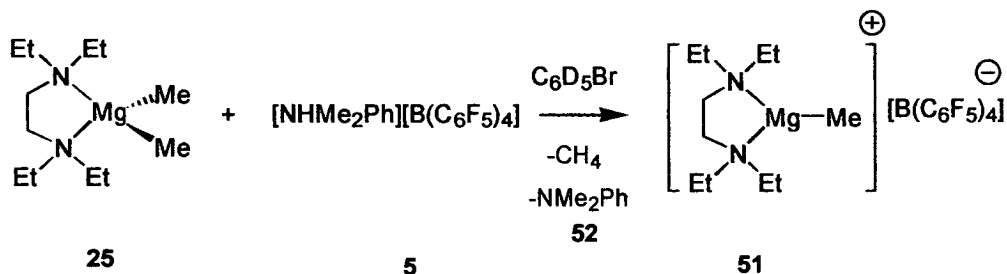
Figure 2.36 Reaction of [Mgη^2(TEEDA)Me₂] with [NHMe₂Ph][B(C₆F₅)₄] (1:1) in C₆D₅Br (in the absence and presence of THF)

(A)

(B)
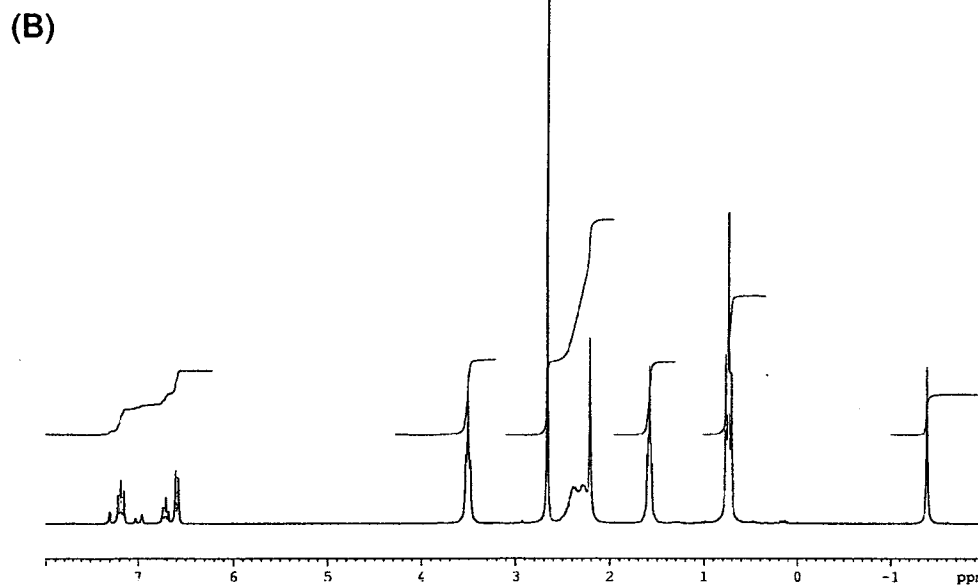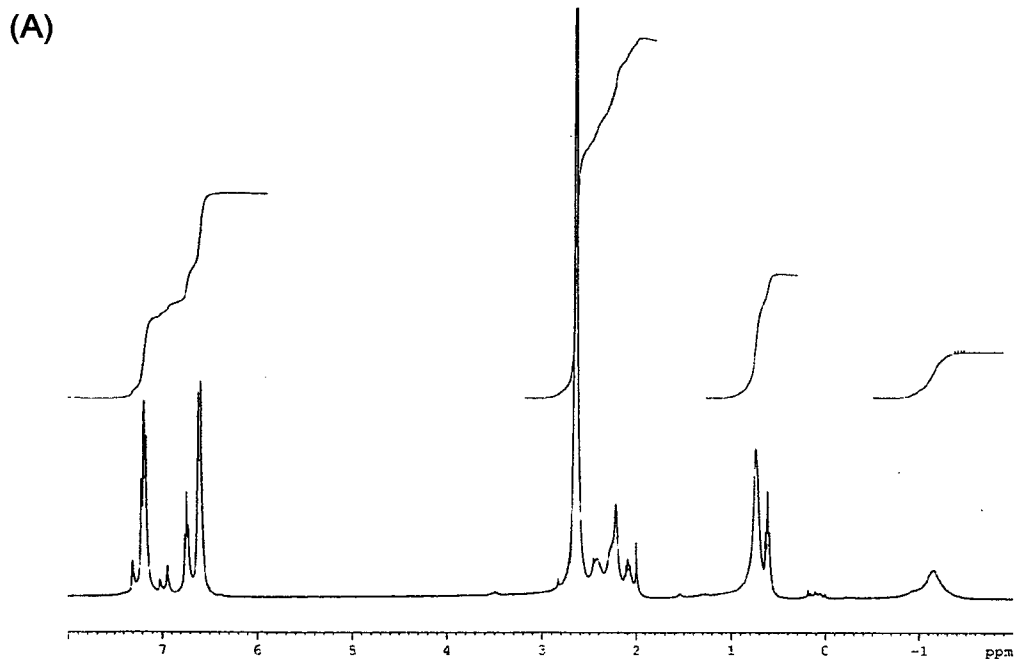
Figure 2.35 ^{1}H NMR spectrum of [Mg(η^2-TEEDA)Me$_2$] with [NHMe$_2$Ph][B(C$_6$F$_5$)$_4$] (1:1) in C$_6$D$_5$Br: (A) in the absence of THF and (B) in the presence of THF.

The ^{19}F NMR spectra, in C_6D_5Br, are identical for the partially soluble reaction product (no THF) and the soluble reaction product (in presence of THF) which correspond to the anion $[B(C_6F_5)_4]^-$: -132.40 ppm (*o*-F), -162.03 ppm (*p*-F) and -166.20 ppm (*m*-F) for the (no THF), and -131.89 ppm (*o*-F), -162.10 ppm (*p*-F), -166.08 ppm (*m*-F) (with THF). The ^{11}B NMR spectrum produced contains a singlet at -13.12 ppm.

The reaction of $[Mg(\eta^3\text{-PMDETA})Me_2]$ with $[NHMe_2Ph][B(C_6F_5)_4]$ produces similar results to that observed for $[Mg(\eta^2\text{-TEEDA})Me_2]$ (Figure 2.37). The ^{1}H NMR of the reaction product in C_6D_5Br reveals free NMe_2Ph (**52**) and THF in solution. The ^{19}F NMR spectra correspond to the maintenance of the anion $[B(C_6F_5)_4]^-$: -131.89 ppm (*o*-F), -161.57 ppm (*p*-F) and −165.75 ppm (*m*-F) (no THF), and -131.86 ppm (*o*-F), - 162.00 ppm (*p*-F), -165.94 ppm (*m*-F) (with THF), in C_6D_5Br. The ^{11}B NMR spectrum displays a singlet at −13.13 ppm.
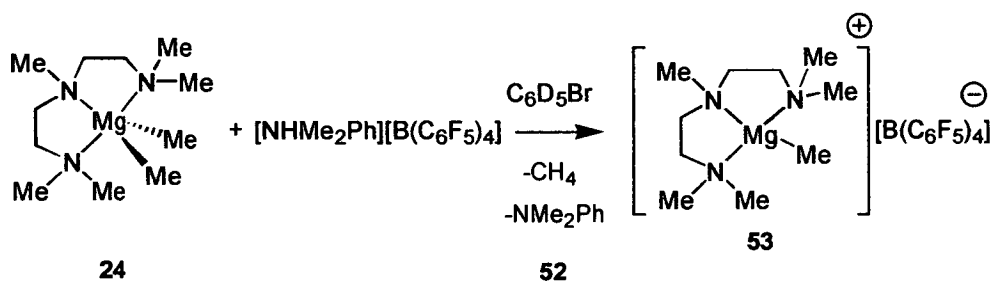
Figure 2.37 Reaction of [Mg(η^3-PMDETA)Me$_2$] with [NHMe$_2$Ph][B(C$_6$F$_5$)$_4$] (1:1) in C$_6$D$_5$Br in the absence and presence of THF.

2.5.3 Activation of [Mg(η^2-TMEDA)(CH$_2$Ph)$_2$] & [Mg(η^2-TEEDA)(CH$_2$Ph)$_2$] with [NHMe$_2$Ph][B(C$_6$F$_5$)$_4$]

Reaction of [Mg(η^2-TMEDA)(CH$_2$Ph)$_2$] (**30**) or [Mg(η^2-TEEDA)(CH$_2$Ph)$_2$] (**31**) with [NHMe$_2$Ph][B(C$_6$F$_5$)$_4$] (**5**) in C$_6$D$_5$Br produces very clean, soluble and easily characterisable products.

The ^{1}H NMR spectra show the formation of two byproducts: toluene and NMe$_2$Ph (Figure 2.39). The NMe$_2$Ph molecule formed is coordinated, with the NMe$_2$ group showing a slight shift from 2.66 ppm in the free ligand to 2.41 ppm for the reaction of {[Mg(η^2-TMEDA)(CH$_2$Ph)$_2$] + [NHMe$_2$Ph][B(C$_6$F$_5$)$_4$]} and 2.48 ppm for the reaction of {[Mg(η^2-TEEDA)(CH$_2$Ph)$_2$] + [NHMe$_2$Ph][B(C$_6$F$_5$)$_4$]}(Figure 2.38). The Me groups in the TMEDA and TEEDA ligands appear to be equivalent. The singlet for the Me groups of the TMEDA ligand is very broad, which could be indicative of fluctional behaviour, which is fast on the NMR time scale.

The ^{19}F NMR spectrum is very clean for both compounds –131.85 ppm (*o-F*), -161.84 ppm (*p-F*) and –165.84 ppm (*m-F*) for [Mg(η^2-TMEDA)(CH$_2$Ph)(NMe$_2$Ph)][B(C$_6$F$_5$)$_4$] (**54**); and –131.83 ppm (*o-F*), -161.78 ppm (*p-F*) and –165.89 ppm (*m-F*) for [[Mg(η^2-TEEDA)(CH$_2$Ph)(NMe$_2$Ph)][B(C$_6$F$_5$)$_4$] (**55**). Again no C$_6$F$_5$ transfer is observed in either reaction. The ^{11}B NMR spectra of **54** and **55** contain singlets at -13.11 ppm and –13.11 ppm respectively.

(A)
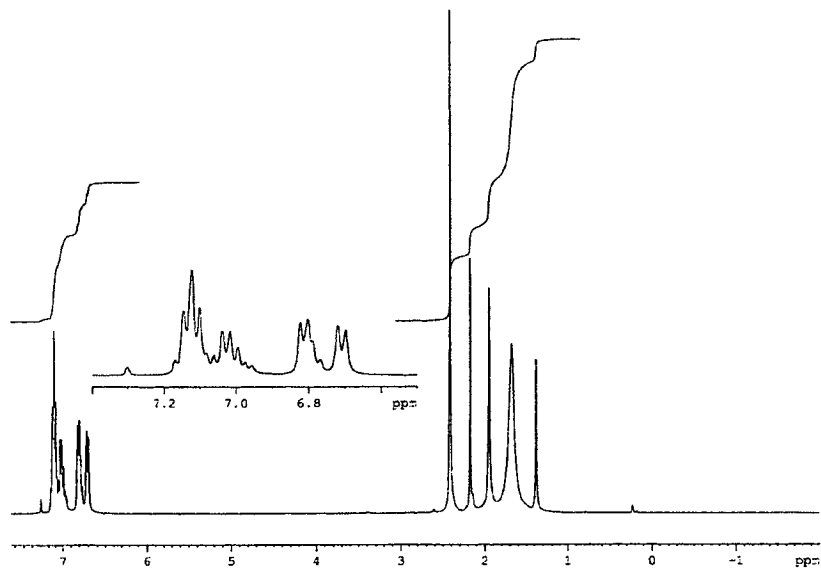
(B)
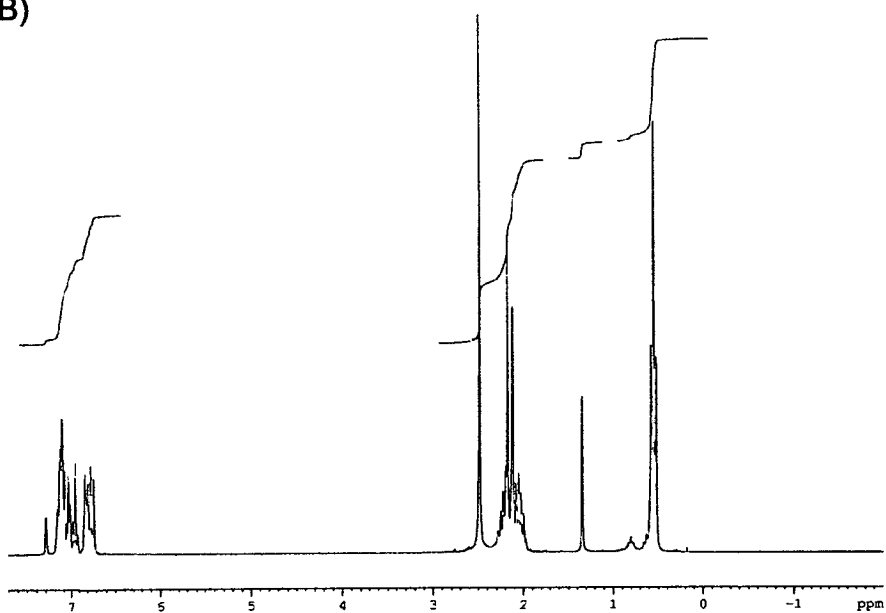
Figure 2.38 ^{1}H NMR spectrum of (A) [Mg(η^2-TMEDA)(CH$_2$Ph)(NMe$_2$Ph)][B(C$_6$F$_5$)$_4$] (54) and (B) [Mg(η^2-TEEDA) (CH$_2$Ph)(NMe$_2$Ph)] [B(C$_6$F$_5$)$_4$] (55); in the presence of toluene and free NMe$_2$Ph

Addition of THF to the reaction mixtures of [Mg(η^2-TMEDA)(CH$_2$Ph)$_2$] + [NHMe$_2$Ph][B(C$_6$F$_5$)$_4$] and [Mg(η^2-TEEDA)(CH$_2$Ph)$_2$] + [NHMe$_2$Ph][B(C$_6$F$_5$)$_4$]

produce the THF solvates [Mg(η^2-TMEDA)(CH$_2$Ph)(THF)] [B(C$_6$F$_5$)$_4$] (**56**) and

[Mg(η^2-TEEDA)(CH$_2$Ph)(THF)] [B(C$_6$F$_5$)$_4$] (**57**) respectively (Figure 2.39).

The THF signals are shifted to a lower frequency of 3.39 ppm /1.51 ppm in the case

of the TMEDA complex and 3.47 ppm/1.54 ppm for the TEEDA complex. With the

NMe$_2$Ph signals in both cases being clearly visible at 2.66 ppm, corresponding to the

aniline being uncoordinated.
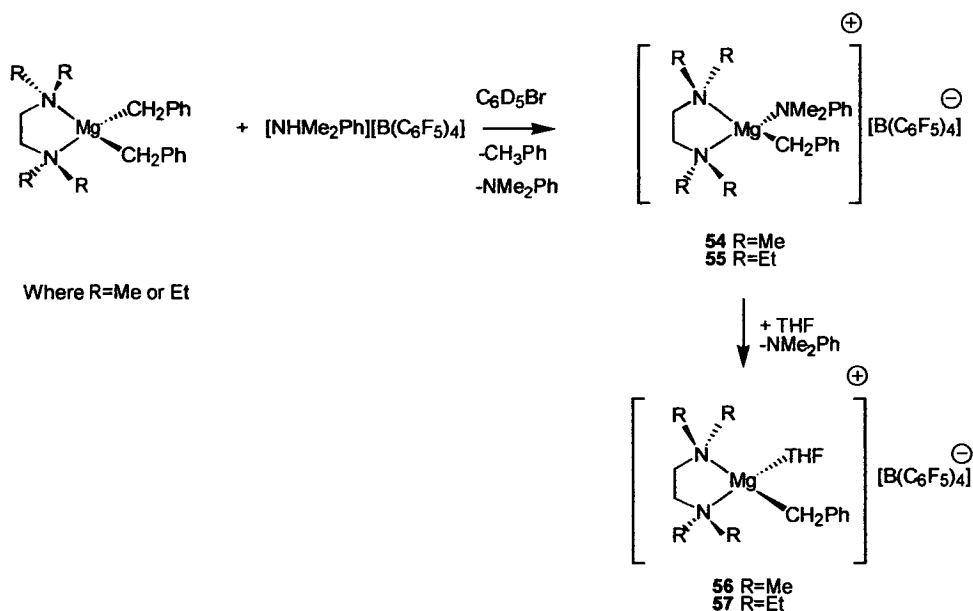
Figure 2.39 Reaction of [Mg(R$_2$NCH$_2$)$_2$(CH$_2$Ph)$_2$] (where R= Me or Et) with [NHMe$_2$Ph] [B(C$_6$F$_5$)$_4$] in the absence or presence of THF

2.6 Activation of Diamine and Triamine MgR$_2$ Complexes with [CPh$_3$][B(C$_6$F$_5$)$_4$]

Reaction of [Mg(η^2-TMEDA)Me$_2$], [Mg(η^2-TEEDA)Me$_2$], [Mg(η^3-PMDETA)Me$_2$],

[Mg(η^2-TMEDA)(CH$_2$Ph)$_2$]and [Mg(η^2-TEEDA)(CH$_2$Ph)$_2$]with [CPh$_3$][B(C$_6$F$_5$)$_4$]

in a variety of solvents (C$_6$D$_6$, Tol-d_8, CD$_2$Cl$_2$ and C$_6$D$_5$Br) produces insoluble

products that can not be identified by NMR. However, addition of an equivalent of

THF produces spectra that are characterisable. Both biproducts MeCPh$_3$ and

PhCH$_2$CPh$_3$ are soluble in C$_6$D$_5$Br and CD$_2$Cl$_2$ and can be identified by ^{1}H NMR

spectroscopy. For reference MeCPh$_3$ produces a methyl signal at 2.03 ppm in

C$_6$D$_5$Br. Whereas, PhCH$_2$CPh$_3$ produces a signal at 3.97 ppm in CD$_2$Cl$_2$.

2.6.1 Activation of [Mg(η²-TEEDA)Me₂] and [CPh₃][B(C₆F₅)₄]

Due to the insolubility of the product formed during the reaction of

[Mg(η²-TEEDA)Me₂] (**25**) with [CPh₃][B(C₆F₅)₄] (**3**) in C₆D₅Br the ¹H NMR

spectrum only contains signals corresponding to CPh₃Me (2.03 ppm, CMe).

The ¹⁹F NMR spectrum shows three principal signals at -133.36 ppm (*o*-F),

-160.64 ppm (*p*-F) and -165.19 ppm (*m*-F)), with a trace of decomposition products

via C₆F₅ transfer (Figure 2.40). The ¹¹B NMR spectrum contains an intense singlet at

−13.30 ppm.
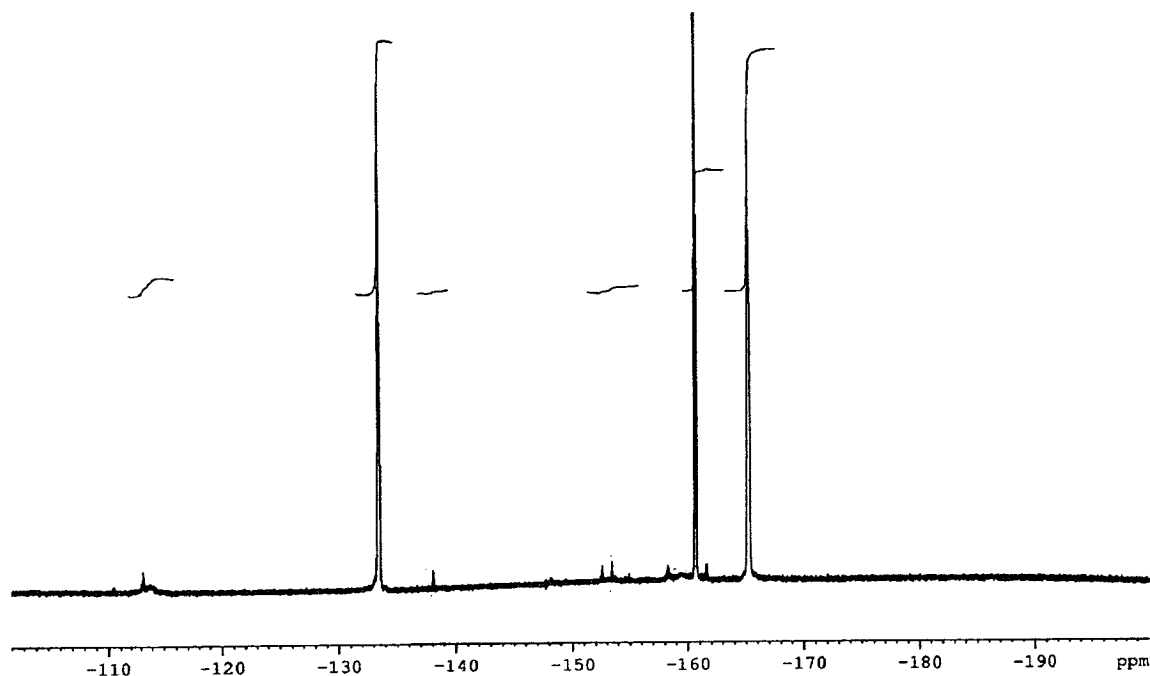
Fig 2.40 ¹⁹F NMR spectrum of the reaction of [Mg(η²-TEEDA)Me₂] with
[NHMe₂Ph][B(C₆F₅)₄] (1:1) in C₆D₅Br

Addition of THF to the reaction mixture produces a soluble product that on ¹H NMR

analysis is identifiable as being [Mg(η²-TEEDA)(Me)][B(C₆F₅)₄] (**51**) (as produced

in the reaction of [Mg(η²-TEEDA)Me₂] with [NHMe₂Ph₂][B(C₆F₅)₄]), where the

complex remains unsolvated.
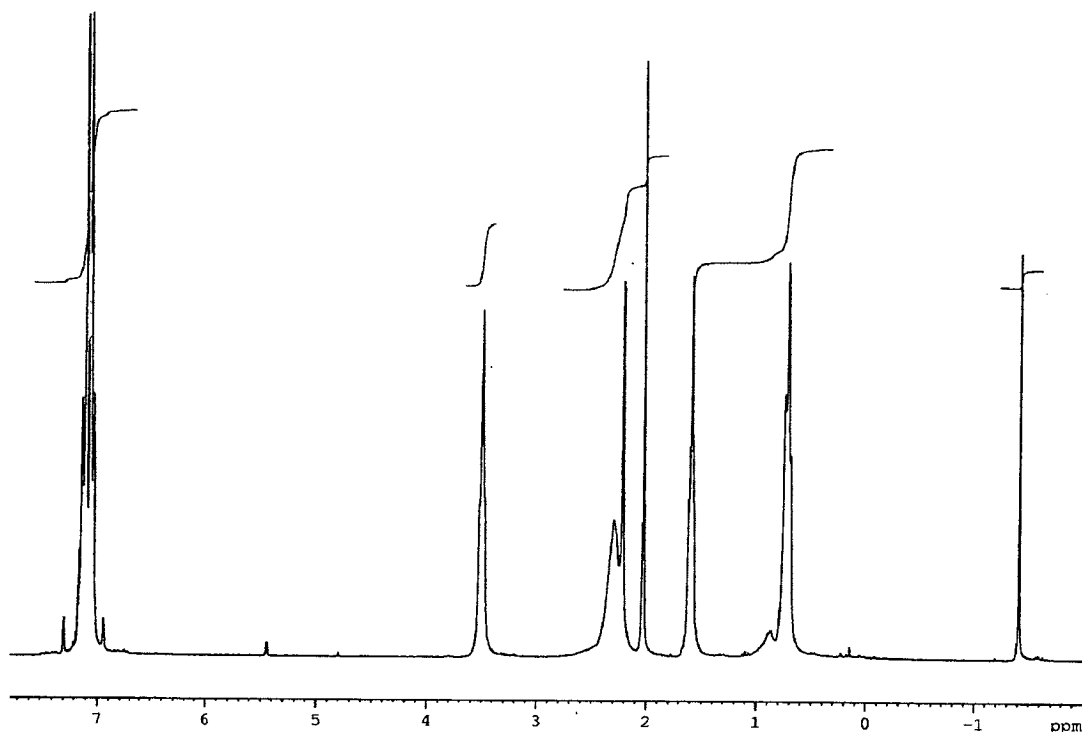
Fig 2.41 Reaction of [Mg(η²-TEEDA)(CH₂Ph)₂] with [CPh₃][B(C₆F₅)₄] (1:1) in C₆D₅Br followed by the addition of THF.

This is similarly the case with the reaction of $[Mg(\eta^3\text{-PMDETA)Me}_2]$ with $[CPh_3][B(C_6F_5)_4]$, where some trace decomposition is observed in the ^{19}F NMR *via* C_6F_5 transfer. The complex $[Mg(\eta^3\text{-PMDETA)Me}][B(C_6F_5)_4]$ (**53**) is produced which on addition to THF remains unsolvated.

2.6.2 Activation of [Mg(η²-TMEDA)(CH₂Ph)₂] & [Mg(η²-TEEDA)(CH₂Ph)₂] with [CPh₃][B(C₆F₅)₄]

The ^1H NMR spectra obtained by the reaction of $[Mg(\eta^2\text{-TMEDA)(CH}_2Ph)_2]$ (**30**) and $[Mg(\eta^2\text{-TEEDA)(CH}_2Ph)_2]$ (**31**) with $[CPh_3][B(C_6F_5)_4]$ in C_6D_5Br are very complex. The ^{19}F NMR spectra, similar to the equivalent dimethyl complexes, show trace evidence of decomposition by C_6F_5 transfer (Figure 2.42). Addition of THF, firstly in the case of $[Mg(\eta^2\text{-TMEDA)(CH}_2Ph)_2]$ produces very noisy ^1H and ^{19}F NMR spectra due to insolubilty. However, in the case of $[Mg(\eta^2\text{-TEEDA)(CH}_2Ph)_2]$ addition of THF clearly produces $[Mg(\eta^2\text{-TEEDA)(CH}_2Ph)(THF)][B(C_6F_5)_4]$ (**57**) (Figures 2.43 and 2.44).

Figure 2.42 Reaction of [Mg(η²-TEEDA)(CH₂Ph)₂] (31) with [CPh₃][B(C₆F₅)₄] (3) and THF

Figure 2.43 ¹H NMR spectrum produced from the reaction [Mg(η²-TEEDA)(CH₂Ph)₂] (31) with [CPh₃][B(C₆F₅)₄] (3) and THF in C₆F₅Br
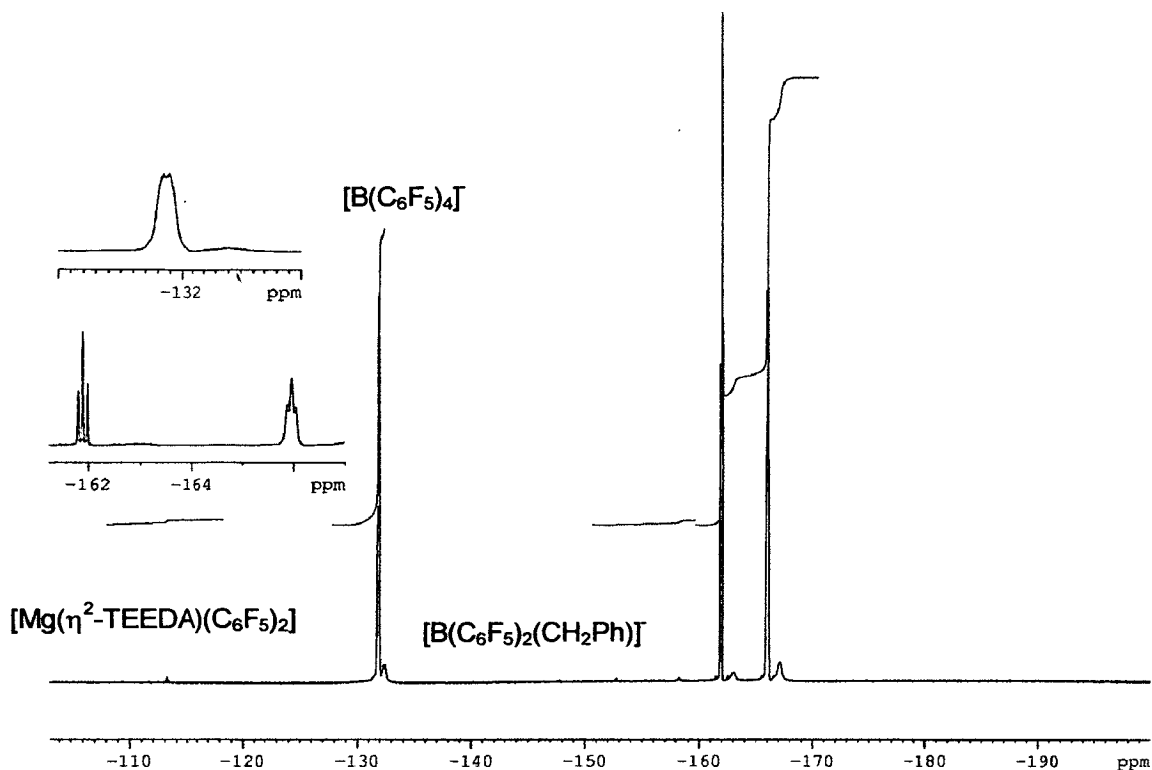
Figure 2.44 ^{19}**F NMR spectrum produced from the reaction of [Mg(η^2-TEEDA)(CH$_2$Ph)$_2$] (31) with [CPh$_3$][B(C$_6$F$_5$)$_4$] (3) and THF in C$_6$F$_5$Br**

2.7 Crystallisation Attempts

A general procedure was followed in a study into growing X-ray diffraction quality crystals of the products of the reactions of [Mg(η^2-TMEDA)(Me)$_2$] (**23**), [Mg(η^2-TEEDA)(Me)$_2$] (**25**),[Mg(η^2-TMEDA)(CH$_2$Ph)$_2$] (**30**) and [Mg(η^2-TEEDA)(CH$_2$Ph)$_2$] (**31**) with B(C$_6$F$_5$)$_3$(**4**), [CPh$_3$][B(C$_6$F$_5$)$_4$](**3**) and [NHMe$_2$Ph][B(C$_6$F$_5$)$_4$] (**5**).

2.7.1 General Procedure

The solid complex (~ 0.4 mmoles) was weighed into a Schlenk tube in the glove box and the corresponding activator (~ 0.4 mmoles) weighed and added. Toluene was added (5 cm^3) and the reaction mixture stirred for 30 mins. The products separated as liquid clathrates, i.e. oils containing the species and solvent, on addition of the toluene.

It is very challenging trying to grow crystals from liquid clathrates but it can be achieved as shown by similar circumstances by the reaction of aluminium alkyl complexes with boron based activators.[22, 23]

The liquids were heated and filtered and the supernatant placed in vials in the glovebox. The solvent was removed in vacuum from the oily/solid remaining in the Schlenk tube, and benzene added, again the liquids were heated and filtered and the supernatant placed in the glovebox. After several weeks, colourless rods were grown from the reactions of $[Mg(\eta^2\text{-}TMEDA)(Me)_2]$ (23) with $[NHMe_2Ph][\ B(C_6F_5)_4]$ (5) in toluene and $[CPh_3][\ B(C_6F_5)_4]$(3) in benzene and $[Mg(\eta^2\text{-}TMEDA)(CH_2Ph)_2]$ (30) with $[NHMe_2Ph][B(C_6F_5)_4]$ (5) in benzene. The product in all cases was structurally determined to be $[N(H)Me_2CH_2CH_2NMe_2][B(C_6F_5)_4]$(61), and must have been formed by hydrolysis in the presence of water (Figures 2.45 and 2.46). All other attempts to grow crystals from these reactions failed.
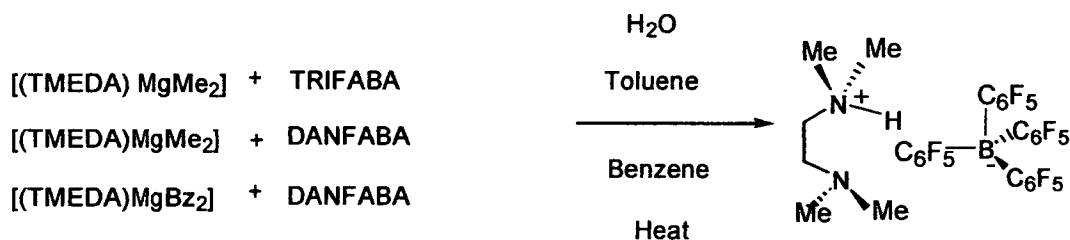
Figure 2.45 Preparation of $[N(H)Me_2CH_2CH_2NMe_2][B(C_6F_5)_4]$(61)
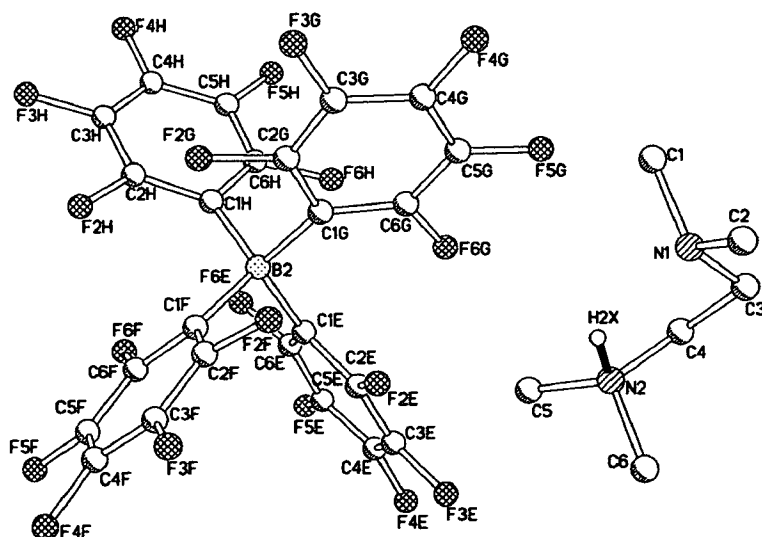
Figure 2.46 Molecular structure of $[N(H)Me_2CH_2CH_2NMe_2][B(C_6F_5)_4]$ (61), with atom labelling, hydrogen atoms omitted for clarity.

Clearly, with the reaction products being susceptible to hydrolysis they should have been manipulated less to enhance the opportunity of obtaining the desired metal cation-anion complexes. The bond lengths and angles from the solid structure of **61** are listed in Tables 2.06-2.07.

B(1)-C(1D)	1.650(4)	C(1D)-C(2D)	1.384(4)	C(1G)-C(6G)	1.380(4)
B(1)-C(1A)	1.650(4)	C(1D)-C(6D)	1.389(4)	C(1G)-C(2G)	1.388(4)
B(1)-C(1B)	1.652(4)	C(2D)-F(2D)	1.351(3)	C(2G)-F(2G)	1.358(3)
B(1)-C(1C)	1.656(4)	C(2D)-C(3D)	1.377(4)	C(2G)-C(3G)	1.371(4)
C(1A)-C(2A)	1.375(4)	C(3D)-F(3D)	1.352(3)	C(3G)-F(3G)	1.343(3)
C(1A)-C(6A)	1.383(4)	C(3D)-C(4D)	1.365(4)	C(3G)-C(4G)	1.371(4)
C(2A)-F(2A)	1.357(3)	C(4D)-F(4D)	1.354(3)	C(4G)-F(4G)	1.338(3)
C(2A)-C(3A)	1.385(4)	C(4D)-C(5D)	1.371(4)	C(4G)-C(5G)	1.373(4)
C(3A)-F(3A)	1.357(3)	C(5D)-F(5D)	1.342(3)	C(5G)-F(5G)	1.344(3)
C(3A)-C(4A)	1.364(5)	C(5D)-C(6D)	1.363(4)	C(5G)-C(6G)	1.382(4)
C(4A)-F(4A)	1.351(3)	C(6D)-F(6D)	1.359(3)	C(6G)-F(6G)	1.360(3)
C(4A)-C(5A)	1.364(4)	B(2)-C(1G)	1.642(4)	C(1H)-C(2H)	1.380(4)
C(5A)-F(5A)	1.347(3)	B(2)-C(1H)	1.646(4)	C(1H)-C(6H)	1.386(4)
C(5A)-C(6A)	1.375(4)	B(2)-C(1F)	1.653(4)	C(2H)-F(2H)	1.356(3)
C(6A)-F(6A)	1.355(3)	B(2)-C(1E)	1.657(4)	C(2H)-C(3H)	1.380(4)
C(1B)-C(6B)	1.378(4)	C(1E)-C(6E)	1.383(4)	C(3H)-F(3H)	1.352(3)
C(1B)-C(2B)	1.387(4)	C(1E)-C(2E)	1.389(4)	C(3H)-C(4H)	1.364(4)
C(2B)-F(2B)	1.365(3)	C(2E)-F(2E)	1.361(3)	C(4H)-F(4H)	1.349(3)
C(2B)-C(3B)	1.369(4)	C(2E)-C(3E)	1.363(4)	C(4H)-C(5H)	1.364(4)
C(3B)-F(3B)	1.347(3)	C(3E)-F(3E)	1.347(3)	C(5H)-F(5H)	1.343(3)
C(3B)-C(4B)	1.369(4)	C(3E)-C(4E)	1.369(4)	C(5H)-C(6H)	1.373(4)
C(4B)-F(4B)	1.344(3)	C(4E)-F(4E)	1.341(3)	C(6H)-F(6H)	1.364(3)
C(4B)-C(5B)	1.366(4)	C(4E)-C(5E)	1.370(4)	C(1)-N(1)	1.455(4)
C(5B)-F(5B)	1.353(3)	C(5E)-F(5E)	1.347(3)	C(2)-N(1)	1.466(4)
C(5B)-C(6B)	1.373(4)	C(5E)-C(6E)	1.380(4)	N(1)-C(3)	1.453(4)
C(6B)-F(6B)	1.358(3)	C(6E)-F(6E)	1.352(3)	C(3)-C(4)	1.528(4)
C(1C)-C(6C)	1.384(4)	C(1F)-C(6F)	1.385(4)	C(4)-N(2)	1.488(4)
C(1C)-C(2C)	1.388(4)	C(1F)-C(2F)	1.390(4)	N(2)-C(5)	1.481(4)
C(2C)-F(2C)	1.348(3)	C(2F)-F(2F)	1.352(3)	N(2)-C(6)	1.489(4)
C(2C)-C(3C)	1.379(4)	C(2F)-C(3F)	1.379(4)	C(7)-N(3)	1.460(5)
C(3C)-F(3C)	1.357(3)	C(3F)-F(3F)	1.348(3)	C(8)-N(3)	1.443(5)
C(3C)-C(4C)	1.359(4)	C(3F)-C(4F)	1.359(4)	N(3)-C(9)	1.478(5)
C(4C)-F(4C)	1.351(3)	C(4F)-F(4F)	1.341(3)	C(9)-C(10)	1.454(6)
C(4C)-C(5C)	1.369(4)	C(4F)-C(5F)	1.376(4)	C(10)-N(4)	1.457(4)
C(5C)-F(5C)	1.353(3)	C(5F)-F(5F)	1.346(3)	N(4)-C(12)	1.456(4)
C(5C)-C(6C)	1.372(4)	C(5F)-C(6F)	1.366(4)	N(4)-C(11)	1.459(4)
C(6C)-F(6C)	1.357(3)	C(6F)-F(6F)	1.354(3)		

Table 2.06 Bond lengths (Å) for [N(H)Me$_2$CH$_2$CH$_2$NMe$_2$][B(C$_6$F$_5$)$_4$] (61)

C(1D)-B(1)-C(1A)	114.0(2)	F(6C)-C(6C)-C(5C)	115.9(2)	F(5F)-C(5F)-C(6F)	120.3(3)
C(1D)-B(1)-C(1B)	112.9(2)	F(6C)-C(6C)-C(1C)	119.3(2)	F(5F)-C(5F)-C(4F)	119.8(3)
C(1A)-B(1)-C(1B)	101.4(2)	C(5C)-C(6C)-C(1C)	124.9(3)	C(6F)-C(5F)-C(4F)	119.9(3)
C(1D)-B(1)-C(1C)	102.1(2)	C(2D)-C(1D)-C(6D)	112.7(3)	F(6F)-C(6F)-C(5F)	115.8(2)
C(1A)-B(1)-C(1C)	113.4(2)	C(2D)-C(1D)-B(1)	127.9(3)	F(6F)-C(6F)-C(1F)	119.4(2)
C(1B)-B(1)-C(1C)	113.6(2)	C(6D)-C(1D)-B(1)	119.3(3)	C(5F)-C(6F)-C(1F)	124.8(3)
C(2A)-C(1A)-C(6A)	113.4(3)	F(2D)-C(2D)-C(3D)	115.1(3)	C(6G)-C(1G)-C(2G)	112.9(3)
C(2A)-C(1A)-B(1)	127.2(3)	F(2D)-C(2D)-C(1D)	121.0(3)	C(6G)-C(1G)-B(2)	127.8(3)
C(6A)-C(1A)-B(1)	118.8(2)	C(3D)-C(2D)-C(1D)	123.9(3)	C(2G)-C(1G)-B(2)	119.1(3)
F(2A)-C(2A)-C(1A)	122.0(3)	F(3D)-C(3D)-C(4D)	119.2(3)	F(2G)-C(2G)-C(3G)	115.6(3)
F(2A)-C(2A)-C(3A)	114.5(3)	F(3D)-C(3D)-C(2D)	120.8(3)	F(2G)-C(2G)-C(1G)	119.1(2)
C(1A)-C(2A)-C(3A)	123.4(3)	C(4D)-C(3D)-C(2D)	120.0(3)	C(3G)-C(2G)-C(1G)	125.3(3)
F(3A)-C(3A)-C(4A)	119.8(3)	F(4D)-C(4D)-C(3D)	120.0(3)	F(3G)-C(3G)-C(4G)	119.6(3)
F(3A)-C(3A)-C(2A)	119.9(3)	F(4D)-C(4D)-C(5D)	120.9(3)	F(3G)-C(3G)-C(2G)	121.4(3)
C(4A)-C(3A)-C(2A)	120.3(3)	C(3D)-C(4D)-C(5D)	119.1(3)	C(4G)-C(3G)-C(2G)	119.0(3)
F(4A)-C(4A)-C(5A)	121.2(3)	F(5D)-C(5D)-C(6D)	121.4(3)	F(4G)-C(4G)-C(3G)	120.9(3)
F(4A)-C(4A)-C(3A)	120.1(3)	F(5D)-C(5D)-C(4D)	119.8(3)	F(4G)-C(4G)-C(5G)	120.4(3)
C(5A)-C(4A)-C(3A)	118.8(3)	C(6D)-C(5D)-C(4D)	118.9(3)	C(3G)-C(4G)-C(5G)	118.8(3)
F(5A)-C(5A)-C(4A)	120.3(3)	F(6D)-C(6D)-C(5D)	115.7(3)	F(5G)-C(5G)-C(4G)	120.1(3)
F(5A)-C(5A)-C(6A)	120.5(3)	F(6D)-C(6D)-C(1D)	118.8(3)	F(5G)-C(5G)-C(6G)	120.0(3)
C(4A)-C(5A)-C(6A)	119.2(3)	C(5D)-C(6D)-C(1D)	125.5(3)	C(4G)-C(5G)-C(6G)	119.9(3)
F(6A)-C(6A)-C(5A)	115.9(3)	C(1G)-B(2)-C(1H)	101.9(2)	F(6G)-C(6G)-C(1G)	121.2(3)
F(6A)-C(6A)-C(1A)	119.2(3)	C(1G)-B(2)-C(1F)	113.1(2)	F(6G)-C(6G)-C(5G)	114.7(3)
C(5A)-C(6A)-C(1A)	124.9(3)	C(1H)-B(2)-C(1F)	115.1(2)	C(1G)-C(6G)-C(5G)	124.1(3)
C(6B)-C(1B)-C(2B)	112.7(3)	C(1G)-B(2)-C(1E)	114.8(2)	C(2H)-C(1H)-C(6H)	112.7(2)
C(6B)-C(1B)-B(1)	127.5(2)	C(1H)-B(2)-C(1E)	112.5(2)	C(2H)-C(1H)-B(2)	127.5(2)
C(2B)-C(1B)-B(1)	119.4(3)	C(1F)-B(2)-C(1E)	100.0(2)	C(6H)-C(1H)-B(2)	119.3(2)
F(2B)-C(2B)-C(3B)	115.9(3)	C(6E)-C(1E)-C(2E)	112.5(3)	F(2H)-C(2H)-C(1H)	120.2(2)
F(2B)-C(2B)-C(1B)	119.2(3)	C(6E)-C(1E)-B(2)	127.3(3)	F(2H)-C(2H)-C(3H)	115.7(2)
C(3B)-C(2B)-C(1B)	125.0(3)	C(2E)-C(1E)-B(2)	119.8(2)	C(1H)-C(2H)-C(3H)	124.1(2)
F(3B)-C(3B)-C(4B)	119.8(3)	F(2E)-C(2E)-C(3E)	116.2(3)	F(3H)-C(3H)-C(4H)	119.8(3)
F(3B)-C(3B)-C(2B)	121.0(3)	F(2E)-C(2E)-C(1E)	118.3(3)	F(3H)-C(3H)-C(2H)	120.3(2)
C(4B)-C(3B)-C(2B)	119.2(3)	C(3E)-C(2E)-C(1E)	125.4(3)	C(4H)-C(3H)-C(2H)	119.9(3)
F(4B)-C(4B)-C(5B)	120.1(3)	F(3E)-C(3E)-C(2E)	120.4(3)	F(4H)-C(4H)-C(5H)	121.3(3)
F(4B)-C(4B)-C(3B)	121.1(3)	F(3E)-C(3E)-C(4E)	120.1(3)	F(4H)-C(4H)-C(3H)	119.6(3)
C(5B)-C(4B)-C(3B)	118.7(3)	C(2E)-C(3E)-C(4E)	119.5(3)	C(5H)-C(4H)-C(3H)	119.1(3)
F(5B)-C(5B)-C(4B)	119.4(3)	F(4E)-C(4E)-C(3E)	120.2(3)	F(5H)-C(5H)-C(4H)	120.6(3)
F(5B)-C(5B)-C(6B)	120.8(3)	F(4E)-C(4E)-C(5E)	121.5(3)	F(5H)-C(5H)-C(6H)	120.5(3)
C(4B)-C(5B)-C(6B)	119.8(3)	C(3E)-C(4E)-C(5E)	118.3(3)	C(4H)-C(5H)-C(6H)	118.9(3)
F(6B)-C(6B)-C(5B)	115.0(3)	F(5E)-C(5E)-C(4E)	119.7(3)	F(6H)-C(6H)-C(5H)	115.5(2)
F(6B)-C(6B)-C(1B)	120.5(2)	F(5E)-C(5E)-C(6E)	120.0(3)	F(6H)-C(6H)-C(1H)	119.2(2)
C(5B)-C(6B)-C(1B)	124.5(3)	C(4E)-C(5E)-C(6E)	120.2(3)	C(5H)-C(6H)-C(1H)	125.3(3)
C(6C)-C(1C)-C(2C)	113.2(3)	F(6E)-C(6E)-C(5E)	114.6(3)	C(3)-N(1)-C(1)	112.5(3)
C(6C)-C(1C)-B(1)	119.8(2)	F(6E)-C(6E)-C(1E)	121.4(3)	C(3)-N(1)-C(2)	112.4(2)
C(2C)-C(1C)-B(1)	126.6(2)	C(5E)-C(6E)-C(1E)	124.0(3)	C(1)-N(1)-C(2)	110.4(3)
F(2C)-C(2C)-C(3C)	115.7(2)	C(6F)-C(1F)-C(2F)	112.6(2)	N(1)-C(3)-C(4)	107.9(2)
F(2C)-C(2C)-C(1C)	121.0(3)	C(6F)-C(1F)-B(2)	119.7(2)	N(2)-C(4)-C(3)	107.4(2)
C(3C)-C(2C)-C(1C)	123.4(3)	C(2F)-C(1F)-B(2)	126.8(2)	C(5)-N(2)-C(4)	112.9(2)
F(3C)-C(3C)-C(4C)	118.7(3)	F(2F)-C(2F)-C(3F)	115.3(2)	C(5)-N(2)-C(6)	111.3(3)
F(3C)-C(3C)-C(2C)	120.7(3)	F(2F)-C(2F)-C(1F)	120.4(3)	C(4)-N(2)-C(6)	112.5(3)

Table 2.07 Bond angles (°) for [N(H)Me₂CH₂CH₂NMe₂][B(C₆F₅)₄] (61)

C(4C)-C(3C)-C(2C)	120.6(3)	C(3F)-C(2F)-C(1F)	124.2(3)	C(8)-N(3)-C(7)	112.6(4)
F(4C)-C(4C)-C(3C)	120.6(3)	F(3F)-C(3F)-C(4F)	120.1(3)	C(8)-N(3)-C(9)	109.3(4)
F(4C)-C(4C)-C(5C)	120.6(3)	F(3F)-C(3F)-C(2F)	119.8(3)	C(7)-N(3)-C(9)	112.8(4)
C(3C)-C(4C)-C(5C)	118.7(3)	C(4F)-C(3F)-C(2F)	120.1(3)	C(10)-C(9)-N(3)	113.3(4)
F(5C)-C(5C)-C(4C)	119.5(3)	F(4F)-C(4F)-C(3F)	120.5(3)	C(9)-C(10)-N(4)	110.6(3)
F(5C)-C(5C)-C(6C)	121.2(3)	F(4F)-C(4F)-C(5F)	121.1(3)	C(12)-N(4)-C(10)	110.9(3)
C(4C)-C(5C)-C(6C)	119.3(3)	C(3F)-C(4F)-C(5F)	118.3(3)	C(12)-N(4)-C(11)	109.6(3)
				C(10)-N(4)-C(11)	110.8(3)

Table 2.07 (Continued) Bond angles (°) for [N(H)Me₂CH₂CH₂NMe₂][B(C₆F₅)₄] (61)

2.8 Summary and Conclusions

The complexes $[Mg(\eta^2\text{-TMEDA})Me_2]$ (**23**), $[Mg(\eta^2\text{-TEEDA})Me_2]$ (**25**), $[Mg(\eta^3\text{-PMDETA})Me_2]$ (**24**), $[Mg(\eta^2\text{-TMEDA})(CH_2Ph)_2]$ (**30**) and $[Mg(\eta^2\text{-TMEDA})(CH_2Ph)_2]$ (**31**) can be easily prepared and characterised. Activation of complexes $[Mg(\eta^2\text{-L})(R)_2]$ (**23-25, 30-31**) with $B(C_6F_5)_3$ (**4**) produces unstable complexes that are susceptible to transfer of C_6F_5 groups to the resulting positive magnesium centre. The process can be monitored by ^{19}F NMR over several hours. In theory, migration of the C_6F_5 group back to boron could produce a single-component catalyst. However the magnesium is clearly more electrophilic/ Lewis acidic than boron in this instance precluding the formation of this species.

Increasing the electron donation and steric bulk of the ligand around the magnesium centre (e.g. in the case of PMDETA) reduces the rate at which the C_6F_5 transfer occurs, thus providing some stability to the reaction product. The counter ion cannot co-ordinate to the magnesium, in the latter case, thus providing a less accessible environment for C_6F_5 transfer.

Activation of complexes $[Mg(\eta^2\text{-L})(R)_2]$ (**23-25, 30-31**) by $[NHMe_2Ph][B(C_6F_5)_4]$ (**5**) produces stable complexes that are not susceptible to addition of C_6F_5, and the bi products methane or toluene depending on R. Increasing the steric bulk of the ligand in $[Mg(\eta^2\text{-L})Me_2]$ (where L= TMEDA, TEEDA or PMDETA) from TMEDA to TEEDA or PMDETA is sufficient to prevent co-ordination of the NMe_2Ph biproduct, to produce $[Mg(\eta^2\text{-L})Me][B(C_6F_5)_4]$(where L=TEEDA or PMDETA). Curiously, changing the R group from Me to CH_2Ph in $[Mg(\eta^2\text{-TMEDA})(R)_2]$ results in the co-ordination of the NMe_2Ph biproduct, to produce $[Mg(\eta^2\text{-L})(NMe_2Ph)(CH_2Ph)][B(C_6F_5)_4]$ (where L=TMEDA or TEEDA). Addition of THF

to $[Mg(\eta^2\text{-}L)Me]^+$ and $[Mg(\eta^3\text{-}L)Me]^+$ helps solubilise the reaction products but there is no evidence of coordination of the solvent. However, addition of THF to $[Mg(\eta^2\text{-}L)(NMe_2Ph)(CH_2Ph)][B(C_6F_5)_4]$ always results in the formation of the THF solvated product.

Minor differences in the ^{19}F chemical shift are probably due to differences in concentration and/or ion association in solution.

Activation of complexes $[Mg(\eta^2\text{-}L)(R)_2]$ (**23-25, 30-31**) with $[CPh_3][B(C_6F_5)_4]$ (**3**) produces stable $[Mg(\eta^2\text{-}L)R][B(C_6F_5)_4]$ complexes, that are slightly susceptible to transfer of C_6F_5, and the bi-products CPh_3Me or $CPh_3(CH_2Ph)$ depending on R.

From the point of view of the formation of the stable potential alkene polymerisation catalysis of the form $[Mg(\eta^2\text{-}L)(R)]^+$ these results indicate that the positively charged Mg centre is too Lewis acidic to be stable in the presence of non coordinated anions based on perfluroaryl borates. Clearly, in order for these C_6F_5 transfer processes to proceed, $[Mg(\eta^2\text{-}L)(R)]^+$ must be more Lewis acidic than $B(C_6F_5)_3$ (Figure 2.47).

$$[(L)Mg\text{-}R]^{\oplus} + [B(C_6F_5)_4]^{\ominus} \longrightarrow [(L)Mg(R)C_6F_5] + B(C_6F_5)_3$$
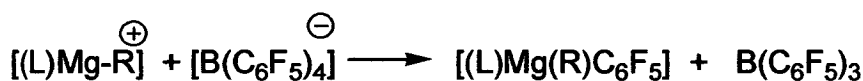
Figure 2.47 Reaction of $[Mg(\eta^2\text{-}L)(R)]^+$ and $[B(C_6F_5)_4]^-$

Some encouraging results are obtained for the less saturated and more hindered complexes containing the tridentate PMDETA ligand, and for those in which the Mg-bound R group is benzyl; in these cases the $[Mg(\eta^2\text{-}L)(R)]^+[A]^-$ salts show some stability towards C_6F_5 transfer from the borate counter ions. However, as will be presented in Chapter 5, even these systems show no ethene polymerisation or oligomerisation activity.

It is unfortunate that suitable X-ray quality crystals of the cationic complexes could not be obtained as the NMR data do not provide any information on the molecularity of these species. It has been found that in the neutral 3-coordinate alkyl complexes the systems dimerise, e.g. $[Mg(\beta\text{-diketiminate})Me]_2$, by alkyl bridging and extreme steric bulk is required to prevent this and stabilise a 3-coordinate complex.[24,25] One

of the benefits of preparing a cationic complex of type $[Mg(\eta^2\text{-L})(R)]^+$ is that an electrostatic barrier to dimerisation is introduced.

2.9 Experimental

2.9.1 General Procedures

All the air/moisture sensitive experimental work was performed under N_2 using standard Schlenk techniques on a vacuum line under dry, oxygen free, nitrogen. Some experimental work and characterisations were carried out in a nitrogen filled glove box (Saffron), fitted with oxygen and water scavenging columns. All solvents were dried and deoxygenated before use.

2.9.2 Solvent and Reagent Pre-treatment

Solvents and reagents where commercially available were bought from Aldrich, Acros or Fischer, with the exception of NMR solvents which were purchased from Goss Scientific. Activators $B(C_6F_5)_3$, $[CPh_3][B(C_6F_5)_3]$ and $[NHMe_2Ph][B(C_6F_5)_3]$ were kindly supplied by SRTCA and were bought from Akzo Nobel and Aldrich where available. Et_2O, toluene, hexane, benzene, and THF were all distilled from Na/ benzophenone under a nitrogen atmosphere. NMR solvents were degassed using three freeze-pump-thaw cycles and stored over molecular sieves. The amines were refluxed over Na and kept under nitrogen, and over molecular sieves in Schlenk flasks.

2.9.3 Instrumentation

Elemental analyses were performed by sealing aluminium capsules containing approx. 1 mg of compound under nitrogen in the glove box, and determined using a Perkin Elmer 2400 CHN Analyser.NMR were recorded on a Gemini 200MHz, Bruker 200Mhz, Bruker 250MHz, Bruker 360 MHz spectometers. Electron impact (EI) mass spectra were obtained either on a Finnigan MAT 4600 quadrapole spectrometer or on a Kratos MS50TC spectrometer. Fast atom bombardment (FAB) mass spectra were obtained on a MS50TC spectrometer. ^1H and ^{13}C NMR spectra were referenced to TMS and ^{19}F NMR were referenced to fluorotrichloromethane $(CFCl_3)$. ^{11}B NMR spectra were referenced to $BF_3(Et_2O)_2$.

[Mg(CH₃)₂] (7)

3M MgMeCl (50.6 cm^3, 151 mmoles) in THF was added to a 500 cm^3 Schlenk flask and diluted with THF (100 cm^3). To this solution 1.6 M MeLi (95 cm^3, 152 mmoles) in Et₂O was added with stirring at room temperature. The reaction mixture was stirred for 2hs, after which time all the solvent was removed in vacuum. Distilled Et₂O was added (250 cm^3) and the cloudy mixture stirred for 30 mins before being filtered to remove LiCl. The solvent was then removed from the filtrate, with heating under vacuum at 120°C for 2hs. The product is obtained as a fine white powder in 99% yield.

^{1}**H NMR** (THF-d₈, 360.13 MHz,): δ -1.82 (s, Mg-CH₃). Elemental analysis: for MgC₂H₆ expect: C:44.18, H:11.12, N:0.00; found : C:42.09, H:5.40, N:0.00.

[Mg(CH₂Ph)₂(THF)₂] (8)

To a stirred suspension of KO^{t}Bu (5.6g, 50 mmoles) in toluene (100 cm^3), 2.5 M BuLi (20 cm^3, 50 mmoles) in hexane is added dropwise via syringe at 0°C. The mixture was allowed to warm at room temperature and stirred for an additional 30 min. The red suspension was filtered through a frit, and the solid washed with toluene (150 cm^3) and hexane (20 cm^3). The volatiles were removed under vacuum yielding benzylpotassium as an orange solid (6.4 g, 49 mmol, 98%).

To a stirred suspension of PhCH₂K (6.4 g, 49 mmol) in THF (30 cm^3) was added 0.71M PhCH₂MgCl (69 cm^3, 49 mmol) in THF, at −78°C. The mixture was allowed to warm at room temperature and was stirred overnight. The volatiles were removed under vacuum and the product was extracted from the KCl with diethylether (100 cm^3). The ether was removed under vacuum till the solid starts to precipitate. Addition of *n*-hexane (15 cm^3) leads to the precipitation of a microcrystalline solid. After filtration the solution the solid is washed with *n*-hexane (15 cm^3), filtered and the solid dried under vacuum to yield the product as a light-yellow microcrystalline solid in 71% yield (12.2 g, 34.8 mmoles).

^{1}**H NMR** (C₆D₆, 360.13 MHz): δ 1.28 (t, J=6.45 Hz, 8H, THF), 1.90 (s, 4H, -C*H₂*), 3.34 (t, J=6.30 Hz, 8H, THF), 6.83 (t, J=7.03 Hz, 2H, p-C₆*H₅*), 7.18 (d, J=7.10 Hz, 4H, *o*-C₆*H₅*), 7.25 (t, J =7.56 Hz, 4H, *m*-C₆*H₅*);

^{13}C{^{1}H} NMR (THF-d_8, 90.55 MHz): 22.80 (CH$_2$-Ph), 25.8 (THF), 67.7 (THF), 115.4 (o-CH), 123.2 (CH), 127.7 (CH), 157.2 (ipso-C).); Elemental analysis: for MgC$_{22}$H$_{30}$O$_2$ expect: C:75.33, H:8.62, N:0.00; found : C:74.22, H:8.42, N:0.00.

[Mg(η^2-TMEDA)Me$_2$] (23)

MgMe$_2$ (1.637g, 30.11mmoles) was dissolved in Et$_2$O (50 cm^3). With stirring TMEDA (4.70 cm^3, 31.14 mmoles) was added dropwise *via* syringe. The pale yellow reaction mixture was allowed to stir for 1h, after which time the solvent was removed in vacuum and a white powder afforded. The white powder was then washed with hexane (20 cm^3) and removed by filtration to yield a white powder (4.071g, 24 mmoles, 77%). ^{1}H NMR (C$_6$D$_6$, 360.13 MHz): -0.97 (s, 6H, MgMe), 1.65 (s, 4H, CH$_2$N), 1.84 (s, 12H, NMe); ^{1}H NMR (CD$_2$Cl$_2$, 300.04 MHz): -1.74 (s, 6H, MgMe), 2.34 (s, 4H, NCH2), 2.50 (s, 12H, NMe); ^{1}H NMR (C$_6$D$_5$Br, 300.04 MHz): -1.25(s, 6H, MgMe), 1.99 (s, 4H, NCH$_2$), 2.01 (s, 12H, NMe); elemental analysis: expect: C:56.33, H:13.00, N: 16.42; found : C:51.96, 51.17, 51.32, 50.96, H: 5.6, 4.83; 12.02, 11.55 N: 15.85, 15.54, 16.30, 17.52. ^{13}C NMR (C$_6$D$_6$, 90.55 MHz): - 14.95 (br, MgCH$_3$), 46.24 (s, NCH$_3$), 56.26 (s, NCH$_2$).

[Mg(η^3-PMDETA)Me$_2$] (24)

MgMe$_2$ (1.01g, 18.60mmoles) was dissolved in Et$_2$O (70 cm^3). With stirring PMDETA (3.90 cm^3, 18.70 mmoles) was added dropwise via syringe. The pale yellow reaction mixture was allowed to stir for 1h, after which time some solvent was removed in vacuum to concentrate the solution and the mother liquor placed in the freezer overnight. Colourless needles were collected by filtration. The product was dried in vacuum and a white powder afforded (2.834g, 16.35 mmoles, 87%).

^{1}H NMR (C$_6$D$_6$, 360.13 MHz): -1.07 (s, 6H, MgMe), 1.54 (br, 4H, NCH$_2$), 1.83 (s(br), 3H, Nme), 2.078 (s, 12H, NMe), 2.21 (br(s), 4H, NCH$_2$);

^{1}H NMR (360.13 MHz,C$_6$D$_5$Br) : -1.35 (s, 6H, MgMe), 1.88 (br, 4H, NCH$_2$), 1.97(s(br), 3H, Nme), 2.23 (s, 12H, NMe), 2.33 (br(s), 4H, NCH$_2$); ^{1}H NMR (THF-d_8, 360.1 MHz): -1.81 (s, 6H, MgMe), 2.23 (s,15H, NMe), 2.49 (d(t), 8H, J=40.74Hz, J=5.74Hz, NCH$_2$), ^{13}C NMR (C$_6$D$_6$, 90.55 MHz): -13.39 (br, MgMe), -12.18 (br, MgMe), 41.90(s, NMe, 1C), 46.77(s, NMe, 4C), 56.34(s, NCH$_2$), 56.96 (s, NCH$_2$). ^{13}C (THF-d_8, 90.55 MHz): -14.70(s, MgMe), 42.08(s, NMe, 1C),

46.13(s, NMe, 4C), 56.96(s, NCH$_2$), 57.02(s, NCH$_2$); **Elemental analysis: expect**: C:58.03, H:29.23, **N: 18.46; found : C:55.70, 56.11, H: 12.86, 9.35; N: 18.60,** 19.07.

[Mg(η^2-TEEDA)Me$_2$] (25)

MgMe$_2$ (1.278g, 23.50mmoles) was dissolved in Et$_2$O (50 cm^3). With stirring TEEDA (5.20 cm^3, 24.38mmoles) was added dropwise via syringe. The pale yellow reaction mixture was allowed to stir for 1h, after which time the solvent was removed in vacuum and a white powder afforded. The white powder was then washed with hexane (10 cm^3) and removed by filtration. The product was extracted into benzene (50 cm^3) and the filtrate collected and the solvent removed to yield a white powder (4.205g, 18.5 mmoles, 79%). **^{1}H NMR** (C$_6$D$_6$, 360.13 MHz): δ-0.92 (s, 6H, MgMe),

0.67 (t, J= 7.26Hz, 12H, NMe), 1.87 (s, 4H, NCH$_2$), 2.18 (m, 4H, NC*H*H),

2.62 (m, 4H, NCH*H*), **^{1}H NMR** (C$_6$D$_5$Br, 360.13 MHz) : -1.22 (s, 6H, MgMe),

0.80 (t, 12H, J = 7.17Hz), 2.18 (s, 4H, NCH$_2$), 2.36 (br, 4H, CH$_2$),

2.68 (br, 4H, CH$_2$); (360MHz,CD$_2$Cl$_2$): -1.73 (s, 6H, MgMe),

1.04 (t, 12H, J = 7.17Hz), 2.63 (s, 4H, NCH$_2$), 2.65 (br(m), 4H, CH$_2$),

2.86 (br(m), 4H, CH$_2$); **^{1}H NMR** (THF-d_8, 360.13 MHz) : -1.77 (s, 6H, MgMe),

0.98 (t, 12H, J = 7.32Hz), 2.48 (s, 4H, NCH$_2$), 2.36 (q, 8H, J = 10.22Hz, CH$_2$),

^{1}H NMR (CD$_2$Cl$_2$, 360.13 MHz): δ -1.73 (s, 6H, MgMe),

1.04 (t, J= 7.16 Hz, 12H, NMe), 2.63 (s, 4H, NCH$_2$),

2.65 (m, J= 7.10 Hz, 4H, NC*H*H), 2.86 (m, J= 6.90 Hz, 4H, NCH*H*),

^{13}C NMR (C$_6$D$_6$, 90.55 MHz): δ -14.35 (s, Mg*C*H$_3$), 8.32 (s, *C*H$_3$), 44.78 (s, *C*H$_2$), 49.79 (s, *C*H$_2$). **^{13}C NMR** (C$_6$D$_5$Br, 90.5 MHz): δ -14.27 (s, Mg*C*H$_3$), 8.10 (s, *C*H$_3$), 44.89 (s, *C*H$_2$), 49.43 (s, *C*H$_2$); **^{13}C{^{1}H} NMR** (CD$_2$Cl$_2$, 90.55 MHz):

δ -15.28 (s, Mg*C*H$_3$), 8.49 (s, *C*H$_3$), 44.87 (s, *C*H$_2$), 50.16 (s, *C*H$_2$);

Elemental analysis: for MgC$_{12}$H$_{30}$N$_2$ expect: C: 63.58, H: 13.34, N: 12.36; **found** : C:59.73, 58.16, 49.18, 48.3, 53.06, 55.44, 55.11; H: 5.96, 5.83;9.61, 6.36, 10.43, 12.41, 12.44; N: 11.65, 11.48, 10.18, 9.97, 9.45, 9.84, 9.83.

Crystal Data for 25

Data was collected on a toe Stadi4 diffractometer using a colourless lath of dimensions 0.78 x 0.31 x 0.16 mm using the ω-θ method in the range of $20 < \theta < 22°$. Of a total of 2881 reflections collected, 2700 ($R_{int}= 0.0129$) were independent. The full difference map extrema were 0.392 and –0.399 eÅ^{-3} with a final R of 6.15% for 137 parameters.

Empirical formula	MgC$_{12}$H$_{30}$N$_2$	$\gamma/°$	90
Formula weight	226.69	Volume / Å^3	1509.4 (7)
Crystal system	Monoclinic	Z	4
Space group	P2$_1$/n	Temperature / K	150 (2)
a / Å	7.482 (2)	Wavelength / Å	1.54178
b / Å	16.835 (5)	Density calc. / Mg/m^3	0.998
c / Å	11.985 (3)	μ(Mo-Kα) / mm^{-1}	0.809
α / °	90	R$_1$[F>4σ(F)]	0.0615
β / °	90.99 (2)	wR$_2$ (all data)	0.1803

[N{CH(CH$_3$)$_2$}$_2$CH$_2$]$_2$ (TIPEDA) (27)

1,2-dibromoethane (52 cm^3, 0.601 moles) was diluted with an EtOH (75 cm^3): H$_2$O (25 cm^3) mixture. With stirring an EtOH (75 cm^3): H$_2$O (25 cm^3) mixture containing diisopropyl amine (169 cm^3, 1.202 moles) was added and the reaction mixture heated to 80°C for 42 hs. The reaction was worked up with KOH (63g) in 150 cm^3 of water, the product was extracted in benzene (200 cm^3). The solvent was removed on a rotary evaporator, distilled (170 °C, 21 mbar) and collected as a yellow oil (12.78g, 9.3%). ^{1}H NMR (C$_6$D$_6$, 360.13 MHz): δ 1.00 (d, J=6.59 Hz, 24H, CH_3),

2.50 (s, 4H, CH_2), 2.94 (spt, 4H, J=6.55 Hz, NCH);

^{13}C NMR (C$_6$D$_6$, 90.55 MHz): δ 21.35 (s, CH$_3$), 47.88 (s, CH$_2$), 49.41 (s, CH).

MS (+EI): 228 (3.5%)

[Mg(η^2-TIPEDA)Me$_2$] (26)

The organomagnesium precursor MgMe$_2$ (0.54g, 9.58 mmoles) was dissolved in Et$_2$O (50 cm^3) with stirring. The ligand was degassed via 3 freeze-pump-thaw cycles, dried over molecular sieves and added (1.440g, 6.30 mmoles) to the MgMe$_2$ solution dropwise *via* syringe. The solvent was removed in vacuum, and the white powdery/oily suspension washed with hexane. The product was extracted into

benzene (80 cm^3), filtered and the solvent removed to produce the yellow oil product (0.102g, 5.7%). ^{1}**H NMR** (C$_6$D$_6$, 360.13 MHz): δ-0.87 ((br)s, 6H, MgMe),

0.99 (d, J= 6.57 Hz, 24H, CH$_2$CH_3), 2.49 (s, 4H, NCH_2), 2.93 (sept, 4H, NCHH).

[Mg(μ-Cl)(η^2-TMEDA)Me]$_2$ (28) and [Mg(μ-Cl)(η^2-TMEDA)Cl]$_2$ (29)

To a stirred solution of TMEDA (2.246g, 0.19 mmoles) in THF (5 cm^3) was added 3M MgMeCl (6.44 cm^3, 0.19 mmoles) in THF. A green solution was observed to form. The THF was removed under vacuum and a white powder obtained which was dried under vacuum with heating (heat gun). The a white powder of the crude product (3.665, 99.3%) was afforded. Toluene (25cm^3) was added to the crude product and after 1 h of stirring the solution was filtered and the volume reduced in vacuum to ~5cm^3 and was placed in the freezer (-20°C). After 1 week colourless block crystals of [Mg(μ-Cl)(η^2-TMEDA)Me]$_2$ (**28**) and [Mg(μ-Cl)(η^2-TMEDA)Cl]$_2$ (**29**) suitable for X-ray diffraction studies were obtained and submitted for analysis. ^{1}**H NMR** (C$_6$D$_6$, 199.97 MHz): δ -1.03 (s, 7H, MgCH_3); 1.81 (s, 22H, NCH_3); 2.08 (s, 71H, N(CH_3)); 2.34 (m, 71H, N(CH_2)); 2.45 (m, 71H, N(CH_2)).

Crystal Data for 28 and 29

Data was collected on a toe Stadi4 diffractometer using a colourless block of dimensions 0.54 x 0.51 x 0.33 mm using the ω-θ method in the range of 20 < θ < 22°. Of a total of 2722 reflections collected, 2051 (R$_{int}$= 0.0140) were independent. The full difference map extrema were 0.267 and –0.263 eÅ^{-3} with a final R of 2.98% for 105 parameters.

Empirical formula	*Mg$_2$C$_{13.60}$H$_{36.80}$Cl$_{2.40}$N$_4$*	*γ /°*	*90*
Formula weight	*390.17*	*Volume / Å^3*	*2190.1 (3)*
Crystal system	*Orthorhombic*	*Z*	*4*
Space group	*Pccn*	*Temperature / K*	*150 (2)*
a / Å	*13.9952 (10)*	*Wavelength / Å*	*1.54178*
b / Å	*15.3913 (15)*	*Density calc. / Mg/m^3*	*1.183*
c / Å	*10.1675 (9)*	*μ(Mo-Kα) / mm^{-1}*	*3.677*
α / °	*90*	*R$_1$[F>4σ(F)]*	*0.0298*
β / °	*90*	*wR$_2$ (all data)*	*0.0808*

[Mg(η²-TMEDA)(CH₂Ph)₂] (30)

To a stirred solution of [Mg(PhCH₂)₂(THF)₂] (0.70g , 2 mmoles) in Et₂O (20 cm³) was added TMEDA (0.3 cm³, 2mmol) (dried over sodium, distilled and stored over molecular sieves 4Å) *via* syringe at room temperature. Stirring was continued overnight. The ether was removed under vacuum until precipitation started to occur. Adding *n*-hexane (5 cm³) leads the solid to precipitate fully. The solution was filtered yielding the product as a white powder (0.46 g, 1.43 mmoles, 71.3%). Colourless crystals were obtained from a solution of [Mg(η²-TMEDA)(CH₂Ph)₂] (30) (0.45 g) in 4 cm³ of toluene and 0.6 cm³ of THF within two days at –20°C.

^{1}H NMR (C₆D₆, 360.13 MHz): δ 1.30 (s, 4H, C*H*₂Ph), 1.51 (s, 12H, C*H*₃), 1.73 (s, 4H, -C*H*₂-C*H*₂), 6.80 (t, J = 7.76 Hz, 2H, *p*-C₆*H*₅,), 7.12 (t, J=7.62 Hz, 4H, *o*-C₆*H*₅,), 7.22 (t, J=7.62 Hz, 4H, *m*-C₆*H*₅,);

^{1}H NMR (THF- *d₈*, 360.13 MHz): δ 1.33 (s, 4H, C*H*₂Ph), 2.15 (s, 12H, C*H*₃), 2.33 (s, 4H, C*H*₂-C*H*₂), 6.30 (t, J=7.09 Hz, 2H, *p*-C₆*H*₅), 6.67 (d, J=7.86 Hz, 4H, *o*-C₆*H*₅), 6.75 (t, J=7.60 Hz, 4H, *m*-C₆*H*₅);

^{1}H NMR (C₆D₅Br, 360.13 MHz): δ 1.53 (s, 4H, MgC*H*₂), 1.78 (s, 12H, NC*H*₃), 1.79 (s, 4H, NC*H*₂), 6.63 (t, J=7.09Hz, 2H, *p*-Ar*H*), 6.93 (d, J =7.85 Hz, 4H, *o*-Ar*H*), 7.06 (t, J =7.56 Hz, 4H, *m*-Ar*H*); ^{13}C NMR (THF- *d₈*, 90.5 MHz): 21.0 (*C*H₂-Ph), 43.9 (*C*H₃), 56.0 (*C*H₂-*C*H₂), 113.6 (o-*C*H), 121.6 (*C*H), 125.9 (*C*H), 155.2 (ipso-*C*).

^{13}C{^{1}H} NMR (C₆D₆, 90.55 MHz): 23.93 (-*C*H₂-Ph), 46.76 (-*C*H₃), 56.82 (-*C*H₂-*C*H₂-), 117.10 (o-*C*H), 125.01 (*C*H), 128.80 (*C*H).

^{13}C NMR (C₆D₅Br, 90.55 MHz): 22.93 (*C*H₂-Ph), 45.77(*C*H₃), 55.71 (-*C*H₂-*C*H₂-), 116.15 (o-*C*H), 123.62 (*C*H), 128.08 (*C*H), 156.22 (*C*ipso).

[Mg(η²-TEEDA)(CH₂Ph)₂] (31)

To a stirred solution of [Mg(PhCH₂)₂(THF)₂] (2.042g , 5.82 mmoles) in Et₂O (50 cm³) was added TEEDA (1.24 cm³, 5.81 mmoles) (dried over sodium, distilled and stored over Molecular sieves 4Å) *via* syringe at room temperature. Stirring was continued overnight. The ether was removed under vacuum until a suspension occurred. Adding *n*-hexane (50 cm³) leads the solid to precipitate. The solution was chilled in ice and filtered yielding the product as a white powder (1.864 g, 84 %). Colourless crystals suitable for X-ray analysis were obtained from a mixed solvent

solution of [Mg(η^2-TEEDA)(CH$_2$Ph)$_2$] (0.446g) in 7 cm^3 of Et$_2$O, 0.2 cm^3 of THF

and 4 cm^3 of *n*-hexane within 7 days at 5°C. **^{1}H NMR** (C$_6$D$_5$Br, 360.13 MHz):

0.61 (t, J=7.01 Hz, 12H, CH$_3$), 1.53 (s, 4H, CH$_2$Ph), 2.06 (s, 4H, NCH$_2$),

2.20 (m, J = 6.99 Hz, 4H, C*H*(H)), 2.47 (m, J = 6.68 Hz, 4H, CH(*H*)),

6.65 (t, J = 7.01 Hz, 2H, *p*-Ar*H*), 6.95 (d, J = 7.89 Hz, 4H, *o*-Ar*H*),

7.08 (t, 4H, J=7.89 Hz, *m*-Ar*H*);

^{1}H NMR (THF-*d*$_8$, 360.13 MHz): 0.97 (t, 12H, CH$_3$), 1.32 (s, 4H, CH$_2$Ph),

2.45 (s, 4H, NCH$_2$), 2.45 (q, J=7.15 Hz, 4H, C*H*(H)), 6.30 (t, J=7.01 Hz, 2H,*m*-Ar*H*),

6.67 (d, J=7.01 Hz, 4H, *m*-Ar*H*), 6.75 (t, J=7.67 Hz, 2H, *m*-Ar*H*).

^{13}C NMR (C$_6$D$_5$Br, 90.55 MHz): 8.23 (*C*H$_3$), 24.19 (Ph*C*H$_2$), 44.36 (N*C*H$_2$),

49.57 (N*C*H$_2$), 116.65 (*p*-Ar*C*H), 124.26 (*m*-Ar*C*H), 128.44 (*o*-Ar*C*H),

156.62 (*C$_{ipso}$*).**^{13}C NMR** (THF-*d*$_8$, 90.55 MHz): 12.84 (-*C*H$_3$), 23.30 (-*C*H$_2$-Ph),

48.53 (-*C*H$_2$), 52.99 (-*C*H$_2$), 115.99 (o-*C*H), 123.85 (*C*H), 128.32 (*C*H),

157.73 (ipso-*C*).

Crystal Data for 31

Data was collected on a Stoe Stadi4 diffractometer using a colourless block of

dimensions 0.40 x 0.30 x 0.18 mm using the π-ω method in the range of 2.5 < θ <

26.5°. Of a total of 13186 reflections collected, 4772 (R$_{int}$= 0.0219) were

independent. The full difference map extrema were 0.278 and –0.179 eÅ^{-3} with a

final R of 4.22% for 244 parameters.

Empirical formula	MgC$_{24}$H$_{38}$N$_2$	γ / °	90
Formula weight	378.87	Volume / Å^3	2347.1
Crystal system	Monoclinic	Z	4
Space group	P2$_1$/n	Temperature / K	150 (2)
a / Å	8.8812 (13)	Wavelength / Å	0.71073
b / Å	21.610 (3)	Density calc. / Mg/m^3	1.072
c / Å	12.2295 (17)	μ(Mo-Kα) / mm^{-1}	0.086
α / °	90	R$_1$[F>4σ(F)]	0.0422
β / °	90.217 (2)	wR$_2$ (all data)	0.1172

B(C$_6$F$_5$)$_3$ (4)

^{19}F NMR (C$_6$D$_5$Br, 235.35 MHz): δ -127.68 (d, J =21.36Hz, 2F, *o*-F),

-142.18 (br, 1F, *p*-F), -159.66 (d, J =21.37Hz, 2F, *m*-F);

^{19}F NMR (CD$_2$Cl$_2$, 235.35 MHz): δ -130.29 (m, 2F, *o*-F), -145.93 (m, 1F, *p*-F),

163.18 (m, 2F, *m*-F);

^{19}**F NMR** (C_6D_6, 282.32 MHz): δ -129.22 (m, 2F, o-F), -142.17 (t, 1F, p-F),

-160.46 (m, 2F, m-F); ^{13}**C NMR** (C_6D_6, 90.55 MHz): 114.04 (s, *ipsoC*),

138.21 (d, J= 249.42 Hz, C-F), 145.25 (d, J= 284.02 Hz, C-F),

148.87 (d, J= 249.75Hz, C-F). ^{11}**B NMR** (C_6D_6, 115.54 MHz): 2.04 (s(br)).

^{19}**F NMR** (C_6D_6/ acetonitrile-d, 235.35 MHz):

δ -134.73 (dd, J=8.21Hz, J= 23.25Hz, 2F, o-F), -156.58 (t, J=20.97 Hz, 1F, p-F),

-164.05 (dd, J=12.05 Hz, J= 23.51Hz, 2F, m-F).

NMe$_2$Ph (52)

^{1}**H NMR** (C_6D_5Br, 360.13 MHz): δ 2.66 (s, 6H, N(CH$_3$)$_2$),

6.60 (d,J = 7.95Hz, 2H, o-ArH), 6.71 (t, J = 7.26Hz, 2H, m-ArH),

7.17 (t, J = 7.22Hz, 2H, p-ArH); ^{13}**C NMR** (C_6D_5Br, 90.55 MHz): δ 40.62 (s, CH_3),

113. 11(s, Ar-CH), 117.06 (s, Ar-CH), 122.73 (s, Ar-CH), 129.44 (s, C).

^{1}**H NMR** (CD_2Cl_2, 360.13 MHz): δ 2.93 (s, NMe, 6H),

6.71 (t, 2H, J = 7.98Hz, m-ArH), 6.74 (d, J = 8.01Hz, 2H, o-ArH),

7.23 (t, J = 7.26Hz, 2H, p-ArH); ^{13}**C NMR** (CD_2Cl_2, 90.55 MHz): δ 40.71(s, CH_3),

112.86 (s, Ar-CH), 116.70 (s, Ar-CH), 129.29 (s, Ar-CH), 151.17 (s, C).

[NHMe$_2$Ph][B(C_6F_5)$_4$] (5)

^{1}**H NMR** (C_6D_5Br, 360.13 MHz): δ 2.46 (s, N(CH_3)$_2$), 6.61 (d, J= 6.15 Hz, Ar-H),

7.09 (d, J= 7.63 Hz, Ar-H);^{1}**H NMR** (C_6D_5Br, 300.04 MHz): δ 2.49 (s, N(CH_3)$_2$),

6.61 (d, J= 8.06 Hz, Ar-H), 7.09 (d, J= 7.87 Hz, Ar-H);

^{19}**F NMR** (C_6D_5Br, 235.35 MHz): δ -132.11(t(br), o-F),

-161.02 (t, J =21.21Hz, p-F), -165.35 (t(br), m-F);

^{19}**F NMR** (C_6D_5Br, 282.32 MHz): δ -132.66 (t(br), o-F),

-161.52 (t, J =19.83 Hz, p-F), -165.86 (t(br), m-F);

^{11}**B NMR** (C_6D_5Br, 115.54 MHz): δ -13.15.

^{1}**H NMR** (CD_2Cl_2, 300.04 MHz): δ 3.42 (s, N(CH_3)$_2$), 7.04 (m, Ar-H),

7.38 (m, Ar-H),7.65 (m, Ar-H);

^{19}**F NMR** (CD_2Cl_2, 282.32 MHz): -133.71 (m(br), o-F),

-163.59 (t, J = 19.84Hz, p-F), -167.70 (t, J =18.31Hz, m-F).

[CPh₃][B(C₆F₅)₄] (3)

^{1}H NMR (CD$_2$Cl$_2$, 300.04 MHz): δ 8.27 (t, J=7.6 Hz, 3H, *p*-Ph),

7.87 (t, J=7.9 Hz, 6H, *m*-Ph), 7.66 (t, J=7.9Hz, 6H, *o*-Ph).

^{13}C NMR (C$_7$D$_8$, 90.55 MHz): δ 122.49 (C$_{ipso}$), 128.02 (*o-C*H), 134.85 (d, C-F),

136.70 (d, *C*-F), 137.35 (ipso-Ph), 139.97 (p/m CH), 140.91 (p/mCH),

146.93 (d, *C*-F), 208.05 (*C*-Ph$_3$), **^{19}F NMR** (C$_6$D$_5$Br, 282.32 MHz):

δ -132.31 (d, J=10.69 Hz, 2F, *o*-F), -162.39 (t, J=21.36 Hz, 1F, *p*-F),

-166.32 (t, J=18.31 Hz, 2F, *m*-F); **^{19}F NMR** (CD$_2$Cl$_2$, 282.32 MHz):

δ -133.58 (s(br), 2F, *o*-F), -164.03 (t, J=19.84 Hz, 1F, *p*-F),

-167.93 (t, J=16.78 Hz, 2F, *m*-F); **^{11}B NMR** (C$_6$D$_6$, 115.55 MHz): -12.90.

[Mg(C₆F₅)Br] (37)

A dilute 1M THF solution of Mg(C$_2$H$_5$)Br (20.2 cm^3, 20.2 mmoles) was chilled in an ice/salt bath. With stirring, a chilled THF (20 cm^3) solution of C$_6$F$_5$Br (2.52 cm^3, 20.2 mmoles) was added dropwise *via* syringe. The solution was allowed to warm to room temperature and stirred for 1h. The solvent was removed in vacuum by gentle heating in a warm water bath (30°C). The product was initially a white/grey oil. The product was frozen in liquid nitrogen and broken into a powder under nitrogen, on warming to room temperature the product remained a solid and was afforded in quantitative yield.

^{19}F NMR (360.13 MHz, THF-*d$_8$*) : δ -115.18 (d, J=21.97 Hz, 2F, *o*-F),

-164.12 (t, J= 19.12Hz, 1F, *p*-F), -165.67 (m, 2F, *m*-F),

^{13}C NMR (90.55 MHz,THF-*d$_8$*) : δ 129.80 (t, J=92.9Hz, *o*-CF), 136.71 (m, *p*-CF),

148.51(dt, J=38.35Hz, *m*-CF).

[Mg(η²-TMEDA)(C₆F₅)Me] (33)

The Grignard Mg(C$_6$F$_5$)Br (2.105g, 7.76 mmoles) was dissolved in THF(10 cm^3), with stirring TMEDA (1.17 cm^3, 0.90g, 7.75 mmoles) was added drop wise, at room temperature. The reaction mixture was allowed to stir for 30mins. The solvent was removed in vacuum and the [Mg(η^2-TMEDA)(C$_6$F$_5$)Br] washed with hexane. The white solid was redissolved in THF (10 cm^3) to produce a yellow solution. At room temperature, a 1.6 M MeLi solution (4.85 cm^3, 7.76 mmoles) in Et$_2$O was added drop

wise and a colour change was observed from yellow/clear to blue/opaque. The solvent was removed in vacuum, and the product extracted from LiCl in toluene. The solution was filtered through a frit and celite. The solvent was removed in vacuum and the purple solid product collected (2.224g, 89%).

^{1}**H NMR** (C$_6$D$_5$Br, 250.13 MHz): δ -1.28 (s, MgCH_3, 3H), 2.02 (s (br), NCH_3, 12H), 2.17 (s (br), NCH$_2$, 4H); ^{19}**F NMR** (C$_6$D$_5$Br, 235.36 MHz):

δ -111.66 (d, J=23.36 Hz, 2F, *o*-F), -158.28 (d, J=19.82 Hz, 1F, *p*-F), -161.04 (t, J=20.50 Hz, 2F, *m*-F); ^{13}**C NMR** (C$_6$D$_5$Br, 90.55 MHz):

δ -14.68 (s, MgCH_3), 46.66 (s, NCH_3), 56.65 (s, NCH$_2$),

122.65 (d, J= 62.84 Hz, *p-C*-F), 125.77 (s, *m-C*-F), 129.05 (d, J= 73.2 Hz, *p-C*-F), 137.87 (s, *ipso-C*) .

Reactions of [Mg(η^2-TMEDA)Me$_2$] (23), [Mg(η^3-PMDETA)Me$_2$] (24), [Mg(η^2-TEEDA)Me$_2$] (25), [Mg(η^2-TMEDA)(CH$_2$Ph)$_2$] (30) and [Mg(η^2-TEEDA)(CH$_2$Ph)$_2$] (31) with [CPh$_3$][B(C$_6$F$_5$)$_4$] (3), B(C$_6$F$_5$)$_3$ (4) and [NHMe$_2$Ph][B(C$_6$F$_5$)$_4$] (5)

General Procedure

In a glovebox the corresponding complex was weighed on top of the activator of choice in a sample vial. With stirring C$_6$D$_5$Br or CD$_2$Cl$_2$ was added (c.a.0.7 cm3) and the reaction mixture allowed to stir for 5 mins at room temperature, before being transferred to a NMR tube and analysed by ^{1}H, ^{19}F, and ^{11}B NMR. The amounts of complex and activator added, and general observations are listed in Table 2.08.

In some cases, where the products were insoluble, pre-dried THF was added after analysis of the reaction product *via* μL syringe, the NMR tube shaken and the sample re-analysed *via* ^{1}H and ^{19}F NMR.

Mg Complex	Activator	MgComp MW	Activator MW	MgC/g	Activator/g	MgC/moles	Activator/moles
TMEDAMgMe$_2$	FABA	170.5802	511.984	0.017	0.051	9.97E-05	9.96E-05
TEEDAMgMe$_2$	FABA	226.6874	511.984	0.011	0.026	4.85E-05	5.08E-05
PMDETAMgMe$_2$	FABA	227.6752	511.984	0.011	0.026	4.83E-05	5.08E-05
TMEDAMgBz$_2$	FABA	322.78	511.984	0.034	0.054	1.05E-04	1.05E-04
TEEDAMgBz$_2$	FABA	378.88	511.984	0.019	0.026	5.01E-05	5.08E-05
TMEDAMgMe$_2$	DANFABA	170.5802	801.2315	0.017	0.082	9.97E-05	1.02E-04
TEEDAMgMe$_2$	DANFABA	226.6874	801.2315	0.023	0.08	1.01E-04	9.98E-05
PMDETAMgMe$_2$	DANFABA	227.6752	801.2315	0.022	0.082	9.66E-05	1.02E-04
TMEDAMgBz$_2$	DANFABA	322.78	801.2315	0.033	0.079	1.02E-04	9.86E-05
TEEDAMgBz$_2$	DANFABA	378.88	801.2315	0.019	0.042	5.01E-05	5.24E-05
TMEDAMgMe$_2$	TRIFABA	170.5802	922.3695	0.017	0.093	9.97E-05	1.01E-04
TEEDAMgMe$_2$	TRIFABA	226.6874	922.3695	0.022	0.092	9.70E-05	9.97E-05
PMDETAMgMe$_2$	TRIFABA	227.6752	922.3695	0.022	0.033	9.66E-05	3.58E-05
TMEDAMgBz$_2$	TRIFABA	322.78	922.3695	0.032	0.092	9.91E-05	9.97E-05
TEEDAMgBz$_2$	TRIFABA	378.88	922.3695	0.019	0.046	5.01E-05	4.99E-05

Table 2.08 Amounts of complex and activator added in the proceeding reaction methods.

Activation of [Mg(η^2-TMEDA)Me$_2$] (23) with B(C$_6$F$_5$)$_3$ (4)

NMR Solvent: C$_6$D$_5$Br, **Observations:** Colourless/clear solution produced

^{1}H NMR (C$_6$D$_5$Br, 360.13 MHz): δ -1.24 (s, MgCH_3), -1.10 (s, 3H, MgCH_3), 0.72 (s, ,9H, B(CH_3)), 0.92 (s(br) , 9H, B(CH_3)), 2.06 (s(br), 72H, NCH$_3$), 2.16 (s(br), 24H, NCH$_2$).

^{19}F NMR (C$_6$D$_5$Br, 235.35 MHz):[Mg(η^2-TMEDA)(C$_6$F$_5$)Me] (33):

δ -112.70 (s(br), 64F, *o*-F), -156.10 (s(br), 32F, *p*-F), -159.93 (s(br), 64F, *m*-F);

[Mg(η^2-TMEDA)(C$_6$F$_5$)$_2$](35): -114.76 (d, J=23.14Hz, 2F, *o*-F),

-153.69 (t, J=19.48Hz, 1F, *p*-F), -158.22 (t, J= 20.76Hz, 2F, *m*-F);

[Mg(η^2-TMEDA)Me{BMe(C$_6$F$_5$)$_3$}] (32): -134.04 (d, J=24.15Hz, 90F, *o*-F),

-160.95 (t, J = 21.0Hz, 45F, *p*-F), -164.53 (t, J =20.8Hz, 90F, *m*-F); BMe(C$_6$F$_5$)$_2$

(34): -133.29 (s(br), 24F, *o*-F), -163.56 (s(br), 12F, *p*-F), -166.69 (s(br), 24F, *m*-F);

BMe$_2$(C$_6$F$_5$) (36) : -132.11 (s(br), 24F, *o*-F), -161.55 (t, J =21.0Hz, 12F,*p*-F),

-165.72 (s(br), 24F, *m*-F).

^{11}B NMR (C$_6$D$_5$Br, 115.54 MHz): δ -13.15 (s), -11.85 (s), 89.47 (s).

20hs later: ^{1}**H NMR** (C$_6$D$_5$Br, 250.13 MHz): δ 0.72 (s, 27H, B(CH_3)),

0.98 (s (br), B(CH_3), 12H), 1.08 ((br), 3H, B(CH_3)), 2.10 (s(br), 144H, NCH$_3$),

2.23 (s (br), 48H, NCH$_2$); ^{19}**F NMR** (C$_6$D$_5$Br, 235.36 MHz):

δ -112.10 (d, J=24.00Hz, 4F, *o*-F), -160.26 (t, J=20.08Hz, 2F, *p*-F),

-161.92 (d, J=21.04Hz, 4F, *m*-F); [Mg (η^2-TMEDA)(C$_6$F$_5$)Me] **(33)**:

-112.89 (d, J=21.57Hz, 2F, *o*-F), -156.77 (s(br), 1F, *p*-F),

-159.66 (t, J=18.57Hz, 2 F, *m*-F); [Mg(η^2-TMEDA)(C$_6$F$_5$)$_2$]**(35)**:

-114.77 (d (m), J=23.88Hz, 16F, *o*-F), -153.73 (t, J=19.39Hz , *p*-F, 8F),

-158.25 (t(m), J=20.57Hz , *m*-F, 16F); -131.85 (s(br), 8F, *o*-F),

-147.92 (m, J=14.03Hz, 4F, *p*-F)), -160.86 (t, J=19.05Hz, 8F , *m*-F);

BMe$_2$(C$_6$F$_5$) **(36)**: -132.08 (d, J=18.26Hz, 24F, *o*-F), -163.38

(t, J=20.98Hz, 12F, *p*-F), -166.16 (t, J=19.58Hz, 24F, *m*-F),-132.43 (s(br), 6F, *o*-F),

-164.30 (s(br), 3F, *p*-F), -167.08 (s(br), 6F, *m*-F).

Activation of [Mg(η^2-TEEDA)Me$_2$] with B(C$_6$F$_5$)$_3$

NMR Solvent: C$_6$D$_5$Br, **Observations:** Colourless/clear solution produced

^{1}**H NMR** (C$_6$D$_5$Br, 360.13 MHz): δ -1.05 (s, 2H, MgCH$_3$), 0.65 (t, CH$_3$),

0.70 (t, CH$_3$), 0.72 (t, CH$_3$), 0.76 (t, CH$_3$), 0.96 (s, BCH_3, 14H), 2.07 (s, 2H),

2.14-2.24 (m, 3H), 2.31 (s), 2.33-2.45 (m), 2.39 (s), 2.55-26.9 (m, 19H),

2.77-2.87 (m, 6H). ^{19}**F NMR** (C$_6$D$_5$Br, 282.35 MHz):

[Mg(η^2-TEEDA)Me(C$_6$F$_5$)] **(39)**: δ -111.74 (d(m), J=21.34 Hz, 20F, *o*-F),

-157.12 (t, J=19.84 Hz, 10F, *p*-F), -160.67 (t, J=20.87 Hz, 20F, *m*-F);

[Mg(η^2-TEEDA)(C$_6$F$_5$)$_2$] **(40)**: -113.19 (d(m), J=19.42 Hz, 18F, *o*-F),

-153.30 (t, J=19.44 Hz, 9F, *p*-F) ,-158.94 (t, J=19.33 Hz, 18F, *m*-F),

[Mg(η^2-TEEDA)Me{BMe(C$_6$F$_5$)$_3$}] **(38)**: -133.25 (d(m), J=20.07 Hz, 60F, *o*-F),

-161.33 (t, J=21.10 Hz, 30F, *p*-F), -165.10 (t, J=20.30 Hz, 60F, *m*-F);

-147.93 (m, 2F, CF), -153.78 (t, J=19.44 Hz, 4F, CF),

-193.19 (s, 2F, CF), -158.48 (t, J= 20.30Hz, 6F, CF);

^{11}**B NMR** (C$_6$D$_5$Br, 115.54 MHz): -11.80

Activation of [Mg(η^3-PMDETA)Me$_2$] with B(C$_6$F$_5$)$_3$

NMR Solvent: C$_6$D$_5$Br, **Observations:** Colourless/clear solution produced

^{1}H NMR (C$_6$D$_5$Br, 250.13 MHz): δ -1.42 (s, 9H, Mg(CH$_3$)), 0.72 (s, 3H,(CH$_3$)),

0.90 (s, 3H, B(CH$_3$)), 1.02(s, 18H, B(CH$_3$)), 1.91(s, 36H, N(CH$_3$)$_2$),

2.02(s, 24H, N(CH$_2$)), 2.12 (s, 24H, N(CH$_2$)), 2.15(s, 9H, N(CH$_3$)).

^{19}F NMR (C$_6$D$_5$Br, 235.36 MHz): [Mg(η^3-PMDETA)(Me)(C$_6$F$_5$)](**42**):

δ -112.44 (dt, J= 18.78Hz, 4F, *o*-F), -152.58 (t, J= 19.43Hz, 2F, *p*-F),

-158.26 (m, J= 19.30Hz, 4F, *m*-F); [Mg(η^3-PMDETA)Me][B(C$_6$F$_5$)$_3$Me](**41**):

-131.85 (d, J=18.48Hz, 30F, *o*-F), -163.39 (t, J=21.05Hz, 15F, *p*-F),

-166.20 (t, J=19.61Hz, 30F, *m*-F); BMe(C$_6$F$_5$)$_2$ (**34**): -132.14 (s(br), 2F, *o*-F),

-163.97 (s(br), 1F, *p*-F), -166.31 (s(br), 2F, *m*-F).

^{11}B NMR (C$_6$D$_5$Br, 115.54 MHz): δ −11.36 (s(br)), 89.14 (s(br)).

Activation of [Mg(η^2- TMEDA)(CH$_2$Ph)$_2$] with B(C$_6$F$_5$)$_3$

NMR Solvent: C$_6$D$_5$Br, **Observations:** Colourless/clear solution produced.

^{1}H NMR (C$_6$D$_5$Br, 360.13 MHz): δ 1.42 (s(br),2H, CH$_2$), 1.96 (s (br), 36H, CH$_3$),

2.09 (s(br), 12H, CH$_3$), 2.60 (s, 4H, CH$_2$), 3.14 (s(br), 2H, CH$_2$),

6.68 (t, J=7.86 Hz, 2H, Ar-*H*), 6.90 (d, J=7.03 Hz, 9H, Ar-*H*),

6.99-7.06 (m, 12H, Ar-*H*), 7.16 (t, J=7.18 Hz, 8H, Ar-*H*).

^{13}C NMR (C$_6$D$_5$Br, 90.55 MHz): δ 37.52 (s, *C*H$_2$), 45.97 (s, *C*H$_3$), 56.43 (s, *C*H$_2$),

125.22 (s, *C*H), 127.86 (s, *C*H), 128.76 (s, *C*H), 128.88 (s, *C*H),

129.35 (s, *C*H),129.54 (s, *C*H), 130.49 (s, *C*H), 135.17 (m(br), *C*H),

135.79 (m(br), *C*), 136.83(m(br), *C*), 137.79 (m(br), *C*), 138.65 (m(br), *C*),

139.84 (s, *C*), 140.19 (s, *C*), 147.66 (s(br), *C*), 148.09 (s(br), *C*), 148.45 (s(br), *C*),

148.71 (s(br), *C*), 150.46 (m(br), *C*), 150.87 (s(br), *C*).

^{19}F NMR (C$_6$D$_5$Br, 235.35 MHz): [Mg(η^2-TMEDA)(C$_6$F$_5$)(CH$_2$Ph)] (**43**):

δ -112.49 (d, J= 19.83 Hz, 2F, *o-F*), -153.99 (s(br), 1F, *p-F*),

-159.92 (s(br), 2F, *m*-F); [B(CH$_2$Ph)(C$_6$F$_5$)$_3$]⁻ (**44**): -131.94 (s(br), *o-F*, 2F),

-161.65 (m, *p-F*, 1F), -164.91 (t, J=21 89 Hz, *m-F*, 2F); [B(CH$_2$Ph)(C$_6$F$_5$)$_2$] (**45**):

-132.04 (s(br), *o-F*, 2F), -161.69 (m, *p-F*, 1F), -165.81 (t, J=18.84, *m-F*, 2F).

^{11}B NMR (C$_6$D$_5$Br, 115.54 MHz): δ −13.14, -9.26, 85.15.

20hs later: ¹H NMR (C₆D₅Br, 250.13 MHz): δ 1.88 (s(br),4H), 2.10 (s, 38H, C*H₃*),

2.13 (s, 38H, C*H₃*), 2.16 (s, 10H, C*H₃*), 2.25 (s, 30H, C*H₂*), 2.60 (s, 23H, C*H₂*),

3.18 (s(br), 3H, C*H₂*), 6.85 (d, J=7.07 Hz, 23H, Ar-*H*),

7.05 (d, J= 6.24 Hz, 18H, Ar-*H*), 7.16 (d, J= 7.16 Hz, 23H, Ar-*H*).

¹⁹F NMR (C₆D₅Br, 235.36 MHz): [Mg(η²-TMEDA)(C₆F₅)(CH₂Ph)] (**43**):

δ -112.18 (d, J= 20.23 Hz, 4F, *o*-F), -156.86 (m, 2F, *p*-F),

-160. 50 (t, J= 20.29 Hz, 4F, *m*-F); [Mg(η²-TMEDA)(C₆F₅)₂] (**46**):

-114.81(d, J= 22.39 Hz, 4F, *o*-F), -153.98 (m, 2F, *p*-F),

-158.33 (t, J= 9.61Hz, 4F, m-F); [B(CH₂Ph)₂(C₆F₅)] (**47**):

-130.66 (d, J= 23.39 Hz, 4F, *o*-F), -162.02 (t, J= 21.00 Hz, 2F, *p*-F),

-166.00 (t, J= 21.05 Hz, 4F, *m*-F); [B(CH₂Ph)(C₆F₅)₂] (**45**): -131.90 (s(br), 2F, *o*-F),

-160.87 (m, 1F, *p*-F), -165.36 (t, J= 21.18 Hz, 2F, *m*-F);

-132.19 (d, J= 20.23 Hz, 4F, *o*-F), -163.09 (t, J= 21.05 Hz, 2F, *p*-F),

-166.05 (t, J= 20.26Hz, 4F, *m*-F), -195.24 (s, 2F).

Activation of [Mg(η²- TEEDA)(CH₂Ph)₂] with B(C₆F₅)₃

NMR Solvent: C₆D₅Br, **Observations:** Colourless/clear solution produced

¹H NMR (C₆D₅Br, 360.13 MHz): δ 0.67 (q, J= 6.12 Hz, 32H, C*H₃*), 0.70

(m, 8H, PhC*H₂*), 1.37 (s, 3H, NC*H₂*), 2.09 (s, 12H, NC*H₂*), 2.12-2.18 (m, 15H),

2.29 (m, 7H), 2.39 (m), 2.50 (m, 7H), 2.61 (s, 4H), 3.19 (s(br), 5H), 6.71

(t, J=7.31 Hz, 4H), 6.77 (d, J=7.26 Hz, 4H), 6.85 (t, J=6.18 Hz, 7H), 6.97

(m, J=7.42 Hz, 10H), 7.04 (m, J=7.33 Hz, 9H), 7.16 (t, J=7.16 Hz, 5H).

¹³C NMR (C₆D₅Br, 90.55 MHz): δ 8.64 (s, C*H₃*), 8.96 (s, C*H₃*), 45.55 (s, C*H₂*),

45.77 (s, C*H₂*), 49.29(s, C*H₂*), 49.63 (s, C*H₂*), 123.90 (s, C*H*), 125.56 (s, C*H*),

128.08 (s, C*H*), 129.22 (s, C*H*), 129.72 (s, C*H*), 132.19 (s, C*H*), 135.70 (s(br), C),

139.80 (s(br), C), 140.51 (s, C), 147.50 (m(br), C), 149.15 (s, C), 151.30 (m(br), C).

¹⁹F NMR (C₆D₅Br, 235.35 MHz): (**48**): δ -111.64 (dt, J=21.69 Hz, 2F, *o*-F),

-156.95 (t, J= 19.87 Hz, 1F, *p*-F), -161.29 (t, J= 17.83 Hz, 2F, *m*-F);

(**49**): δ -113.46 (t, J= 19.57 Hz, 4F, *o*-F), -153.35 (d, J= 18.80 Hz, 2F, *p*-F),

-158.77 (t, J= 10.04 Hz, 4F, *m*-F);-131.01 (d, J= 25.96 Hz, 30F, *o*-F),

-161.73 (t, J= 21.45 Hz, 15F, *p*-F), -165.57 (t, J= 19.35 Hz, 30F, *m*-F);

-131.85 (d, J= 11.59 Hz, 2F, *o*-F), -160.66 (t, J= 11.23 Hz, 1F, *p*-F),

-166.68 (t, J= 17.83 Hz, 2F, *m*-F).

^{11}**B NMR** (C$_6$D$_5$Br, 115.54 MHz): δ –9.20, -13.15, 85.10.

Activation of [Mg(η^2-TMEDA)Me$_2$] with [NHMe$_2$Ph][B(C$_6$F$_5$)$_4$]

NMR Solvent: CD$_2$Cl$_2$, **Observations:** Colourless/clear solution produced

^{1}**H NMR** (CD$_2$Cl$_2$, 360.13 MHz): δ -1.42 (s, 3H, Mg(C*H$_3$*)), 2.45 (s, 12H, N(C*H$_3$*)),

2.65 (s, 4H, N(C*H$_2$*)) , 2.91 (s, 3H, N(C*H$_3$*)Ph), 3.61 (s, 3H, N(C*H$_3$*)Ph),

6.66 (d, J= 7.22 Hz, 1H, Ar-*H*), 6.72 (d, J= 8.24 Hz, 1H, Ar-*H*),

7.20 (t, J= 8.02 Hz, 1H, Ar-*H*), 7.52 (t, J= 4.35 Hz, 1H, Ar-*H*),

7.68 (t, J= 4.09 Hz, 1H, Ar-*H*);

^{19}**F NMR** (CD$_2$Cl$_2$, 235.35 MHz): δ -133.51 (d, J= 9.83 Hz, *o*-F),

-163.84 (t, J= 20.43 Hz, *p*-F), -167.79 (t, J= 18.34 Hz, *m*-F);

^{11}**B NMR** (CD$_2$Cl$_2$, 115.54 MHz): δ -13.58;

^{13}**C NMR** (CD$_2$Cl$_2$, 90.55 MHz): δ –17.31 (s, C*H$_3$*), 40.72 (s, N(CH$_3$)$_2$Ph),

46.45 (s, N(CH$_3$)$_2$Ph), 53.44 (s, N(CH$_3$)$_2$*C*H$_2$), 56.48 (s, N(*C*H$_2$)), 119.96 (s, *o*-*C*H),

124.06 (s(br), *C*), 132.06 (s, *p*-*C*H), 132.87 (s, *m*-*C*H),

136.70 (d, J= 245.63 Hz, *C*-F), 138.64 (d, J= 245.62 Hz, *C*-F),

148.55 (d, J= 239.35 Hz, *C*-F).

Activation of [Mg(η^2-TEEDA)Me$_2$] with [NHMe$_2$Ph][B(C$_6$F$_5$)$_4$]

NMR Solvent: C$_6$D$_5$Br, **Observations:** Gas evolved on adding solvent, white precipitate present, i.e. suspension.

^{1}**H NMR** (C$_6$D$_5$Br, 250.13 MHz): (**51**): δ - 1.15 (s(br), 13H, Mg(C*H$_3$*)), 0.61

(t, J= 7.12 Hz, 8H, C*H$_3$*CH$_2$), 0.73 (s(br), 27H, C*H$_3$*CH$_2$), 2.00 (s, 2H), 2.09 (m, 5H),

2.22 (s(br), 15H), 2.41-2.45 (s(br), 7H); (**52**): δ 2.64 (s, 70H, N(C*H$_3$*)$_2$Ph), 6.60

(d, J=7.92 Hz, 20H, Ar-*H*), 6.73 (t, J=7.20 Hz, 10H, Ar-*H*), 7.18 (m, 20H, Ar-*H*);

^{19}**F NMR** (C$_6$D$_5$Br, 235.3 MHz): (**51**): δ -132.40 (d, J = 8.92Hz, 2H, *o*-F),

-162.03 (t, J = 21.10Hz, 1H, *p*-F), -166.20 (t, J = 17.65Hz, 2H, *m*-F).

^{11}**B NMR** (C$_6$D$_5$Br, 115.5 MHz): (**51**): δ -13.12.

[Mg(η^2-TEEDA)Me$_2$] + [NHMe$_2$Ph][B(C$_6$F$_5$)$_4$] + THF

NMR Solvent: C$_6$D$_5$Br,

^{1}H NMR (C$_6$D$_5$Br, 250.13 MHz): **(51)**:δ -1.38 (s, 3H, Mg(CH_3)),

0.73 (t, J= 7.10 Hz, 12H, CH_3CH$_2$), 1.57 (m (br), 6H, THF-CH_2),

2.21 (s, 4H, N(CH_2)), 2.30 (m, 4H, N(C(H)H)), 2.39 (m, 4H, N(C(H)H)),

3.50 (m (br), 6H, THF-CH_2); **(52)**: 2.66 (s, 6H, N(CH_3)),

6.59 (d, J= 8.02Hz, 2H, Ar-H), 6.71 (t, J= 7.26 Hz, 1H, Ar-H),

7.18 (t, J= 7.29 Hz, 2H, Ar-H).

^{19}F NMR (C$_6$D$_5$Br, 235.36 MHz): **(51)**:δ -131.89 (d, J= 10.32 Hz, 2F, *o*-F),

-162.10 (t, J= 21.03 Hz, 1F, *p*-F), -166.08 (t, J= 18.26 Hz, 2F, *m*-F).

Activation of [Mg(η^3-PMDETA)Me$_2$] with [NHMe$_2$Ph][B(C$_6$F$_5$)$_4$]

NMR Solvent: C$_6$D$_5$Br, **Observations:** Colourless/clear solution produced

^{1}H NMR (C$_6$D$_5$Br, 360.13 MHz): **(53)**: δ -1.42 (s, 3H, Mg(CH$_3$)), 1.77 (br, 2H),

1.85 (s, 11H), 1.88 (s, 8H), 1.90 (s(br), 4H), 2.07 (br, 4H);

(52): 2.66 (s, 48H, N(CH$_3$)), 6.60 (d, J=7.77Hz, 16H), 6.72 (t, J=7.16Hz, 8H),

7.19 (t, J=6.74Hz, 16H).

^{19}F NMR (C$_6$D$_5$Br, 235.3 MHz): **(53)**: δ -131.89 (m(br), 2F, *o*-F),

-161.57 (t, J =21.11 Hz, 1F, *p*-F), -165.75 (m(br), 2F, m-F).

^{11}B NMR (C$_6$D$_5$Br, 115.54 MHz): -13.13 (s).

[Mg(η^3-PMDETA)Me$_2$] + [NHMe$_2$Ph][B(C$_6$F$_5$)$_4$] + THF

^{1}H NMR (C$_6$D$_5$Br, 250.13 MHz): **(53)**: δ -1.62 (s, 3H, Mg(CH$_3$)),

1.55 (t(br), 4H, THF), 1.83 (s, 6H, N(CH$_3$)), 1.87 (s, 3H, N(CH$_3$)),

1.90 (s, 6H, N(CH$_3$)), 2.02-2.12 (m(br), 4H, N(CH$_2$)),

2.15-2.17 (m(br), 4H, N(CH$_2$)), 3.51 (t(br), 4H, THF);

(52): 2.66 (s, 6H, N(CH$_3$)), 6.59 (d, J=8.68 Hz, 2H, Ar-H),

6.71 (t, J=7.36 Hz, 1H, Ar-H), 7.18 (t, J=7.27Hz, 2H, Ar-H)

^{19}F NMR (C$_6$D$_5$Br, 235.36 MHz): **(53)**: δ -131.86 (m(br), 2F, *o*-F),

-162.00 (t, J =21.07 Hz, 1F, *p*-F), -165.94 (t, J=18.39Hz, 2F, m-F).

Activation of [Mg(η²-TMEDA(PhCH₂)₂] with [NHMe₂Ph][B(C₆F₅)₄]

NMR Solvent: C₆D₅Br, **Observations:** Colourless/clear solution produced.

¹H NMR (C₆D₅Br, 360.13 MHz): **(54):** δ 1.38 (s, 2F, Mg(C*H*₂)),

1.68 (s(br), 12F, N(C*H*₃)₂), 1.95 (s, 4H, NC*H*₂), 2.17 (s, 3H, Tol-C*H*₃),

2.41 (s, 6H, N(C*H*₃)₂Ph), 6.71 (d, J=7.94 Hz, 2H, Ar-*H*),

6.79 (d, J=4.49Hz, 4H, Ar-*H*), 6.82-7.08 (m, 4H, Ar-*H*), 7.10-7.16 (m, 5H, Ar-*H*).

¹⁹F NMR (C₆D₅Br, 235.35 MHz): **(54):**δ -131.85 (d, J = 10.95 Hz, 2F, *o-F*),

-161.84 (t, J = 21.09 Hz, 1F, *p-F*), -165.84 (t, J = 18.52 Hz, 2F, *m-F*).

¹¹B NMR (C₆D₅Br, 115.54 MHz): **(54):** δ -13.11 (s).

[Mg(η²-TMEDA)(PhCH₂)₂] +[NHMe₂Ph][B(C₆F₅)₄ + THF

NMR Solvent: C₆D₅Br

¹H NMR (C₆D₅Br, 250.13 MHz): **(56) + (52):** δ 1.33 (s, 2H, Mg(C*H*₂)),

1.51 (s, 4F, THF), 1.89 (s, 12H, N(C*H*₃)₂), 2.00 (s, 4H, NC*H*₂),

2.18 (s, 3H, Tol-C*H*₃), 2.66 (s, 6H, N(C*H*₃)₂Ph), 3.39 (s, 4H, THF),

6.59 (d, J=8.19 Hz, 1H, Ar-*H*), 6.71-6.78 (m, 5H, Ar-*H*), 6.95-7.08 (m, 5H, Ar-*H*),

7.12-7.21 (m, 4H, Ar-*H*).**¹⁹F NMR** (C₆D₅Br, 235.35 MHz): **(56):**

δ -131.90 (d, J= 10.55 Hz, 2F, *o*-F), -161.99 (t, J= 21.05 Hz, 1F, *p*-F),

-166.00 (t, J=18.39 Hz, 2F, *m*-F).

Activation of [Mg(η²-TEEDA)(PhCH₂)₂] with [NHMe₂Ph][B(C₆F₅)₄]

NMR Solvent: C₆D₅Br, **Observations:** Colourless/clear solution produced.

¹H NMR (C₆D₅Br, 360.13 MHz): **(55):**δ 0.55 (t, J= 7.02 Hz, 12H, CH₂C*H*₃),

1.34 (s, 2H, C*H*₂Ph), 2.05 (m, J=6.85 Hz, CH(*H*)CH₃, 4H), 2.12 (s, Tol-C*H*₃, 3H),

2.17 (s, NC*H*₂, 4H), 2.19-2.28 (m, J=6.75 Hz, 4H, C*H*(H)CH₃),

2.48 (s, 6H, N(C*H*₃)₂), 6.75 (d, J=8.28 Hz, 2H, Ar-*H*), 6.81 (d, J=7.95 Hz, 3H, Ar-*H*),

6.95 (t, J= 7.23 Hz, 2H, Ar-*H*), 7.04 (t, J= 6.45 Hz, 2H, Ar-*H*),

7.06-7.24 (m, 6H, Ar-*H*).

¹⁹F NMR (C₆D₅Br, 235.35 MHz): **(55):** δ -131.83 (d, J = 10.42Hz, 2F, *o-F*),

-161.78 (t, J = 21.12 Hz, 1F, *p-F*), -165.89 (t, J = 18.46 Hz, 2F, *m-F*).

¹¹B NMR (C₆D₅Br, 115.54 MHz): -13.09 (s).

Activation of [Mg(η^2-TEEDA)(PhCH$_2$)$_2$ with [NHMe$_2$Ph][B(C$_6$F$_5$)$_4$] + THF

NMR Solvent: C$_6$D$_5$Br,

^{1}**H NMR** (C$_6$D$_5$Br, 250.13 MHz): **(57)** + **(52)**: δ 0.68 (t, J= 7.07 Hz, 12H, CH$_2$C*H$_3$*),

1.31 (s, 2H, C*H$_2$*Ph), 1.54 (t, J=6.37 Hz, 6H, THF), 2.18 (s, 4H, NC*H$_2$*),

2.27 (m(br) , 8H, CH(*H*)CH$_3$), 2.66 (s, 6H, NC*H$_3$*), 6.59 (d, J=8.04 Hz, 1H, Ar-*H*),

6.72 (t, J= 7.27 Hz, 2H, Ar-*H*), 6.77 (d, J=7.34 Hz, 2H, Ar-*H*),

7.01-7.09 (m, 6H, Ar-*H*), 7.12-7.22 (m, 4H, Ar-*H*).

^{19}**F NMR** (C$_6$D$_5$Br, 235.36 MHz): **(58)**: δ -131.88 (d, J = 10.71Hz, 2F, *o*-*F*),

-161.92 (t, J = 21.07 Hz, 1F, *p*-*F*), -165.97 (t, J = 18.53 Hz, 2F, *m*-*F*).

Activation of [Mg(η^2-TMEDA)Me$_2$] with [CPh$_3$][B(C$_6$F$_5$)$_4$]

NMR Solvent: C$_6$D$_5$Br, **Observations:** Orange solution with an orange oil

clatherate. ^{1}**H NMR** (C$_6$D$_5$Br, 360.13 MHz): δ 1.74 (s, 24H, C*H$_3$*),

1.83 (s, 8H, C*H$_2$*), 1.93 (s, 12H, C*H$_3$*), 1.98 (s, 4 H, C*H$_2$*).;

(58): 2.03 (s, 33H, C*H$_3$*Ph), 7.01-7.18 (m, 198H, Ar-*H*).

^{19}**F NMR** (C$_6$D$_5$Br, 235.35 MHz): δ -113.28 (m, J=11.00 Hz, 2F, *o*-F),

-153.42 (t, J= 21.00 Hz, 1F, *p*-F), -158.25 (t, J=19.21 Hz, 2F, *m*-F);

-133.42 (s(br), 30F, *o*-F), -160.64 (t, J= 21.19 Hz, 15F, *p*-F),

-165.19 (s(br), 30F, *m*-F),

^{19}**F NMR** (CD$_2$Cl$_2$, 235.35 MHz): δ -114.91 (d, J=10.33 Hz, 2F, *o*-F),

-155.11 (t, J= 18.61 Hz, 1F, *p*-F), -161.00 (t, J=18.67 Hz, 2F, *m*-F);

-134.19 (s(br), 24F, *o*-F), -162.57 (t, J= 20.44 Hz, 12F, *p*-F),

-167.12 (s(br), 24F, *m*-F).^{11}**B NMR** (C$_6$D$_5$Br, 115.54 MHz): -12.88 (s), 89.70 (s(br),

^{11}**B NMR** (CD$_2$Cl$_2$, 115.54 MHz): -13.55, 89.53.

Activation of [Mg(η^2-TEEDA)Me$_2$] with [CPh$_3$][B(C$_6$F$_5$)$_4$]

NMR Solvent: C$_6$D$_5$Br, **Observations:** dark green suspension.

^{1}**H NMR** (C$_6$D$_5$Br, 250.13 MHz): **(51)**: δ 0.60 (s(br), 4H, C*H$_3$*),

0.85 (s(br), 1H), 2.04 (s(br), 9H, C*H$_3$*), 2.11(s(br), 2 H, C*H$_2$*), 2.14 (s(br), 2H, C*H$_2$*),

7.08-7.11(m, 34H, Ar-*H*). ^{19}**F NMR** (C$_6$D$_5$Br, 235.36 MHz): **(51)**:

δ -133.17 (s(br), 2F, *o*-F), -160.36 (t, J=21.00 Hz, 1F, *p*-F), -165.35 (s(br, 2F, *m*-F);

^{11}**B NMR** (C$_6$D$_5$Br, 115.54 MHz): δ -13.30 (s).

Activation of [Mg(η²-TEEDA)Me₂] with [CPh₃][B(C₆F₅)₄] + THF

NMR Solvent: C₆D₅Br,

¹H NMR (C₆D₅Br, 250.13 MHz): **(51)**: δ -1.40 (s, 3H, MgC*H₃*), 0.72 (t, J=6.57 Hz, 12H, C*H₃*), 1.60 (m(br), 4H, THF), 2.22 (s, 4H, NC*H₂*), 2.30 (s(br), 8H, NC*H₂*), 3.50 (m(br), 4H, THF); **(58)**: 2.03 (s, 3H, CPh₃C*H₃*) , 7.04-7.21(m, 15H, CPh₃). **¹⁹F NMR** (C₆D₅Br, 235.36 MHz): **(51)**:

δ -131.89 (d, J=10.68 Hz, 2F, *o*-F), -162.11 (t, J=21.02 Hz, 1F, *p*-F), -166.12 (t, J=18.47 Hz, 2F, *m*-F).

Activation of [Mg(η³-PMDETA)Me₂] with [CPh₃][B(C₆F₅)₄]

NMR Solvent: C₆D₅Br, **Observations:** yellow solution with an orange/brown oil clatherate.

¹H NMR (C₆D₅Br, 360.13 MHz): **(53)**: δ -1.42 (s(br), 4H), 1.73 (s, 2H), 1.75 (s, 3H), 1.89 (s), 1.92 (s), 1.94 (s), 2.02 (s, 6H), 2.08-2.17 (m, 14H), 5.45 (s, 1H), 6.94-7.16 (m, 54H); **(58)**: 2.03 (s, 11H).

¹⁹F NMR (C₆D₅Br, 235.35 MHz): δ -131.97 (d, J=10.73 Hz, 6F, *o*-F), -161.60 (t, J=22.48 Hz, 3F, *p*-F), -165.78 (t, J=17.80 Hz, 6F, *m*-F); **(53)**: -132.30 (br, 2F, *o*-F), -162.0 (br, 1F, *p*-F), -166.78 (br, 2F, *m*-F).

¹¹B NMR (C₆D₅Br, 115.54 MHz): -12.80 (s).

Activation of [Mg(η³-PMDETA)Me₂] with [CPh₃][B(C₆F₅)₄] + THF

NMR Solvent: C₆D₅Br.

¹H NMR (C₆D₅Br, 360.13 MHz): **(53)**:δ -1.60 (s(br), 4H), 1.56 (s, 16H, THF), 1.86 (s), 1.88 (s), 1.91 (s), 2.07-2.39 (s, 16H), 3.56 (m, 16H), 5.45 (s, 1H), 6.95-7.18 (m, 51H); **(58)**: 2.04 (s, 16H).

¹⁹F NMR (C₆D₅Br, 235.35 MHz): **(53)**:δ -131.84 (d, J=10.94 Hz, 10F, *o*-F), -161.97 (t, J=21.08 Hz, 5F, *p*-F), -165.94 (t, J=18.41 Hz, 10F, *m*-F); -132.31 (s(br), 2F, *o*-F), -162.57 (s(br), 1F, *p*-F), -166.84 (s(br), 2F, *m*-F).

Activation of [Mg(η^2-TEEDA)(CH$_2$Ph)$_2$] with [CPh$_3$][B(C$_6$F$_5$)$_4$]

NMR Solvent: C$_6$D$_5$Br, **Observations:** Orange clear solution.

^{1}H NMR (C$_6$D$_5$Br, 250.13 MHz): **(59)** + **(60)**: δ 0.64 (s, J=7.15Hz,12H, C*H*$_3$), 1.41 (s, 2H, C*H*$_2$), 2.18 (s, 3H), 2.19 (s, 4H), 2.2-2.28 (m, 8H, NC*H*$_2$), 3.84 (m, 6H), 6.66-6.70 (m, 3H, Ar-*H*), 6.85-7.22 (m, 17H, Ar-*H*).

^{19}F NMR (C$_6$D$_5$Br, 235.36 MHz): δ -113.91(d, J=12.88 Hz, 2F, *o*-F), -152.66 (t, J=19.20 Hz, 1F, *p*-F), -158.59 (t, J=19.17 Hz, 2F, *m*-F); **(59)**: -131.95 (d, J=12.88Hz, 44F, *o*-F), -161.00 (t, J=21.34 Hz, 22F, *p*-F), -165.81 (t, J= 19.17Hz, 44F, *m*-F);-132.50 (s(br), 8F, *o*-F), -162.78 (s(br), 4F, *p*-F), -167.11 (s(br), 8F, *m*-F).**^{11}B NMR** (C$_6$D$_5$Br, 115.54 MHz): δ -13.13 (s).

Activation of [Mg(η^2-TEEDA)(CH$_2$Ph)$_2$] with [CPh$_3$][B(C$_6$F$_5$)$_4$] + THF

NMR Solvent: C$_6$D$_5$Br,

^{1}H NMR (C$_6$D$_5$Br, 250.13 MHz): **(57)** + **(60)**: δ 0.67 (t, J=6.48 Hz, 12H, C*H*$_3$), 1.31 (s, 2H, PhC*H*$_2$), 1.56 (m(br), 8H, THF), 2.17 (s, 4H, NC*H*$_2$), 2.18-2.28 (m (br), 8H, NC*H*$_2$), 3.47 (s(br), 8H, THF), 3.83 (s, 2H, CH$_2$CPh$_3$), 6.62-7.21 (m, 25H, Ar-*H*). **^{19}F NMR** (C$_6$D$_5$Br, 235.36 MHz): **(57)**: δ –131.95 (d, J=12.88Hz, 44F, *o*-F), -161.00 (t, J=21.34 Hz, 22F, *p*-F), -165.81 (t, J= 19.17Hz, 44F, *m*-F); **(49)**: δ -113.91(d, J=12.88 Hz, 2F, *o*-F), 152.66 (t, J=19.20 Hz, 1F, *p*-F), -158.59 (t, J=19.17 Hz, 2F, *m*-F); **(45)**:-132.50 (s(br), 8F, *o*-F), - 162.78 (s(br), 4F, *p*-F), -167.11 (s(br), 8F, *m*-F).

^{11}B NMR (C$_6$D$_5$Br, 115.54 MHz): δ -13.13 (s).

[N(H)Me$_2$CH$_2$CH$_2$NMe$_2$][B(C$_6$F$_5$)$_4$](61)

Crystal Data for [N(H)Me$_2$CH$_2$CH$_2$NMe$_2$][B(C$_6$F$_5$)$_4$](61)

Data was collected on a SMART diffractometer using a colourless rod of dimensions 0.25 x 0.08 x 0.08 mm using the π-φ method in the range of $5 < \theta < 48°$. Of a total of 21436 reflections collected, 11839 (R_{int}= 0.0351) were independent. The full difference map extrema were 0.885 and –0.573 eÅ^{-3} with a final R of 4.77% for 969 parameters.

Empirical formula	*C$_{30}$H$_{17}$BF$_{20}$N$_2$*	*γ / °*	*83.1880 (10)*
Formula weight	*796.27*	*Volume / Å^3*	*3029.1 (3)*
Crystal system	*Triclinic*	*Z*	*4*
Space group	*P-1*	*Temperature / K*	*150 (2)*
a / Å	*8.9362 (5)*	*Wavelength / Å*	*0.71073*
b / Å	*17.1486 (10)*	*Density calc. / Mg/m^3*	*1.746*
c / Å	*21.2132 (13)*	*μ(Mo-Kα) / mm^{-1}*	*0.189*
α / °	*71.0380 (10)*	*R$_1$[F>4σ(F)]*	*0.0477*
β / °	*81.0820 (10)*	*wR$_2$ (all data)*	*0.1110*

2.10 References

1   Britovsek, G.P.; Gibson, V.C.; Wass, D.F.; *Angew.Chem.Int.Ed.*, **1999**, *38*, 429-447

2   Chen; E.Y.X; Marks, T.J.; *Chem.Rev.*; **2000**; *100*; 1391-1434.

3   Horton, A.D.; de With, J.; *J.Chem.Soc.; Chem. Comm.*; **1996**, 1375-1376.

4   Viebrock, H.; Weiss, E.; *J.Organomet.Chem.*, **1994**, *464*, 121-126.

5   Yasuda, H.; Yamauchi, M.; Nakamura, A.; Sei, T.; Kai, Y.; Yasuoka, N.; Kasi, N.;
    Bull.Chem.Soc.Jpn.; 1980, 53, 1089-1100.

6   Marsch, M.; Harms, K.; Massa, W.; Boche, G.; *Angew.Chem.Int.Ed.Engl.*; **1987**, *26*, 696-697.

7   Gardiner, M.G.; Raston, C.L.; *Organomet.*, **1995**, *14*, 1339-1353.

8   Morley, C.P.; Jutzi., P.; Kruger, C.; Wallis, J.M.; *Organomet.*, **1987**, *6*, 1084-1090.

9   Clegg, W.; Craig, F.J.; Henderson, K.W.; Kennedy, A.R.; Mulvey, R.E.; O'Neil, P.A.; Reed, D.;
    Inorg.Chem.; **1997**, *36*, 6238-6246.

10 Henderson, K.W.; Kennedy, A.R.; Mulvey, R.E.; Clegg, W.; O'Neil, P.A; *J.Organomet.Chem.*;
    1992, *439*, 237-250.

11 Schubert,B.; Behrens, U.; Weiss, E.; *Chem.Ber.*, **1981**, *114*, 2640-2643.

12 Grieser, T.; Kopf, J.; Thoennes, D.; weiss, E.; *J.Organomet.Chem.*, **1980**, *191*, 1-6.

13 Shepherd, R.G.; Wilkinson, R.G.; *J.Med.Pharm.Chem.*, **1962**, 823-825.

14 Barnett, N.D.R.; Clegg, W.; Mulvey, R.E.; O'Neil, P.A.; Reed, D.; *J.Organomet.Chem.*, **1996**,
    510, 297-300.

15 Thoennes, D.; Weiss, E.; *Chem.Ber.*; **1978**, *111*, 3381-3384.

16 Johnson, C.;Toney, Stucky, G.D.; *J.Organomet.Chem.*, **1972**, *40*, C11.

17 Viebrock, H; Ablen, D.; Weiss, E.; *Z.Naturforschung.B*; **1994**, *49*, 89-99.

18 Herber, C.; *Project report*, C.O. Bailey, P.J.; Department of Chemistry, University of Edinburgh,
    July **2000**.

19 Horton, A.D.; de With, J.; van der Linden, A.; van de Weg, H.; *Organomet.*, **1996**, *15*, 2672-
    2674.

20 Pellecchia, C.; Immirizi, A.; Grassi, A.; Zambelli, A.; *Organomet.*, **1993**, *12*, 4473-4478.

21 a.Jukes, A.E.; Gilman, H.; *J.Organomet.Chem.*, **1969**, *17*, 145-148; b. Respess, W.L.; Tamborski,
    C.; *J.Organomet.Chem.*, **1968**, *11*, 619-622.

22 Ihara, E.; Young, V.G.; Jordan, R.F.; *J.Am.Chem.Soc.*, **1998**, *120*, 8277-9278.

23 Radzewich, C.E., Guzei, I.A.; Jordan, R.F.; *J.Am.Chem.Soc.*, **1999**, *121*, 8673-8674.

24 Bailey, P.J.; Coxal, R.A.; Dick, C.M.; Fabre, S.; Parsons, S.; *Organometallics*, **2001**, *20*, 798-801.

25 Gibson, V.C.; Segal, J.A.; white, A.J.P.; Williams, D.J.; *J.Am.Chem.Soc.*, **2000**, *122*, 7120-7121.

CHAPTER THREE REACTION OF MAGNESIUM ALKYLS WITH α-DIIMINES

Our initial goal was to produce monomeric dialkyl magnesium diimine complexes, which we could activate and investigate as alkene polymerisation catalysts. We chose α-diimine ligand systems because of their wide use as a support to active transition metal (such as Pd, Ni) catalysts reported in the literature.[1-15] The proposed complexes displayed in Figure 3.01 offer a variety of potential functionalisation, which will allow exploration of the effect of each on their reactivity and specificity in ethene polymerisation. The Ar-BIAN (where BIAN= bis(imino)acenaphthene) ligand in **1** provides a rigid backbone in comparison with the other systems. Compounds **1**, **2** and **3** will allow comparison of the effect of steric bulk on the backbone. The amidoimine complex **4** would allow comparison of a neutral catalyst that does not require activation and has asymmetry which may offer stereoselectivity if used for propene polymerisation.
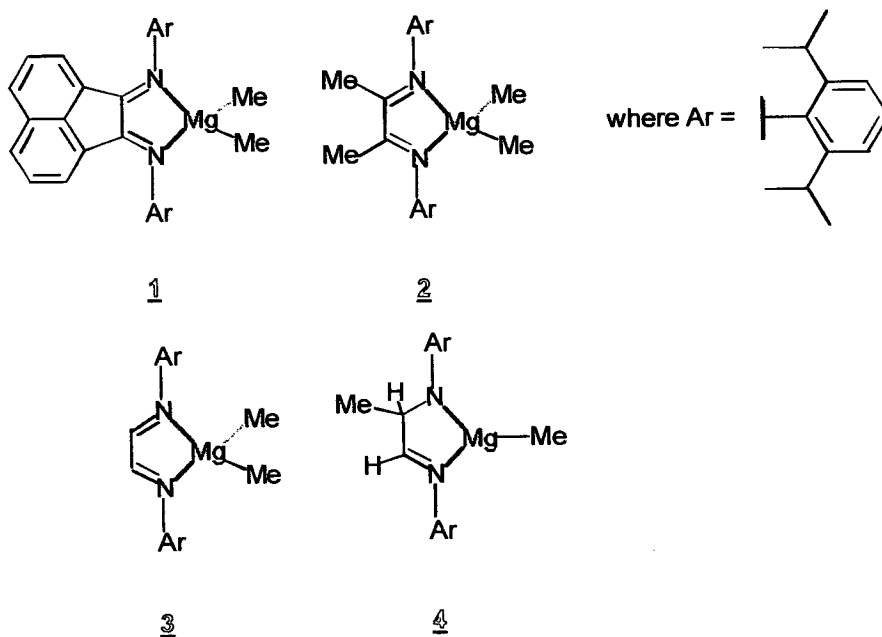
Figure 3.01 Desired monomeric magnesium dimethyl diimine and monomethyl iminoamide complexes for alkene polymerisation research.

3.1 Transition Metal (Pd, Ni, Pt, V) Based α-diimine Complexes As Active Ethene Polymerisation Catalysts

3.1.1 Pd and Ni α-diimine Ethene Polymerisation Catalysts

Brookhart and Johnson have extensively studied the single site polymerisation properties of bulky aryl-substituted α-dimine based systems, mainly with late transition metals such as Ni and Pd (Figures 3.03 & 3.04). [1-7, 9-15] Their catalyst systems are very reactive to alkene polymerisation, and have stimulated our group to use similar ligand systems in our investigation of the preparation, isolation, characterisation and ethene polymerisation testing of new magnesium alkyl complexes. A recent review by Brookhart, Johnson and Ittel comprehensively covers the homo-and copolymerisation of late-metal catalysts which include those of Pd, and Ni α-diimine systems. [1]
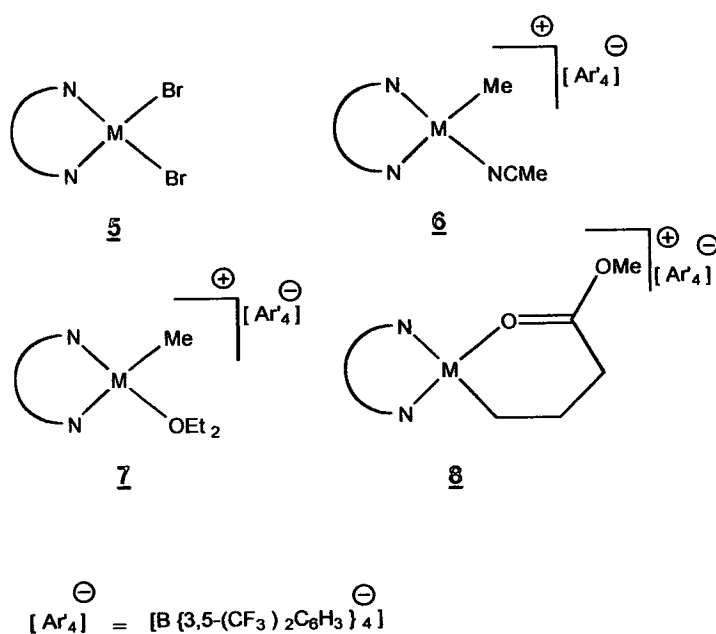
Figure 3.02 Pd and Ni catalysts 5-8
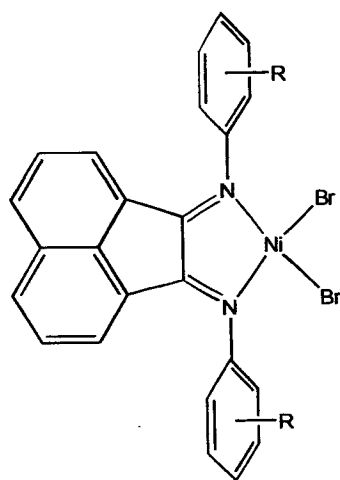
9 :[2,3,11,14] R= 2,6-(iPr)2
10 :[3,14] R=2-tBu
11 :[14] R= 2,5-(tBu)2
12 :[14] R= 2,4,6-Me3
13 :[11] R=2-CF3
14 :[11] R=2-CF3,4-Me
15 :[11] R=2-(C6F5)
16 :[11] R=2-(C6F5), 4-Me
17 :[9,11] R=2-Me
18 :[11] R= 2,6-Me
19 :[9] R=4-CF3
20 :[6,9] R=H
21 :[6,9] R=4-Me
22 :[9] R=4-OMe
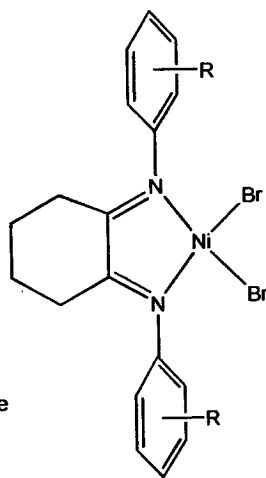
23 :[11] R= 2,6-(iPr)2
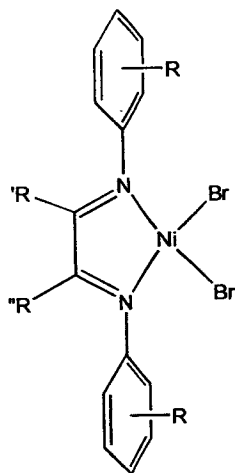
24 :[11] R= 2,6-(iPr)2, R'=Et, R''=Me
25 :[6] R=4-MeC6H4, R'=R''=Me
26 :[2] R=2,6-(iPr)2, R'=R''=H
27 :[2] R=2,6-(iPr)2, R'=R''=Me
28 :[2] R=2,6-Me2, R'=R''=H
29 :[2] R=2,6-Me2, R'=R''=Me
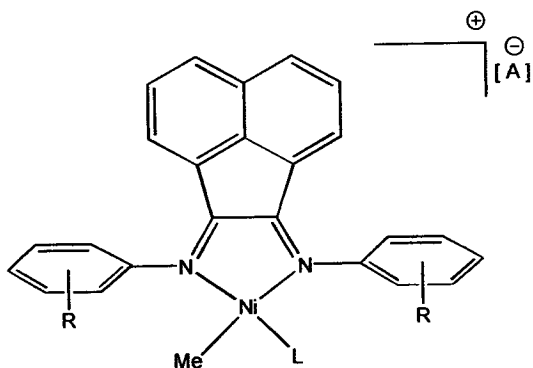
30 :[5] R=2,6-Me2, L= Et2O, A =B{3,5-(CF3)2C4H3}4
31 :[5] R=2,6-Me2, L= OH, A =B{3,5-(CF3)2C4H3}4
32 :[5] R=2,6-(iPr)2, L= Et2O, A =B{3,5-(CF3)2C4H3}4
33 :[5] R=2,6-(iPr)2, L= OH, A =B{3,5-(CF3)2C4H3}4
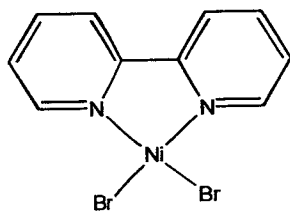
34 :[6]
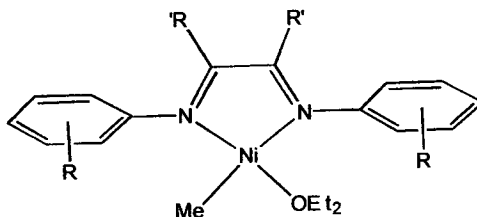
35 :[2] R=2,6-(iPr)2, R'=H

Figure 3.03 Ni(α-dimine) based ethene polymerisation catalysts studied by Brookhart and co-workers

119

36:       R= 2,6-(^{i}Pr)$_2$, R'= Me, L= NCMe, A =B (C$_6$F$_5$) $_4$

37 :[14]   R=2,6-(^{i}Pr)$_2$, R'= Me, L= E t$_2$O, A =SbF $_6$

38 :[4,7, 12] R=2,6-(^{i}Pr)$_2$, R'= H, L= E t$_2$O, A =B {3,5-(CF$_3$) $_2$C$_6$H$_3$ } $_4$

39 :[12]   R=2,6-(^{i}Pr)$_2$, R'= H, L= NCMe, A =B {3,5-(CF$_3$) $_2$C$_6$H$_3$ } $_4$

40 :[4,7,12] R=2,6-(^{i}Pr)$_2$, R'= Me, L= E t$_2$O, A =B {3,5-(CF$_3$) $_2$C$_6$H$_3$ } $_4$

41 :[1,10,12] R=2,6-(^{i}Pr)$_2$, R'= Me, L= NCMe, A =B {3,5-(CF$_3$) $_2$C$_6$H$_3$ } $_4$

42 :[12]   R=2-^{t}Bu, R'=Me, L= E t$_2$O, A =B {3,5-(CF$_3$) $_2$C$_6$H$_3$ } $_4$

43 :[12]   R=2-^{t}Bu, R'=Me, L= NCMe, A =B {3,5-(CF$_3$) $_2$C$_6$H$_3$ } $_4$

44 :[15]   R=2,6-Me$_2$, R'= Me, L= NCMe, A =B {3,5-(CF$_3$) $_2$C$_6$H$_3$ } $_4$

45 :[15]   R=4-Me, R'=Me, L= NCMe, A =B {3,5-(CF$_3$) $_2$C$_6$H$_3$ } $_4$

46 :[7]   R=2,6-Me$_2$, R'=Me, L= E t$_2$O, A =B {3,5-(CF$_3$) $_2$C$_6$H$_3$ } $_4$

47 :[15]   A =B {3,5-(CF$_3$) $_2$C$_6$H$_3$ } $_4$

48 :[13]

49 :[4,7,12] R=2,6-(^{i}Pr)$_2$, L= E t$_2$O, A =B {3,5-(CF$_3$) $_2$C$_6$H$_3$ } $_4$

50 :[12]   R=2,6-(^{i}Pr)$_2$, L= NCMe, A =B {3,5-(CF$_3$) $_2$C$_6$H$_3$ } $_4$

51 :[12]   R=2-^{t}Bu, L= E t$_2$O, A =B {3,5-(CF$_3$) $_2$C$_6$H$_3$ } $_4$

52 :[12]   R=2-^{t}Bu, L= NCMe, A =B {3,5-(CF$_3$) $_2$C$_6$H$_3$ } $_4$

53 :[12]   R=2,6-Me$_2$, L= E t$_2$O, A =B {3,5-(CF$_3$) $_2$C$_6$H$_3$ } $_4$

54 :[12]   R=2,6-Me$_2$, L= NMe, A =B {3,5-(CF$_3$) $_2$C$_6$H$_3$ } $_4$

55 :[10]   R=2,6-(^{i}Pr)$_2$, R'= Me, A =B {3,5-(CF$_3$) $_2$C$_6$H$_3$ } $_4$

56 :[14]   R=2,6-(^{i}Pr)$_2$, R'= Me, A =SbF$_6$

57 :[14]   R=2,6-(^{i}Pr)$_2$, R'= Me, A =[B {2,4-(CF$_3$) $_2$C$_6$H$_3$ } $_4$]

58 :[1]   R=2,6-(Me)$_2$, R'= Me, A = {3,5-(CF$_3$) $_2$C$_6$H$_3$ } $_4$

Figure 3.04 Pd(α-dimine) based ethene polymerisation catalysts studied by Brookhart and co-workers

These catalysts have been investigated for the polymerisation of ethene, α-olefins and cyclic olefins, as well as for the co-polymerisation of non-polar olefins with an array of functionalised olefins.

R= ^{i}Pr
R'= H, Me or R',R'= 1,8-naphth-diyl
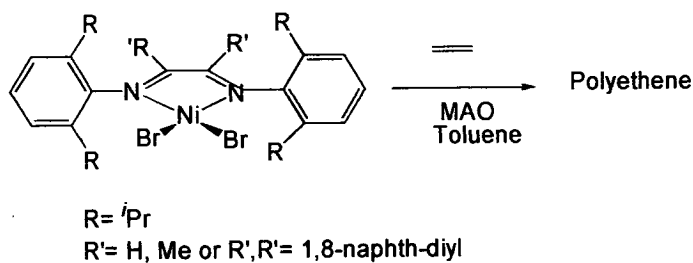
Figure 3.05 Example of ethene polymerisation by activation of [Ni(α-diimine)Br₂] with MAO.

The late transition metals have a greater functional group tolerance and reduced poisoning susceptibility in the presence of polar comonomers on co-polymerisation, in comparison to early transition metals (titanium, zirconium, chromium), which makes Pd and Ni good systems for the co-polymerisation reactions of ethane with polar co-monomers under mild conditions. In general, the catalysts incorporate highly electrophilic cationic square planar Pd(II) and Ni(II) centres.[1] The α-diimine systems are sterically bulky, and on complexation their crystal structures reveal that the aryl ring substituents are orthogonal to the square plane, and the substituents in the ortho-position sit above and below the plane (Figure 3.05). It has been observed that the larger the steric bulk of either the backbone or ortho-substituents the more rigidly the plane of the aryl ring becomes locked perpendicular to the coordination plane. This is mechanistically important when it comes to ethene polymerisation as it suggests that you can tailor the bulk of the ligand to adjust the hindrance at the axial sites to your needs.

The catalyst employs a non-coordinating counter ion to provide an accessible coordination site for incoming unsaturated species, the most commonly used ones being: $[B\{3,5-(CF_3)_2C_4H_3\}_4]^-$, $[B(C_6F_5)_4]^-$, and $[SbF_6]^-$.

The most important variables that control the catalyst activity, lifetime, initiation, and decay as well as the polymer molecular weight, molecular weight distributions, and the extent of polymer branching are the ligand structure, co-catalyst, temperature and olefin concentration. Brookhart has investigated several catalyst systems, Figure

3.02. The α-diimine based polymersiation catalysts of Pd and Ni can be prepared in situ, for example by the reaction of the dihalide catalyst precursor 5 with MAO.[1,2,3,6,8,11,14] Or the catalytic species can be prepared and isolated as cationic organometallic species which are typically stabilised by relatively weak donor ligands such as acetonitrile 6 or diethylether 7.[1,2,4,5,7,10,12,14,15]

Low temperature NMR studies of the polyethene chain production in the reaction of cationic Ni and Pd α-diimine centres with ethene, have allowed the elucidation of the mechanism for ethylene polymerisation and polymer branch formation. In general the catalyst resting state is the alkyl ethene complex 59 (Figure 3.06). The metal, in the alkyl β-agostic cation complex (60) can rapidly migrate along the polymer chain *via* β-hydride elimination/reinsertion reactions. Chain growth is dependent on the rate of migratory insertion, which causes branching. The chain transfer is quite slow relative to chain propagation, for the Pd and Ni systems, and consequently high molecular weight polymers are produced. The migration barriers were calculated from NMR results and range between 17-18 kcal/mol for Pd systems and 13-14 kcal/mol for Ni systems. The barrier differences explain the observations that Ni systems have higher activities.[5]
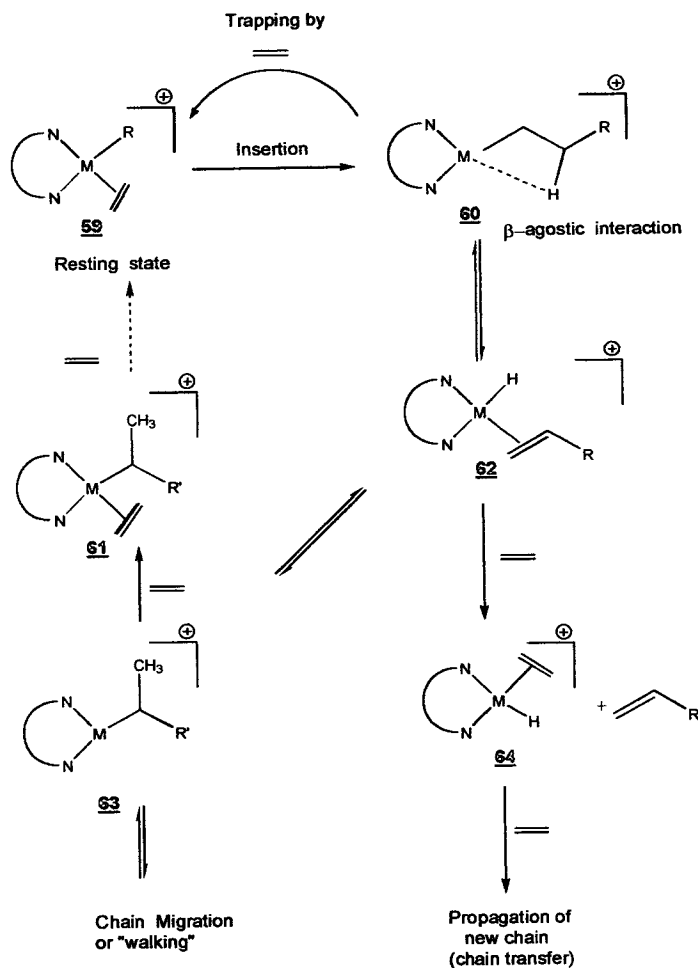
Figure 3.06 Mechanism showing insertion, chain propagation, and chain migration reactions in the ethene polymerisation reaction of diimine Ni/Pd alkyl systems.

The migration insertion barrier height is also affected by the bulk of the diimine ligand. Increasing the steric bulk of the aryl substituents on the donor nitrogen atoms was shown to increase the ground state energy of the resting state relative to the migratory transition state, thus lowering the migratory insertion barrier. There are two possible routes that result in chain transfer either by: 1) associative displacement from the alkene hydride intermediate *via* β-hydride elimination before ethylene coordination, or 2) direct β-hydride transfer to monomer from the alkyl-olefin resting state (Figure 3.07).[11]

Chain transfer *via* associative exchange
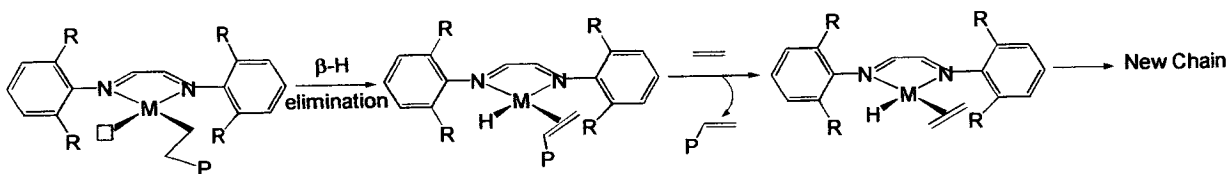
Chain transfer to monomer
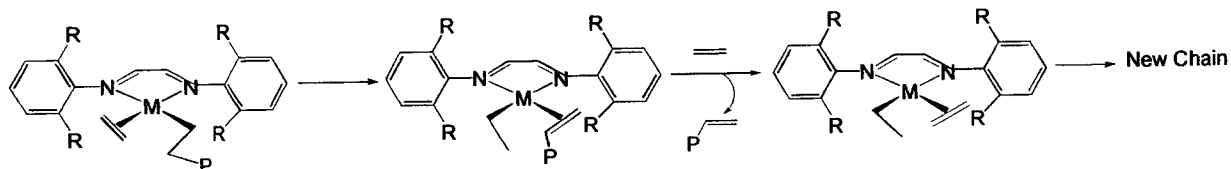
M= Pd or Ni

Figure 3.07 Two reaction routes resulting in chain transfer 1) associative route, 2) direct β-hydride transfer route.[11]

The palladium systems produce highly branched polyethenes, which is indicative of high rates of chain walking relative to insertion. However the nickel systems seem to produce more linear α-olefins in comparison with the palladium systems (Tables 3.01 and 3.02). Another trend that is apparent, on comparison of the ethene polymerisation reactions of both the Pd and Ni systems, is the reduction of the molecular weight (M_n) of the polymer on reduction of the steric bulk of: 1) the backbone and or 2) ortho substituents on the aryl substituents, as expected. The steric effects are significantly reduced in the nickel species the number of branches are significantly reduced (not observed for Pd) and the polymer molecular weight (M_n) also decreases. Thus more linear α-olefins are produced in preference because of the increased chain-transfer rates.[1]

Complex	Key no.	Reference	moles of cat (X10⁻⁶)	monomer	Pressure	Temp (°C)	Time (min)	Toluene (cm³)	Mn (X10⁻⁴)	Mw/Mn	branches (per 1000 C)
[{(2,6-Me$_2$Ph)$_2$DABH$_2$}NiBr$_2$] / MAO	28	2	17	ethene	1 atm	0	30	100	4.3	2.5	1.2
[{(2,6-Me$_2$Ph)$_2$DABH$_2$}NiBr$_2$] / MAO	28	2	17	ethene	1 atm	25	30	100	1.4	2.9	29
[{(2,6-Me$_2$Ph)$_2$DABMe$_2$}NiBr$_2$] / MAO	29	2	17	ethene	1 atm	0	10	100	17	2.6	20
[{(2,6-^{i}Pr$_2$Ph)$_2$DABH$_2$}NiBr$_2$] / MAO	26	2	1.7	ethene	1 atm	0	15	100	11	2.7	7
[{(2,6-^{i}Pr$_2$Ph)$_2$DABH$_2$}NiBr$_2$] / MAO	26	2	1.7	ethene	1 atm	25	15	100	3.1	2.5	38
[{(2,6-^{i}Pr$_2$Ph)$_2$DABMe$_2$}NiBr$_2$] / MAO	27	2	1.6	ethene	1 atm	0	15	100	52	1.6	48
[{(2,6-^{i}Pr$_2$Ph)$_2$DAB(Et)(Me)}NiBr$_2$] / MMAO	24	11	1.8	ethene	1 atm	35	30	100	17.1	not given	101
[{(2,6-^{i}Pr$_2$Ph)$_2$DAB(Et)(Me)}NiBr$_2$] / MMAO	24	11	0.95	ethene	200 psig	35	10	100	76.6	not given	28
[{(2,6-^{i}Pr$_2$Ph)$_2$DAB(CH$_2$)$_4$}NiBr$_2$] / MMAO	23	11	1.8	ethene	1 atm	35	30	100	26.8	not given	108
[{(2,6-^{i}Pr$_2$Ph)$_2$DAB(CH$_2$)$_4$}NiBr$_2$] / MMAO	23	11	0.89	ethene	200 psig	35	10	100	84.4	not given	39
[{Ph$_2$DAB(An)}NiBr$_2$]	20	1	not given	ethene	15 atm	35	not given	not given	oligomers	not given	85% linear α-olefins
[{Ph$_2$DAB(An)}NiBr$_2$]	20	1	not given	ethene	56 atm	35	not given	not given	oligomers	not given	85% linear α-olefins
[{(2-MePh)$_2$DAB(An)}NiBr$_2$] / MMAO	17	11	10	ethene	1 atm	35	30	100	0.092	not given	3
[{(2-MePh)$_2$DAB(An)}NiBr$_2$] / MMAO	17	11	5	ethene	200 psig	35	20	100	0.13	not given	2
[{(2-CF$_3$Ph)$_2$DAB(An)}NiBr$_2$] / MAO	13	11	2	ethene	1 atm	30	30	100	0.41	not given	31
[{(2-CF$_3$Ph)$_2$DAB(An)}NiBr$_2$] / MAO	13	11	1.1	ethene	200 psig	35	20	100	0.38	not given	5
[{(2-C$_6$F$_5$Ph)$_2$DAB(An)}NiBr$_2$] / MMAO	15	11	2.8	ethene	1 atm	35	20	100	0.102	not given	29
[{(2-C$_6$F$_5$Ph)$_2$DAB(An)}NiBr$_2$] / MMAO	15	11	1.7	ethene	200 psig	35	20	100	0.097	not given	5
[{(2, 4-Me$_2$Ph)$_2$DAB(An)}NiBr$_2$] / MMAO	18	11	2	ethene	1 atm	35	30	100	1.43	not given	24
[{(2, 4-Me$_2$Ph)$_2$DAB(An)}NiBr$_2$] / MMAO	18	11	1.5	ethene	200 psig	35	10	100	5.92	not given	13
[{(2-CF$_3$,4-Me)Ph$_2$DAB(An)}NiBr$_2$] / MMAO	14	11	2	ethene	1 atm	35	30	100	24	not given	75
[{(2-CF$_3$,4-Me)Ph$_2$DAB(An)}NiBr$_2$] / MMAO	14	11	2	ethene	200 psig	35	20	100	40	not given	27
[{(2,6-^{i}Pr$_2$Ph)$_2$DAB(An)}NiBr$_2$] / MMAO	9	11	1.6	ethene	1 atm	35	30	100	12.5	not given	106
[{(2,6-^{i}Pr$_2$Ph)$_2$DAB(An)}NiBr$_2$] / MMAO	9	11	0.83	ethene	200 psig	35	10	100	33.7	not given	24
[{(2,6-^{i}Pr$_2$Ph)$_2$DAB(An)}NiBr$_2$] / MAO	9	2	17	ethene	1 atm	0	30	100	17	2.3	74
[{(2,6-^{i}Pr$_2$Ph)$_2$DAB(An)}NiBr$_2$] / MAO	9	2	0.83	ethene	1 atm	not given	30	100	65	2.4	24
[{(2,6-^{i}Pr$_2$Ph)$_2$DAB(An)}NiBr$_2$] / MAO	9	2	0.83	ethene	1 atm	25	30	100	19	2.2	71
[{(2,6-^{i}Pr$_2$Ph)$_2$DAB(An)}NiBr$_2$] / MAO	9	2	0.83	ethene	4 atm	0	30	200	61	2.3	5
[{(2-C$_6$F5, 4-Me)Ph$_2$DAB(An)}NiBr$_2$] / MMAO	16	11	3.7	ethene	1 atm	35	20	100	4.14	not given	34
[{(2-C$_6$F5, 4-Me)Ph$_2$DAB(An)}NiBr$_2$] / MMAO	16	11	0.5	ethene	200 psig	35	20	100	7.37	not given	4

Table 3.01 Ethene polymerisation experiments of [(diimine)NiBr$_2$] activated with MAO or MMAO; where MAO is methylaluminiumoxane, and MMAO is "modified" methylaluminiumoxane (see references).

Complex	Key no.	Reference	moles of cat (X10⁻⁶)	monomer	Pressure	Temp (°C)	Time (h)	Solvent	Mn (X10⁻⁴)	Mw/Mn	branches (per 1000 C)
[{(2,6-^{i}Pr$_2$Ph)$_2$DABH$_2$}Pd(Me)(OEt$_2$)][BAF]	38	2	100	ethene	1 atm	25	24	50cm³ CH$_2$Cl$_2$	0.06	3	116
[{(2,6-^{i}Pr$_2$Ph)$_2$DABMe$_2$}Pd(Me)(OEt$_2$)][BAF]	40	2	100	ethene	1 atm	25	17	100cm³ CH$_2$Cl$_2$	2.9	3.9	103
[{(2,6-^{i}Pr$_2$Ph)$_2$DABH$_2$}Ni(Me)(OEt$_2$)][BAF]	35	2	0.83	ethene	1 atm	0	0.5	75cm³ CH$_2$Cl$_2$	9.2	3	6
[{(2,6-^{i}Pr$_2$Ph)$_2$DABMe$_2$}Pd(Me)(NCMe)][BAF]	41	10	5	ethene	400 psig	5	5	100 cm³ C$_6$H$_5$Cl	640	1.04	93
[{(2,6-^{i}Pr$_2$Ph)$_2$DABMe$_2$}Pd(Me)(NCMe)][BAF]	41	10	5	ethene	200 psig	5	5	100 cm³ C$_6$H$_5$Cl	690	1.03	99
[{(2,6-^{i}Pr$_2$Ph)$_2$DABMe$_2$}Pd(Me)(NCMe)][BAF]	41	10	5	ethene	100 psig	5	5	100 cm³ C$_6$H$_5$Cl	630	1.03	95
[{(2,6-^{i}Pr$_2$Ph)$_2$DABMe$_2$}Pd(Me)(NCMe)][BAF]	41	10	5	ethene	1 atm	5	5	100 cm³ C$_6$H$_5$Cl	220	1.15	not given
[{(2,6-^{i}Pr$_2$Ph)$_2$DABMe$_2$}Pd(CH$_2$CH$_2$CH$_2$CO$_2$Me)][BAF]	54	10	5	ethene	400 psig	5	1	100 cm³ C$_6$H$_5$Cl	130	1.09	108
[{(2,6-^{i}Pr$_2$Ph)$_2$DABMe$_2$}Pd(CH$_2$CH$_2$CH$_2$CO$_2$Me)][BAF]	54	10	5	ethene	400 psig	5	2	100 cm³ C$_6$H$_5$Cl	270	1.06	101
[{(2,6-^{i}Pr$_2$Ph)$_2$DABMe$_2$}Pd(CH$_2$CH$_2$CH$_2$CO$_2$Me)][BAF]	54	10	5	ethene	400 psig	5	3	100 cm³ C$_6$H$_5$Cl	390	1.05	109
[{(2,6-^{i}Pr$_2$Ph)$_2$DABMe$_2$}Pd(CH$_2$CH$_2$CH$_2$CO$_2$Me)][BAF]	54	10	5	ethene	400 psig	5	4	100 cm³ C$_6$H$_5$Cl	490	1.05	86
[{(2,6-^{i}Pr$_2$Ph)$_2$DABMe$_2$}Pd(CH$_2$CH$_2$CH$_2$CO$_2$Me)][BAF]	54	10	5	ethene	400 psig	5	5	100 cm³ C$_6$H$_5$Cl	590	1.05	93
[{(2,6-^{i}Pr$_2$Ph)$_2$DABMe$_2$}Pd(CH$_2$CH$_2$CH$_2$CO$_2$Me)][BAF]	54	10	5	ethene	400 psig	5	6	100 cm³ C$_6$H$_5$Cl	710	1.04	96
[{(2,6-^{i}Pr$_2$Ph)$_2$DABMe$_2$}Pd(CH$_2$CH$_2$CH$_2$CO$_2$Me)][BAF]	54	10	5	ethene	400 psig	5	14.9	100 cm³ C$_6$H$_5$Cl	1640	1.06	not given
[{(2,6-^{i}Pr$_2$Ph)$_2$DABMe$_2$}Pd(CH$_2$CH$_2$CH$_2$CO$_2$Me)][BAF]	54	10	5	ethene	400 psig	5	24.2	100 cm³ C$_6$H$_5$Cl	2360	1.06	not given
[{(2,6-^{i}Pr$_2$Ph)$_2$DABMe$_2$}Pd(CH$_2$CH$_2$CH$_2$CO$_2$Me)][BAF]	54	10	5	ethene	400 psig	5	5	100 cm³ C$_6$H$_5$Cl	580	1.05	102
[{(2,6-^{i}Pr$_2$Ph)$_2$DABMe$_2$}Pd(CH$_2$CH$_2$CH$_2$CO$_2$Me)][BAF]	54	10	5	ethene	300 psig	5	5	100 cm³ C$_6$H$_5$Cl	660	1.05	96
[{(2,6-^{i}Pr$_2$Ph)$_2$DABMe$_2$}Pd(CH$_2$CH$_2$CH$_2$CO$_2$Me)][BAF]	54	10	5	ethene	200 psig	5	5	100 cm³ C$_6$H$_5$Cl	590	1.06	96
[{(2,6-^{i}Pr$_2$Ph)$_2$DABMe$_2$}Pd(CH$_2$CH$_2$CH$_2$CO$_2$Me)][BAF]	54	10	5	ethene	100 psig	5	5	100 cm³ C$_6$H$_5$Cl	510	1.08	94
[{(2,6-^{i}Pr$_2$Ph)$_2$DABMe$_2$}Pd(CH$_2$CH$_2$CH$_2$CO$_2$Me)][BAF]	54	10	5	ethene	1 atm	5	5	100 cm³ C$_6$H$_5$Cl	250	1.27	98
[{(2,6-^{i}Pr$_2$Ph)$_2$DABMe$_2$}Pd(CH$_2$CH$_2$CH$_2$CO$_2$Me)][BAF]	54	10	2.5	ethene	400 psig	5	5	100 cm³ C$_6$H$_5$Cl	590	1.06	92
[{(2,6-^{i}Pr$_2$Ph)$_2$DABMe$_2$}Pd(CH$_2$CH$_2$CH$_2$CO$_2$Me)][BAF]	54	10	5	ethene	400 psig	5	5	100 cm³ C$_6$H$_5$Cl	580	1.05	102
[{(2,6-^{i}Pr$_2$Ph)$_2$DABMe$_2$}Pd(CH$_2$CH$_2$CH$_2$CO$_2$Me)][BAF]	54	10	7.5	ethene	400 psig	5	5	100 cm³ C$_6$H$_5$Cl	570	1.06	96
[{(2,6-^{i}Pr$_2$Ph)$_2$DABMe$_2$}Pd(CH$_2$CH$_2$CH$_2$CO$_2$Me)][BAF]	54	10	15	ethene	400 psig	5	5	100 cm³ C$_6$H$_5$Cl	610	1.05	93
[{(2,6-^{i}Pr$_2$Ph)$_2$DABMe$_2$}Pd(CH$_2$CH$_2$CH$_2$CO$_2$Me)][BAF]	54	1	not given	ethene	2 atm	not given	not given	not given	2.97	3.5	102
[{(2,6-^{i}Pr$_2$Ph)$_2$DABMe$_2$}Pd(CH$_2$CH$_2$CH$_2$CO$_2$Me)][BAF]	54	1	not given	ethene	11 atm	not given	not given	not given	4.9	2.7	100
[{(2,6-^{i}Pr$_2$Ph)$_2$DABMe$_2$}Pd(CH$_2$CH$_2$CH$_2$CO$_2$Me)][BAF]	54	1	not given	ethene	29 atm	not given	not given	not given	4.96	3	98

Table 3.02 Ethene polymerisation experiments of catalysts: [(diimine)Pd(Me)(OEt$_2$)][BAF], [(diimine)}Pd(Me)(NCMe)][BAF] and [(diimine)Pd(CH$_2$CH$_2$CH$_2$CO$_2$Me)][BAF]; where [BAF]= [B{3,5-(CF$_3$)$_2$C$_6$H$_3$}$_4$

3.2 The Reaction of α–diimines with Main Group and Zinc Organometallics

Over the last thirty years there has been a modest amount of research into the reactions of α-diimines with magnesium, aluminium, zinc and gallium and their alkyls. This brief review will discuss the findings of the literature by initially discussing the relevant magnesium chemistry discovered followed by other relevant findings for other metals.

3.2.1 The Reaction of Magnesium and MgR$_2$ with α-diimines

The majority of the work indicates the reaction of magnesium and magnesium complexes with α-diimine ligands leads to the production of radical species. This was determined as long ago as 1976 when the reaction of α-diimines with magnesium metal or MgCl$_2$ was reported to produce the triplet biradical species (α-diimine)$_2$Mg.[16] The complex was analysed by EPR in a glass matrix at -170°C and determined to be formed by two radical anions and Mg^{2+} cation. From simulation calculations for the production of (α-diimine)$_2$M, where M= Mg, Zn, Sr they determined that in the radical species the linear planes of the NCCN moiety in each ligand lie perpendicular to each other thus providing a tetrahedral species, as shown in Figure 3.08.

65
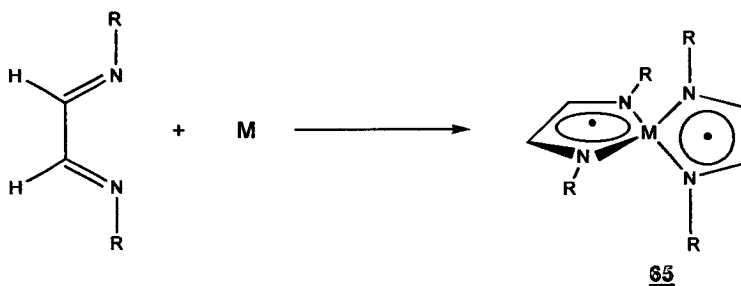
Figure 3.08 The reaction of α-diimines with alkaline earths

In 1982 and 1985 Kaim reported his significant findings on the reaction of magnesium and aluminium dialkyls with 2,2'-bipyridines (**Bipy**) and 1,10-phenanthrolines (**Phen**) (Figure 3.09).[17,18]
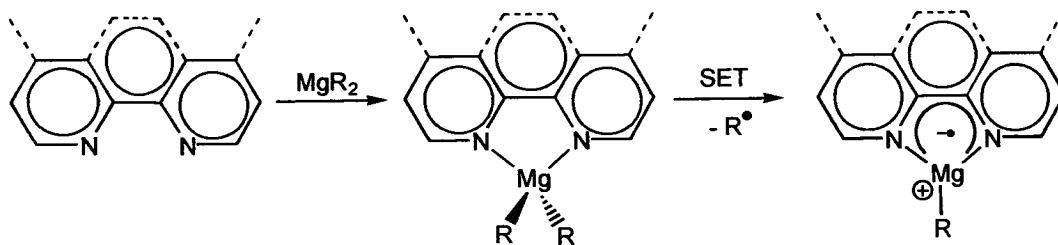
Figure 3.09 Reaction of Phen with dialkylmagnesium.

Full EPR analysis of the reaction mixtures provided evidence for the co-ordination of the radical anion to the electrophilic metal center. He suggested a "non-conventional" reaction pathway for these systems, shown in Figure 3.10. Upon direct coordination of the metal with the diimine it was proposed that a neutral complex [Mg(diimine)R$_2$] was initially produced. This was immediately followed by an electron transfer into the π^* orbital of the ligand. At this stage in the presence of a nucleophilic ligand, L, a bridge between the two metal centers M-L-M' would be created allowing electron exchange between those electron centers. Complete transfer of an electron *via* homolytic bond cleavage between the magnesium and an alkyl group, induced by additional activation e.g. UV or thermal energy, would generate the metal radical complex and an alkyl radical which are in a short-lived solvent cage. The existence of a solvent cage was demonstrated by trapping experiments in matrices and by the detection of their triplet EPR spectra.

Diimine + MgR$_2$ $\longrightarrow$ [Diimine$^{\delta-}$, MgR$^{\delta+}$]   **SET**= Single electron transfer

Charge transfer complex

$\downarrow$ **SET**

[Diimine$^{-\bullet}$, Mg] + $\overset{\bullet}{\text{R}}$ $\longleftarrow$ ^{1,3}[Diimine$^{-\bullet}$, Mg$\overset{+\bullet}{\text{R}}$] $\longrightarrow$ [(Diimine)MgR]

Escape   **Cage** $\downarrow$ **Hydrolysis**

Products
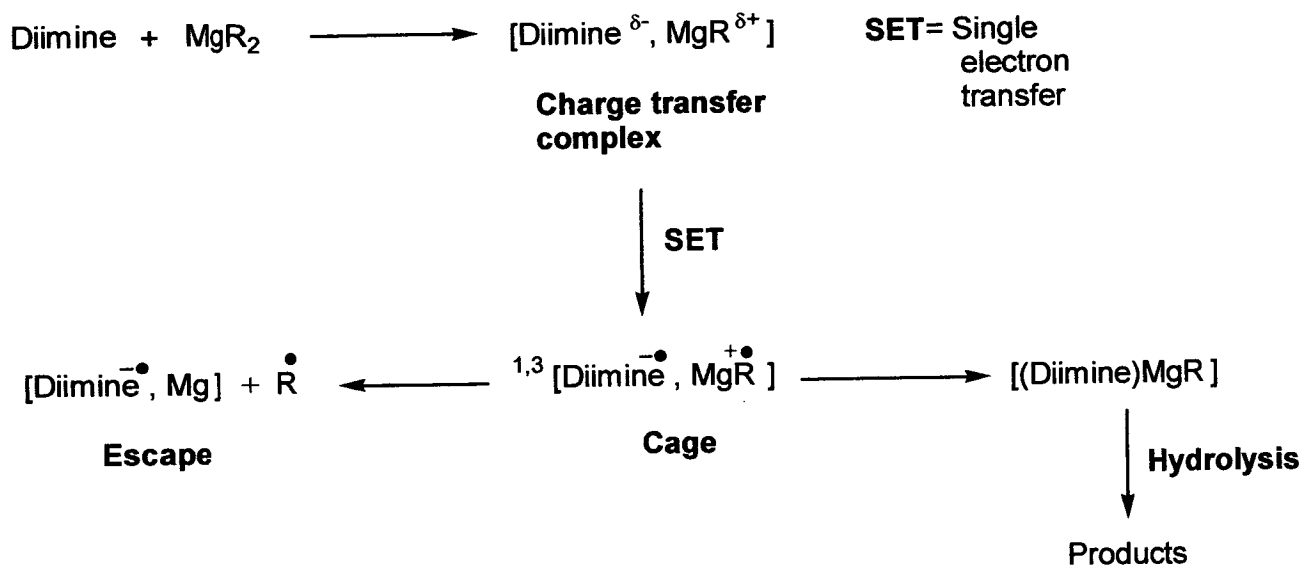
Figure 3.10 Mechanism proposed by Kaim for the reaction of α-diimines with dialkylmagnesium

In 1994, Raston and co-workers reported work similar to that carried out Corvaja and Pasimeni in 1976.[19,16] They investigated the reactions of activated magnesium and zinc in THF, and of sonified lithium in hexane, with (^{t}BuN=CH)$_2$. They found that the reactions produced triplet, ligand-centred biradical complexes of formula [M(diimine)$_2$] (where M = Mg, or Zn) or a ligand-centred radical where M = Li (Figure 3.11). Similarly, they found [Mg(diimine)$_2$] could be prepared by reacting activated magnesium (Mg*) or MgH$_2$ with (^{t}BuN=CH)$_2$ in THF, or MgCl$_2$ with [Li(diimine)$_2$]. They report the frozen-solution EPR data and the crystal structures of all three radical complexes.
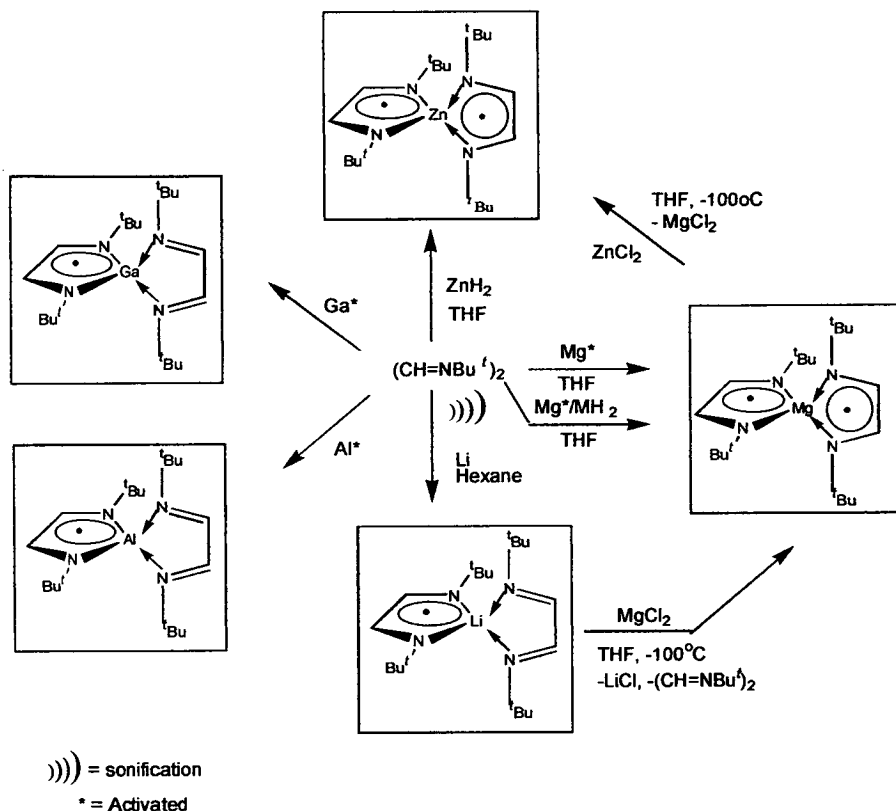
Figure 3.11 The synthesis of [M (diimine)$_2$] radicals where M = Mg, Zn and Li.

In the same year Thiele and co-workers, made a significant discovery revealing the reaction of the diimines (RN=CPh-CPh=NR) where (R=Ph, 4-MePh, 4-MeOPh) with magnesium in dimethoxyethane (DME) produces a mixture of complexes, firstly [Mg(dimine)$_2$(DME)] in which the ligands have been reduced to the radical anion, and secondly producing highly reactive complexes of formula [Mg(dimine)$_2$(DME)$_2$] in which the ligand has been doubly reduced to the diamagnetic enediamide (Figure 3.12).[20] The complexes were characterised from their respective crystal structures. The structure of [Mg(PhN-CPh=CPh-NPh)(DME)$_2$] displays a C=C double bond length of 1.372 (4) Å in the NCCN moiety, supporting the enediamide formulation.

66   67
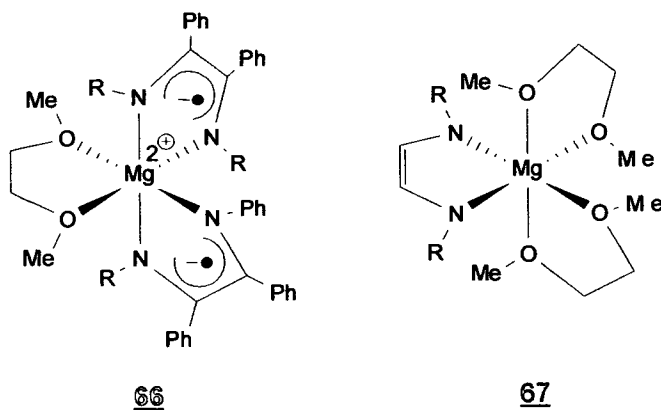
Figure 3.12 Structures of complexes A] [Mg(dimine)$_2$(DME)] and B] [Mg(dimine)(DME)$_2$]

The reaction of phenanthroline with ethyl magnesium bromide was studied experimentally by UV-VIS spectroscopy and computationally by Tuulmets an co-workers.[21] They summarized that [MgEtBr(phen)] is stable as calculated by *ab initio* calculations, and they attributed the stability to the atomic charge at the magnesium atom. A study of the bonding of the ligands in the EtMgBr fragment found the ligands to bind in an ionic fashion. They confirmed by *ab initio* and DFT calculations that the π* transitions in the Phen ligand cause all the intensive bands in the UV-Vis absorption spectrum.[21]

3.2.2 The Reaction of Aluminum, Zinc and Gallium Alkyls with α-diimines

3.2.2.1 Aluminium

In 1979 Vrieze, et al, published an interesting paper on the reaction of AlMe₃ with various α-diimines (R-N=CH)₂ where R= 2,6-Me₂Ph, 2,4,6-Me₃Ph, 4-ClPh, 4-MePh, or 4-MeOPh.[22] Over all they identified the production of 3 different complexes: 68, 69 and 70 (Figure 3.13), with no mention of radical species.
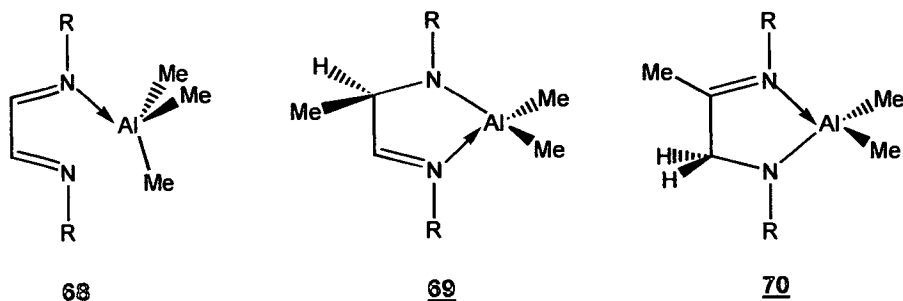
Figure 3.13 Products 68, 69 and 70 identified in the reaction of AlMe₃ with α-diimines.

The co-ordination product 68 was identified for R= 2,6-$(CH_3)_2C_6H_3$ and 2,4,6-$(CH_3)_3C_6H_2$. In complex 68 the ligand is coordinated to the metal by one σ(N) dative bond, the R groups in the ^1H NMR spectra are equivalent because of rapid ligand exchange. Complex 69 is thought to be produced by the rotation of the (Me)-Al group around the Al-N bond, until one of the Al-(Me) methyl groups is aligned in the proximity of the Np_π orbital at the non-coordinated end of the molecule. An

Al-(Me) bond is weakend by bonding interactions which results in the methyl migration of a methyl group from the aluminium to the N-C carbon atom, and the formation of a Al-N bond occurs, producing complexes of type 69 where Al is part of a five membered chelate ring. For R=4-ClPh, 4-CH_3Ph and 4-CH_3OPh, depending on the temperature, an intermolecular rearrangement (*via* hydrogen migration) can occur to produce complex 70. The proposed reaction scheme for the formation of 68, 69 and 70 is shown in Figure 3.14.
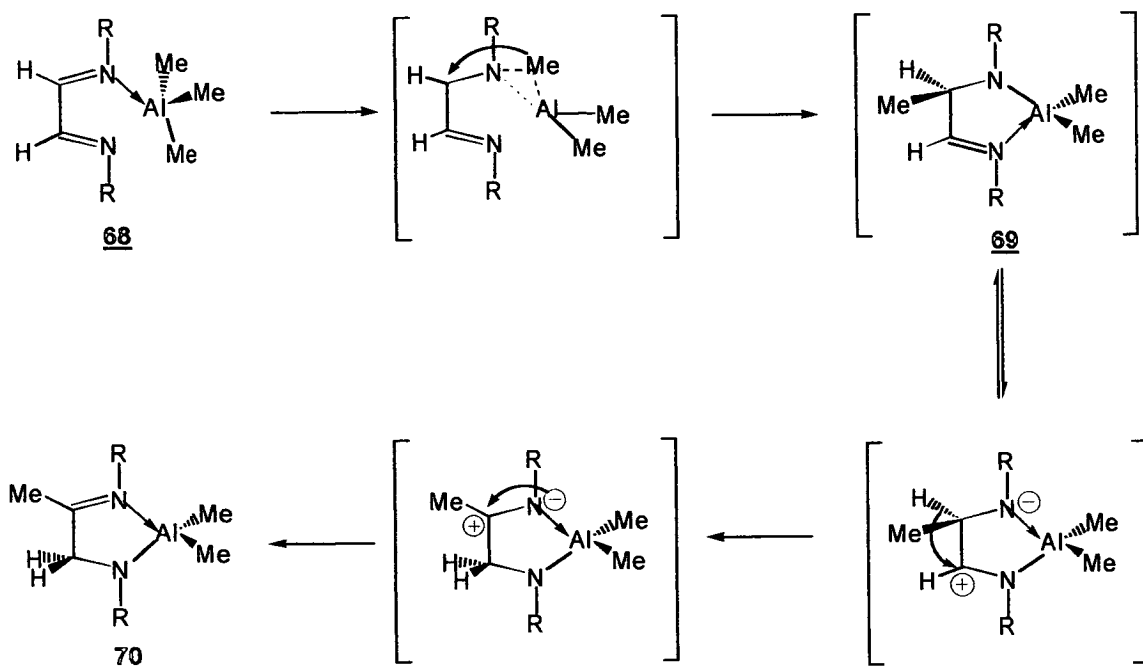
Figure 3.14 Proposed mechanism for the reaction of 68→69→70

In 1993, Vrieze and co-workers published a similar but extended study on the reaction of AlEt₃ with (ᵗBu-N=CH)₂ and (ᵗBu-NCH-2-C₅H₄N) (ᵗBu-Pyca) (Figure 3.15).[23] Again they summarized that initially the AlEt₃ only forms four co-ordinate monodentate complexes with these ligands. They observed the presence of persistent organometallic radical complexes this time, which were studied by EPR spectroscopy, and furthermore they identified the ethyl transfer reaction to either of the C or N nitrogen atoms in the N=C-C=N ligand backbone.
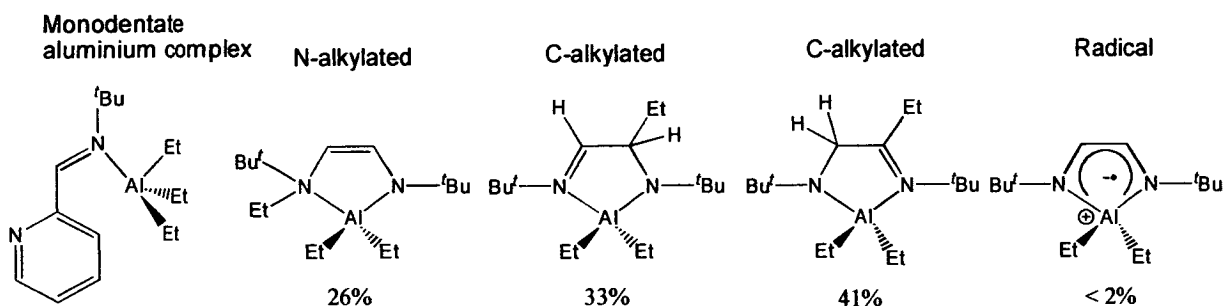
Figure 3.15 4-coordinate complex [Al(ᵗBu-Pyca)Et₂] and the secondary products produced from [Al(ᵗBu-N=CH)₂Et₂]

No further amendment to the mechanism was suggested, although one for an analogous zinc alkyl system was given (See later section 3.24). In 1998, Gibson et al, produced crystalline complexes of [AlMe₂{(2,6-^{i}Pr)₂PhN-CH₂C(Me)=N{(2,6-^{i}Pr)₂Ph}] (71) and [AlMe₂{(2,6-^{i}Pr)₂PhN-CH(Me)-2-Pyca}](72) in which aluminium is bonded to imino-amide and pyridyl-amide ligands respectively (Figure 3.16).[25]

71   72
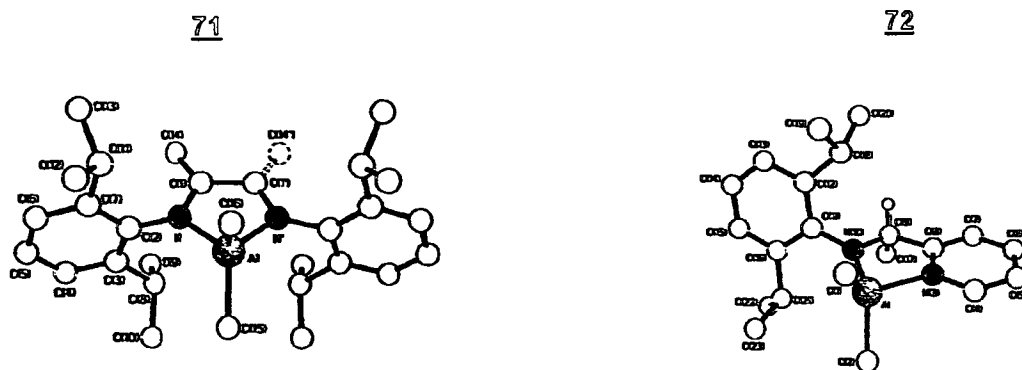
Figure 3.18 Molecular structures of [AlMe₂{(2,6-^{i}Pr)₂PhN-CH₂C(Me)=N{(2,6-^{i}Pr)₂Ph}] (71) and B:[AlMe₂{(2,6-^{i}Pr)₂PhN-CH(Me)-2-Pyca}] (72)

In 1999, Raston et al reported the reaction of LiAlH₄ with (^{t}Bu-N=CH)₂ which produces various products depending on the order of addition or the stoichiometry of the reactants.[26] The products have been identified as the lithium diamidoaluminium dihydride [Li{N(^{t}Bu)CHCH₂N^{t}Bu}₂AlH₂] (73), the dimeric diamidoaluminium hydride [cis-{μ-N(^{t}Bu)CH₂CH₂N^{t}Bu]AlH₂] (74), the heteroleptic lithium tetraamidinoaluminium species [(Et₂O)Li{N(^{t}Bu)CH₂}₂(CHN-^{t}Bu)₂Al] (75), and the dimeric lithium aluminium hydride adduct [{HN(^{t}Bu)CH(^{t}Bu)CHN^{t}Bu]Li(μ-H)₂AlH₂}₂] (76) as shown in Figure 3.17.
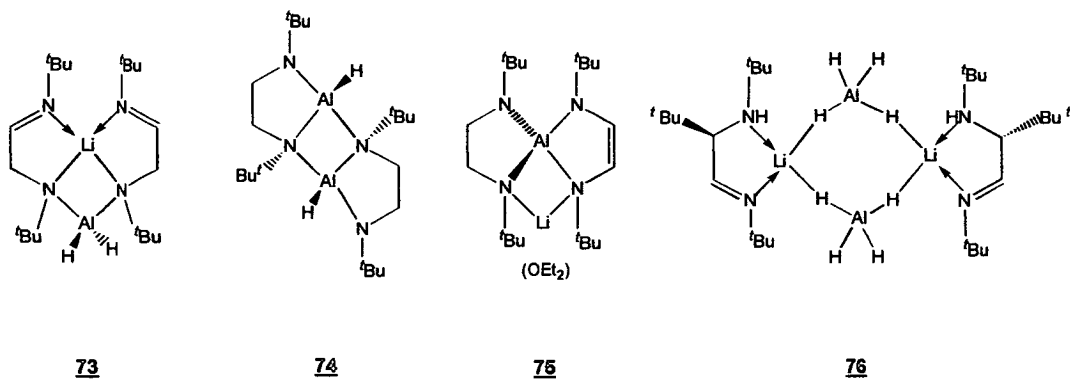
Figure 3.17 Products 73 to 76 identified in the reaction of LiAlH₄ with (^{t}Bu-N=CH)₂

Compounds 73 to 76 were isolated as air and moisture sensitive crystalline solids and were characterized by standard analytical techniques. Addition of an ethereal solution of the ligand to a chilled ethereal solution of LiAlH₄ in a 1:1 ratio produces complex 74, however addition in a 2:1 ratio produces complex 75. In contrast, the addition of an ethereal solution of LiAlH₄ to a chilled ethereal solution of (^{t}Bu-N=CH)₂, in both a 1:1 or a 2:1 ratio, produces solely complex 73. Complex 73 was found to decompose to 75 over a period of several weeks at room temperature, refer to Figure 3.18.
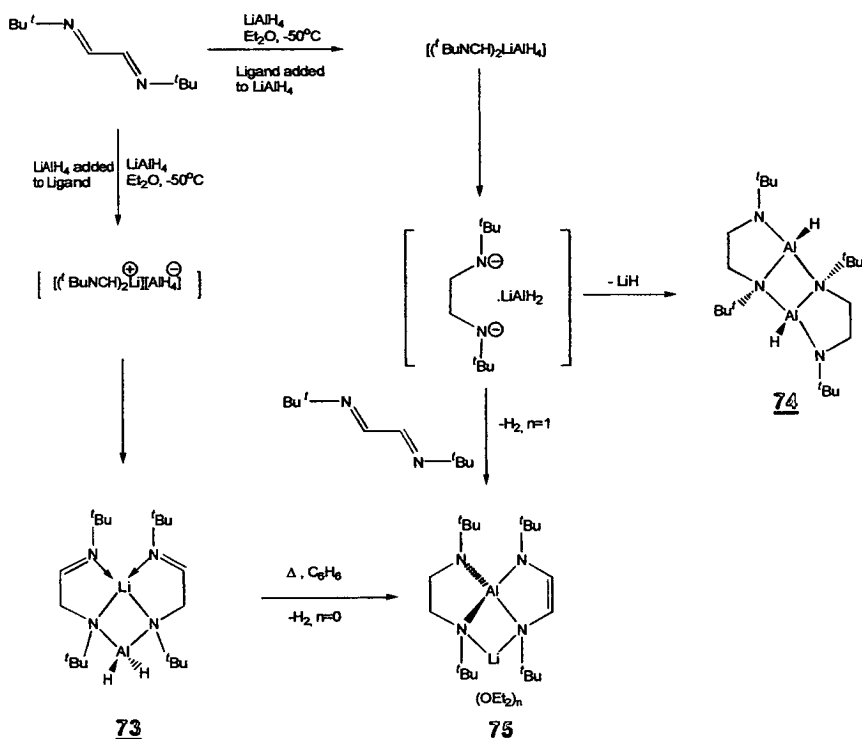
Figure 3.18 Proposed reaction profile for the reaction of LiAlH₄ with (^{t}BuN=CH)₂

3.2.2.2 Zinc

The nature of the reaction of zinc alkyls with α-diimines is discussed in several papers, [19, 23, 24] of which the results from Gardiner et al have been discussed in section 3.21.[19] As with the reaction of AlEt$_3$, Vreize and co-workers investigated the reaction of ZnEt$_2$ with (^{t}Bu-N=CH)$_2$ and (^{t}Bu-NCH-2-C$_5$H$_4$N) (^{t}Bu-Pyca).[23] They found that initially the ZnEt$_2$ only forms four co-ordinate bidentate complexes with these ligands. However, they subsequently observed the presence of persistent organometallic radical complexes, which were studied by EPR spectroscopy, and identified ethyl transfer to either of the C or N atoms in the N=C-C=N ligand backbone, as shown in Figures 3.19 and 3.20. In addition, a C-C coupled dimer, which exists in equilibrium with the radical species in solution, was detected and characterised by X-ray crystallography.
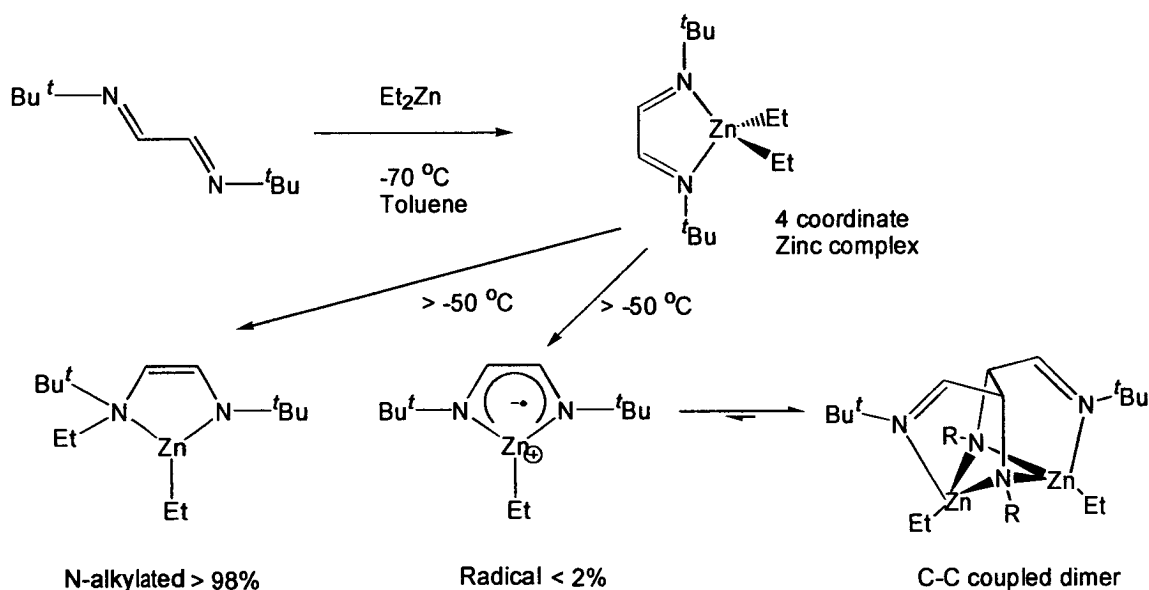
Figure 3.19 Reaction products produced during the reaction of ZnEt$_2$ with (^{t}Bu-N=CH)$_2$
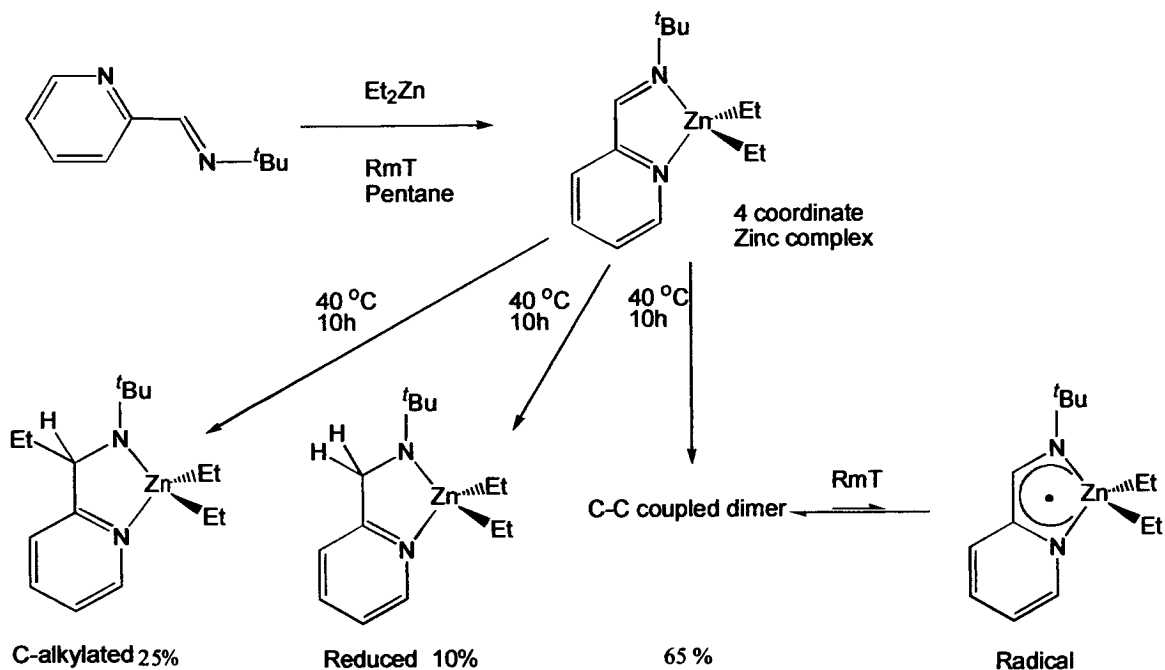
Figure 3.20 Reaction products produced during the reaction of ZnEt₂ with ᵗBu-Pyca

As a result of all these findings the mechanism in Figure 3.21 was proposed for the reaction of Zn with α-diimines. After complexation the product can either form a radical pair in a "solvent cage" **80**, similar to that reported by Kaim,[18] or eliminate ethene *via* β–hydride elimination **79** (when the alkyl group contains a β-hydrogen). The radical pair **80** can either react together to produce the N-alkylated or C-alkylated products **81** and **84**, or the ethyl radical can escape, and the radical complex can persist, (**83**). From molecular weight determinations they report that in solution complex **83** exists as a dimer, with the two Zn atoms bridged by a newly formed quadridentate dianionic ligand comprising of two C-C coupled diimine ligands **85**. On formation of the zinc hydride complex **79**, the complex can undergo a SET to produce another radical ion pair **78**, which on reaction with one another can either reform **79**, or hydrogenate one of the carbon atoms forming the imino-amide complex **82**.
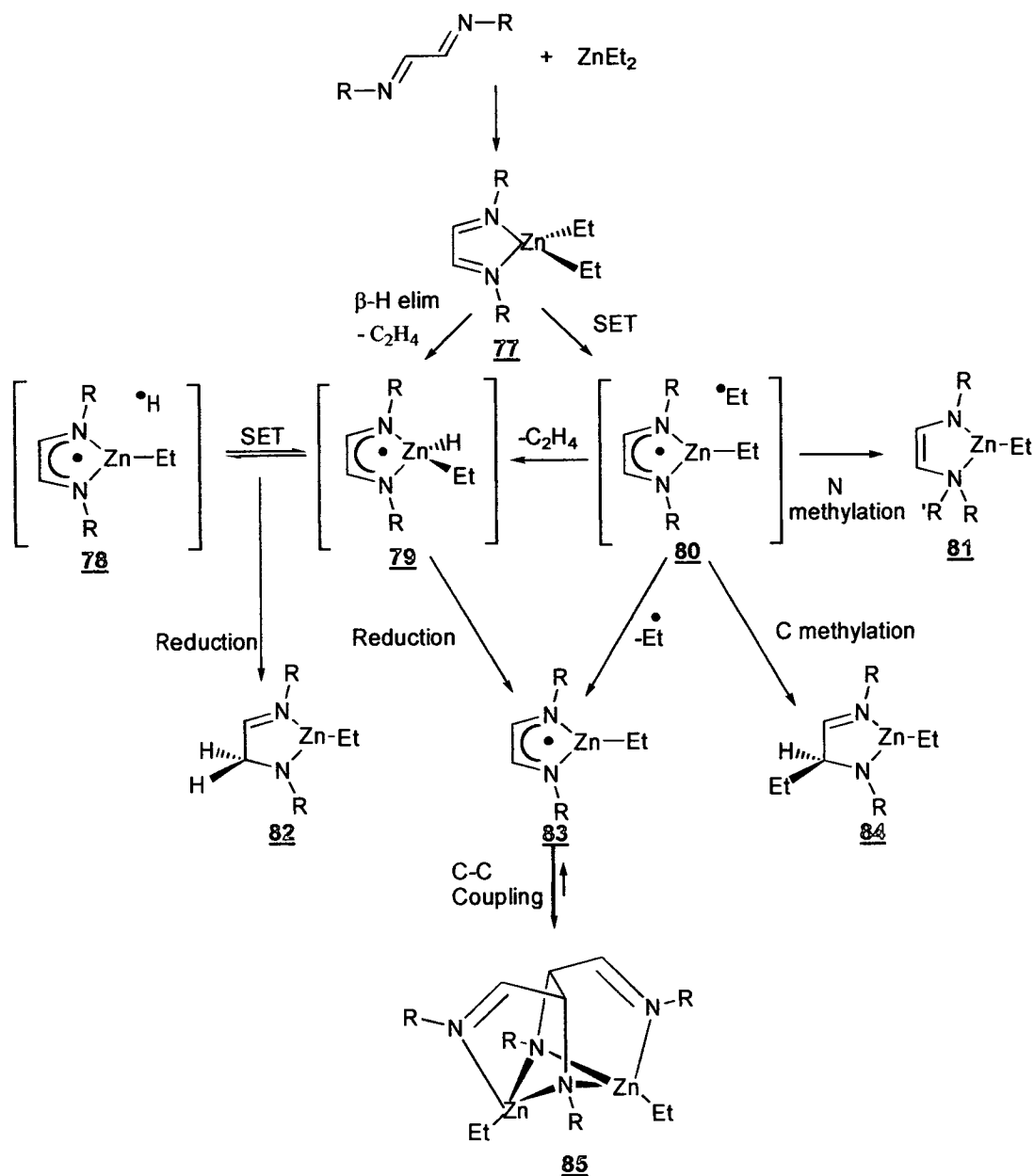
Figure 3.21 Reaction mechanism for the reaction of zinc alkyls with α-diimines

In 1991 Stoll, Kaim and Van Koten reported their findings on the theoretical and experimental study of diamagnetic and paramagnetic products from thermal and light-induced alkyl transfer between zinc or magnesium substrates and α-diimines $(RN=CH)_2$ where R= ^{t}Bu, H, Me.[24] The experimental was all carried out using various zinc alkyls ZnR_2 where R'=Me, Et, ^{i}Pr, o-Xyl, Ph, and the α-diimine $(^tBuN=CH)_2$, with only passing magnesium/diimine theoretical calculations being

discussed. They suggest the same reaction mechanism as Vrieze (Figure 3.21), minus the β-hyrdide elimination products, i.e. minus $\underline{78}$, $\underline{79}$ and $\underline{82}$.

3.2.2.3 Gallium

Radical chemistry dominates the reaction of gallium compounds with α-diimine ligands. As mentioned earlier (section 3.2.1) the radical $[Ga\{({}^{t}BuN=CH)_2\}_2]$ can be obtained by the cocondensation reaction of Ga vapour with $({}^{t}BuN=CH)_2$. [19, 28] Pott et al, report the reaction of Cp*Ga with different N-substuted α-diimine ligands.[27] Complexes of type $\underline{87}$ (Figure 3.22) are isolable, when the R substituents are 2,6-diisopropylphenyl or 2,6-diethylphenyl groups. The crystal structure of the former has been determined. The reaction of 2 equivalents of $({}^{t}BuN=CH)_2$ with Cp*Ga affords the radical $[Ga\{({}^{t}BuN=CH)_2\}_2]$ ($\underline{88}$), which has already been reported.[19, 28] The suggested reaction pathway for the production of $\underline{87}$ and $\underline{88}$ is given in Figure 3.22. Initially a [4+2] cycloaddition occurs to produce complex $\underline{87}$. The elimination of the Cp* substituent and the addition of another ligand produces the radical complex $[Ga\{({}^{t}BuN=CH)_2\}_2]$ $\underline{88}$.
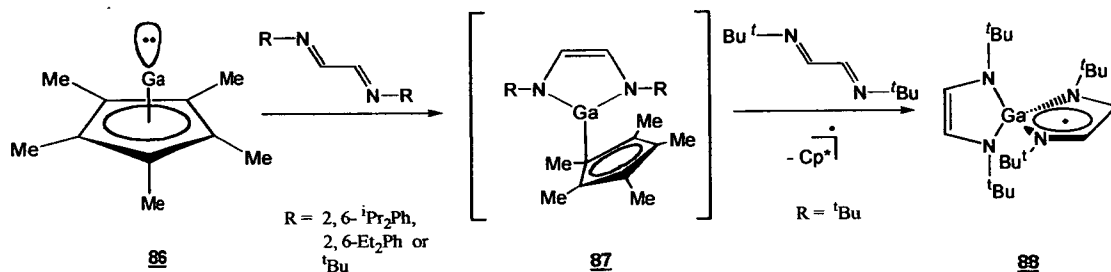
Figure 3.22 Reaction scheme for the reaction of Cp*Ga with ligands of type (RN=CH)₂

3.2.3 Summary of Zn, Mg, Li, Al and Ga Based Radical Complexes EPR Analyses Results

The following section consists of a summary of the EPR analysis results observed in the papers reviewed, so as to be used as a useful comparison to those obtained in our investigation of the reaction of dimethyl magnesium with various α-diimines (Tables 3.03 and 3.04). The collated results list the solvents used, the g_{av} values and the coupling constants, where given, for the systems shown. [17, 22, 23, 24]

Metal Fragment	Ligand	Reference	g_{av}	Solvent	a(^{14}N)/ mT	a(^{1}H)/mT	a(x)/mT
ZnMe$_2$	{(^{t}Bu)NCH}$_2$	24	Not given	hexane	0.485	0.585	0.050 (ZnCH$_3$)
ZnMe$_2$	{(^{t}Bu)NCH}$_2$	24	Not given	benzene	0.485	0.585	0.050 (ZnCH$_3$)
ZnMe$_2$	{(^{t}Bu)NCH}$_2$	24	Not given	benzene	Not given	Not given	Not given
ZnMe$_2$	{(^{t}Bu)NCH}$_2$	24	Not given	THF	0.552	0.552	0.298 (6 X ^{13}C), 0.179(1 X ^{67}Zn)
ZnMe$_2$	{(t-Amyl)NCH}$_2$	24	Not given	THF	0.552	0.552	Not given
ZnMe$_2$	{(o-Xyl)NCH}$_2$	24	Not given	THF	0.466	0.672(CH$_3$)	Not given
ZnEt$_2$	{(^{t}Bu)NCH}$_2$	24	Not given	THF	0.491	0.585	0.043 (ZnCH$_2$)
ZnEt$_2$	{(^{t}Bu)NCH}$_2$	24	Not given	Et$_2$O	0.528	0.56	Not given
ZnEt$_2$	{(^{t}Bu)NCH}$_2$	24	Not given	Et$_2$O	0.528	0.56	Not given
Zn^{i}Pr$_2$	{(^{t}Bu)NCH}$_2$	24	Not given	Et$_2$O	0.49	0.585	0.026 (ZnCH), 0.29 (6 X ^{13}C), 0.18(1 X ^{67}Zn)
Zn^{i}Pr$_2$	{(^{t}Bu)NCH}$_2$	24	Not given	Et$_2$O	Not given	Not given	Not given
Zn^{t}Bu$_2$	{(^{t}Bu)NCH}$_2$	24	Not given	Et$_2$O	0.508	0.578	Not given
Zn^{t}Bu$_2$	{(^{t}Bu)NCH}$_2$	24	Not given	Et$_2$O	0.557	0.557	Not given
Zn(o-Xyl)$_2$	{(^{t}Bu)NCH}$_2$	24	Not given	Et$_2$O	0.47	0.596	Not given
ZnPh$_2$	{(^{t}Bu)NCH}$_2$	24	Not given	THF	0.553	0.553	0.287 (6 X ^{13}C), 0.14(1 X ^{67}Zn)
Mg	{(^{t}Bu)NCH}$_2$	22	2.0036	hexane	Not given	Not given	Not given
Zn	{(^{t}Bu)NCH}$_2$	22	2.0068	THF	0.466(2)	0.623 (2)	Not given
Li	{(^{t}Bu)NCH}$_2$	22	2.0034	THF	0.466(2)	0.49(2)	0.13(6) (1 X ^{7}Li)
Al	{(^{t}Bu)NCH}$_2$	22	2.0012	THF	0.50(2)	0.50(2)	0.50(1) (^{27}Al)
Ga	{(^{t}Bu)NCH}$_2$	22	2.0024	THF	0.264(2)	Not given	1.839(1) (^{69,71}Ga)
ZnMe$_2$	{(^{t}Bu)NCH}$_2$	23	2.0021	Not given	0.487	0.587	Not given
ZnEt$_2$	{(^{t}Bu)NCH}$_2$	23	2.0021	Not given	0.487	0.587	Not given
Zn^{i}Pr$_2$	{(^{t}Bu)NCH}$_2$	23	2.0021	Not given	0.487	0.587	Not given
ZnCl$_2$	{(^{t}Bu)NCH}$_2$	23	2.0024	Not given	0.56	0.56	0.058 (^{35,37}Cl), 0.44 (^{67}Zn)
ZnPh$_2$	BIPY	23	2.0029	Not given	0.318	Not given	Not given
AlEt$_3$	{(^{t}Bu)NCH}$_2$	23	2.0028	Not given	0.537	0.563	0.793 (^{27}Al)
AlEt$_3$	BIPY	23	2.003	Not given	0.3	Not given	0.436 (^{27}Al)

Table 3.03 Summary of the EPR results for the reaction of Zn and main group metal compounds with α-diimine ligands. (1mT= 10G)

Metal Fragment	Ligand	Reference	g_{av}	Solvent	a(^{14}N)/ mT	a(^{1}H$_{(3)}$)/mT	a(^{1}H$_{(4)}$)/mT	a(^{1}H$_{(5)}$)/mT	a(^{1}H$_{(6)}$)/mT
K	BIPY	17	Not given	Et$_2$O	0.261	0.122	0.106	0.464	0.057
MgPh$_2$	BIPY	17	Not given	Et$_2$O	0.229	0.153	0.092	0.463	0.061
K	4,4'-dimethylBIPY	17	Not given	Et$_2$O	0.293	0.067	0.194	0.387	0.031
MgPh$_2$	4,4'-dimethylBIPY	17	Not given	Et$_2$O	0.262	0.12	0.168	0.429	0.049

Metal Fragment	Ligand	Reference	g_{av}	Solvent	a(^{14}N)/ mT	a(^{1}H$_{(2)}$)/mT	a(^{1}H$_{(3)}$)/mT	a(^{1}H$_{(4)}$)/mT	a(^{1}H$_{(5)}$)/mT
K	Phen	17	Not given	Et$_2$O	0.28	0.041	0.36	0.28	0.041
MgPh$_2$	Phen	17	Not given	Et$_2$O	0.262	0.054	0.428	0.112	0.054
K	4,7-dimethylPhen	17	Not given	Et$_2$O	0.29	0.021	0.29	0.326	0.064
MgPh$_2$	4,7-dimethylPhen	17	Not given	Et$_2$O	0.255	not given	0.305	0.225	0.049

Table 3.04 Summary of the EPR results for the reaction of diphenyl magnesium and potassium metal compounds with α-diimine ligands. (1mT= 10G)

3.3 Preparation of the α-diimine and Imino-amide Ligands

Our research interests were initially to react neutral diimine ligands such as glyoxal bis (2,6-diisopropylphenyldiimine) (62), glyoxal bis (2,6-dimethylphenyldiimine) (63), diacetal-bis (2,6-diisopropylphenyldiimine) (64), and 2,6-diisopropylphenylbis(imino) acenaphthene (65) with alkyl magnesium compounds to produce neutral complexes that would require activation before use as cationic alkene polymerisation catalysts (Figure 3.23).
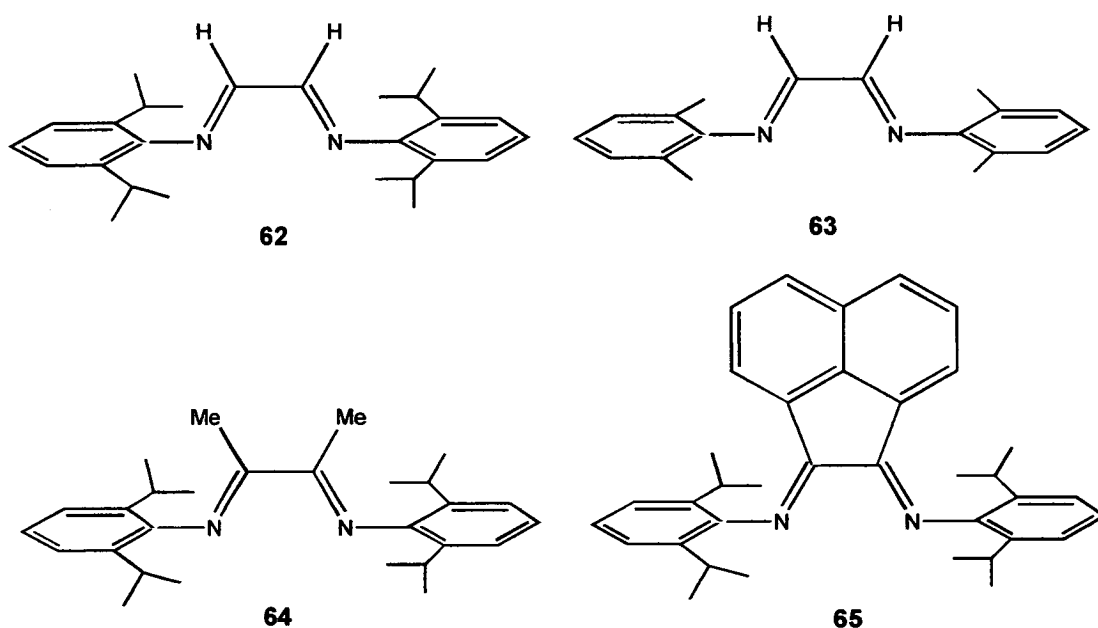
Figure 3.23 Structural formulae of 62, 63, 64 and 65.

Diimines are prepared by the nucleophilic addition reaction of the corresponding dicarbonyl compound with the appropriate primary amine (Figure 3.24). The initial addition product undergoes dehydration to form the imine. Elimination occurs with this orientation and the preferred product is the imine rather than the enamine.
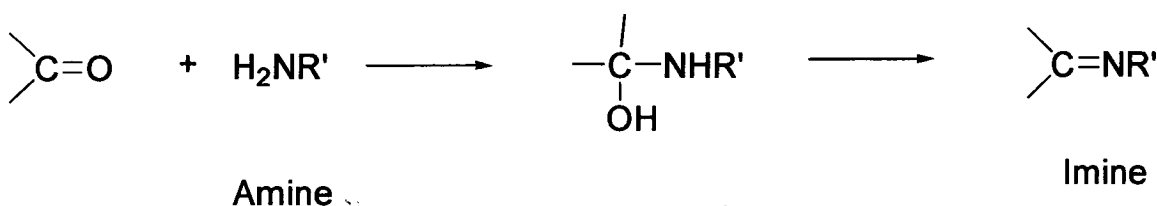
Figure 3.24 The reaction of carbonyls with a primary amine to produce an imine

Ligands **62** and **63** are prepared under mild conditions (Figure 3.25).[29, 30] The amine is added dropwise to a water/methanol solution of glyoxal at 33°C and stirred for one hour. Each product precipitates as a bright yellow powder, and can be crystallized from ethanol in yields of 45-47%. Formation of the imine can be established by NMR spectroscopy: e.g. a singlet in the ^{1}H NMR spectrum between 8.00-8.20 ppm where a HC=N group is present, and by the quaternary singlet in the ^{13}C NMR between 160-168 ppm due to the C=N unit. Preparation of the bulky ligands **64** and **65** involves using a weak acid, such as formic or acetic acid, as a catalyst. Compound **64** is prepared by adding 2,3-butadione to a methanol and acetic solution of 2,6-diisopropylamine. The reaction mixture was stirred for 20 hours at room temperature and the yellow precipitate of **64** collected and then crystallised from methanol in 56% yield.[31] Compound **65** was prepared by refluxing a mixture of acenaphthenequinone with 2,6-diisopropylamine in acetic acid for one hour.[32] An orange solid is afforded, and after washings with hexane the final product can be crystallised from ethanol. Complexes **62-65** were analysed by standard spectroscopic techniques.

During the reaction of **65** with dimethyl magnesium in section 3.53b, ligand **65** was crystallized as single orange rod crystals and the crystal structure determined by X-ray diffraction (Figure 3.26). The aromatic rings attached to the nitrogen twist so that they are positioned in an orthogonal arrangement to the bulky ligand backbone, thus producing a low energy conformer in which there is minimum steric interaction with the isopropyl groups.

62: R = H, R' = [i]Pr
63: R = H, R' = Me
64: R=Me, R' = [i]Pr

65: R= (acenaphthene), R' = [i]Pr
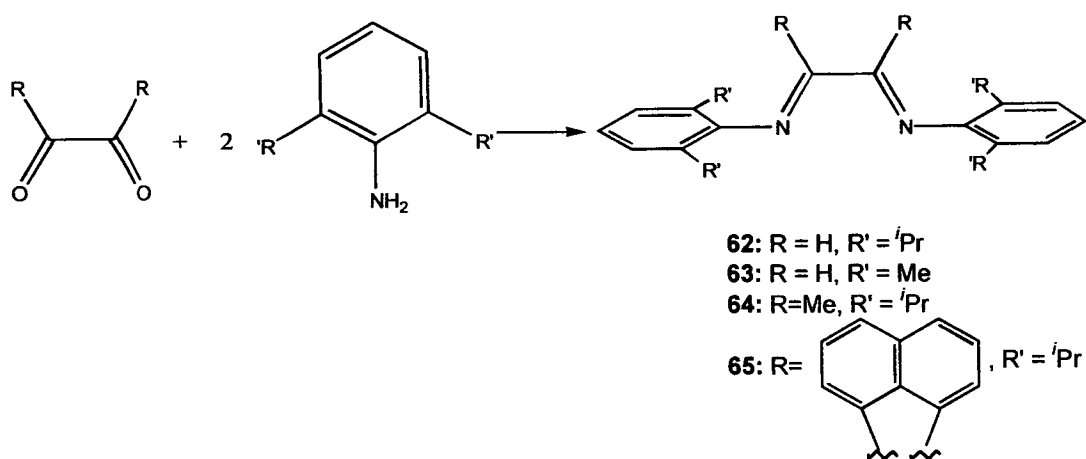
Figure 3.25 Synthesis of 62-65
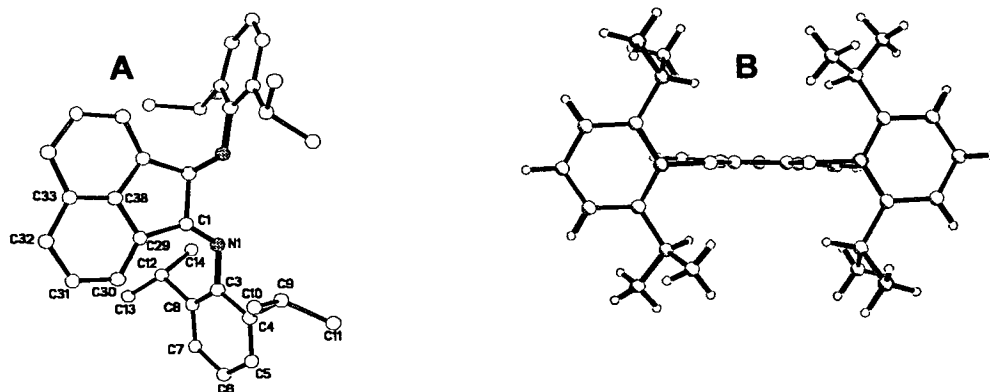
Figure 3.26 Molecular structure of 65: A displaying the atom labeling with the hydrogen atoms are omitted for clarity; and B showing the planarity of the NCCN unit and the orthogonality of the aromatic rings to the NCCN plane

A list of the bond lengths and angles obtained for **65** are shown in Table 3.05. In the five membered ring C(1)-C(29)-C(38)-C(29)#1-C(1)#1 the bond angles are C(1)#1-C(1)-C(29)=106.1(2)° , C(1)-C(29)-C(38)= 107.7(4)° and C(29)-C(38)-C(29)#1= 112.4(5)°, the angle about C(38) has been widened by around 4° because of the geometry imposed by the fused aromatic rings, this causes a contraction of the other angles in the 5-membered ring to accommodate this constraint. The double bond between C(33)-C(38)= 1.389(8) Å, consequentially means the conjugated C(29)-C(38) and C(29)#1-C(38) bond lengths are between a single and double bond [1.425(5) Å]. In the NCCN moiety the bond length of N(1)-C(1)=1.283(5) Å, which is consistent with a N=C double bond. The distance C(1)-C(1)#1=1.547(8) Å, is consistent with a single C-C bond, and the bond angle N(1)-C(1)-C(1)#1= 119.6(2)° is consistent with an sp^2 conjugated system.

N(1)-C(1)	1.283 (5)
C(1)-C(1)#1	1.547 (8)
C(33)-C(38)	1.389 (8)
C(29)-C(38)	1.425 (5)
C(29)#1-C(38)	1.425 (5)
N(1)-C(1)-C(1)#1	119.6 (2)
C(1)#1-C(1)-C(29)	106.1 (2)
C(1)-C(29)-C(38)	107.7 (4)
C(29)-C(38)-C(29)#1	112.4 (5)

Table 3.05 Selected bond lengths (Å) and angles (°) for 65.
With symmetry transformations used to generate equivalent atoms: #1 –x+1, y, -z+3/2.

3.4 Reaction of Magnesium Alkyls with α-diimine Ligands

At the outset we expected the reaction of magnesium alkyls with α-diimines would produce neutral mononuclear complexes in which the ligand would be chelated in a bidentate fashion to the magnesium. Complexation studies were undertaken using the commercially available Grignard, methyl magnesium chloride (Figure 3.27). However, the majority of the research has been centred around preparing dimethyl magnesium complexes.

where X = Cl or Me

62: R = H, R' = ^{i}Pr
63: R = H, R' = Me
64: R=Me, R' = ^{i}Pr

65: R= [structure] , R' = ^{i}Pr
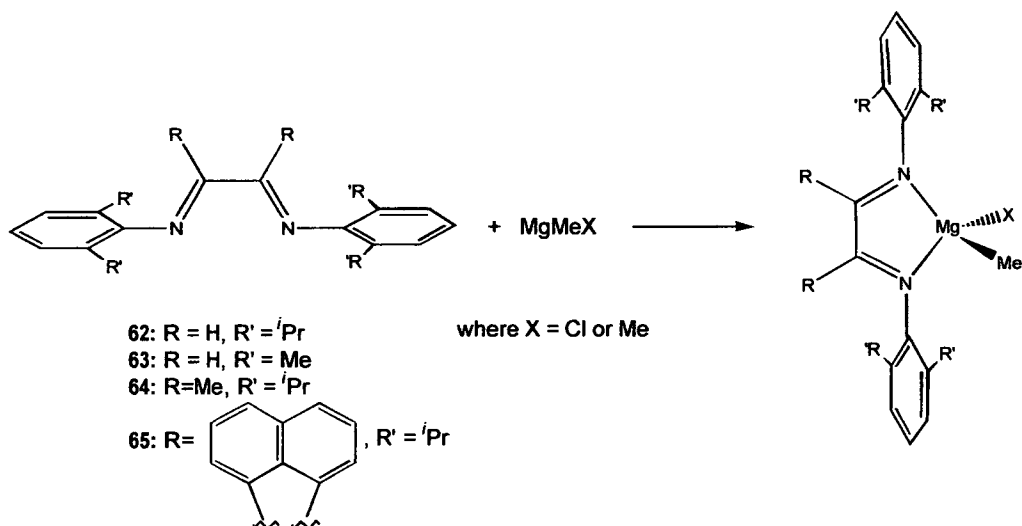
Figure 3.27 Diagram showing the expected products produced by reacting α–diimines with magnesium alkyls

3.4.1 Reaction of the Grignard MgMeCl with Ligands 63 & 65

3.4.1.1 Reaction of 63 with MgMeCl

Addition of [Me$_2$PhN=CH]$_2$ (**63**) with MgMeCl in the presence of THF produced an orange solution. The solvent was removed under vacuum and an orange oil obtained, the NMR of which was obtained. The sample was redissolved in THF to produce a more concentrated solution which was now red in colour, and placed in the freezer for 1 week, after which time colourless block crystals of a cage complex with molecular formula [Mg$_{13}$C$_{48.60}$H$_{99.20}$Cl$_{14}$O$_{18.40}$] (**66**) were isolated and their structure determined (Figures 3.28 and 3.29).
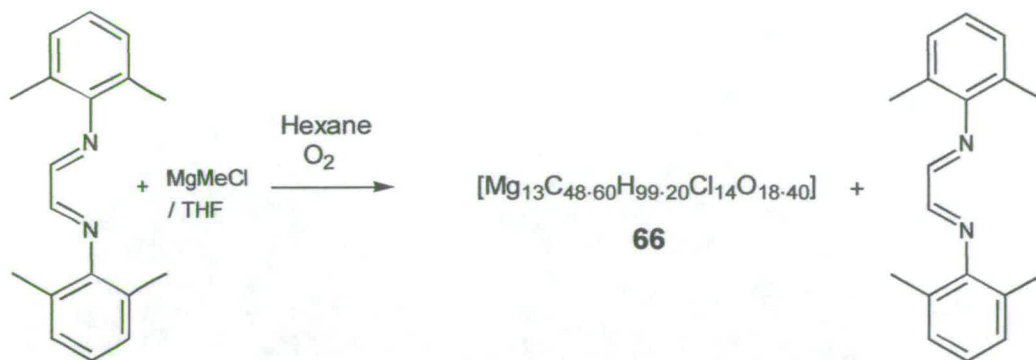
Figure 3.28 Diagram showing the synthesis of 66

Compound **66** is produced by oxidation of the Grignard in the presence of THF and EtOH (trace amount present from the recrystallisation of the diimine), and does not contain any diimine. The molecular structure of **66** is displayed in Figure 3.29.
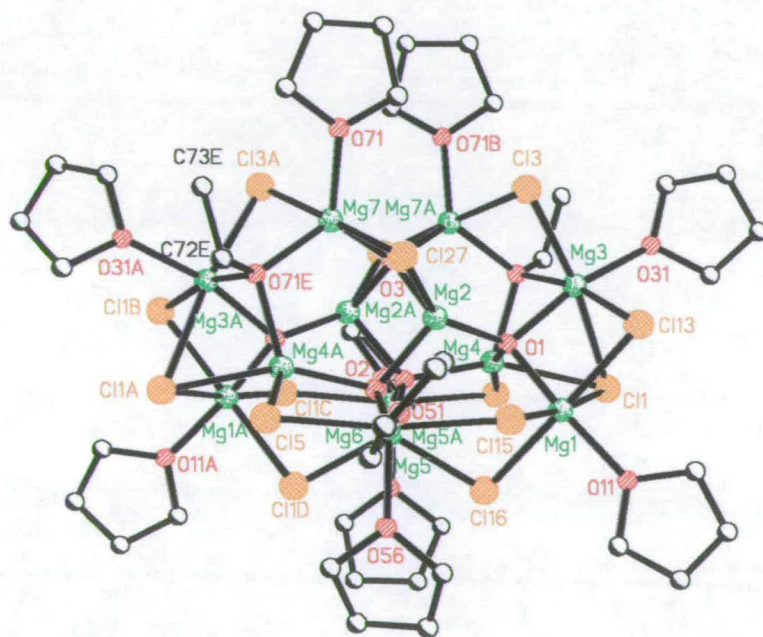
Figure 3.29 Molecular structure of 66 showing some of the numbering scheme

146

3.4.1.1a Magnesium Environments in 66

The structure of **66** is a cage containing 13 magnesium atoms, which are bridged by oxide, ethoxy or chloride ligands. The cage has C2 symmetry, with the C2 axis bisecting atoms O(3) and Mg(6). There are several magnesium co-ordination environments Mg(2) and Mg(6) [therefore Mg(2A)] are distorted tetrahedral, Mg(4), Mg(5) and Mg(7) [and therefore Mg(4A), Mg(5A) and Mg(7A)] are distorted trigonal bipyramidal, Mg(1) and Mg(3) [and therefore Mg(1A) and Mg(3A)] are distorted octahedral. The distorted tetrahedral magnesium environments are displayed more clearly in Figure 3.30 and are also elucidated in Table 3.06. The magnesium-magnesium distances are in general between 3.0-3.4 Å. The structure is composed of several fused 6-membered rings which are in a skewed boat conformation, e.g. Mg(7A)-Cl(27)-Mg(2)-O(1)-Mg(3)-Cl(13), which are in turn fused to several diamond shaped 4 membered rings, e.g. O(1)-Mg(1)-Cl(13)-Mg(3) at the edge of the structure.

Figure 3.30 Diagram displaying the distorted tetrahedral environment about Mg(2) and Mg(6).

Mg(2)-O(1)	1.892 (6)	Mg(2)-Mg(7A)	3.236 (4)
Mg(2)-O(3)	1.984 (5)	Mg(2)-Mg(4)	3.309 (4)
Mg(2)-O(2)	1.989 (6)	Mg(2)-Mg(4A)	3.382 (4)
Mg(2)-Cl(27)	2.411 (4)	Cl(27)-Mg(2)-O(2)	96.82 (19)
Mg(2)-Mg(7)	3.012 (4)	Cl(27)-Mg(2)-O(3)	92.16 (17)
Mg(2)-Mg(6)	3.071 (4)	Cl(27)-Mg(2)-O(1)	141.8 (2)
Mg(2)-Mg(2A)	3.174 (5)	O(1)-Mg(2)-O(2)	110.6 (3)
Mg(2)-Mg(5)	3.203 (4)	O(1)-Mg(2)-O(3)	104.9 (2)
		O(2)-Mg(2)-O(3)	105.4 (2)

Mg(6)-O(2)	1.957 (6)	O(2)-Mg(6)-O(2A)	111.2 (4)
Mg(6)-O(2A)	1.957 (6)	O(2)-Mg(6)-Cl(16)	111.64 (16)
Mg(6)-Cl(1D)	2.375 (3)	O(2)-Mg(6)-Cl(1D)	101.55 (16)
Mg(6)-Cl(1D)	2.375 (3)	O(2A)-Mg(6)-Cl(16)	101.55 (16)
Mg(6)-Mg(2A)	3.071 (4)	O(2A)-Mg(6)-Cl(1D)	111.64 (16)
Mg(6)-Mg(4A)	3.135 (3)	Cl(16)-Mg(6)-Cl(1D)	119.48 (19)
Mg(6)-Mg(5A)	3.443 (3)		

Table 3.06 Selected bond lengths (Å) and angles (°) about Mg(2) and Mg(6) in 66

Similarly the distorted trigonal bipyramidal magnesium environments are displayed more clearly in Figure 3.31 and are also elucidated in Table 3.07, and the distorted octahedral magnesium environments are displayed more clearly in Figure 3.32 and are also elucidated in Table 3.08.
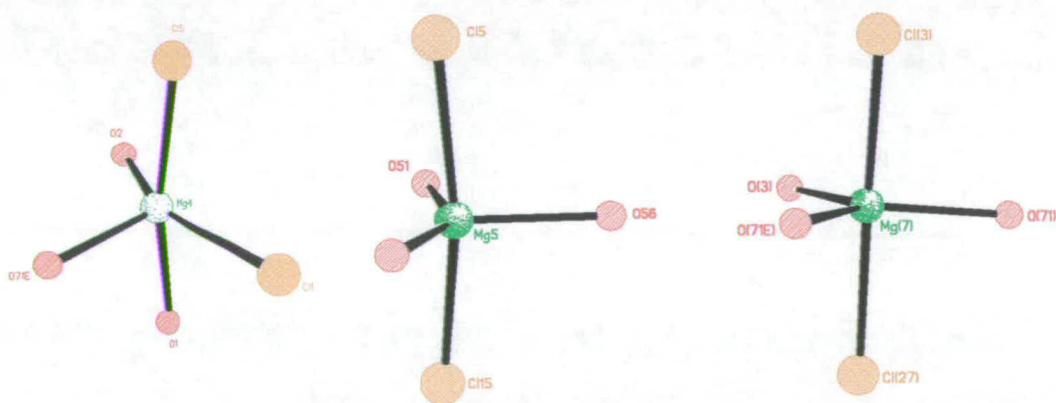
Figure 3.31 Diagram displaying the distorted trigonal bipyramidal environments about Mg(4), Mg(5) and Mg(7).

Mg(4)-O(2A)	1.995 (6)	O(1)-Mg(4)-Cl(1)	78.81 (18)
Mg(4)-O(1)	2.000 (6)	O(1)-Mg(4)-O(2A)	100.9 (2)
Mg(4)-O(71A)	2.091 (6)	Cl(1)-Mg(4)-Cl(5A)	88.72 (12)
Mg(4)-Cl(5A)	2.436 (4)	O(2A)-Mg(4)-Cl(5A)	88.80 (19)
Mg(4)-Cl(1)	2.611 (3)	O(1)-Mg(4)-O(71A)	82.1 (2)
Mg(4)-Mg(5A)	3.107 (4)	Cl(1)-Mg(4)-O(71A0	88.40 (18)
Mg(4)-Mg(6)	3.135 (3)	Cl(5A)-Mg(4)-O(71A)	101.4 (2)
Mg(4)-Mg(7A)	3.320 (4)	O(2A)-Mg(4)-O(71A)	117.0 (2)
Mg(4)-Mg(2A)	3.382 (4)		

Mg(5)-O(2)	1.966 (6)	O(2)-Mg(5)-O(56)	113.0 (3)
Mg(5)-O(56)	2.046 (6)	O(2)-Mg(5)-O(51)	147.1 (3)
Mg(5)-O(51)	2.093 (6)	O(51)-Mg(5)-O(56)	99.8 (3)
Mg(5)-Cl(5)	2.459 (4)	O(2)-Mg(5)-Cl(15)	94.84 (19)
Mg(5)-Cl(15)	2.462 (4)	O(51)-Mg(5)-Cl(15)	84.66 (19)
Mg(5)-Mg(4A)	3.107 (4)	O(56)-Mg(5)-Cl(15)	94.9 (2)
Mg(5)-Mg(6)	3.443 (3)	O(2)-Mg(5)-Cl(5)	88.84 (19)
		O(51)-Mg(5)-Cl(5)	86.2 (2)
		O(56)-Mg(5)-Cl(5)	93.8 (2)

Mg(7)-O(3)	1.944 4	O(71)-Mg(7)-O(71E)	119.9 (3)
Mg(7)-O(71E)	2.020 (6)	O(71)-Mg(7)-O(3)	124.2 (3)
Mg(7)-O(71)	2.054 (6)	O(71E)-Mg(7)-O(3)	115.9 (3)
Mg(7)-Cl(13A)	2.507 (4)	O(3)-Mg(7)-Cl(27)	88.15 (13)
Mg(7)-Cl(27)	2.580 (4)	O(71)-Mg(7)-Cl(27)	88.6 (2)
Mg(7)-Mg(3A)	3.210 (4)	O(71E)-Mg(7)-Cl(27)	91.53 (19)
Mg(7)-Mg(2A)	3.236 (4)	O(3)-Mg(7)-Cl(3A)	95.75 (14)
Mg(7)-Mg(4A)	3.320 (4)	O(71)-Mg(7)-Cl(13A)	90.4 (2)
Mg(7)-Mg(7A)	3.482 (6)	O(71E)-Mg(7)-Cl(13A)	85.49(19)

Table 3.07 Selected bond lengths (Å) & angles (°) about Mg(4), Mg(5) and Mg(7) in 66.
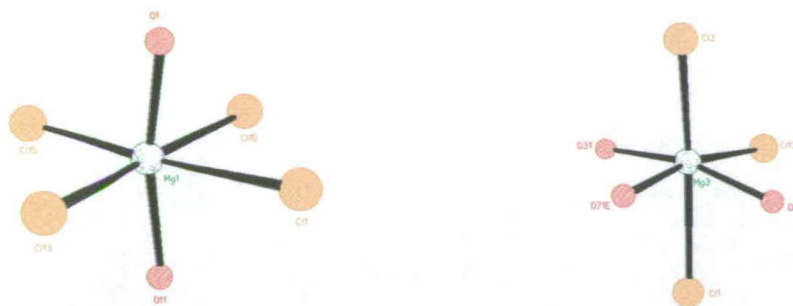
Figure 3.32 Diagram displaying the distorted octahedral Mg(1) and Mg(3) environments.

Mg(1)-O(1)	1.947 (6)	O(1)-Mg(1)-Cl(15)	96.3 (2)
Mg(1)-O(11)	2.056 (6)	O(1)-Mg(1)-Cl(1)	78.20 (19)
Mg(1)-Cl(13)	2.438(4)	Cl(1)-Mg(1)-O(11)	89.0 (2)
Mg(1)-Cl(13)	2.561 (4)	Cl(15)-Mg(1)-O(11)	96.4 (2)
Mg(1)-Cl(16)	2.649(4)	Cl(15)-Mg(1)-Cl(16)	93.07 (12)
Mg(1)-Cl(1)	2.670 (4)	Cl(1)-Mg(1)-Cl(16)	89.49 (12)
Mg(1)-Mg(3)	2.961 (4)	O(1)-Mg(1)-Cl(16)	89.99 (19)
Mg(1)-Mg(4)	3.169 (4)	O(11)-Mg(1)-Cl(16)	89.3 (2)
Mg(1)-Mg(2)	3.301 (4)	Cl(15)-Mg(1)-Cl(13)	92.01 (13)
		Cl(1)-Mg(1)-Cl(13)	85.23 (11)
		O(1)-Mg(1)-Cl(13)	87.16 (19)
		O(11)-Mg(1)-Cl(13)	92.4 (2)

Mg(3)-O(1)	1.995 (6)	O(1)-Mg(3)-Cl(13)	88.1 (2)
Mg(3)-O(31)	2.081 (7)	O(1)-Mg(3)-O(71A)	81.4 (2)
Mg(3)-O(71A)	2.123 (6)	Cl(13)-Mg(3)-O(31)	91.7 (2)
Mg(3)-Cl(3)	2.461 (4)	O(31)-Mg(3)-O(71A)	96.9 (3)
Mg(3)-Cl(13)	2.491 (4)	O(1)-Mg(3)-Cl(3)	98.47 (19)
Mg(3)-Cl(1)	2.708 (4)	Cl(13)-Mg(3)-Cl(3)	103.75 (13)
Mg(3)-C(32')	2.758 (15)	O(31)-Mg(3)-Cl(3)	95.7 (2)
Mg(3)-Mg(4)	2.868 (4)	O(71A)-Mg(3)-Cl(3)	84.54 (18)
Mg(3)-Mg(7A)	3.210 (4)	O(1)-Mg(3)-Cl(1)	76.51 (18)
		Cl(13)-Mg(3)-Cl(1)	85.79 (11)
		O(31)-Mg(3)-Cl(1)	89.0 (2)
		O(71A)-Mg(3)-Cl(1)	85.24 (18)

Table 3.08 Selected bond lengths (Å) and angles (°) about Mg(1) and Mg(3) in 66

3.4.1.1b Oxide, Ethoxide and THF Bridges in 66

There are three types of oxygen containing ligands that act as bridges in **66** (Figure 3.33 and Table 3.09):

1) 4-coordinate distorted tetrahedral Mg_4-μ_4O, e.g. O(1), O(2), and O(3).

The average Mg_4-μ_4O bond length is 1.966Å (Table 3.09), which is consistent with the average obtained from literature values literature values (1.952 (8)Å).[33] This co-ordination mode is very rare with the oxygen being solely co-ordinated to 4 magnesium atoms. There is only one other structure reported in the CSD.[33]

2) 4-coordinate distorted tetrahedral oxygen centre bonded to an ethoxy group and 3-magnesium atoms Mg_3-μ_3O-Et, e.g. O(71E). In a Mg_3-μ_3O-Et fragment, the average Mg_3-μ_3O bond length is 2.078Å (Table 3.10), which falls in the range average bond lengths (2.066-2.101Å) obtained from the literature (Table 3.11).[33-37] Similarly the average Mg-μ_3O-Mg bond angle (98.3°) and the average Et-μ_3O-Mg bond angle (118.7°) is also comparable to literature averaged values in the Mg_3-μ_3O-Et fragment (96.3-97.7° and 118.9° respectively). The structures of the crystals mentioned from the literature are shown in Figure 3.34.

3) 3-coordinate oxygens in the THF molecule, e.g. O(31), O(71), O(11).
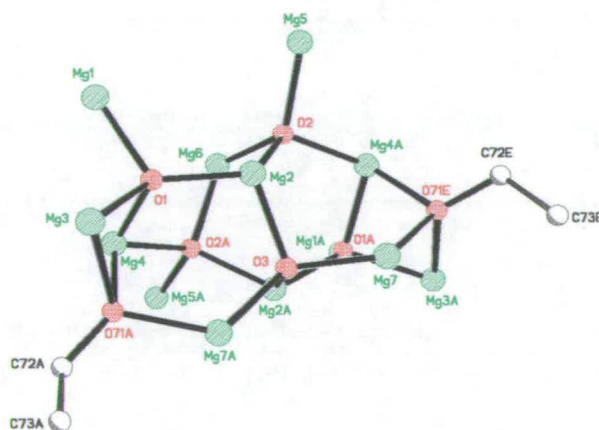
Figure 3.34 Diagram displaying the distorted tetrahedral environment about O(1)-O(3) and at O(71) and O(71A).

O(1)-Mg(1)	1.947 (6)	Mg(1)-O(1)-Mg(2)	118.6 (3)
O(1)-Mg(2)	1.892 (6)	Mg(1)-O(1)-Mg(3)	97.4 (2)
O(1)-Mg(3)	1.995 (6)	Mg(1)-O(1)-Mg(4)	106.8 (3)
O(1)-Mg(4)	2.000 (6)	Mg(2)-O(1)-Mg(3)	121.3 (3)
		Mg(2)-O(1)-Mg(4)	116.4 (3)
		Mg(3)-O(1)-Mg(4)	91. 8 (3)

O(2)-Mg(2)	1.989 (6)	Mg(2)-O(2)-Mg(5)	108.2 (3)
O(2)-Mg(5)	1.966 (6)	Mg(2)-O(2)-Mg(6)	102.2 (3)
O(2)-Mg(6)	1.957 (6)	Mg(2)-O(2)-Mg(4A)	116.2 (3)
O(2)-Mg(4A)	1.995 (6)	Mg(5)-O(2)-Mg(6)	122.7 (3)
		Mg(5)-O(2)-Mg(4A)	103.0 (3)
		Mg(4A)-O(1)-Mg(6)	105.0 (2)

O(3)-Mg(2)	1.984 (5)	Mg(2)-O(3)-Mg(2A)	106.2 (4)
O(3)-Mg(2A)	1.984 (5)	Mg(2)-O(3)-Mg(7)	100.15 (12)
O(3)-Mg(7)	1.944 (4)	Mg(2)-O(3)-Mg(7A)	110.96 (13)
O(3)-Mg(7A)	1.944 (4)	Mg(2A)-O(3)-Mg(7)	110.96 (13)
		Mg(2A)-O(3)-Mg(7A)	110.15 (12)
		Mg(7A)-O(3)-Mg(7)	127.2 (4)

Average	1.966	Average	109.7

Table 3.09 Selected bond lengths (Å) and angles (°) at Mg-μ_4O fragment.

O(71E)-Mg(7)	2.020 (6)	Mg(7)-O(71E)-Mg(3A)	101.5 (3)
O(71E)-Mg(3A)	2.123 (6)	Mg(7)-O(71E)-Mg(4A)	107.7 (3)
O(71E)-Mg(4A)	2.091 (6)	Mg(3A)-O(71E)-Mg(4A)	85.8 (2)
Average	2.078	Average	98.3

O(71E)-C(72E)	1.435 (10)	Mg(4A)-O(71E)-C(72E)	116.8 (5)
		Mg(7)-O(71E)-C(72E)	118.9 (5)
		Mg(3A)-O(71E)-C(72E)	120.6 (5)
		Average	118.7

Table 3.10 Selected bond lengths (Å) and angles (°) at Mg$_3$-μ_3O-C fragment.

Mg-μ₄O

Mg₃-μ₃O-C
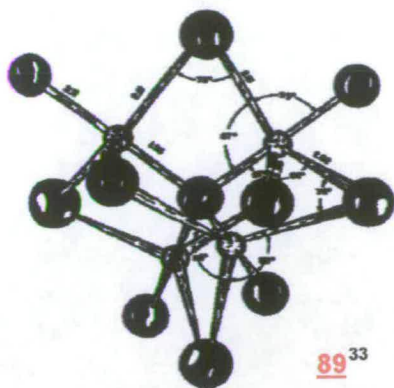
89 [33]
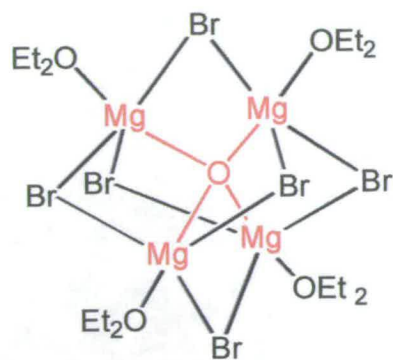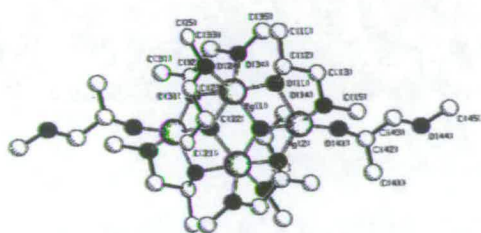
90 [34]
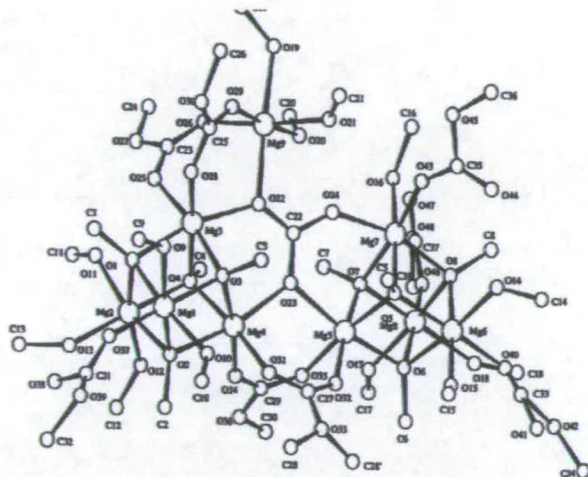
91 [35]
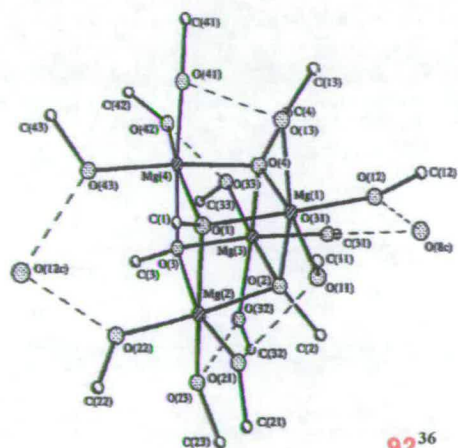
92 [36]
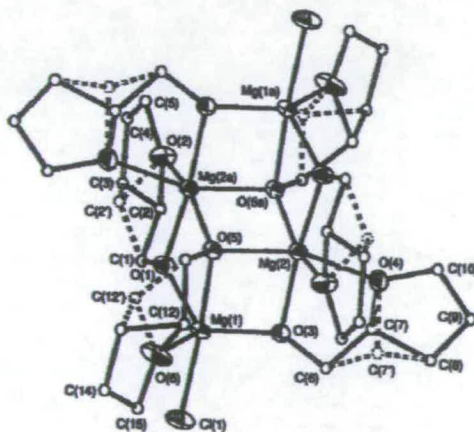
93 [37]

Figure 3.34 Structures from the literature containing Mg-μ₄O or Mg-μ₃O-C.

3.4.1.1c Chloride Bridges in 66

The chloride bridges in **66** are mainly μ_2-Cl, however there are two μ_3-Cl bridging chlorides (e.g. Cl(1)), (Figure 3.29, Table 3.11). A CSD search revealed that there are a handful of structures containing μ_3Cl-Mg bridges, e.g. compounds **94**-**97** (Figure 3.35), a selection of bond lengths and angles are summarised for comparison with those observed in **66** (Table 3.12).[38-41] The μ_2-Cl bond lengths and angles are comparable to those obtained in the literature e.g. for **66** the average μ_2-Cl bond length is 2.493 Å compared with 2.496Å **94**-**97**. In contrast the μ_3-Cl bond lengths and angles are very different on comparison to compounds **94**-**97**. The Mg-Cl-Mg angles are significantly shorter [65.23 (10)-73.73 (11)° **66**, 79.6 (1)-89.8 (2)° **94**-**97**] than those reported and the Mg-Cl bond distances are significantly longer [2.670 (4)-3.169 (4) Å **66**, 2.495 (9)-2.779 (5)Å **94**-**97**].

μ_2-Cl	Distance (Å)	Mg-μ_2Cl-Mg	Angle (°)
Cl(3)-Mg(7)#1	2.507 (4)	Mg(7)#1-Cl(3)-Mg(3)	80.50 (11)
Cl(3)-Mg(3)	2.461 (4)	Mg(3)-Cl(13)-Mg(1)	71.74 (11)
Cl(13)-Mg(3)	2.491 (4)	Mg(1)-Cl(16)-Mg(6)	99.89 (13)
Cl(13)-Mg(1)	2.561 (4)	Mg(5)-Cl(15)-Mg(1)	120.53 (13)
Cl(16)-Mg(1)	2.649 (4)	Average	93.15
Cl(16)-Mg(6)	2.375 (3)		
Cl(15)-Mg(5)	2.462 (4)		
Cl(15)-Mg(1)	2.438 (4)		
Average	2.493		

μ_3-Cl	Distance (Å)	Mg-μ_3Cl-Mg	Angle (°)
Cl(1)-Mg(1)	2.670 (4)	Mg(1)-Cl(1)-Mg(3)	66.80 (10)
Cl(1)-Mg(3)	2.961 (4)	Mg(3)-Cl(1)-Mg(4)	65.23 (10)
Cl(1)-Mg(4)	3.169 (4)	Mg(1)-Cl(1)-Mg(4)	73.73 (11)
Average	2.933	Average	68.58

Table 3.11 Selected bond lengths and angles from the crystal structure of 66

94 [38]

[GaCl$_4$]$^-$

95 [39]

[^{i}PrInBr$_{2.7}$Cl$_{0.3}$]$^-$
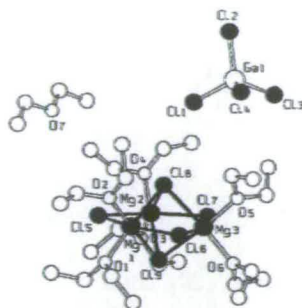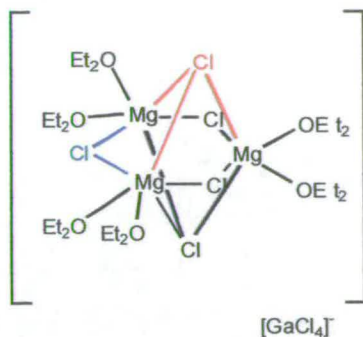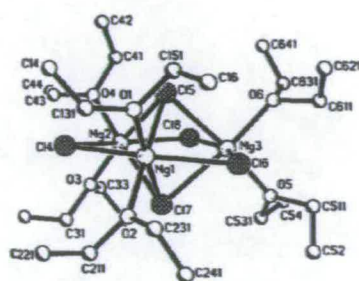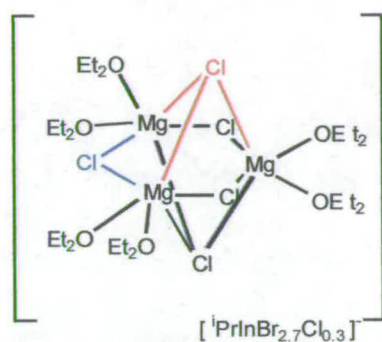
96 [40]
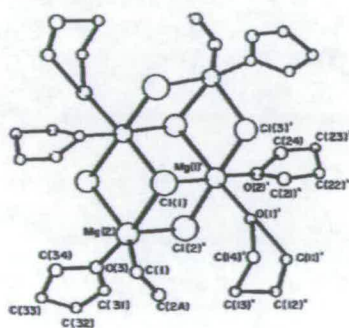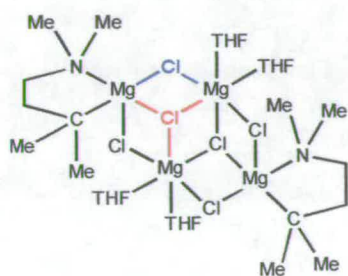
97 [41]
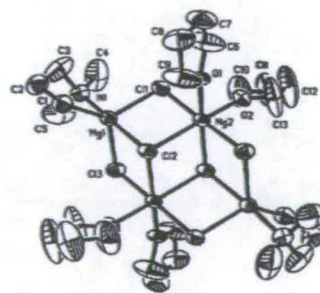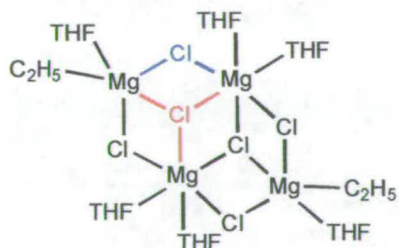
Figure 3.35 Some crystal structures reported containing Mg$_2$-μ_2Cl and Mg$_3$-μ_3Cl fragments

Complex	μ_2-Cl	Distance (Å)
94	Mg-Cl	2.502
94	Mg-Cl	2.484 (2)
94	Mg-Cl	2.514 (2)
95	Mg(1)-Cl(4)	2.610 (5)
95	Mg(2)-Cl(4)	2.585 (4)
95	Mg(1)-Cl(6)	2.549 (5)
95	Mg(3)-Cl(6)	2.518 (5)
95	Mg(2)-Cl(8)	2.578 (4)
95	Mg(3)-Cl(8)	2.551 (5)
96	Mg(2)-Cl(1)	2.479 (5)
96	Mg(1)-Cl(1)	2.397 (5)
96	Mg(1)-Cl(3)	2.401(5)
97	Mg(1)Cl(2)	2.506 (9)
97	Mg(1)-Cl(3)	2.472 (9)
97	Mg(2)-Cl(3)	2.395 (11)
97	Mg(2)-Cl(2)'	2.406 (10)
	Average	2.496

Complex	μ_3-Cl	Distance (Å)
94	Mg-Cl	2.548
94	Mg-Cl	2.535(3)
94	Mg-Cl	2.563 (2)
95	Mg(1)-Cl(5)	2.533 (5)
95	Mg(2)-Cl(5)	2.595 (5)
95	Mg(3)-Cl(5)	2.565 (4)
95	Mg(1)-Cl(7)	2.567 (5)
95	Mg(2)-Cl(7)	2.524 (5)
95	Mg(3)-Cl(7)	2.597 (5)
96	Mg(2)-Cl(2)	2.524 (4)
96	Mg(1)-Cl(2)	2.779 (5)
97	Mg(1)-Cl(1)'	2.508 (10)
97	Mg(1)-Cl(1)	2.495 (9)
	Average	2.564

Complex	μ_2-Cl	Angle (°)
95	Mg(1)-Cl(4)-Mg(2)	79.2 (1)
95	Mg(1)-Cl(6)-Mg(3)	81.5 (1)
95	Mg(2)-Cl(8)-Mg(3)	80.5 (1)
96	Mg(1)-Cl(1)-Mg(2)	100.4 (2)
97	Mg(1)-Cl(2)-Mg(2)	99.8 (4)
97	Mg(1)-Cl(3)-Mg(2)	98.8 (4)
	Average	90

Complex	μ_3-Cl	Angle (°)
95	Mg(1)-Cl(5)-Mg(2)	80.4 (2)
95	Mg(1)-Cl(5)-Mg(3)	80.9 (1)
95	Mg(2)-Cl(5)-Mg(3)	79.9 (1)
95	Mg(1)-Cl(7)-Mg(2)	81.2 (1)
95	Mg(1)-Cl(7)-Mg(3)	79.6 (1)
95	Mg(2)-Cl(7)-Mg(3)	80.6(1)
96	Mg(1)-Cl(2)-Mg(2)	89.8 (2)
97	Mg(1)-Cl(1)-Mg(1)'	96.4 (3)
97	Mg(1)-Cl(1)-Mg(2)	88.5 (3)
97	Mg(1)'-Cl(1)-Mg(2)	89.8 (3)
	Average	84.7

Table 3.12 Bond lengths and angles reported for Mg$_2$-μ_2Cl and Mg$_3$-μ_3Cl in complexes A-D

3.4.1.2 Reaction of 65 with MgMeCl in the Presence of Oxygen

The reaction of methyl magnesium chloride with **65** in THF and hexane, produces a strongly red coloured solution, which in the presence of oxygen yields crystals of $[Mg(\mu\text{-}OCH_3)\{(2,6\text{-}^iPr_2Ph)BIAN(Me)\}]_2$ (**67**), (Figure 3.36). Initially, the formation of complex **67** was puzzling, as the stoichiometry does not seem to add up. However, if you consider how non-polar solvents affect the Schlenk equilibrium, as reported by Tulmetts,[42-43] it is possible to propose that in hexane/THF solvent the Schlenk equilibrium is shifted towards dimethyl magnesium and magnesium dichloride. Subsequent reaction of **65** with dimethyl magnesium produces $[Mg\{(^iPr_2Ph)_2BIAN\}Me\{\mu\text{-}Me\}]_2$ (**A**) (Figure 3.37). The terminal methyl groups in **A** undergo homolytic bond cleavage to produce a biradical dimer and two methyl radicals (**B**). The methyl radicals on addition to the BIAN ligands of the dimer complex would produce **C** and reaction of complex **C** with oxygen would produce **67**. Complex **67** was characterised by its crystal structure shown in Figure 3.36.
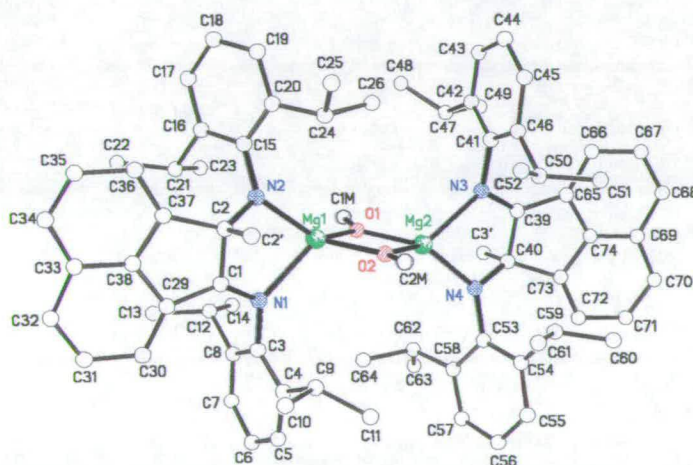
Figure 3.36 Diagram displaying the molecular structure and atom labeling of 67, The hydrogen atoms are omitted for clarity
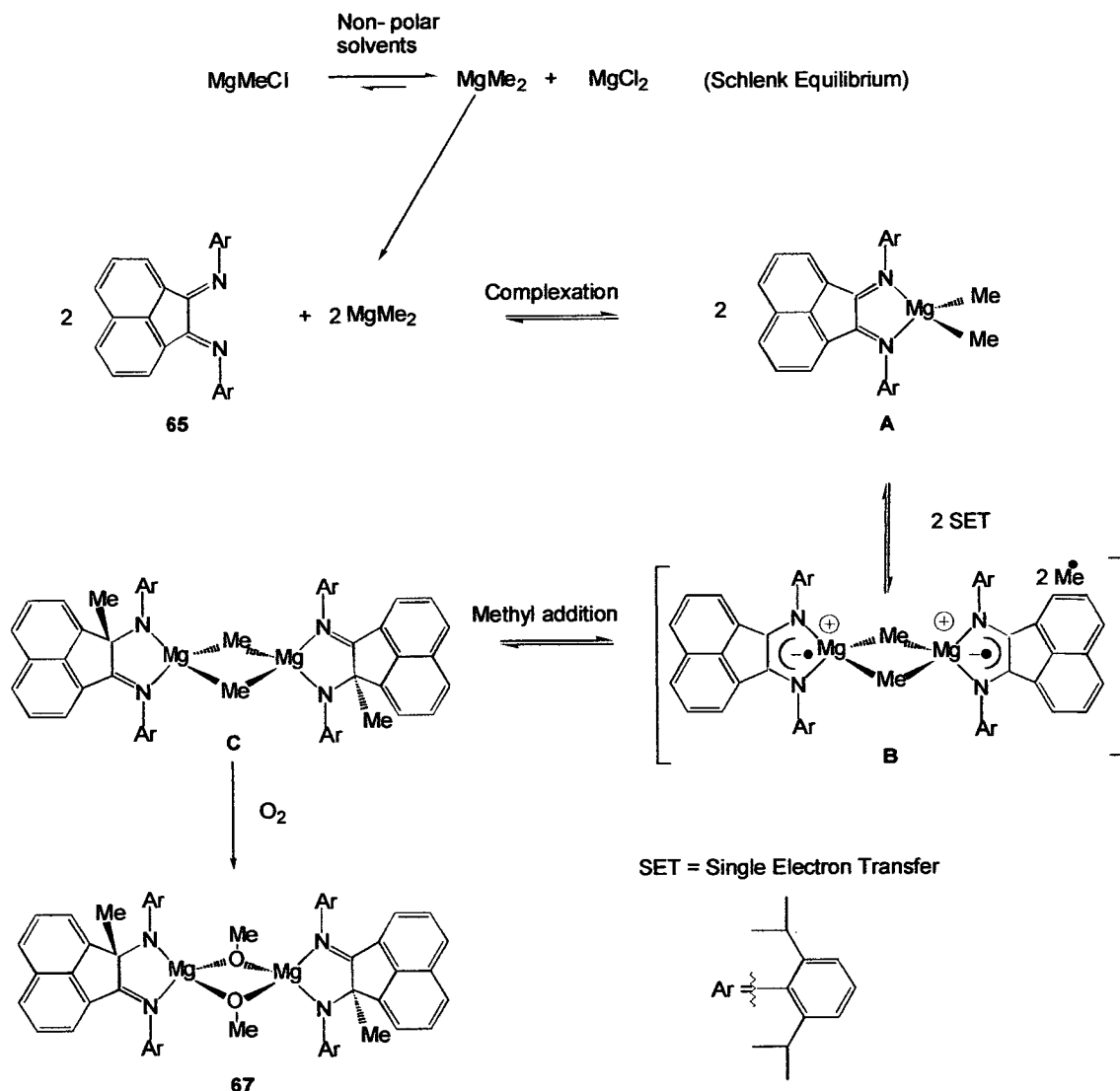
Figure 3.37 Hypothesized reaction mechanism in the synthesis of 67

Both magnesium centres are 4 coordinate and are distorted tetrahedral. Refer to Table 3.13 for significant bond lengths and angles. In the NCCN moiety, the carbon-nitrogen bond lengths on comparison convey that bonds C(2)-N(2) and N(4)-C(40) are single [C(2)-N(2) = 1.440(9) Å, N(4)-C(40)= 1.433(9)Å], where as bonds C(1)-N(1) and N(3)-C(39) are double bonds [C(1)-N(1)= 1.276(9) Å, N(3)-C(39)= 1.290(8)Å], as expected. The magnesium-nitrogen bond lengths differ; the bonds to the amide nitrogen atoms [Mg(1)-N(2) 1.989(7) Å and Mg(2)-N(4) (1.973(7)Å] being shorter than those to the imine nitrogen [Mg(1)-N(1) (2.180(7) Å and Mg(2)-N(3) (2.169(7) Å]. The magnesium-oxygen bond lengths of the bridging methoxy

groups are Mg(1)-O(1) = 1.944(6) Å, and Mg(1)-O(2) = 1.958(6) Å. The five membered rings are distorted from a perfect geometry as a result of the both the geometry imposed by the fused aromatic rings and by the geometries of C(1) and C(2).

Mg(1)-O(1)	1.944 (6)	Mg(2)-O(1)	1.937 (6)
Mg(1)-O(2)	1.985 (6)	Mg(2)-O(2)	1.942 (6)
Mg(1)-Mg(2)	2.902 (4)		
Mg(1)-N(1)	2.180 (7)	Mg(2)-N(3)	2.169 (7)
Mg(1)-N(2)	1.989 (7)	Mg(2)-N(4)	1.973 (7)
N(1)-C(1)	1.276 (9)	N(3)-C(39)	1.290 (8)
N(2)-C(2)	1.440 (9)	N(4)-C(40)	1.433 (9)
C(1)-C(2)	1.538 (10)	C(39)-C(40)	1.529 (9)
C(2)-C(2')	1.567 (10)	C(40)-C(3')	1.588 (10)
N(2)-Mg(1)-O(1)	131.3 (3)	N(4)-Mg(2)-O(2)	126.9 (3)
N(1)-Mg(1)-O(2)	112.5 (3)	N(3)-Mg(2)-O(1)	117.0 (3)
N(2)-Mg(1)-N(1)	80.9 (3)	N(3)-Mg(2)-N(4)	80.8 (3)
O(2)-Mg(1)-O(1)	83.2 (3)	O(2)-Mg(2)-O(1)	83.8 (3)
N(2)-C(2)-C(1)	108.8 (6)	N(4)-C(40)-C(39)	109.2 (6)
C(2)-C(1)-N(1)	118.5 (7)	C(40)-C(39)-N(3)	118.0 (7)
C(1)-N(1)-Mg(1)	108.7 (5)	C(39)-N(3)-Mg(2)	109.5 (5)
C(2)-N(2)-Mg(1)	109.0 (5)	C(40)-N(4)-Mg(2)	111.2 (50
C(2)-C(1)-C(29)	109.7 (7)	C(40)-C(39)-C(65)	110.4 (6)
C(1)-C(29)-C(38)	105.5 (7)	C(39)-C(65)-C(74)	105.8 (7)
C(29)-C(38)-C(37)	113.8 (7)	C(65)-C(74)-C(73)	113.0 (6)
C(38)-C(37)-C(2)	107.2 (7)	C(74)-C(73)-C(40)	107.2 (7)
C(37)-C(2)-C(1)	101.7 (6)	C(73)-C(40)-C(39)	100.5 (6)
N(2)-C(2)-C(2')	112.2(6)	N(4)-C(40)-C(3')	113.3 (6)
Mg(1)-O(1)-Mg(2)	96.6 (3)	Mg(1)-O(2)-Mg(2)	96.3 (3)

Table 3.13 Selected bond lengths (Å) and angles (°) for 67

3.5 Reaction of α-diimine Ligands with Dimethyl Magnesium

The products obtained by the reaction of MgMe$_2$ with α-diimines **62**, **64** and **65** could not be characterised by NMR as their spectra were observed only as broad signals. This observation combined with the highly coloured reaction mixtures lead us to believe that the reaction may produce radical products. Consequently we analysed each of the Et$_2$O mother liquors using EPR spectroscopy.

3.5.1 Evidence of Radical Species

3.5.1.1 EPR Evidence

Addition of $MgMe_2$ to ligands **62**, **64** and **65** at room temperature in Et_2O produces strongly orange/red coloured paramagnetic solutions of **68**, **69** and **70** respectively as shown by EPR analysis. The results for the different diimine ligands in solution are shown in Table 3.14. The spectra have been simulated using Win EPR to enable accurate calculation of the spectral parameters. The radicals are ligand centred and delocalised across the N=C-C=N backbone, shown by coupling with both N atoms and each of the H atoms or CH_3 groups on the imine carbon atoms (where present).
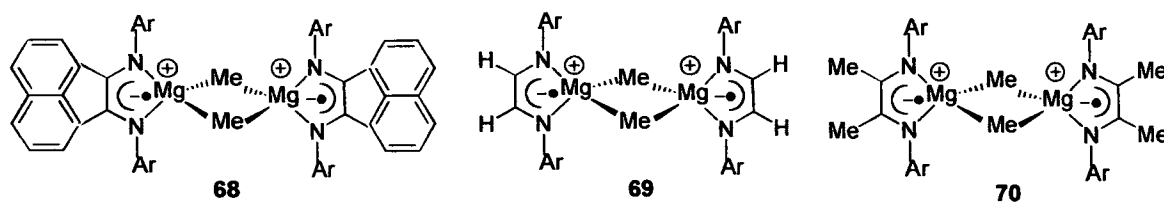
Figure 3.38 Structural formulae of 68, 69 & 70.

Complex	No. of peaks	Equiv. N's	Equiv. H's	a^N / G	a^H / G	g / G
68	5	2	0	4.6	0	2.012
69	7	2	2	5.3	5.3	2.013
70	11	2	6	5.59	5.59	2.012

Table 3.14 Results of EPR analyses in Et_2O of 68, 69 & 70.

The EPR spectra are asymmetric, the a^N and a^H couplings are identical and comparable to the line width as shown in Figure 3.39. The 5 lined spectrum for **68** is produced by coupling of the free electron to the 2 equivalent nitrogens with $I = 1$, therefore $(2nI +1)= 5$. Refer to Figure 3.40 to observe the coupling pattern. Subsequent coupling to H's (where present) results in a greater multiplicity of peaks. In the case of **69** the 5 nitrogen peaks are split into triplets (by 2 H) to yield a 7 lined spectrum with ratios 1:3:6:7:6:3:1. Where as for **70** each of the 5 lines are split into septets of equal coupling constant to produce an 11 lined signal with ratios 1:2:3:5:8:9:8:5:3:2:1. The g values suggest the electron is very delocalised and the coupling patterns indicate it is delocalised over the ligand NCCN backbone. X-Ray crystallographic analysis of **68** shows it to adopt a methyl bridged dimeric structure

(see later), and it is therefore assumed that **69** and **70** also adopt such a structure in which Mg is 4-coordinate. The observed EPR spectra for these species indicate that
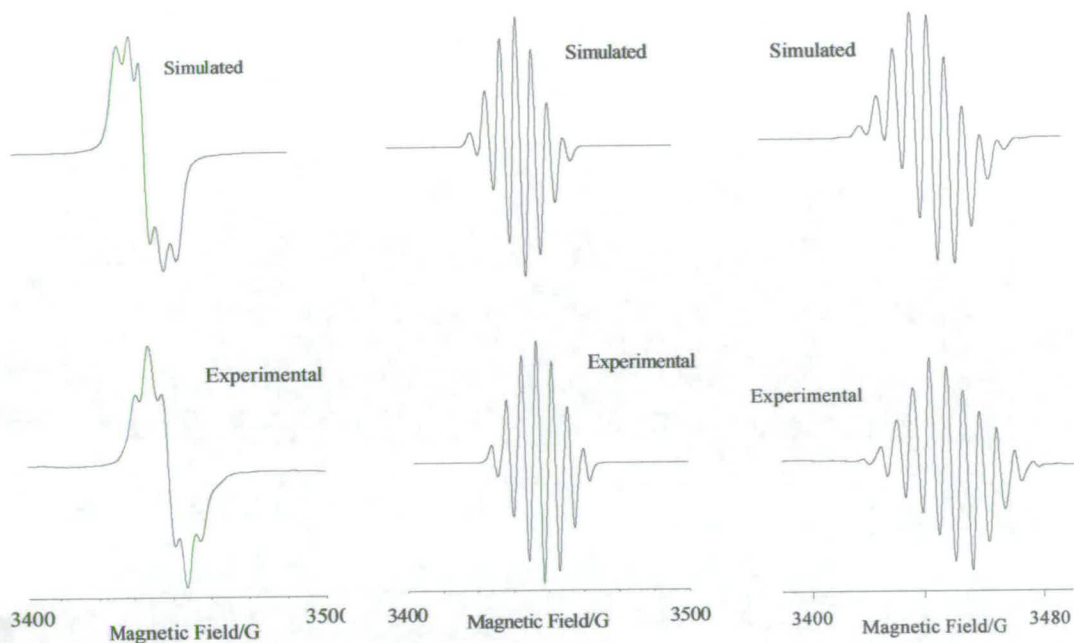
they are triplet species.

68　　　　　　　69　　　　　　　70

Figure 3.39 Simulated and experimental EPR Spectra of 68, 69 and 70
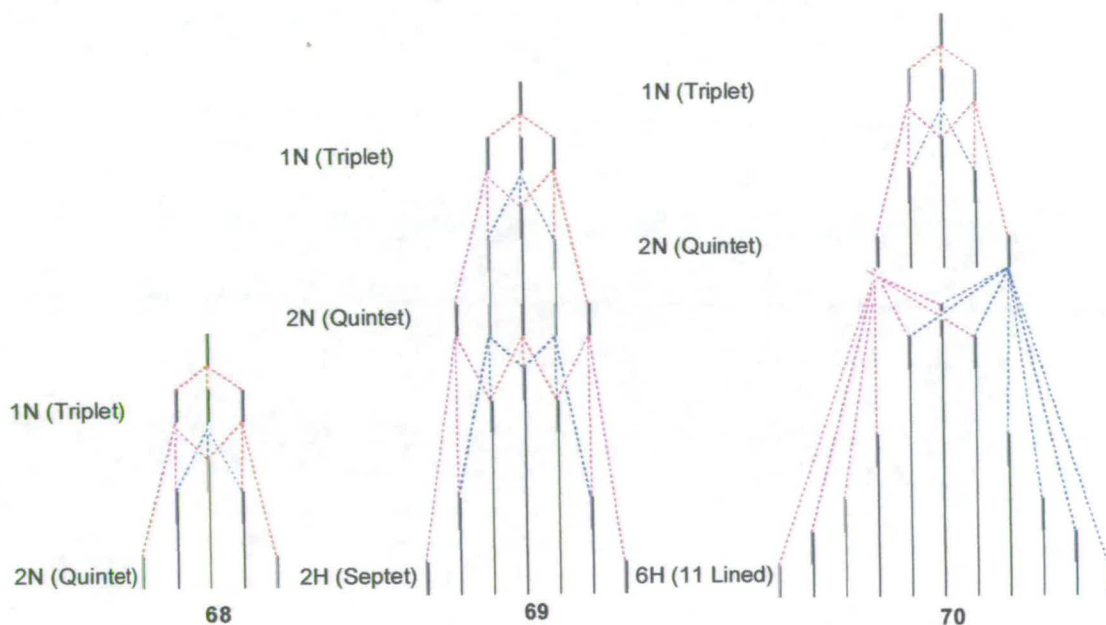
Figure 3.40 Diagram showing the EPR splitting patterns of 68, 69 & 70

The formation of these triplet diradical species is considered to take place *via* the neutral direct co-ordination product (LMgMe₂), which must undergo a homolytic bond cleavage between the alkyl group and the magnesium, to produce a methyl radical and a radical complex (Figure 3.41). During the bond cleavage the free electron is transferred from the metal to the ligand and delocalised into the low energy conjugated π^* system followed by dimer formation *via* methyl bridges. This is consistent with the work of Kaim and Kaupp on the complexation of Mg and Zn alkyls with diimines.[18,24]
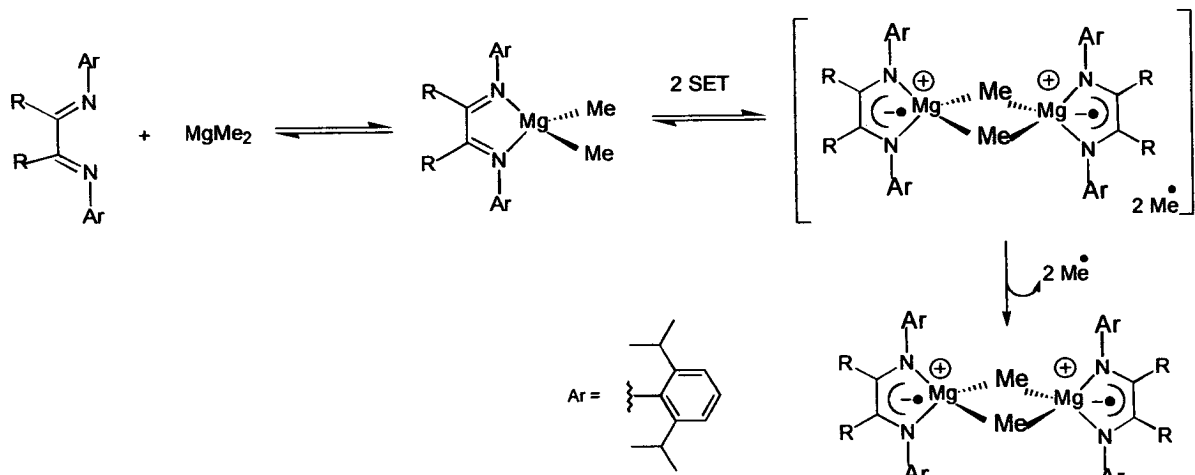
Figure 3.41 Preparation of diimine based radical magnesium alkyl complexes.

3.5.1.2 Structural Evidence

Ligand **65** is only partially soluble in many solvents including THF and Et₂O. Reaction of **65** with MgMe₂ at room temperature in Et₂O produced a highly coloured red suspension. The suspension was filtered, concentrated in vacuum and layered with hexane, and after two days in the fridge at 5°C produced a red tablet crystal of the radical dimer [Mg(μ-Me){(2,6^{i}Pr₂Ph)BIAN}]₂ (**68**). An X-ray crystal structure determination of **68** was undertaken and the molecular structure is shown in Figure 3.42, and significant bond lengths and angles are given in Table 3.15. To our knowledge this is the first structural evidence of a magnesium alkyl radical complex. The majority of the structurally characterised complexes obtained in this chapter are dimeric (as shown in the preceding sections), therefore the reaction mechanism for the production of the radical species may be more accurately described as in Figure 3.43.
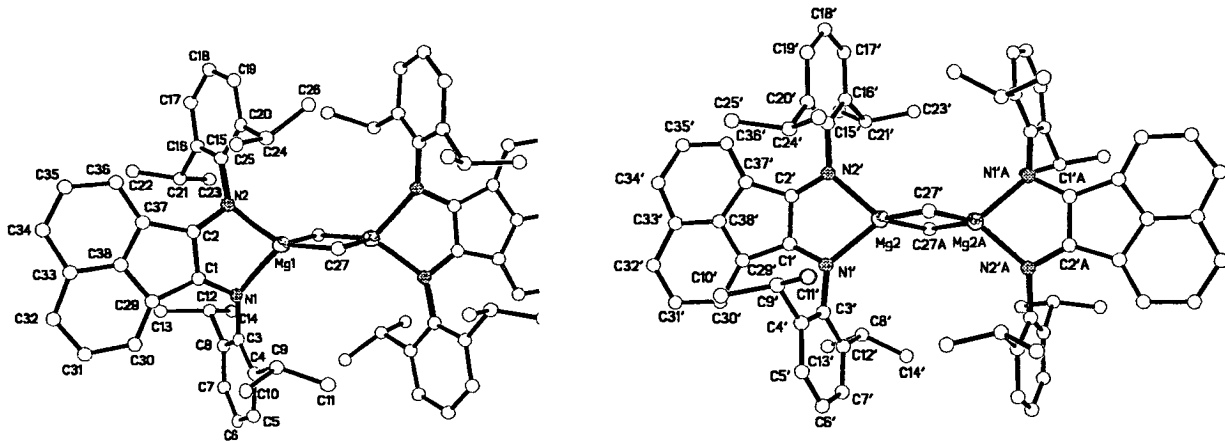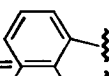
Figure 3.42 The two dimeric molecules of 68 found in the unit cell, the hydrogen atoms have been omitted for clarity and only selected atoms labelled.
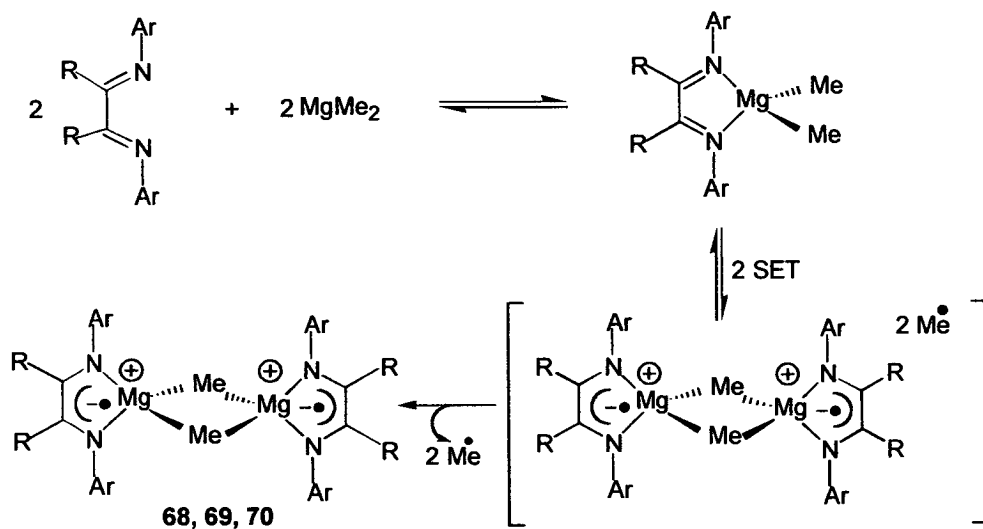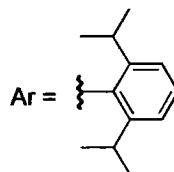
Figure 3.43 Suggested reaction route to radical dimers 68, 69 & 70

Mg(1)-(C27)#1	2.205 (6)	Mg(2)-(C27')#2	2.270 (6)
Mg(1)-C(27)	2.263 (5)	Mg(2)-C(27')	2.200 (6)
Mg(1)-Mg(1)#1	2.704 (3)	Mg(2)-Mg(2')#2	2.724 (3)
Mg(1)-N(2)	2.065 (4)	Mg(2)-N(2')	2.048 (4)
Mg(1)-N(1)	2.066 (5)	Mg(2)-N(1')	2.050 (4)
N(2)-C(2)	1.333 (6)	N(2')-C(2')	1.320 (6)
N(1)-C(1)	1.345 (6)	N(1')-C(1')	1.336 (5)
C(1)-C(2)	1.422 (7)	C(1')-C(2')	1.437 (7)

N(2)-Mg(1)-C(27)#1	118.8 (2)	N(2')-Mg(2)-C(27')#2	115.1 (2)
N(1)-Mg(1)-C(27)	113.9 (2)	N(1')-Mg(2)-C(27')	119.5 (2)
N(2)-Mg(1)-N(1)	84.54 (17)	N(2')-Mg(2)-N(1')	83.62 (16)
C(27)-Mg(1)-C(27)#1	105.52 (18)	C(27')-Mg(2)-C(27')#2	104.9 (2)
N(2)-C(2)-C(1)	120.5 (4)	N(2')-C(2')-C(1')	119.3 (4)
C(2)-C(1)-N(1)	120.4 (4)	C(2')-C(1')-N(1')	119.0 (4)
C(1)-N(1)-Mg(1)	106.2 (3)	C(1')-N(1')-Mg(2)	107.6 (3)
C(2)-N(2)-Mg(1)	106.5 (3)	C(2')-N(2')-Mg(2)	108.1 (3)
C(1)-C(29)-C(38)	103.5(5)	C(1')-C(29')-C(38')	104.8 (4)
C(29)-C(38)-C(37)	114.1 (40	C(29')-C(38')-C(37')	111.9 (4)
C(38)-C(37)-C(2)	105.9 (4)	C(38')-C(37')-C(2')	106.4 (4)
C(37)-C(2)-C(1)	107.3 (4)	C(37')-C(2')-C(1')	107.7 (4)
Mg(1)-C(27)-Mg(1)#1	74.48 (18)	Mg(2)-C(27')-Mg(2)#2	75.1 (2)

Table 3.15 Selected bond lengths (Å) and angles (°) for 68, with symmetry transformations used to generate equivalent atoms: #1 –x+2, -y+1, -z+1; #2 –x+1, -y, -z.

The magnesium centre is distorted tetrahedral [N(1)-Mg(1)-N(2) = 84.54(17)°, N(1)-Mg(1)-C(27) = 113.9(2)° and N(2)-Mg(1)-C(27) = 116.4(2)°]. The Mg(1)-C(27) bond length is 2.263(5) Å, and the bond lengths in the NCCN part of the ligand backbone [C(1)-C(2) = 1.422(7) Å, C(1)-N(1) = 1.345(6) Å, C(2)-N(2) = 1.333(6) Å] are in between those of double and single bonds found in the free diimine ligand [C(1)-C(2) =1.547(8) Å, C(1)-N(1) = 1.283(5) Å] (refer to section 3.30). Such a result is indicative of delocalisation and reinforces the evidence that the free electron of the radical species resides on the ligand. Reproduction of the crystals of **68** proved impossible and subsequent reactions lead to the preparation of other new compounds, suggesting the reaction is not clean and that there are in fact a number of products produced simultaneously and in competition with each other depending on the reaction conditions.

3.5.2 Evidence of Doubley Reduced Species

3.5.2.1 Synthesis of [Mg{(2,6-^{i}Pr$_2$Ph)BIAN}(THF)$_3$]

Changing the solvent and reaction conditions in the reaction of **65** with MgMe$_2$ allowed the isolation and characterisation of the monomer species [Mg{(2,6-^{i}Pr$_2$Ph)BIAN}(THF)$_3$] **71** in which the BIAN ligand has been doubly reduced. The ligand formed a suspension in a mixture of THF and toluene and was chilled in liquid nitrogen, addition of a chilled solution of MgMe$_2$ in THF produced a highly coloured red suspension on warming to room temperature. Filtration of the suspension followed by concentration in vacuum and storage for 16 days at 5°C produced a mixture of orange rod crystals of ligand **65** whose crystal structure we had previously determined (section 3.3), and red needle crystals of **71**.

In **71** the ligand is a dianionic diamide donor, which has been doubly reduced on complexation with dimethyl magnesium as a result of two single electron transfer processes (SET) due to the homolytic bond cleavage of both magnesium-methyl bonds (Figure 3.44).
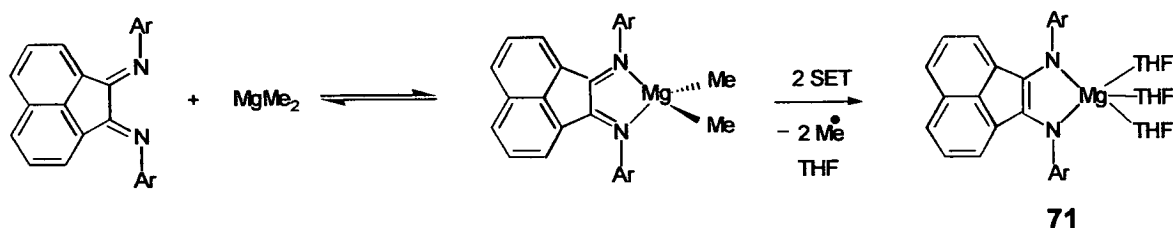
Figure 3.44 Synthesis of 71

Elucidation and refinement of the crystal data of the red needles containing **71**, revealed that the crystal system is orthorhombic, with space group P$_{bca}$. The R$_1$ factor is reasonable at 6.39% for [5535 data]. The molecular structure is displayed in Figure 3.45. There is one molecule of **71** in the asymmetric unit and 8 molecules of **71** in the unit cell. The magnesium centre is 5-coordinate and adopts a distorted square based pyramidal geometry with atom O(3) at the apex. Refer to Table 3.16 for significant bond lengths and angles. In the NCCN moiety, the magnesium-nitrogen bond lengths are comparable to single bonds [Mg(1)-N(1) = 2.060(2) Å, Mg(1)-N(2)= 2.071(2) Å], whereas the C(1)-C(2) bond length is characteristic of a double bond

[C(1)-C(2)= 1.398(3) Å], (Figure 3.44). In the five membered ring C(1)-C(29)-C(38)-C(37)-C(2) the bond angles are C(2)-C(1)-C(29) = 108.9(2)°, C(1)-C(29)-C(38) = 106.4(2)°, C(29)-C(38)-C(37) = 110.0(2)°, C(38)-C(37)-C(2) = 106.5(2)°, and C(37)-C(2)-C(1) = 108.3(2)°. The angle about C(38) is smaller as a result of the double bond between C(1) and C(2). The bond distances between the magnesium centre and the oxygen atoms on the three THF molecules are unremarkable, with the bond length between Mg(1) and O(3) (the apex of the square based pyramid) being the shortest of the three lengths [Mg(1)-O(1) = 2.1113(19) Å, Mg(1)-O(2) = 2.1335(19) Å, Mg(1)-O(3) = 2.0621(19) Å].
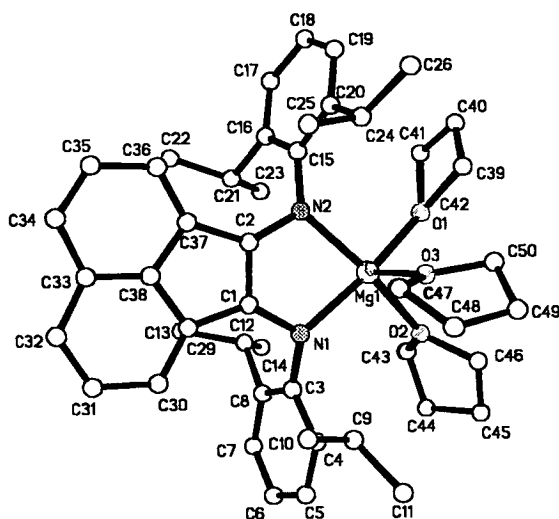
Figure 3.45 Molecular structure of 71 displaying atomic numbering scheme, the hydrogen atoms have been omitted for clarity

Mg(1)-N(1)	2.060(2)	C(38)-C(37)	1.418(3)	O(1)-Mg(1)-O(3)	95.33(8)
Mg(1)-N(2)	2.071(2)	C(37)-C(2)	1.467(3)	N(2)-Mg(1)-O(3)	103.92(8)
C(1)-C(2)	1.398(3)	Mg(1)-N(1)-C(1)	107.37(15)	N(1)-Mg(1)-O(3)	109.23(8)
C(1)-N(1)	1.402(3)	N(1)-C(1)-C(2)	119.6(2)	O(2)-Mg(1)-O(3)	93.56(8)
C(2)-N(2)	1.385(3)	C(1)-C(2)-N(2)	120.2(2)	C(2)-C(1)-C(29)	108.9(2)
Mg(1)-O(1)	2.1113(19)	Mg(1)-N(2)-C(2)	107.37(16)	C(1)-C(29)-C(38)	106.4(2)
Mg(1)-O(2)	2.815(3)	O(1)-Mg(1)-O(2)	83.58(8)	C(29)-C(38)-C(37)	110.0(2)
Mg(1)-O(3)	2.0621(19)	N(2)-Mg(1)-O(1)	94.47(8)	C(38)-C(37)-C(2)	106.5(2)
C(1)-C(29)	1.457(3)	N(1)-Mg(1)-N(2)	84.84(8)	C(37)-C(2)-C(1)	108.3(2)
C(29)-C(38)	1.425(4)	N(1)-Mg(1)-O(2)	89.62(8)		

Table 3.16 Selected bond lengths (Å) and angles (°) for 71

The NMR and IR spectra are difficult to assign due to the co-crystallisation of **71** with the diimine ligand. The spectra produced by the complex and the contaminant overlap and make elucidation of the data impossible. However, for completeness each peak in the NMR and IR spectra have been given but not identified.

3.5.3 Evidence of Methyl Migration

Reaction of α-diimines with $MgMe_2$ also produces complexes which have undergone methylation as shown in Figure 3.46. We postulate that this occurs due to attack at the δ^+ carbons on the NCCN backbone of the ligand, by the free methyl radicals.
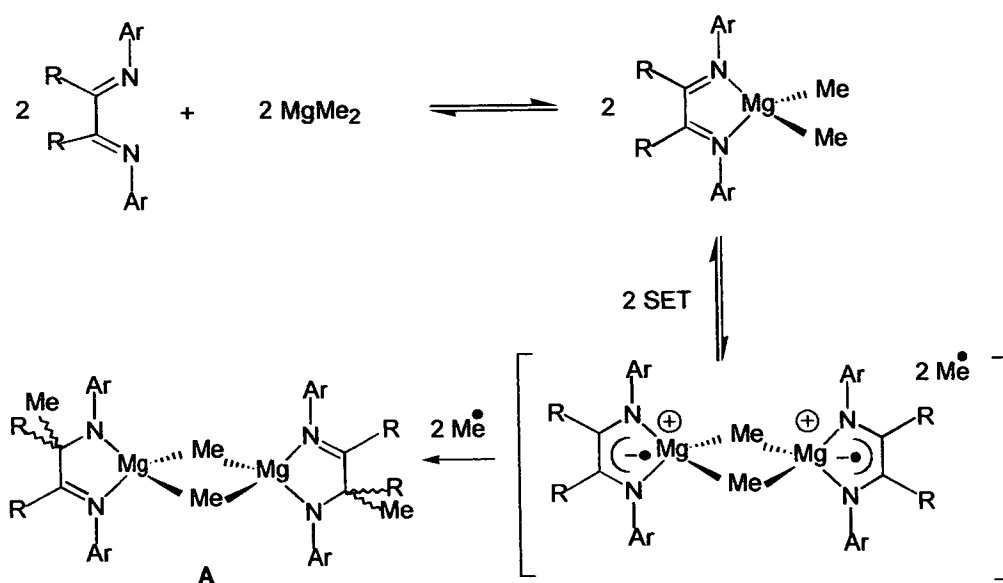
Figure 3.46 Reaction scheme of suggested route to imino-amide magnesium alkyl complexes.

3.5.3.1 Synthesis of [Mg(μ₂-Me){(2,6-^{i}Pr₂Ph)NC(Me)₂C(Me)N(2,6-^{i}Pr₂Ph)}]₂

A low temperature reaction of dimethylmagnesium with **64** in a mixture of THF and toluene was performed by chilling separate reactant solutions and combining them by transferring the ligand solution by cannula. On warming to room temperature a strong clear orange solution was obtained, which on concentration and after being

left at room temperature for 1 day, and then 5 days in the freezer at -20°C, yielded red block crystals of **72**. The molecular structure of **72** is displayed in Figure 3.47.
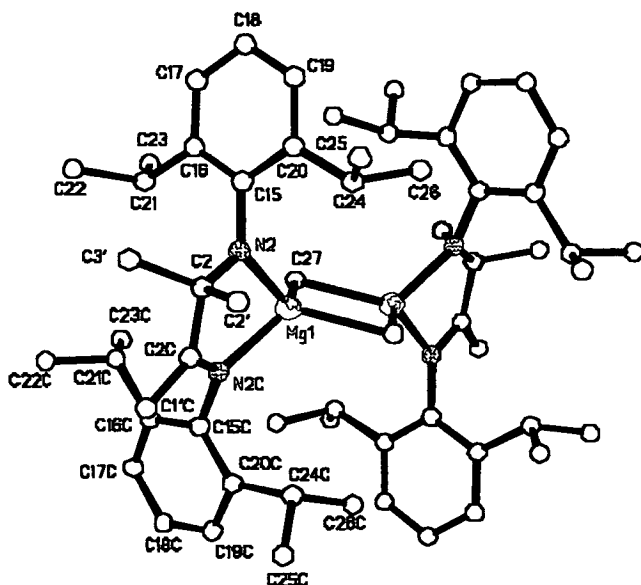
Figure 3.47 Molecular structure and atom labelling of
[Mg(μ₂-Me){(2,6-ⁱPr₂Ph)NC(Me)₂C(Me)N(2,6-ⁱPr₂Ph)}]₂ 72, the hydrogen atoms
have been omitted for clarity.

Refinement of the structure revealed the empirical formula $C_{71}H_{108}Mg_2N_4O$, containing **72** and both a THF and a toluene solvent molecule. There is a quarter of the molecule in the asymmetric unit and two molecules of **72** in the unit cell. The structure contains disorder, in part one of the data each carbon atom in the ligand NCCN backbone has been methylated, refer to Figure 3.48. However, in part two of the structure the NCCN backbone is completely unmethylated, as a result of the nature of the disorder the bond lengths and angles are averaged and thus the bond lengths of C(2)-N(2) and C(2C)-N(2C) are identical 1.370(2)Å and neither can be assigned as a single bond, which would be observed when either C had been methylated making the C-N an amide bond. Significant bond lengths and angles are given in Table 3.17.

Part 1   Part 2
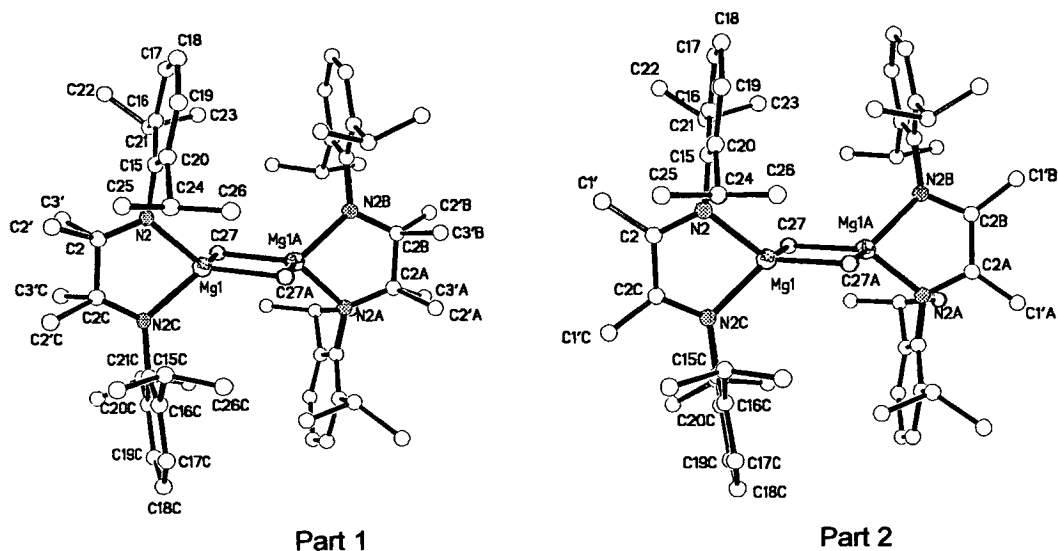
Figure 3.48 Diagram showing the 2-fold disorder in the crystal structure of
[Mg(μ₂-Me){(2,6-^{i}Pr₂Ph)NC(Me)₂C(Me)N(2,6-^{i}Pr₂Ph)}]₂ (72), the hydrogen atoms are
omitted for clarity and only a selection of the atoms are labelled.

N(2)-Mg(1)	2.0422 (14)	N(2)-Mg(1)-N(2)#1	81.08 (8)
N(2)-C(2)	1.370 (2)	C(27)-Mg(1)-C(27)#1	104.32 (8)
C(2)-C(2)#1	1.505 (4)	C(27)-Mg(1)-N(2)	114.74 (6)
Mg(1)-C(27)	2.2499 (25)	C(27)-Mg(1)-N(2)#1	114.74 (6)
Mg(1)-C(27)#1	2.2041 (25)	Mg(1)-N(2)-C(2)	112.09 (11)
Mg(1)-Mg(1)#1	2.7326 (15)	N(2)-C(2)-C(2)#1	114.82 (9)
C(2)-C(1')	1.458 (4)		
C(2)-C(2')	1.563 (4)		
C(2)-C(3')	1.608 (4)		

Table 3.17 Selected bond lengths (Å) and angles (°) for 72
With symmetry operations used to generate equivalent atoms: #1 x, -y, z

Analysis of **72** by NMR in THF-d₈ produces the spectrum displayed in (Figure 3.50). In the presence of THF, complex **72** would be expected to be the solvated monomer (Figure 3.49), however the crystal structure of the dimer contains THF yet the structure is an unsolvated dimer. The NMR spectrum of the crystals of **72**, that were the subject of X-ray analysis, show the presence of free THF and free toluene which were present in the lattice. The small signals at 1.72 ppm and 3.58 ppm are assigned

to the residual protons in THF-d_8, and there is no evidence of solvation. A singlet MgMe peak is observed at chemical shift −1.79 ppm, and the methyl hydrogens on the amide carbon at 1.27 ppm, in contrast to the methyl hydrogens on the imine carbon at 2.25 ppm. There are two septets present, 3.02 ppm and 3.98 ppm, due to the two inequivalent (^{i}Pr$_2$CH) environments.
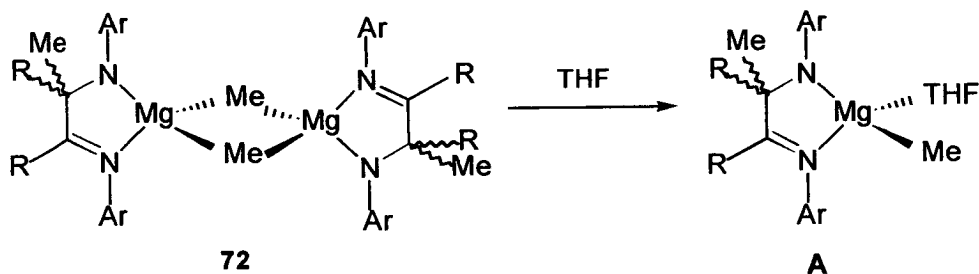
Figure 3.49 THF solvation of 72 to produce A.
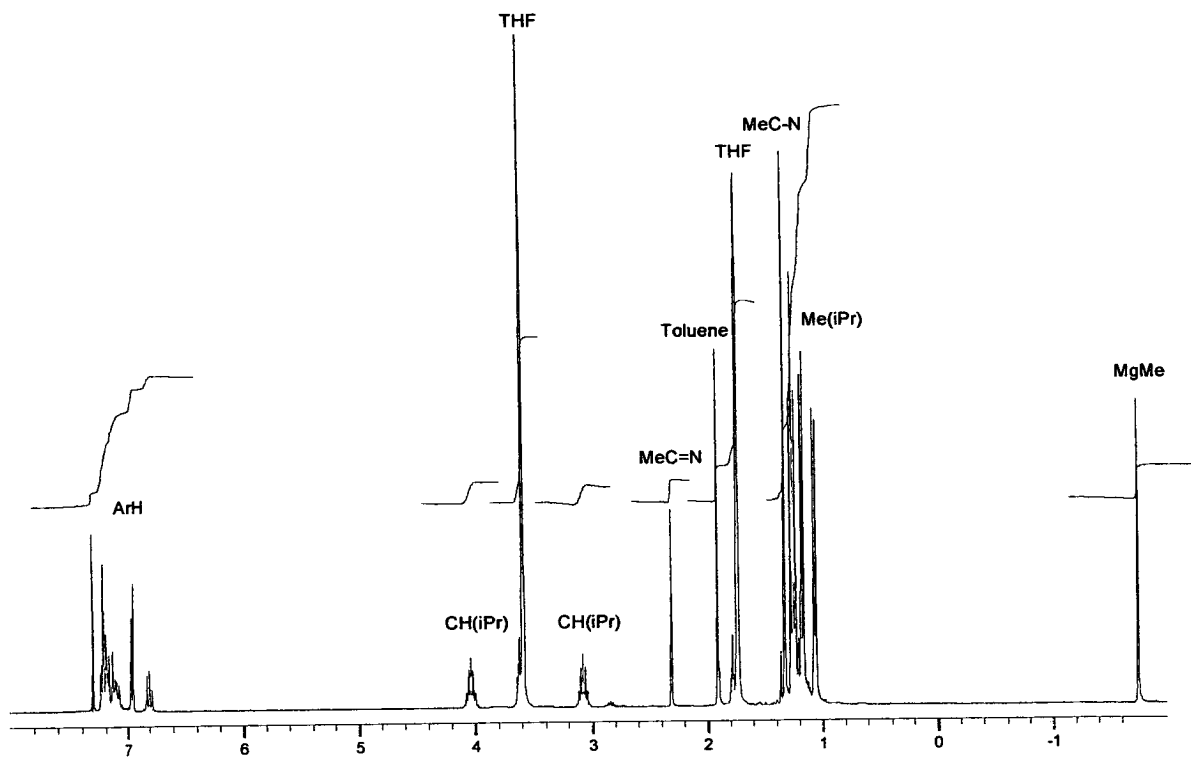
Figure 3.50 ^{1}H NMR of crystals of 72 in THF-d$_8$

3.5.3.2 Synthesis of [Mg(μ-OH){(2,6-^{i}Pr$_2$Ph)NC(Me)$_2$C(Me)N(2,6-^{i}Pr$_2$Ph)}]$_2$

The crystallization of 72 under non-anhydrous conditions produces 73, which can be isolated as an orange powder on removal of the solvent under vacuum. Orange block crystals of 73 suitable for X-ray analysis were obtained from hexane solution over 6 days at room temperature.
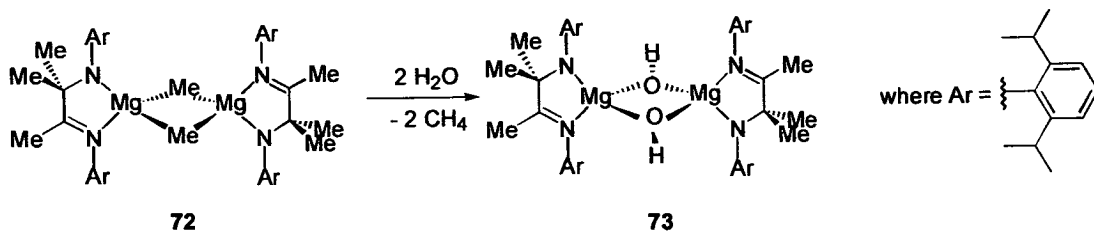
Figure 3.51 Suggested reaction of 72 with water to produce 73

The reaction must have proceeded to the stage of forming complex 72, before the water has reacted with the complex, implying that the formation of 72 is very rapid. Reaction of 72 with two water molecules results in the substitution of the bridging methyl groups with hydroxy groups upon the protonolysis of the methyl groups to produce methane gas (Figure 3.51).

The crystal data obtained for 73 shows there is half a molecule in the asymmetric unit and two molecules of 73 in a unit cell. Each molecule is 2-fold disordered at the carbon atoms in the NCCN moiety, i.e. N(1)-C(1)-C(2)-N(2) in part 1 and

N(1)-C(1A)-C(2A)-N(2) in part 2. In part 1 it is the carbon next to [N(2)] that has been methylated [C(2)], where as in part 2 it is the carbon next to [N(1)] that has been methylated [C(1A)], refer to Figure 3.52. The magnesium centre is distorted tetrahedral, refer to Table 3.18 for the bond angles about Mg(1). The Mg(1)-O(1) distance [2.320(3)Å] is longer than the Mg-O(THF) bond distances for 71 [Mg(1)-O(1)= 2.1113(19) Å, Mg(1)-O(2)= 2.1335(19) Å, Mg(1)-O(3)= 2.0621(19) Å], because in 73 the hydroxide oxygen is acting a bridge. Comparison of the Mg-N bond distances reveals little difference in the distance for Mg(1)-N(1)= 2.020(4) Å, in which the [N(1)] atom is an imine nitrogen, and Mg(1)-N(2)= 2.057(4) Å , in which the [N(2)] atom is an amide nitrogen. However, the amide nature of [N(2)] and the imino nature of [N(1)] is displayed on comparison of the N(2)-C(2) bond length [1.45(2) Å] and the N(1)-C(1) bond length [1.31(2) Å] , which are

Part 1
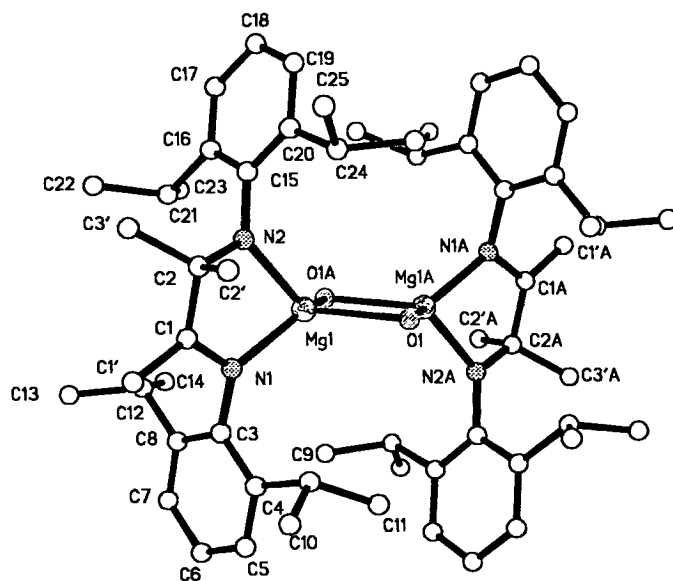
Part 2
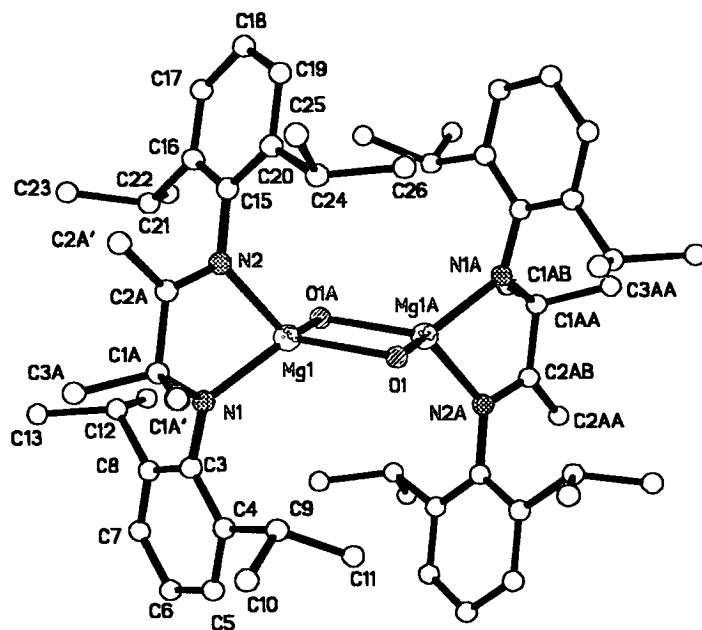
Figure 3.52 Diagram displaying the two disordered parts and the atom labelling of 73, the hydrogen atoms are omitted for clarity and a selection of atoms are labelled

clearly single and double bonds respectively. Atom C(2) is distorted tetrahedral (sp^3) and atom C(1) clearly of trigonal (sp^2) geometry.

Mg(1)-O(1)	2.320 (3)	N(2)-Mg(1)-O(1)#1	117.38 (14)
Mg(1)O(1)#1	2.284 (3)	N(1)-Mg(1)-O(1)	116.37 (14)
Mg(1)-Mg(1)#1	2.839 (3)	N(1)-Mg(1)-N(2)	81.47 (14)
Mg(1)-N(2)	2.057 (4)	O(3)-Mg(1)-O(1)	103.85 (10)
Mg(1)-N(1)	2.020 (4)	N(2)-C(2)-C(1)	106.5 (16)
N(2)-C(2)	1.45 (2)	N(2)-C(2A)-C(1A)	120.1 (10)
N(2)-C(2A)	1.288 (14)	C(2)-C(1)-N(1)	120.2 (18)
N(1)-C(1)	1.31 (2)	C(2A)-C(1A)-N(1)	107.9 (9)
N(1)-C(1A)	1.473 (11)	C(1)-N(1)-Mg(1)	112.9 (9)
C(1)-C(2)	1.520 (10)	C(1A)-N(1)-Mg(1)	111.3 (5)
C(1A)-C(2A)	1.521 (9)	C(2)-N(2)-Mg(1)	111.7 (8)
C(2)-C(2')	1.513 (7)	C(2A)-N(2)-Mg(1)	112.5 (5)
C(2)-C(3')	1.539 (17)		
C(1)-C(1')	1.548 (16)		
C(2A)-C(2A')	1.548 (15)		
C(1A)-C(1A')	1.520 (6)		
C(1A)-C(3A')	1.531 (15)		

Table 3.18 Selected bond lengths (Å) and angles (°) for 73 with symmetry transformations used to generate equivalent atoms: #1 –x, -y+2, -z

3.5.4 Comparison of the Molecular Structures of 65, 67, 68, 71 and 73

For clarity, the atom labeling in this section is specified in Figure 3.53 to aid with the direct comparison of bond lengths and angles. Refer to Tables 3.19 and 3.20 for the significant bond lengths and angles of each compound.

65   **68**   **71**

72   **67**
                                73
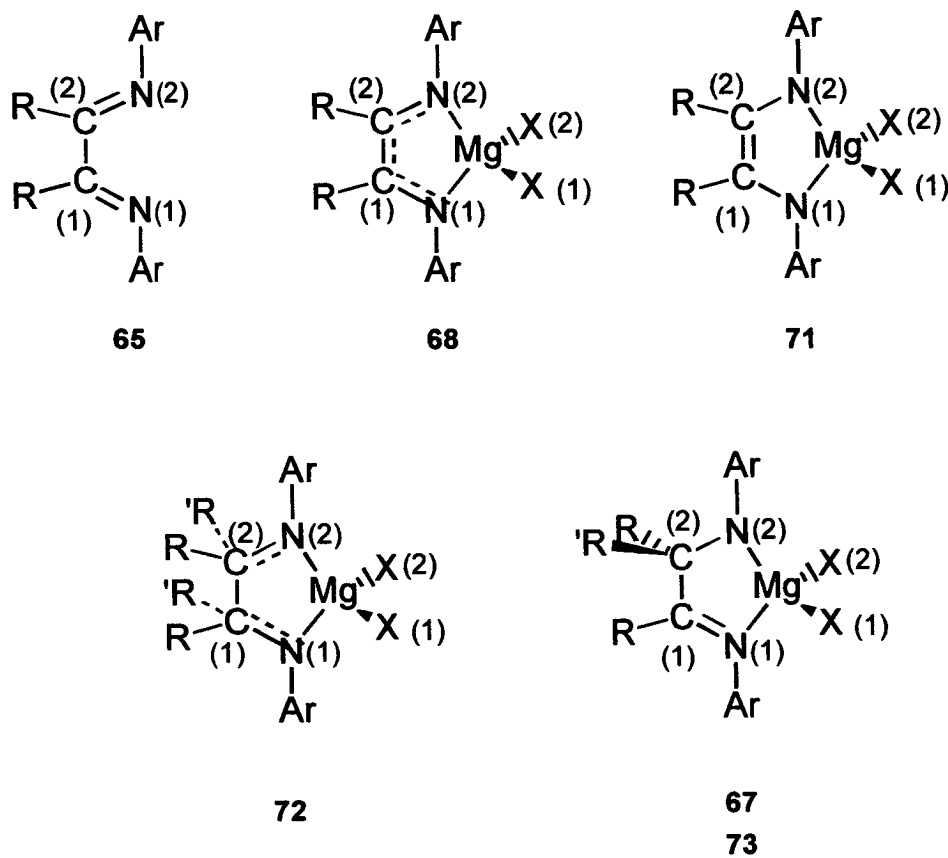
Figure 3.53 The numbering scheme for 65 (α-diimine ligand); 68 (Radical complex); 71 (Dianionic ligand based complex); 67, 72 & 73 (imino-amide complex).

	65	67	68 Molecule 1	68 Molecule 2	71	72	73 Part1	73 Part2
N(1)-C(1)	1.283 (5)	1.276 (9)	1.345 (6)	1.336 (5)	1.402 (3)	1.370 (2)	1.31 (2)	1.288 (14)
N(2)-C(2)	1.283 (5)	1.440 (9)	1.333 (6)	1.320 (6)	1.385 (3)	1.370 (2)	1.45 (2)	1.473 (11)
C(1)-C(2)	1.547 (8)	1.538 (10)	1.422 (7)	1.437 (7)	1.398 (3)	1.505 (4)	1.520 (10)	1.521 (9)
N(1)-Mg(1)	-	2.180 (7)	2.066 (5)	2.050 (4)	2.060 (2)	2.0422 (14)	2.020 (4)	2.020 (4)
N(2)-Mg(1)	-	1.989 (7)	2.065 (4)	2.048 (4)	2.071 (2)	2.0422 (14)	2.057 (4)	2.057 (4)
Mg(1)-X(1)	-	1.985 (6)	2.263 (5)	2.270 (6)	2.113 (19)	2.2041 (25)	2.320 (3)	2.284 (3)
Mg(1)-X(2)	-	1.944 (6)	2.205 (6)	2.200 (6)	2.815 (3)	2.2499 (25)	2.284 (3)	2.3201 (3)
N(2)-Mg(1)-X(2)	-	131.3 (3)	118.8 (2)	115.1 (2)	-	114.74 (6)	117.38 (14)	117.38 (14)
N(1)-Mg(1)-X(1)	-	112.5 (3)	113.9 (2)	119.5 (2)	-	114.74 (6)	116.37 (14)	116.37 (14)
N(2)-Mg(1)-N(1)	-	80.9 (30	84.54 (17)	83.62 (16)	-	81.08 (8)	81.47 (14)	81.47 (14)
X(1)-Mg(1)-X(2)	-	83.2 (3)	105.52 (18)	104.9 (2)	-	104.32 (8)	103.85 (10)	103.85 (10)
N(2)-C(2)-C(1)	119.6 (2)	108.8 (6)	120.5 (4)	119.3 (4)	120.2 (2)	114.82 (9)	106.5 (16)	107.9 (9)
C(2)-C(1)-N(1)	119.6 (2)	108.5 (7)	120.4 (4)	119.0 (4)	119.6 (2)	114.82 (9)	120.2 (18)	120.2 (18)
C(1)-N(1)-Mg(1)	-	108.7 (5)	106.2 (3)	107.6 (3)	107.37 (15)	112.09 (11)	112.9 (9)	111.3 (5)
C(2)-N(2)-Mg(1)	-	109.0 (5)	106.5 (3)	108.1 (3)	107.37 (16)	112.09 (11)	111.7(8)	112.5 (5)

Table 3.19 Selected bond lengths (Å) and angles (°) for 65, 67, 68, and 71-73

3.5.4.1 The NCCN Fragment

The average N-C(sp^2), N-C(sp^3), C(sp^2)-C(sp^2) and C(sp^3)-C(sp^3) bond lengths are quoted as 1.279 (8)Å, 1.469 (14)Å, 1.460 (15)Å and 1.524 (14) Å respectively in the international tables for crystallography.[44] The N(1)-C(1) bond length for the free diimine ligand corresponds to a double bond (1.283(5)Å). Comparison of the NCCN bond distances for all the structures **65, 67, 68, 71-73** (Table 3.19), show that the NCCN fragments correspond to the structures given in Figure 3.53. The results of a CSD search of similar NCCNMg moieties (Figure 3.54) are tabulated in Table 3.20. A CSD search for the amide equivalent of the NCCNMg fragment revealed 37 hit samples and the mean NC, CC and MgN distances were calculated.
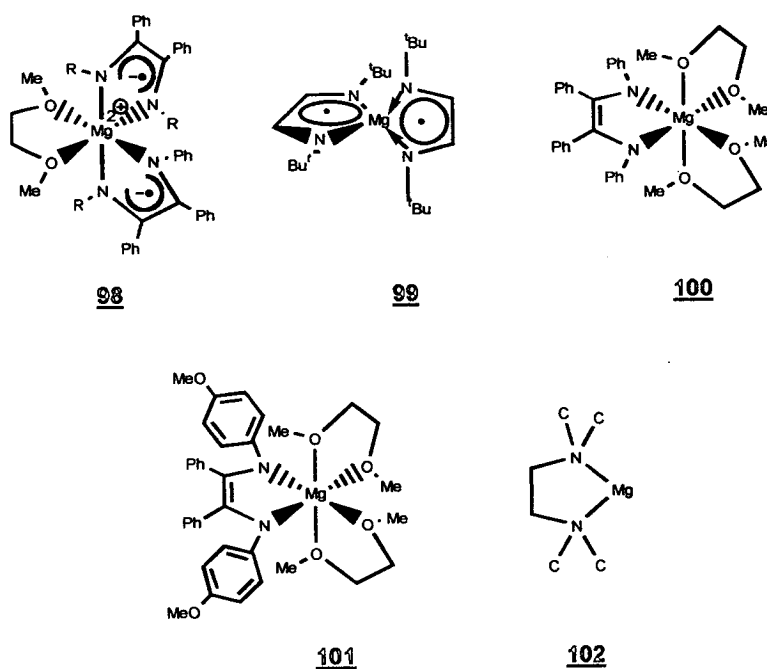
Figure 3.54 Molecules A-E obtained during a CSD search

	No.of hits	Mg(1)-N(1)	N(1)-C(1)	C(1)-C(2)	N(2)-C(2)	Mg(2)-N(2)
Dimine Radicals	2					
98		2.070 (7)	1.32 (1)	1.41 (1)	1.32 (1)	2.067 (7)
99		2.149 (2)	1.343 (4)	1.343 (4)	1.434 (5)	2.147 (3)
Dianionic Ligand	2					
100		2.066 (3)	1.414 (4)	1.372 (4)	1.416 (6)	2.096 (30
101		2.056 (2)	1.403 (4)	1.369 (4)	1.423 (3)	2.066 (2)
Amine	37					
102		2.280 (9)	1.469 (5)	1.500 (8)	1.475 (4)	2.281 (9)

Table 3.20 Selected average bond lengths (Å) calculated from searches on the CSD.

The bond lengths for the NCCN unit for **68**, for both molecules 1 and 2, are consistent with the literature, and similarly the bond lengths observed in the NCCN unit for **71** are comparable with those found in 100 and 101. The imino amide ligand based complexes have no Mg precident in the literature. In **72** both NC bond lengths appear to be N=C double bonds and the CC bond a single bond. This is a consequence of the disorder observed in the molecule which causes an averaging of the N=C and N-C distances. On considering the valency and co-ordinative saturation of C(1), then C(1)-N(1) must be a single bond. In contrast, The imine nature of the N(1)-C(1) imine bond and the N(2)-C(2) amide bond are clearly displayed in complexes **67** and **73** (parts 1 and 2). The amide N(2)-C(2) bond lengths in **67** and **73** are comparable to those observed in the literature.

3.5.4.2 The N-Mg Bond Lengths

From Table 3.20 it is evident that the neutral chelating diamines have longer N-Mg bond lengths [2.280 (9)-2.281(9)Å] compared with the bond lengths observed for the monoanionc delocalised radical complexes [2.070 (7)-2.149 (2) Å]. The dianionic ligand based complexes have similar bond lengths to the monoanionic systems [2.056 (2) –2.096 (3)Å]. Comparison of the MgN bond lengths in complexes **67-68** and **71-73** reveals that the N(1)-Mg(1) bond length in **67** to be greater than that of N(2)-Mg(2). The Mg(1)-N(1) bond length is comparable to the bond length of a neutral chelating diimine. The N(2)-Mg(1) bond length is shorter at 1.989 (7)Å and indicative of the N atom being monoanionic. The Mg(1)-N(2) and Mg(1)-N(1) bond lengths in **72** are averaged due to the nature of the disorder in the molecule and can be ignored. The N(1)-Mg(1) bond lengths in **73** are slightly shorter than the N(2)-Mg(1) bond lengths, but not significantly so, and are as short as those quoted for the doubly reduced species, however there is not a large enough basis set in the literature (2 compounds) to say whether this result is unusual. The N-Mg bond lengths in complex **71** are consistent with 100 and 101, and similarly the MgN bond lengths with 98 and 99, Tables 3.19 and 3.20.

3.5.4.3 Comparison of the Mg-C and Mg-O Bond Lengths

CSD searches were implemented to determine the average bond lengths for terminal Mg-Me groups and bridging μ_2Me-Mg, and μ_2CO-Mg groups, (Table 3.21). As expected the bridging methyl groups with a higher coordination number longer greater Mg-Me bond lengths [2.289 (17) -2.327(11)Å] in comparison to a Mg-Me terminal bond length [2.145 (6)Å]. We have only characterised two magnesium methyl complexes (68 and 72). In these the methyls are bridging and the Mg-CH$_3$ bond lengths correspond with those obtained for such groups in the literature [2.200 (6) -2.270 (6)Å (68), 2.2041 (25) -2.2499 (25)Å (72)]. The bridging μ_2OH ligand in 73 has a Mg-O length of 2.320(3)-2.284(3)Å and is quite a rare moiety with only one reported in the literature. A search for terminal Mg-OH groups produced no hits.
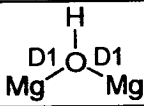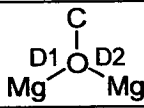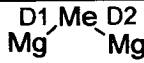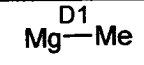
Moiety	No.of Hits	Bond	D1	D2
H D1 O D1 Mg Mg	1 Hit	MgO	1.951	-
C D1 O D2 Mg Mg	25Hits	MgO	1.987	1.999
D1 Me D2 Mg Mg	5 Hits	MgMe	2.327	2.289
D1 Mg—Me	14 Hits	MgMe	2.145	-

Table 3.21 Table of the mean bond lengths calculated from a CSD search of the given moieties.

In contrast, a CSD search for a Mgμ_2-OC fragment produced 25 hits, and the mean Mg-μ_2O bond length was between 1.987 (9) Å [D1] and 1.999 (7)Å [D2]. Comparison with the Mgμ_2OMe bond lengths in 67, reveal corresponding values of 1.985 (6) Å [D1] and 1.944 (6)Å [D2].

3.6 Summary of the Reaction of Magnesium Alkyls with α-diimines

In conjunction with results reported here, and work reported by Van Koten and Klerks on the reaction of ZnR_2 and AlR_3 with α-diimines, a pathway for the reaction of α-diimines with $MgMe_2$ can be proposed (Figure 3.55). The reactants initially complex to form the primary neutral complex $[Mg(CH_3)_2(diimine)]$ which up to now has not been characterised by NMR due to the facile homolytic cleavage of the methyl magnesium bonds to produce a methyl radical and the magnesium complex radical, even at low temperatures. The electron that is transferred to the magnesium resides in the π^* orbital of the diimine ligand. The resultant methyl radical can escape leaving a persistent magnesium complex radical that is ligand centred, which can be observed by EPR in solution (**68, 69, 70**), and identified as a triplet diradical dimer in the solid state (**68**). If the liberated methyl radical does not escape, it can alternatively recombine with the Mg complex radical adding to the carbon atom of one of the C=N to produce an imino-amide species, which on isolation in the solid state can be identified as a dimeric species bridged by two methyl groups (**72**). Subsequent reaction with water or oxygen can produce the hydroxy- bridged dimeric species $[(Mg(\mu_2\text{-}OH)_2\{diimine(Me)\}]_2$ (**73**) or the methoxy bridged species

$[Mg(\mu_2\text{-}OMe)\{diimine(Me)\}]_2$ (**67**) respectively. At very low temperatures, in a solvent mixture of toluene and THF, complete elimination of both methyl ligands from the neutral $[Mg(Me)_2(diimine)]$ complex, *via* two single electron transfers, produces a monomeric, THF solvated, Mg complex containing a doubly reduced dianionic diamide ligand $[Mg(diamide)(THF)_3]$ (**71**).

A radical such as $[Mg^+(\mu_2\text{-}Me)(diimine^-)]_2$ would make an ideal polymerisation catalyst as they would not require activation as the Mg centre is positively charged; and the molecule is neutral over all and so should be soluble in non-polar solvents. However, the fact that the complex is a dimer may present problems.
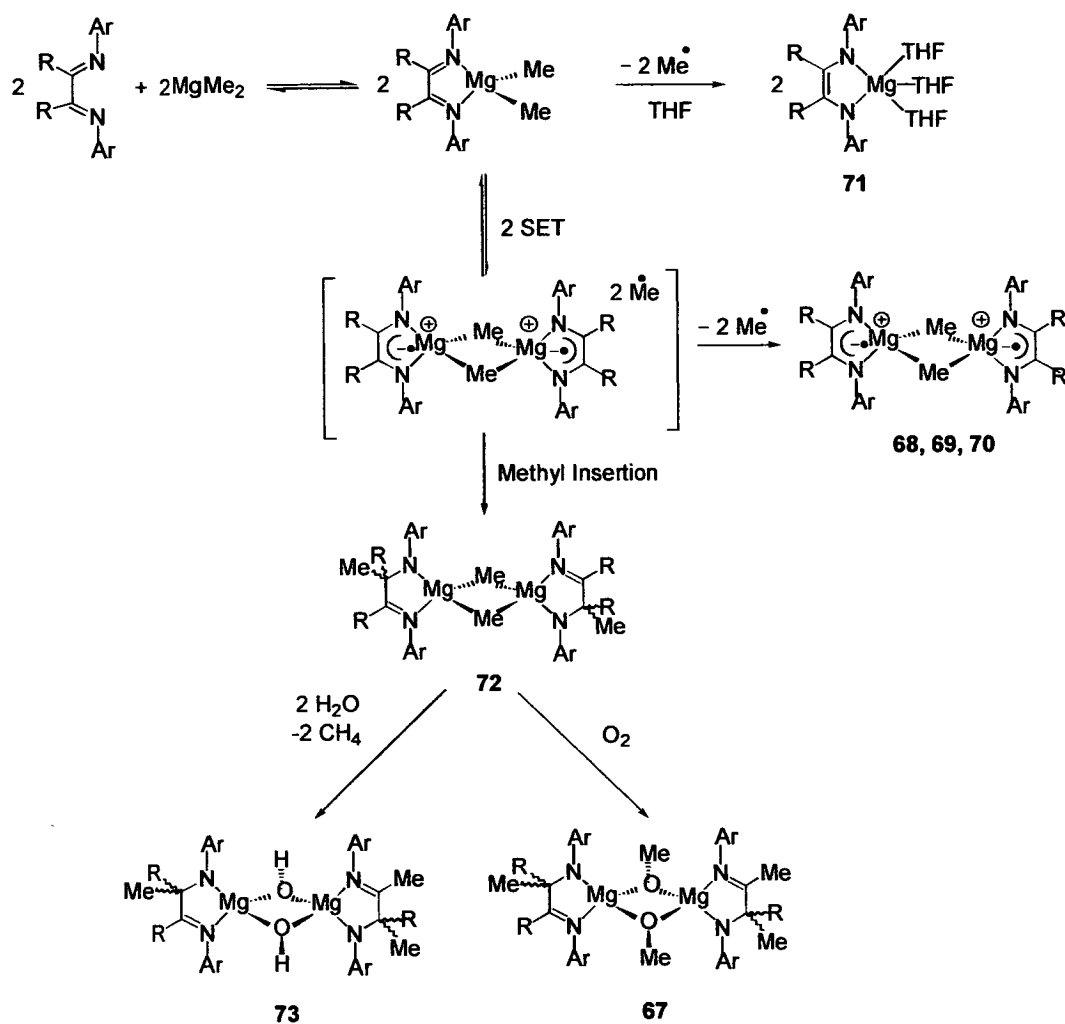
Figure 3.55 Hypothesised reaction mechanism on reacting MgMe₂ with α-diimine

3.7 Experimental

3.7.1 General Procedures.

All the air/moisture sensitive experimental work was performed under N_2 using standard Schlenk techniques on a vacuum line under dry, oxygen free, nitrogen. Some experimental work and characterisations were carried out in a nitrogen filled glove box (Saffron), fitted with oxygen and water scavenging columns. All solvents were dried and deoxygenated before use. Solvents and reagents where commercially available were bought from Aldrich, Acros or Fischer. With exception of NMR solvents which were purchased from Goss Scientific. Et_2O, toluene, hexane, benzene, and THF were all distilled from Na/benzophenone under a nitrogen atmosphere. NMR solvents were degassed using three freeze-pump-thaw cycles and stored over molecular sieves. The diimines powders were placed under vacuum and then under nitrogen before complexation reactions.

3.7.2 Instrumentation

Elemental analyses were performed by sealing aluminium capsules containing approx. 1mg of compound under nitrogen in the glove box, and determined using a Perkin Elmer 2400 CHN Analyser. NMR were recorded on a Gemini 200MHz, Bruker 200Mhz, Bruker 250MHz and Bruker GPX 360MHz spectometers. IR spectra were obtained on a Perkin Elmer Paragon 1000 FT-IR spectometer as potassium bromide discs or as liquid thin films. Electron impact (EI) mass spectra were obtained either on a Finnigan MAT 4600 quadrapole spectrometer or on a Kratos MS50TC spectrometer. Fast atom bombardment (FAB) mass spectra were obtained on a MS50TC spectrometer. EPR spectra were recorded on a Bruker ER200D spectrometer at room temperature.

[(2,6-^{i}Pr$_2$Ph)NCH]$_2$ (62)

2,6-Diisopropylaniline (73.709 g, 416 mmoles) was added dropwise with stirring to a warm 40% solution of glyoxal (24.183 g, 417 mmoles) in methanol (225 cm^3). The mixture was warmed at 33°C for 1h after which time a yellow precipitate had formed. The solid was filtered and re-crystallised from boiling ethanol (100 cm^3) with a yield of 73.078g (194.05 mmoles, 47%). **CHN:** Found C 83.30, H 9.62, N 7.25; $C_{26}H_{36}N_2$ requires C 82.93, H 9.64, N 7.44. **^{1}H NMR** (199.97 MHz, CDCl$_3$):

δ 1.14 (d, J = 6.95Hz, 24H, (^{i}Pr-CH_3), 2.87 (spt, 4H, J = 6.95Hz, (^{i}Pr-CH)),

7.11 (m, 6H, Ar-H), 8.03 (s, 2H, NCH). ^{13}C NMR (62.89 MHz, CDCl$_3$):

δ 23.25 (s, ^{i}Pr-CH_3), 27.90 (s, ^{i}Pr-CH), 123.04 (s, m-ArCH), 124.99 (s, p-ArCH),

136.55 (s, Ar-C), 147.86 (s, Ar-C), 162.96 (s, N=CH).

MS (+FAB): m/z = 377 (59.9%). **IR (KBr, cm^{-1}):** ($\nu_{C=N}$) 1625.2.

[(2,6-Me$_2$Ph)NCH]$_2$ (63)

2,6-Dimethylaniline (8.015 g, 66.1 mmoles) was added drop wise with stirring to solution of glyoxal (2.304 g, 39.7mmoles) in methanol (75 cm^3) at 33°C. The mixture was stirred at 33°C for 1h after which time a yellow precipitate had formed. The solid was filtered and re-crystallised from boiling ethanol with a yield of 3.97g (15.0 mmoles, 45.37%). **CHN:** Found C 81.28, H 7.74, N 10.65;

C$_{18}$H$_{20}$N$_2$ requires C 81.78, H 7.63, N 10.60.

^{1}**H NMR** (250.13 MHz, CDCl$_3$): δ 2.19 (s, 12H, (CH_3)),

7.01 (t, J = 8.26Hz, 2H, o-ArH), 7.10 (d, J = 7.75Hz, 4H, m-ArH),

8.13 (s, 2H, NCH). ^{13}**C NMR** (62.89 MHz, CDCl$_3$): δ 18.09 (s, CH_3),

124.62 (s, o-ArCH), 126.26 (s, Ar-C), 128.13 (s, m-ArCH),

149.68. (s, Ar-C), 163.3 (s, N=CH). **MS (+FAB):** m/z = 265 (88.6%).

IR (KBr, cm^{-1}): ($\nu_{C=N}$) 1617.1. **IR (nujol, cm^{-1}):** ($\nu_{C=N}$) 1618.8, 1592.7.

[(2,6-^{i}Pr$_2$Ph)NCMe]$_2$ (64)

2,6-diisopropylaniline (9.544 g, 53.8 mmoles) was added to a 250 cm^3 round bottomed flask containing MeOH (50 cm^3), and with stirring formic acid (1cm^3) added. 2,3-butandione (2.317 g, 26.9 mmoles) was then added dropwise and the reaction mixture stirred for 20h. The product (8.789 g, 21.7 mmoles, 80.7%), a yellow solid, was filtered off and recrystallised from MeOH (75 cm^3). The recrystallised product (6.093 g, 15.1 mmoles, 56.0%) was filtered and washed with cold MeOH and dried under vacuum.

CHN: Found C 83.08, H 10.00, N 6.96; C$_{28}$H$_{40}$N$_2$ requires C83.11, H 9.96, N 6.93.

^{1}**H NMR** (250.13 MHz, CDCl$_3$): δ1.21 (d, 24H, J = 5.71Hz, (^{i}Pr-CH_3));

2.08 (s, 6H, CH_3CN), 2.72 (spt, 4H, J = 6.83Hz, ^{i}Pr-CH), 7.19 (m, 6H, Ar-H).

^{13}**C NMR:** (62.89 MHz, CDCl$_3$): δ 16.44 (s, C=C-CH_3), 22.58 (s, ^{i}Pr-CH_3),

22.58 (s, ^{i}Pr-CH_3), 28.41 (s, ^{i}Pr-CH), 122.88 (s, m-ArCH), 123.67 (s, o-ArCH),

134.89 (s, Ar-C), 146.06 (s, Ar-C) 168.05 (s, N=C).

MS (+FAB): m/z = 405 (60.8%). **IR** (nujol, cm^{-1}): ($v_{C=N}$) 1590.1; 1642.4.

[(2,6-^{i}Pr$_2$Ph)BIAN] (65)   BIAN= bis(imino)acenapthene

A mixture of acenaphthenequinone (1.022 g, 5.61 mmoles) and 2,6-

diisopropylaniline (1.998 g, 11.3 mmoles) in acetic acid (15 cm^3) was heated to

reflux. After 1h the mixture was cooled to room temperature and the orange solid

filtered off. The product was washed with acetic acid, hexane and air dried.

Recrystallisation from ethanol yielded 49 (2.336 g , 4.78 mmoles, 85.2% yield).

CHN: Found C85.72, H 8.08, N 5.54; C$_{36}$H$_{40}$N$_2$ requires C 86.35, H 8.05, N 5.60.

^{1}**H NMR** (250.13 MHz, CDCl$_3$): δ 0.96 (d, J = 6.95Hz, 12H, (^{i}Pr-CH_3);.

1.23 (d, J = 6.95Hz, 12H, (^{i}Pr-CH_3)), 3.04 (spt, 4H, J = 6.82Hz, (^{i}Pr-CH),

6.63 (d, 2H, J = 7.20Hz, ArH), 7.27 (m, 6H, ArH), 7.38 (pst, 2H, ArH),

7.84 (d, 1H, J = 8.25Hz , ArH). ^{13}**C NMR** (62.89 MHz, CDCl$_3$):

δ   22.98 (s, (^{i}Pr-CH_3)), 23.25 (s, (^{i}Pr-CH_3), 28.46 (s, (^{i}Pr-CH), 123.19 (s, Ar-CH),

123.31 (s, Ar-CH), 124.15 (s, Ar-CH), 127.70 (s, Ar-CH), 128.72 (s, Ar-C),

129.35 (s, Ar-CH), 130.95 (s, Ar-C), 135.25 (s, Ar-C), 140.69 (s, Ar-C),

147.36 (s, Ar-C), 160.82 (s, N=C). **MS (+FAB):** m/z = 501 (70.4%).

IR (Nujol, cm^{-1}): ($v_{C=N}$): 1593.7; 1641.3.

Crystal Data for 65

Data was collected on a SMART diffractometer using an orange rod of dimensions

0.16 x 0.08 x 0.04 mm using the ω-θ method in the range of 40< θ < 44°. Of a total

of 3112 reflections collected, 260 (R$_{int}$= 0.1272) were independent. The full

difference map extrema were 0.346 and –0.197 eÅ^{-3} with a final R of 8.28% for 177

parameters.

Empirical formula	$C_{36}H_{40}N_2$	γ /°	90
Formula weight	500.70	Volume / Å³	2917.8 (8)
Crystal system	Monoclinic	Z	4
Space group	C2/c	Temperature / K	293 (2)
a / Å	15.468 (3)	Wavelength / Å	1.54178
b / Å	8.8082 (12)	Density calc. / Mg/m³	1.140
c / Å	21.466 (3)	μ(Mo-Kα) / mm⁻¹	0.495
α / °	90	$R_1[F>4\sigma(F)]$	0.0828
β / °	93.91 (2)	wR_2 (all data)	0.2405

$[Mg_{13}C_{48.60}H_{99.20}Cl_{14}O_{18.40}]_{1.4}$ (66)

With stirring **63** (0.166 g, 0.627 mmoles) was dissolved in THF (1 cm³). The Gringard MgMeCl was added as a 3M THF solution (0.2 cm³, 0.600 mmoles) and a colour change from yellow to orange was observed. The product was dried under vacuum and an orange oil obtained. The product was crystallised from THF in the freezer at $-20°C$ after 2 weeks in an NMR tube. Yield= 0.068 g (0.038 mmoles, 6.33%). Complex **67** was characterized by ^{1}H NMR and by X-ray crystal structure analysis. ^{1}**H NMR** (250.13 MHz, CDCl₃): δ 0.00 (s), 0.76 (s), 0.82 (s), 0.91 (s), 0.96 (s), 1.09 (s(br), THF), 1.30 (s), 1.63 (s), 1.65 (s), 1.68 (s), 1.79 (s), 1.816 (s), 1.93 (s), 2.05 (s), 2.26 (s), 3.27 (d), 3.39 (s(br)), 3.73 (s), 3.84 (s), 5.10 (s), 6.57 (s), 6.67 (d), 6.70 (d), 6.88 (s), 6.93 (s), 6.96 (s), 7.72 (s).

Crystal Data for 66

Data was collected on a SMART diffractometer using an orange rod of dimensions 0.19 x 0.19 x 0.15 mm using the ω-θ method in the range of 20< θ < 22°. All the 5011 reflections collected were independent, (R_{int}= 0.0000). The full difference map extrema were 0.346 and -0.197 eÅ⁻³ with a final R of 8.28% for 177 parameters.

Empirical formula	C$_{36}$H$_{40}$N$_2$	γ / °	90
Formula weight	500.70	Volume / Å^3	2917.8 (8)
Crystal system	Monoclinic	Z	4
Space group	C2/c	Temperature / K	293 (2)
a / Å	15.468 (3)	Wavelength / Å	1.54178
b / Å	8.8082 (12)	Density calc. / Mg/m^3	1.140
c / Å	21.466 (3)	μ(Mo-Kα) / mm^{-1}	0.495
α / °	90	R$_1$[F>4σ(F)]	0.0828
β / °	93.91 (2)	wR$_2$ (all data)	0.2405

[Mg(μ_2-OMe){(2,6-^{i}Pr$_2$Ph)BIAN(Me)] (67)

Hexane was added to **65** (0.027 g, 0.054 mmoles)(1cm^3) and the ligand dissolved forming an orange solution. With stirring 3M MgMeCl in THF was added (0.10 cm^3, 0.3 mmoles) drop wise via syringe. On removing the solvent in vacuum a red solid was afforded. The product was crystallized as a single red block crystal from hexane (2 cm^3) after being stored in an NMR tube in the fridge at °C for one week.

Crystal Data for 67

Data was collected on a Stoe Stadi4 diffractometer using a red tablet of dimensions 0.19 x 0.19 x 0.12 mm using the ω-θ method in the range of 20< θ < 22°. Of a total of 7380 reflections collected, 7238 (R$_{int}$= 0.0360) were independent. The full difference map extrema were 0.244 and –0.261 eÅ^{-3} with a final R of 8.68% for 757 parameters.

Empirical formula	C$_{77.50}$H$_{97.50}$Mg$_2$N$_4$O$_2$ [Mg$_2$(OMe)$_2$L$_2$].0.25C$_6$H$_{14}$	γ / °	90
Formula weight	1165.72	Volume / Å^3	7524.2(10)
Crystal system	Orthorhombic	Z	4
Space group	P2$_1$2$_1$2$_1$	Temperature / K	220(2)
a / Å	15.8537 (11)	Wavelength / Å	1.54184
b / Å	21.2530(18)	Density calc. / Mg/m^3	1.029
c / Å	22.3310(19)	μ(Mo-Kα) / mm^{-1}	0.614
α / °	90	R$_1$[F>4σ(F)]	0.0868
β / °	90	wR$_2$ (all data)	0.211

[Mg(μ2-Me){(2,6-^{i}Pr$_2$Ph)BIAN}]$_2$ (68)

Crystal

A solution of MgMe$_2$ (0.503 g, 1.004 mmoles) in Et$_2$O (35 cm^3) was added by cannula to an Et$_2$O (25 cm^3) solution of **66** (0.116 g, 2.133 mmoles). A colour change of orange to black to dark red was observed. The reaction mixture was sonicated in an ultrasound cleaning bath for 5 mins and then left to stir overnight. The solution was filtered through celite. A suitable crystal for X-ray analysis was grown in 10 cm^3 of the filtrate layered with 4 cm^3 of hexane at –26°C for 2 days.

Crystal Data for 68

Data was collected on a Stoe Stadi4 diffractometer using a red tablet of dimensions 0.50 x 0.42 x 0.19 mm using the ω-θ method in the range of 20< θ < 22°. Of a total of 9159 reflections collected, 9159 (R$_{int}$ = 0.0000) were independent. The full difference map extrema were 0.538 and –0.507 eÅ^{-3} with a final R of 9.70% for 719 parameters.

Empirical formula	C$_{81.50}$H$_{103.50}$Mg$_2$N$_4$ [Mg$_2$Me$_2$L$_2$]1.25(C$_6$H$_{14}$)	γ /°	100.09(4)
Formula weight	1187.80	Volume / Å^3	3688(3)
Crystal system	Triclinic	Z	2
Space group	P$_1$	Temperature / K	150(2)
a / Å	14.513(9)	Wavelength / Å	1.54178
b / Å	14.781(9)	Density calc. / Mg/m^3	1.070
c / Å	18.381(9)	μ(Mo-Kα) / mm^{-1}	0.613
α / °	93.43(4)	R$_1$[F>4σ(F)]	0.0970
β / °	106.93(40	wR$_2$ (all data)	0.2867

EPR

An Et$_2$O (25 cm^3) solution of **65** (0.040 g, 0.081 mmoles) was stirred overnight and MgMe$_2$ (4 mg, 0.073 mmoles) in Et$_2$O (25 cm^3), was added by cannula. A colour change of orange to black to dark red was observed. The solution was transferred to a quartz flat cell in the glove box and the EPR analysis completed. The EPR analysis parameters were CF 3440, Gain 3.2 x 10^4, Mod 4 Gpp, SW 200, Phase 0°, Power 100

mW, Freq 9.71 GHz; after simulation using WinEPR: g=2.0117, 2N a^N=4.6, Lorenzian line width 4.7 G.

[Mg (μ_2-Me){(2,6-^{i}Pr$_2$Ph)NC(H)}$_2$]$_2$ (69)

A yellow solution of **62** (0.070 g, 18.59 mmoles) in Et$_2$O (50 cm^3) was added to solid MgMe$_2$ (0.010 g, 18.39mmoles) with stirring. An orange solution formed. A sample of the mother liquor was prepared in a flat quartz cell for EPR analysis in the glove box and the EPR spectrum recorded. The EPR analysis parameters were CF 3450, Gain 3200, Mod 4 Gpp, SW 200, Phase 180°, Power 100 mW, Freq 9.71 GHz; after simulation using WinEPR: g=2.01253, 2N a^N=5.3, 2H a^H=5.3, Lorenzian line width 3.004 G.

[Mg(μ_2-CH$_3$){(2,6-^{i}Pr$_2$Ph)NCMe}]$_2$ (70)

A solution of **64** (2.173 g, 10.8 mmoles) in Et$_2$O (25 cm^3) was added to an Et$_2$O (25 cm^3) solution of MgMe$_2$ (0.585 g, 5.37 mmoles) with stirring. An orange solution formed. The solution was allowed to stir for 1h. The mother liquor (1.73 cm^3) was diluted with Et$_2$O (48 cm^3) and a sample prepared for EPR analysis in the glove box and the EPR spectrum recorded. The EPR analysis parameters were CF 3440, Gain 4 x 10^4, Mod 4 Gpp, SW 200, Phase 180°, Power 100 mW, Freq 9.71 GHz; after simulation using WinEPR: g=2.0123, 2N a^N=5.54, 6H a^H=5.54, Lorenzian line width 4.00 G.

[Mg (THF)$_3${(2,6-^{i}Pr$_2$Ph)BIAN}] (71)

A solution of MgMe$_2$ (0.220 g, 4.046 mmoles) in toluene (10cm^3) and THF (1cm^3) was chilled slightly in liquid N$_2$. This solution was transferred *via* cannula into a solution of **65** (1.1912 g, 3.818 mmoles) in toluene (10cm^3) and THF (7cm^3). A deep red solution was obtained. The solution was allowed to slowly warm to room temperature. The reaction mixture contained a mixture of an orange solid, **65**, and the red solution. The opaque solution was transferred to a fresh Schlenk and allowed to stand at room temperature over night. The solution was placed in the fridge over night at 5 °C but no crystals were obtained, it was then placed in the freezer at –20 °C

for 2 weeks. To the eye there was a reasonable crop of a mixture the crystals unfortunately they re-dissolved at room temperature, the crystals were of poor quality. The solution was gently heated and became slightly green in colour, the reaction mixture was placed in the fridge over night and crystals suitable for X-ray analysis were obtained: orange rods of **65** and red needles of **71**. The yield of crystals obtained was 0.722g (0.820 mmoles, 0.215%) but contained a mixture of **65**, and **71**.

IR (Nujol, cm^{-1}): ($v_{C=N}$): 1651.5; 1580.1.

^{1}H NMR (360.13 MHz, THF-d_8): 0.08 (s), 1.02 (d, J=7.02Hz, CH_3), 1.14 (s), 1.18 (d, J= 6.56 Hz, CH_3), 1.69 (s, THF), 1.73 (s, THF), 1.90 (s, THF), 2.27 (s, CH_3Ph), 2.96 (m(br), CH(CH$_3$)$_2$), 3.24 (m(br), CH(CH$_3$)$_2$), 3.55 (s, THF), 3.58 (s, THF), 3.83 (s(br), THF), 4.02 (s(br), THF), 5.48 (s), 5.82 (s), 6.04 (d), 6.39 (s(br)), 6.70 (m), 6.80 (s(br)), 6.86 (t), 6.89-7.26 (m(br)), 7.66 (d), 7.82 (d), 7.92 (d).

^{13}C NMR (90.55 MHz, THF-d_8): 23.76 (s), 24.56 (s), 26.36 (s), 28.25 (s), 28.84 (s), 68.01 (s, CH$_2$), 119.96 (s, CH), 124.21 (s, CH), 124.93 (s, CH), 126.01 (s, CH), 126.45 (s, CH), 126.45 (s, CH), 127.46 (s, CH), 128.88 (s, CH), 129.64 (s, CH), 140.00 (s, C), 146.27 (s, C).

Crystal Data for 71

Data was collected on a SMART diffractometer using a red needle of dimensions 0.13 x 0.05 x 0.04 mm using the ω & π scans method in the range of 5< θ < 40°. Of a total of 54563 reflections collected, 10210 (R_{in} = 0.1260) were independent. The full difference map extrema were 0.719 and –0.315 e Å with a final R of 6.39% for 605 parameters.

Empirical formula	$C_{58.50}H_{76}MgN_2O_3$ [Mg(L)(THF)$_3$].1.5MeC$_6$H$_5$	γ /°	90
Formula weight	879.52	Volume / Å^3	9980(2)
Crystal system	Orthorhombic	Z	8
Space group	Pbca	Temperature / K	150(2)
a / Å	22.475(3)	Wavelength / Å	0.71073
b / Å	18.271(3)	Density calc. / Mg/m^3	1.171
c / Å	24.304(3)	μ(Mo-Kα) / mm^{-1}	0.082
α / °	90	R$_1$[F>4σ(F)]	0.0639
β / °	90	wR$_2$ (all data)	0.1615

[Mg(μ₂-Me){(2,6-ⁱPr₂Ph)NC(Me)₂C(Me)N(2,6-ⁱPr₂Ph)}]₂ (72)

MgMe₂ (0.300 g, 5.518 mmoles) was dissolved in THF (1cm³) and toluene (10cm³) and then chilled in liquid nitrogen. A chilled solution of **63** (2.287 g, 5.62 mmole) in toluene (10cm³) and THF (0.2cm³) was added via cannula, and the reaction mixture allowed to gradually warm to room temperature. The orange/clear solution was allowed to stand at room temperature overnight and placed in the freezer the next day. After 5 days red block crystals suitable for X-ray structure analysis were formed (0.510 g, 10%).

CHN: Found C 78.63, H 10.15, N 5.99; $C_{60}H_{92}N_4Mg_2$ requires C 78.50, H 10.10, N 6.10. **¹H NMR** (360.13 MHz, THF-d_8): δ -1.79 (s, 3H, MgCH_3),

1.01 (d, J = 6.81Hz, 6H, (ⁱPr-CH_3)), 1.11 (d, J = 6.84Hz, 6H, (ⁱPr-CH_3)),

1.19 (d, J = 7.04Hz, 6H, (ⁱPr-CH_3)), 1.21 (d, J = 6.91Hz, 6H, (ⁱPr-CH_3)),

1.27 (s, 6H, (C(CH_3)₂), 2.25 (s, 3H, (N=C(CH_3)),

3.02 (sept, J = 6.81Hz, 4H, (ⁱPr-CH)), 3.98 (sept, J = 6.89Hz, 4H, (ⁱPr-CH)),

6.75 (t, J = 7.32Hz, 4H, o-ArCH), 6.91 (d, J = 7.55Hz, 8H, m-ArCH),

7.13-7.19 (m, 12H, ArCH), **¹³C NMR** (90.55 MHz, THF-d_8): 19.04 (s, CH₃),

24.33 (s, CH₃), 24.56 (s, CH₃), 24.66 (s, CH₃), 27.04 (s, CH₃), 28.38 (s, CH),

28.72 (s, CH), 30.12 (s), 32.65 (s), 121.67 (s, CH), 123.11 (s, CH), 124.62 (s, CH),

126.54 (s, CH), 128.89 (s, CH), 129.01 (s, CH), 140.09 (s, C), 150.12 (s, C).

IR (Nujol, cm⁻¹): ($v_{C=N}$): 1589.2; 1609.8.

Crystal Data for 72

Data was collected on a SMART diffractometer using a red block of dimensions 0.31 x 0.30 x 0.30 mm using the ω and π method in the range of 5< θ < 53°. Of a total of 9392 reflections collected, 3459 (Rint= 0.0373) were independent. The full difference map extrema were 0.294 and –0.392 e Å⁻³ with a final R of 5.26% for 170 parameters.

Empirical formula	$C_{71}H_{108}Mg_2N_4O$ $[\{Mg(L)(CH_3)\}_2].C_7H_8.C_4H_8O$	$\gamma /°$	90
Formula weight	1082.23	Volume / $Å^3$	3301.6(10)
Crystal system	Monoclinic	Z	2
Space group	C2/m	Temperature / K	150(2)
a / Å	18.459(3)	Wavelength / Å	0.71073
b / Å	18.337(3)	Density calc. / Mg/m^3	1.089
c / Å	12.190(2)	$\mu(Mo\text{-}K\alpha)$ / mm^{-1}	0.080
α / °	90	$R_1[F>4\sigma(F)]$	0.0526
β / °	126.851(2)	wR_2 (all data)	0.1454

$[Mg(\mu_2\text{-}OH)\{(2,6\text{-}^iPr_2Ph)NC(Me)_2C(Me)N(2,6\text{-}^iPr_2Ph)\}]_2$ (73)

A solution of **64** (2.173 g, 5.37 mmoles) in Et_2O (25 cm^3) was added to an Et_2O (25 cm^3) solution of MgMe$_2$ (0.585 g, 10.8 mmoles) with stirring. An orange solution formed immediately. The solution was allowed to stir overnight. Some of the mother liquor was taken for EPR analysis (see **70**). The solvent was removed in vacuum and an orange powder was formed. The product was extracted in hexane (80cm^3) and filtered through celite. Crystals suitable for X-ray analysis were grow at room temperature after 6 days.

Crystal Data for 73

Data was collected on a SMART diffractometer using a orange block of dimensions 0.58 x 0.46 x 0.23 mm using the ω and π scans in the range of $4< \theta < 59°$. Of a total of 21742 reflections collected, 8308 (R_{int}= 0.1289) were independent. The full difference map extrema were 0.409 and −0.515 e Å with a final R of 11.04% for 328 parameters.

Empirical formula	$C_{60}H_{94}Mg_2N_4O_2$ $[Mg(L)(OH)]_2$	$\gamma /°$	90
Formula weight	952.01	Volume / $Å^3$	2893.6(6)
Crystal system	Monoclinic	Z	2
Space group	P2$_1$/n	Temperature / K	150(2)
a / Å	13.5017(15)	Wavelength / Å	0.71073
b / Å	14.3619(16)	Density calc. / Mg/m^3	1.093
c / Å	15.5783(17)	$\mu(Mo\text{-}K\alpha)$ / mm^{-1}	0.084
α / °	90	$R_1[F>4\sigma(F)]$	0.1104
β / °	106.688(2)	wR_2 (all data)	0.3859

3.8 References

1 Ittel, S.D, Johnson, L.K, Brookhart, M., *Chem.Rev.*, **2000**, *100*, 1169-1203.

2 Johnson, L.K; Killian, C.M.; Brookhart, M., *J.Am.Chem.Soc.*, **1995**, *117*,6414-6415.

3 Killian, C.M.; Temple, D.J.; Johnson, L.K; White, P.S.; Brookhart, M., *J.Am.Chem.Soc.*, **1997**, *118*,11664-11665.

4 Johnson, L.K; Stefan, M.; Brookhart, M., *J.Am.Chem.Soc.*, **1996**, *118*, 267 -268.

5 Svejda, S.A; Johnson, L.K; Brookhart, M., *J.Am.Chem.Soc.*, **1999**, *121*, 10634-10645.

6 Killian, C.M.; Johnson, L.K; White, P.S.; Brookhart, M., *Organomet.*, **1997**, *16*,2005-2007.

7 Mecking, S.; Johnson, L.K; Wang, L.; Brookhart, M., *J.Am.Chem.Soc.*, **1998**, *120*, 888-899.

8 Yang, K.; Lachicotte, R.J.; Eisenberg, R., *Organomet.*, **1998**, *17*, 5102-5113.

9 Svejda,S.A; Brookhart, M., *Organomet.*, **1999**, *18*, 65-74.

10 Gottfried, A.C.; Brookhart, M., *Macromol.*, **2001**, *32*, 1140-1142.

11 Gates, D.P; Svejda, S.A; Orate, E.; Killian, C.M.; Johnson, L.K; White, P.S.; Brookhart, M., *Macromol.*, **2000**, *33*, 2320-2334.

12 Temple, D.J.; Johnson, L.K.; Huff, R.L.; White, P.S.; Brookhart, M., *J.Am.Chem.Soc.*, **2000**, *122*, 6686-6700.

13 Yagyu T.; Kohtaro, K.; Brookhart, M., *Organomet.*, **2000**, *19*, 2125-2129.

14 McCord, E.F; McLain, S.J.; Nelson, L.T.J; Arthur, S.D; Coughlin, E.B.; Ittel, S.D.; Johnson, L.K.; Temple, D.; Killian, C.M.; Brookhart, M., *Macromol.*, **2001**, *34*, 362-371.

15 LaPointe, A.M.; Brookhart, M., *Organomet.*, **1998**, *17,* 1530-1537.

16 Corvaja, C.; Pasimeni, L., *Chem.Phys.Lett.*, **1976**, *39*, 261-264.

17 Kaim, W., *J.Am.Chem.Soc.*, **1982**, *104*, 3833-3837.

18 Kaim, W., *Acc.Chem.Res.*, **1985**, *18*, 160-166.

19 Gardiner, M.G.; Hanson, G.R.; Henderson, M.J.; Lee, F.C.; Raston, C.L., *Inorg.Chem.*, **1994**, *33*, 2456-2461.

20 Lorenz, V.; Thiele, K.H.; Neumuller, B., *Z.anorg.allg.Chem.*, **1994**, *620*, 691-696.

21 Tammiku, J.; Burk, P.; Tuulmets, A., *Main Group Metal Chem.*, **2000**, *23*, 301-307.

22 Klerks, J.M.; Stufkens, D.J.; Van Koten, G.; Vrieze, K., *J.Organomet.Chem.*, **1979**, *181*, 271-2283.

23 Van Koten, G.; Jastrzebski, J.T.B.H; Vrieze, K., *J.Organomet.Chem.*, **1983**, *250*, 49-61.

24 Kaupp, M.; Stoll,H.; Preuss, H.; Kaim, W.; Stahl, T.; Van Koten, G.; Wissing, E.; Smeets, W.J.J.; Spek, A.L.., *J.Am.Chem.Soc.*, **1991**, *113*, 5606-5618.

25 Gibson, V.; Redshaw, C.; White. A.J.P; Williams, D.J., *J.Organomet.Chem.*, **1998**, *550*, 453-456.

26 Gardiner,M.G.; Raston, C.L., *Inorg.Chem.*, **1999**, *38*, 4467-4472.

27 Pott, T.; Jutzi, P.; Neumann, B.; Stammler, H.G., *Organomet.*, **2001**, 20, *10*, 1965-1967.

28 Cloke, F.G.N.; Hanson, G.R; Henderson, M.J.; Hitchcock, P.B.; Raston, C.L., *J.Chem.Soc., Chem.Comm.*, **1989**, 1002.

29 Kleigmen, J.M.; Barnes, R.K., *Tetrahedron*, **1970**, *26*, 2555-2560; Kleigmen, J.M.; Barnes, R.K., *Tetrahedron letters*, **1969**, *24*, 1969.

30 Kleigmen, J.M.; Barnes, R.K., *J.Org.Chem.*, **1970**, *35*, 9, 3142-3143.

31 Diek, H., Svoboda, M. Greiser, T., *Z.Naturforsch.B Anorg.Chem.*, **1981**, *36*, 7, 823-832.

32 Asslet, R.V., *.et al, Recl.Trav.Chim.Pays-Bas*, **1994**, *113*, 88-98.

33 Stucky, G.; Rundle, R.E., *J.Am.Chem.Soc.*, **1964**, *86*, 4821-4830.

34 Albaric, L.; Hovnanian, N.; Julbe, A.; Guizard, C.; Alvarez-Larena, A.; Piniella, J.F., *Polyhedron*, **1997**, *16*, 4, 587-592.

35 Arunasalam, V.C.; Baxter, I.; Darr, J.A.; Drake, S.R.; Hursthouse, M.B.; Malik, K.M.A.; Mingos, M.P., *Polyhedron*, **1998**, *17*, 5-6, 641-657.

36 Starikova, Z.A.; Yanovsky, A.I.; Turevskaya, E.P.; Turova, N.Y., *Polyhedron*, **1997**, *16*, 6, 967-974.

37 Sobota, P.; Utko, J.; Janas, Z.; Szafert, S., *Chem.Comm.*; **1996**, 1923-1924.

38 Loos, D.; Eichkorn, K.; Magull, J.; Ahlrichs, R.; Schnockel, H., *Z.Anorg.Allg,Chem.*, **1995**, *621*, 1582-1588.

39 Werner, B.; Krauter, T.; Neumuller, E., *Z.Anorg.Allg, Chem.*, **1995**, *621*, 346-358.

40 Toney, J.; Stucky, G.D., *J.Organomet.Chem.*, **1971**, *28*, 5-20.

41 Casellato, U.; Ossola, F., *Organomet.*, **1994**, *13*, 4105-4108.

42 Tuulmets, A.; Mikk, M.; Panov, D., *Main Group Metal Chemistry*, **1997**, *20*, 1, 1-5.

43 Tuulmets, A.; Mikk, M.; Panov, D., *J.Organomet.Chem.*, **1996**, *523*, 133-138.

44 Wilson, A.J.C., International Tables for Crystallography, Volume C, Kluwer Academic Publishers, Dordrecht, 1992.

CHAPTER FOUR METHYL MAGNESIUM [CH(Ph₂PNSiMe₃)₂]⁻ LIGAND COMPLEXES

4.1 Preparation of $CH_2(Ph_2PNSiMe_3)_2$ (74)

Bis(iminodiphenylphosphorano)methane $CH_2(Ph_2PNSiMe_3)_2$ (74) is readily prepared by oxidation of bis(diphenylphosphino)methane with Me_3SiN_3

(Figure 4.01).[1] Formation of the iminophosphorano group can be identified by the P=N stretch in the IR spectrum in the range of 1238 to 1377 cm^{-1}. There is a shift in the ^{31}P chemical shift from -21.09 ppm for bis(diphenylphosphino)methane to

δ -3.91 ppm for 74 the iminophosphorano ligand. The carbon bridge between the phosphorus group contains two hydrogens, therefore the ligand is neutral as indicated by the triplet observed in the ^{13}C (3π/4 dept) spectrum δ 37.71 ($J^{P-C} = 67.27$ Hz).
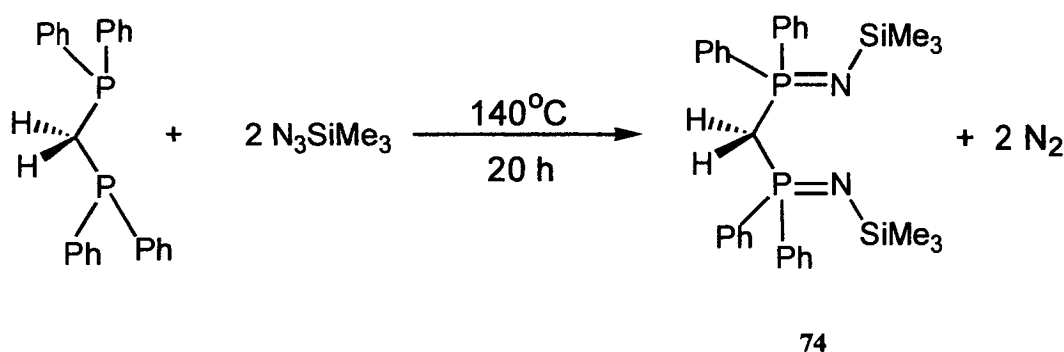

74

Figure 4.01 Preparation of $CH_2(Ph_2PNSiMe_3)_2$ (74)

The protons on the central carbon of 74 are acidic by analogy to the P(III) species $CH_2(PPh_2)_2$ and are easily lost to produce the corresponding mono anionic ligand. The nitrogen atoms provide donors capable of co-ordinating to a metal.

4.2 Complexation Chemistry

There are many bonding modes of bis(iminophosphorano)methanide ligands such as $CH_2(PPh_2=N-Ar)_2$ and the corresponding anions $[HC(PPh_2=NR)_2]^-$ reported in the literature (Figure 4.02).[2-20]
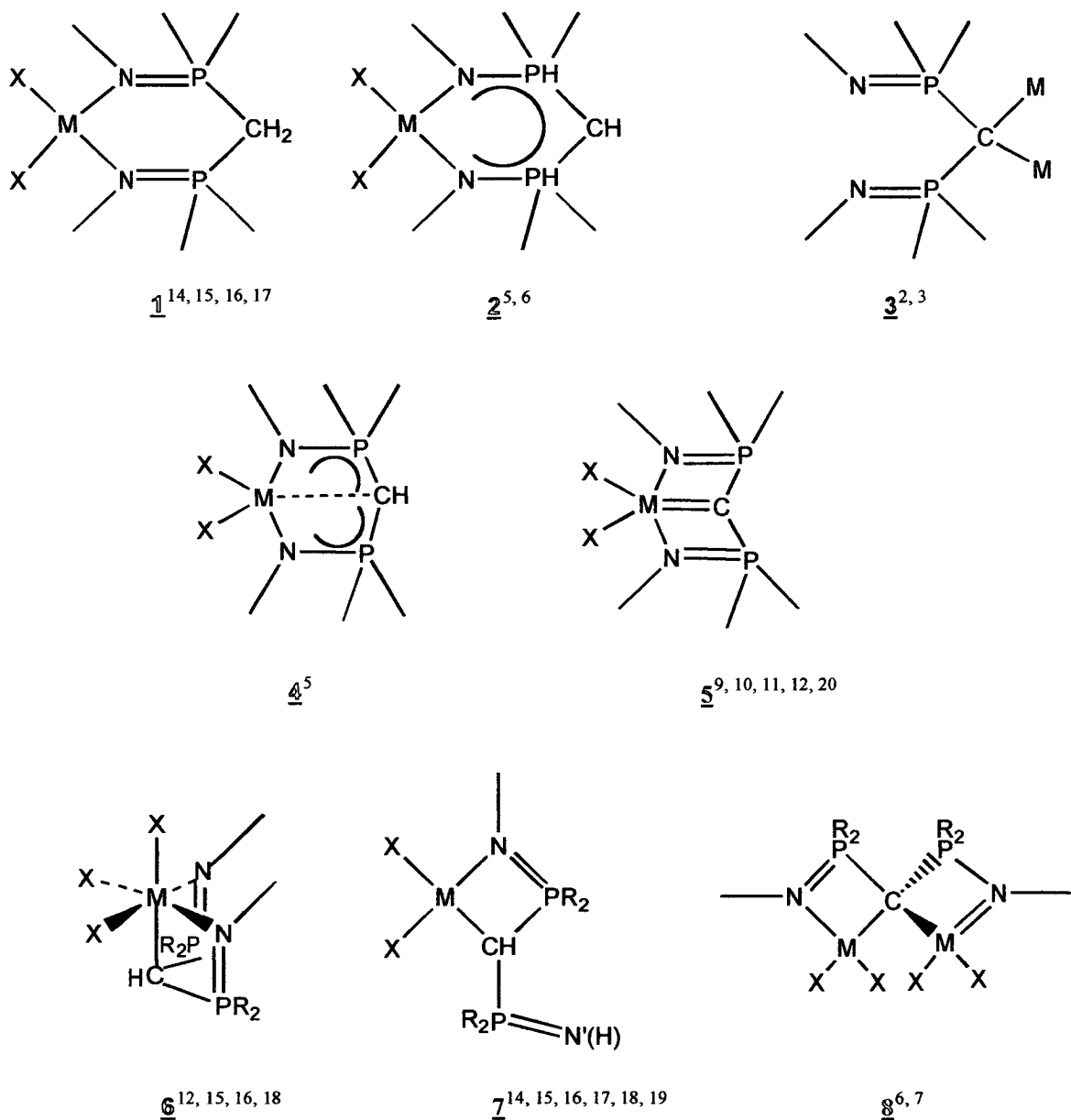

Figure 4.02 Bonding modes of $CH_2(PPh_2=N-Ar)_2$ with MX_2

4.2.1 Alkali and Main Group Metal Complexes

4.2.1.1 Sodium, Lithium and Potassium (Group I) Complexes

The reaction of $CH_2\{Ph_2PN(SiMe_3)\}_2$ (74) with two equivalents of R'Li (where R'=Me, Ph), results in the dilithiation of the central atom of 74 to produce colourless crystals of (9) (Figure 4.03).[2,3] The ^1H NMR spectrum shows the absence of the methylene resonance of the P-CH₂-P backbone. A singlet at 19.1 ppm is observed in the ^{31}P NMR spectrum and no $^{13}C\{^1H\}$ NMR signal was observed. The successful synthesis of the doubly deprotonated dilithiated salt can be attributed to the enhanced acidity of the P-CH₂-P backbone protons in the bisimine system.

Elucidation of the crystal structure of 9 revealed a four metal-centred cage, with the four lithium atoms forming a square plane which is capped at either side by the C atoms of the two P-C-P fragments. The Li₄C₂ fragment is almost perfectly octahedral, but is slightly distorted.

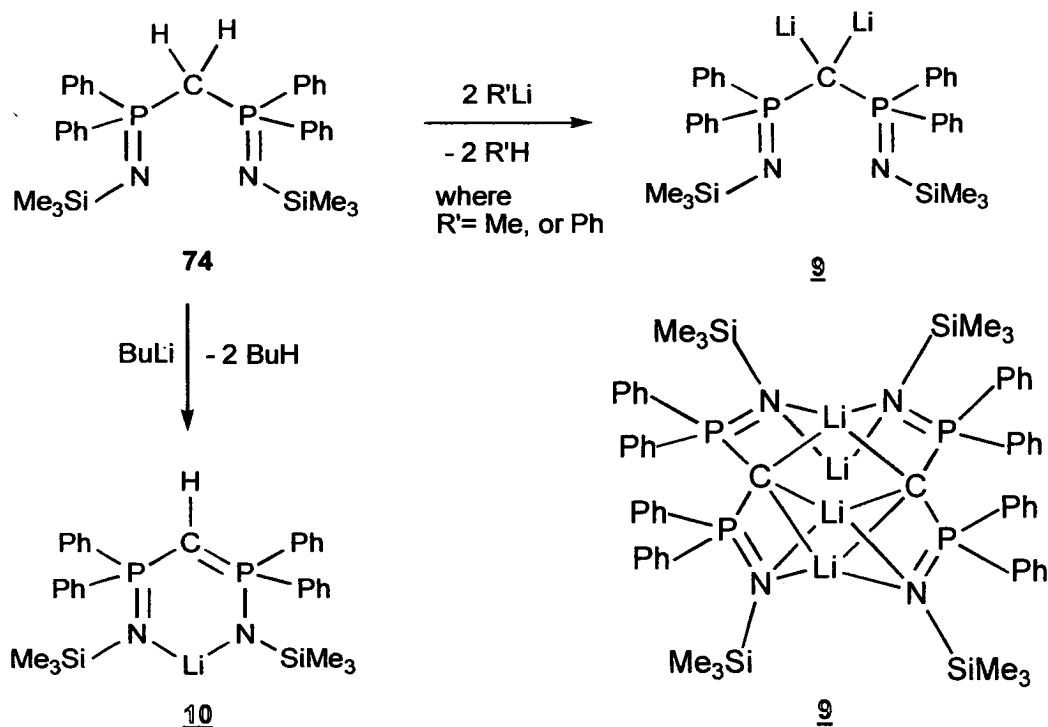
Figure 4.03 The reaction of 74 with R'Li (where R'=Me,Bu or Ph) to produce 9 or 10

The reaction of 74 with one equivalent of BuLi in THF produced Li[CH(Ph₂PNSiMe₃)₂] (10) (Figure 4.03), in which the Li⁺ cation is thought to be

coordinated by the phosphinimine nitrogen. The ^{1}H NMR spectrum contains a triplet at 3.62 ppm and the ^{31}P NMR a singlet at 17.5 ppm. Unfortunately no X-ray quality crystals were obtained.

McDonald et al, reported the preparation of dimeric bis(iminophosphorano) methanide complexes [M{μ_2-κN,κC,κN'-CH(Ph$_2$P=NSiMe$_3$)$_2$}]$_2$, where M= Li (**11**) or Na (**12**), by the reaction of **74** with MN(SiMe$_3$)$_2$ (M=Li or Na) in toluene at room temperature (Figure 4.03).[4] The NMR spectra were very similar for both structures suggesting almost identical, dynamically averaged structures in solution. It was the elucidation of the crystal structures that allowed the differences between the two structures to be determined. The ligand in each dimeric product has been singly deprotonated and has a different mode of coordination to the metal. In complex **11** each lithium atom is four coordinate binding to a nitrogen atom from each ligand and the central carbon atom from each ligand. The Li$_2$C$_2$ core of the structure consists of a twisted four membered ring. In contrast complex **12** consists of sodium atoms that are bridged by nitrogen atoms only, reflecting the chemical difference between Li and Na. The Na$_2$C$_2$ core of the structure consists of a twisted four membered ring, in which the Na atoms are three coordinate.

11   **12**
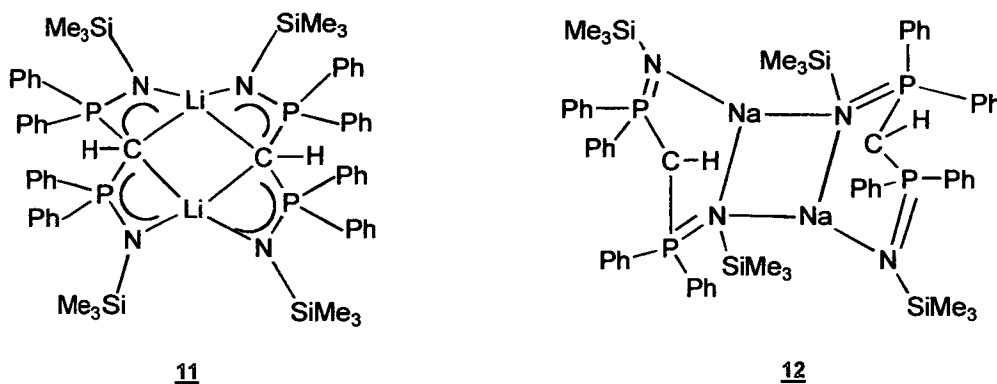
Figure 4.03 Diagram showing the structural formulae of 11 and 12

McDonald et al, reported the preparation of the first solvated monomeric group I complexes of bis(iminophosphorano) methanide ligands.[5] The crystal structure of the first complex [Li{HC(Cy$_2$P=NSiMe$_3$)$_2$-κC,κN,κN'}(OEt$_2$)](**13**), prepared by the reaction of an ether solution of methyl lithium with CH$_2$(Cy$_2$P=NSiMe$_3$)$_2$, shows the lithium atom is four coordinate and significantly binds to the singly deprotonated

carbanionic center. The crystal structures of the sodium and potassium complexes [M{HC(Ph$_2$P=NSiMe$_3$)$_2$-κN,κN'}(THF)$_2$] (M= Na (14), K (15)), prepared by the reaction of CH$_2$(Ph$_2$P=NSiMe$_3$)$_2$ with MH in the presence of THF, also show the metal centre to be four coordinate, but do not show significant metal-carbanion interaction (Figure 4.05). However the potassium complex shows π-acid and agostic interactions with the other parts of the ligand which do not appear in the sodium system. The potassium complex thus has a lower molecular (and crystal) symmetry than the sodium complex. In all cases, structures 13, 14 and 15 show extensive delocalisation within the internal metallacyclic ring structures.

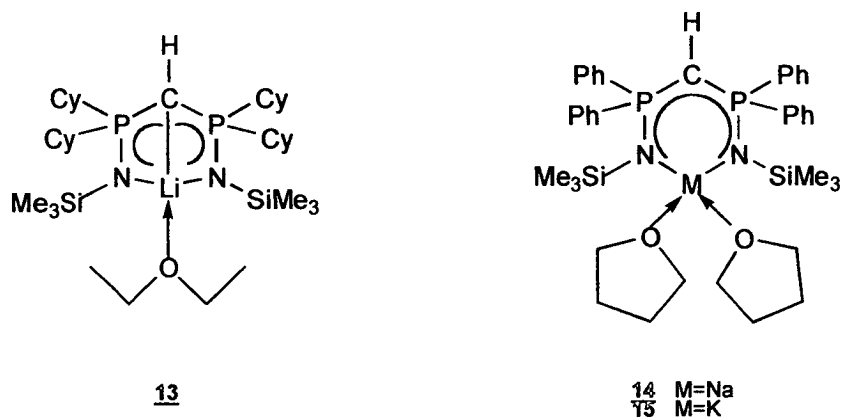**Figure 4.05 Diagram showing the structural formulae of 13, 14 and 15**

4.2.1.2 Aluminium Complexes

McDonald et al, have described the first examples of group 13 bis(iminophosphorano)methide complexes of aluminium.[6] They investigated the reaction of AlMe$_3$ with CH$_2$(Ph$_2$P=NSiMe$_3$)$_2$ (74) in toluene under different reaction conditions. Treatment with one equivalent of AlMe$_3$ at ambient temperature produced the monomer complex [AlMe$_2${HC(Ph$_2$P=NSiMe$_3$)$_2$-κ^{2}N,N'}] (16)

(Figure 4.06). The crystal structure of 16 reveals the core atoms form a 6-membered metallacyclic ring which has a distorted boat conformation. Treatment with two equivalents of AlMe$_3$ at 120°C produced the doubly deprotonated dimer complex [(AlMe$_2$){μ$_2$-C(Ph$_2$P=NSiMe$_3$)$_2$-κ^{4}C,C',N,N'}] (17) in which the ligand has been doubly deprotonated (Figure 4.06). The crystal structure of 17 reveals a dimer containing a doubly deprotonated bimetallic bridging methanidiide ligands with a

novel spirocyclic carbene center. Stepwise synthesis of the mono- and bimetallic methanide and methanediide complexes has also been achieved.

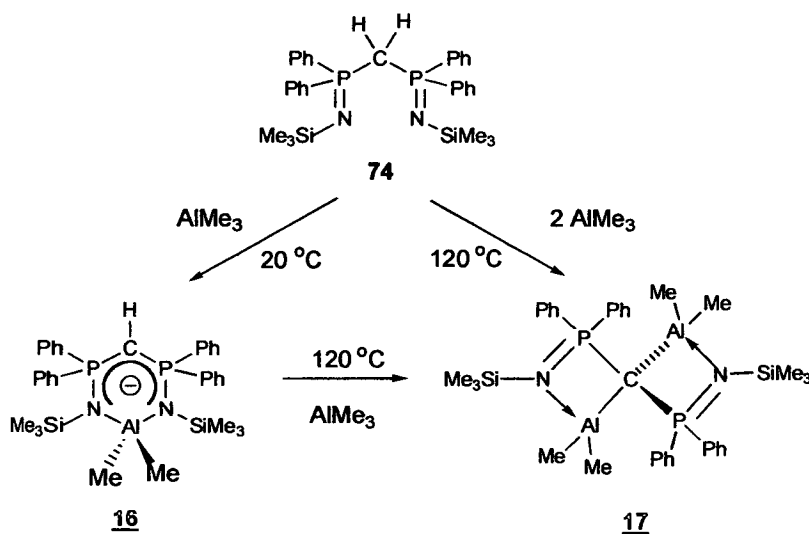**Figure 4.06 Synthesis of 16 and 17**

The bimetallic methandiide complex 17 can insert unsaturated heteroallenes (adamantylisocyanate, or dicyclohexylcarbodiimide), under reflux, to form novel metallobicyclic compounds through a new C=C bond formation reaction *via* cleavage of the two aluminium-carbon bonds by one molecule of a heteroallene (Figure 4.07).[7]
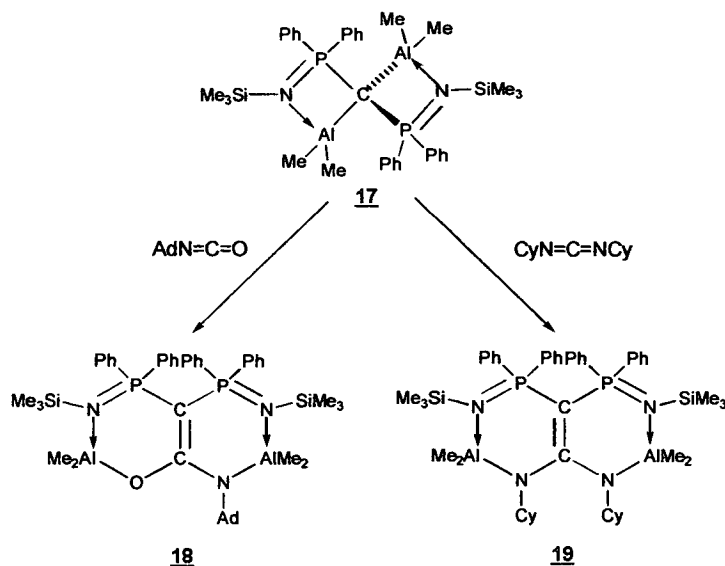

Figure 4.07 Structural formulae of 18 and 19

4.2.2 Transition Metal Complexes

4.2.2.1 Group 12 Metal Complexes

Cavell et al, have reported that the reaction of $CH_2(PPh_2NSiMe_3)_2$ (**74**) with dimethyl zinc, at room temperature in toluene, produces $[ZnMe\{HC(Ph_2P=NSiMe_3)_{2-\kappa}2N,N'\}]$ (**20**) (Figure 4.08), along with the evolution of methane gas.[8]

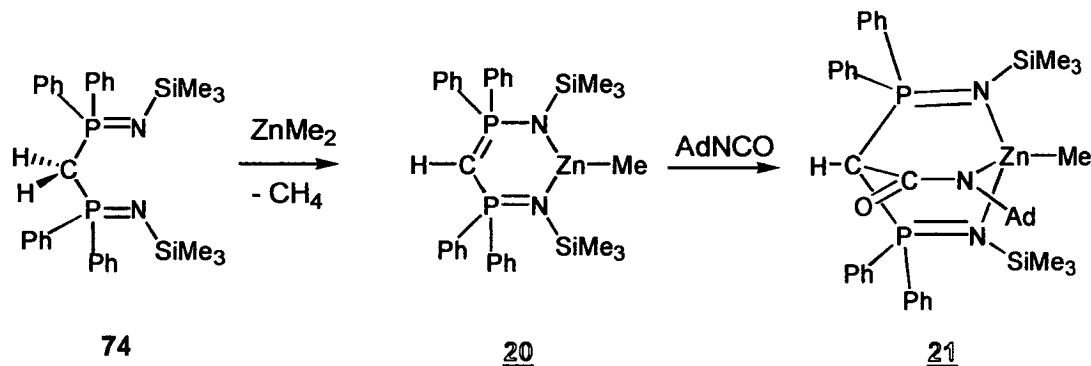

74   **20**   **21**

Figure 4.08 Synthesis of 20 and 21

Complex **20** has been identified by standard spectroscopic techniques and by X-ray structure analysis. In the monomeric complex **20**, the monomethylated zinc is chelated by the monoanionic (iminoamide)phosphorano ligand. The CH group on the ligand was identified by a negative triplet signal in the $^{13}C\{^1H\}$NMR signal at 28.4 ppm, the ^{31}P NMR spectrum contains a singlet at 26.2ppm. The P=N stretch was observed at 1259 and 1244 cm^{-1} in the IR spectrum. In the molecular structure of **20**, the core atoms that make up the six memebered ring are in a distorted boat conformation and the zinc is in a distorted trigonal planar geometry.

Reactions of **20** with adamant nitrile (AdCN) and isonitriles (Ar'NC) were fruitless even under harsh conditions. However, reaction of **20** with adamant isocyanate results in nucleophilic addition of the methanide carbon to the adamant carbon to form a tripodal ligand, giving a four co-ordinated zinc complex, as in $[ZnMe\{HC\{C(O)N(Ad)\}(Ph_2P=NSiMe_3)_{2-\kappa}3N,N',N''\}]$ (**21**). Complex **21** was identified by ^1H, $^{13}C\{^1H\}$, $^{31}P\{^1H\}$, IR, CHN, and by X-ray structure analysis. They suggested that the relative inertness of the methyl group attached to the Zn could be attributed to the steric protection by the bulky $SiMe_3$ and Ad groups provided by the ligand.

4.3 Reaction of CH₂(PPh₂NSi(CH₃)₃)₂ and MgMe₂

Here we describe the first monoanionic bis(iminophosphorano)methane ligand chemistry with group II metals.

4.3.1 Synthesis of [Mg(Me){CH(PPH₂NSIMe₃)₂}(THF)] (75)

The reaction of $CH_2\{PPh_2NSi(Me)_3\}_2$ (**74**) with $MgMe_2$ in THF provides the monomeric solvated complex $[Mg(Me)\{CH(PPh_2NSiMe_3)_2\}(THF)]$ (**75**), following evolution of methane gas resulting from the mono deprotonation of the CH_2 group on the ligand back bone by methyl group from the magnesium centre (Figure 4.09). Removal of the solvent in vacuum produces a white oil, which on cooling in liquid nitrogen produces a fine white powder. Unfortunately **75** could not be isolated in the form of X-Ray quality crystals. The complex has been characterised using standard spectroscopic techniques. The ^{31}P NMR spectrum consists of one sharp singlet at 24.76 ppm, which is shifted to a higher frequency than that in the corresponding free ligand at –3.91 ppm (Figure 4.11). The sharp singlet indicates that each phosphorus environment is equivalent. The ^{13}C $\pi/2$ Dept NMR spectrum revealed a positive triplet signal at 27.45 ppm ($J^{C\text{-}P}$=110.55 Hz) for the bridging CH group coupled to two phosphorus nuclei. A broad ^{1}H signal for the single methine proton in **75** was observed at 1.86 ppm in the ^{1}H NMR spectrum rather than the expected triplet (Figure 4.10).
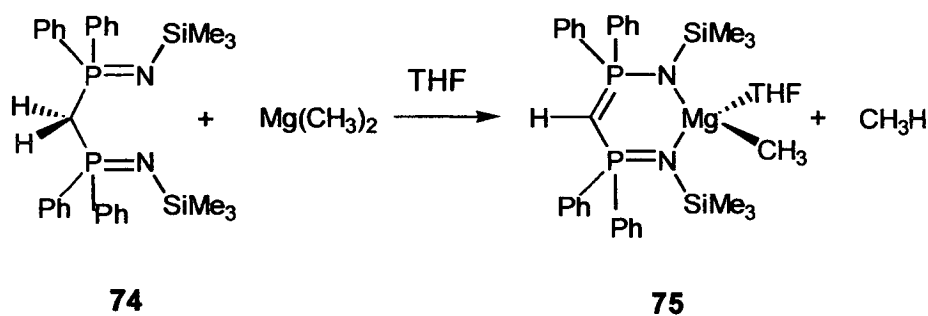

74   **75**
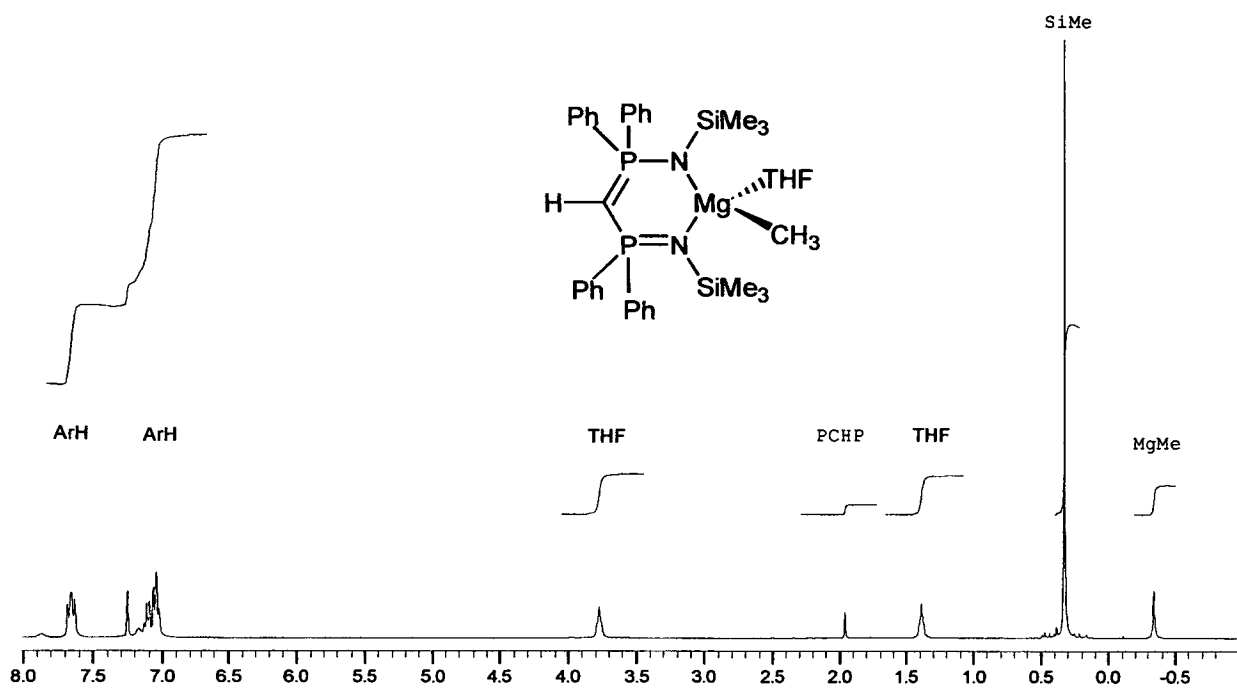
Figure 4.09 Reaction of MgMe₂ and 74 to produce 75

Figure 4.10 ^{1}H NMR spectrum of 75 in C$_6$D$_6$.
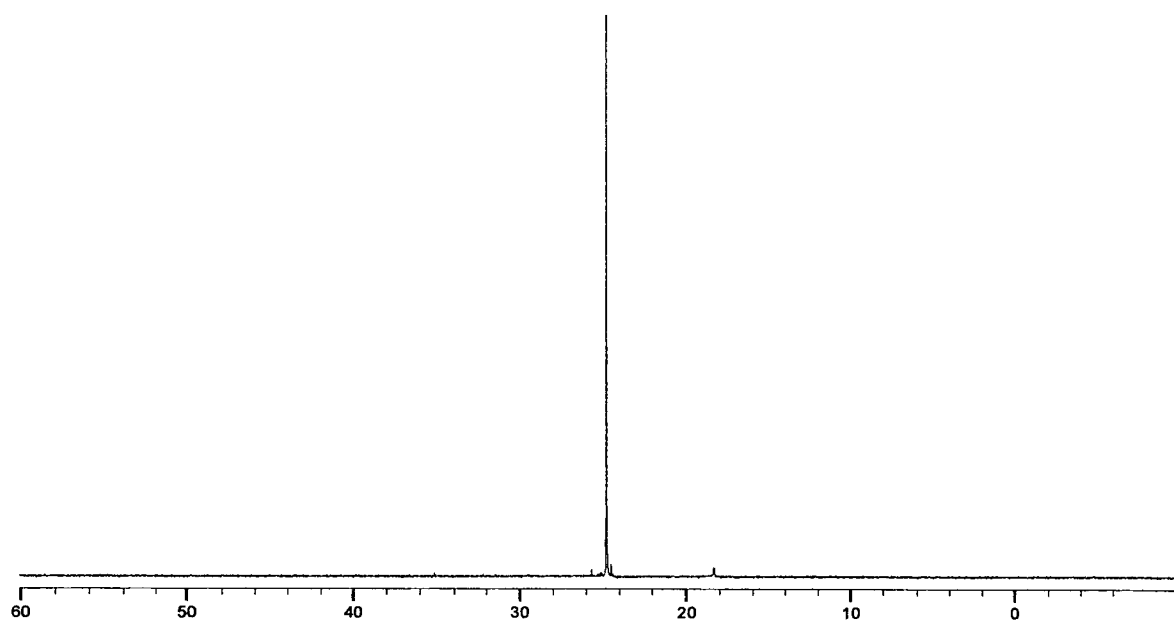
Figure 4.11 ^{31}P{^{1}H} NMR spectrum of 75 in C$_6$D$_6$.

4.3.2 Synthesis of [Mg(μ₂-Me){CH(PPh₂NSiMe₃)₂}]₂ (76)

The coordinated THF may be removed from the solid complex **75** in vacuum at room temperature as indicated by the absence of the THF signals in the NMR spectra of the resulting species, (Figures 4.12 and 4.13). Crystals suitable for X-ray analysis were grown from a concentrated toluene solution over 2 weeks at 5°C (Figure 4.15). The complex has also been characterised using standard spectroscopic techniques.
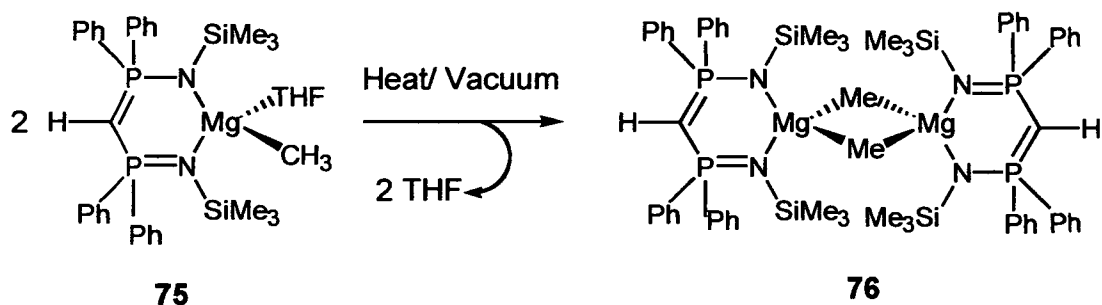
Figure 4.12 Preparation of 76

Complex **76** displays strong absorptions between 1082.8 and 1169.5 cm^{-1}, which are due to the P=N stretching modes. The ^{31}P NMR spectrum consists of one sharp singlet at δ 24.44 ppm, which is shifted to a higher frequency than that in the corresponding free ligand at –3.91 ppm. The sharp singlet indicates that each phosphorus environment is equivalent. The ^{13}C π/2 Dept NMR spectrum revealed a positive triplet signal at 26.90 ppm (J^{C-P}= 99.5 Hz) for the CH group coupled to two phosphorus nuclei. Again a broad ^{1}H signal for the single methine in **76** was observed 1.94 ppm, rather than the expected triplet.
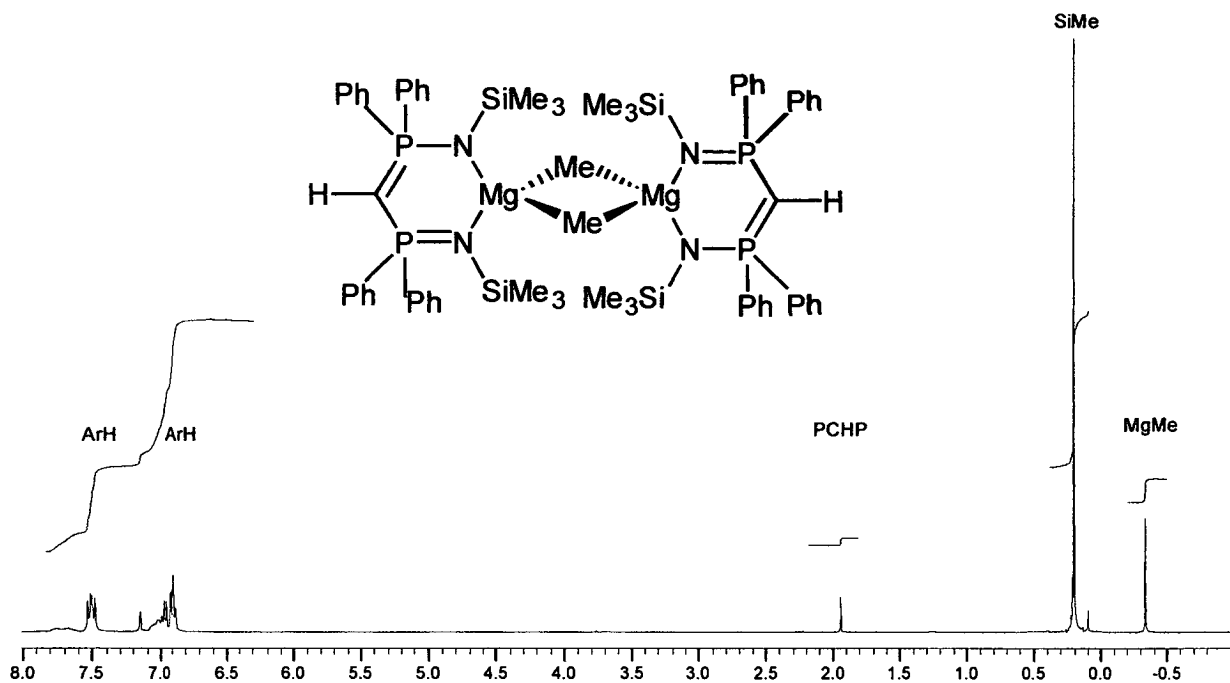
Figure 4.13 ¹H NMR spectrum of 76 in C₆D₆.
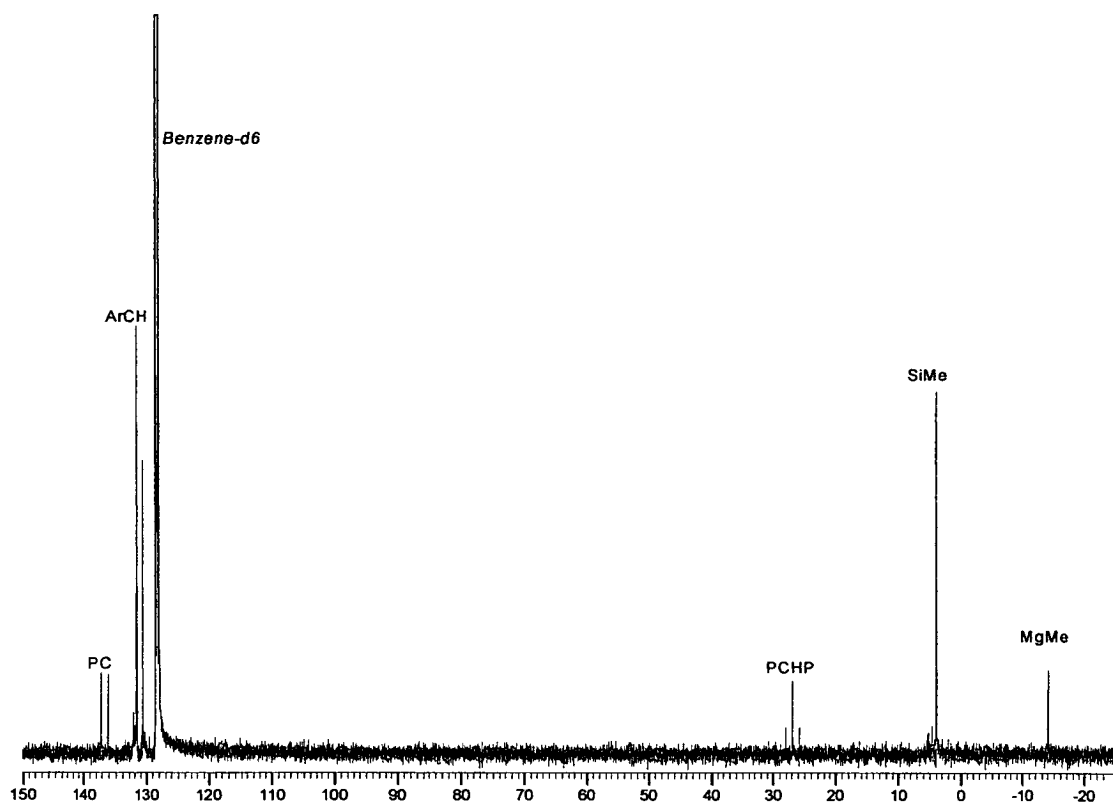
Figure 4.14 ¹³C NMR spectrum of 76 in C₆D₆.

Inspection of the crystal structure reveals that the unsolvated complex is a dimer [Mg(μ$_2$-Me){CH(PPh$_2$NSiMe$_3$)$_2$}]$_2$ (**76**), bridged through the methyl groups. The molecular structure and the labelling scheme for **76** are given in Figure 4.30. The crystal system is monoclinic, and the space group P2$_1$/c. The R$_1$ factor is 6.32% with [6018 data]. The dimer contains no disorder. The core structure, is similar to that reported for [AlMe$_2${HC(PPh$_2$NSiMe$_3$)$_2$}](16) and [ZnMe{HC(Ph$_2$P=NSiMe$_3$)$_2$- $_κ$2N,N'}](20) consisting of a six membered ring with Mg(1), N(1),P(1), C(13), P(2), N(2) atoms which are puckered into a distorted boat conformation.[5,8] The magnesium atoms are four coordinate, with a distorted tetrahedral geometry {N(1)-Mg(1)-N(2) = 101.62 (10) °, N(1)-Mg(1)-C(32) = 116.97(11)°, N(2)-Mg(1)-C(32) = 127.16 (11)°, C(13)-Mg(1)-C(32A) = 83.90 (11)°}.
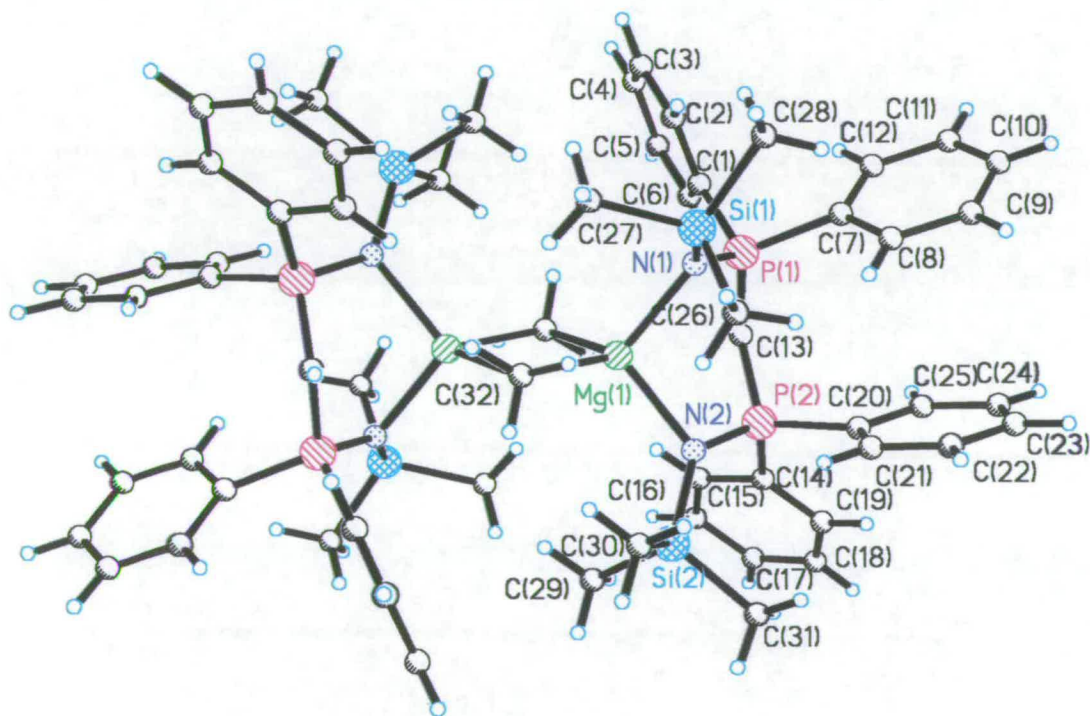
Figure 4.15 Molecular structure of 76 showing the atom-labeling scheme

Selected bond lengths and angles are given in Table 4.01. Only half of the complex has been solved, i.e. the [MgMe{HC(PPh$_2$NSiMe$_3$)$_2$}] fragment is used to symmetry generate the other half of the dimer *via* a C$_2$ axis which lies

perpendicular to the Mg(1)-C(32) plane and parallel to N(1) and N(2) . The bond distances within the ligand frame work in complex **76** differ on comparison to with the related values in the free ligand.[21] The P=N distances are lengthened and therefore the bonds are weakend, reinforcing the lower energy of the ν(P=N) modes observed in the IR spectrum compared with the free ligand, whereas the endocyclic P-C bond distances are shorter. The P-C-P bond angle is decreased slightly 124.15 (17)° compared with 124.94 (15)° in the free ligand. All combined these observations suggest there is a delocalisation of π electron density within the metallocyclic ring system.

	76	74
Mg(1)-C(32)	1.989 (3)	-
Mg(1)-N(1)	2.143 (3)	-
Mg(1)-N(2)	2.099 (3)	-
N(1)-P(1)	1.594 (3)	1.536 (2)
N(2)-P(2)	1.597 (2)	1.536 (2)
P(1)-C(13)	1.723 (3)	1.825 (1)
P(2)-C(13)	1.726 (3)	1.825 (1)
N(1)-Mg(1)-N(2)	101.62 (10)	-
N(1)-Mg(1)-C(32)	116.97 (11)	-
N(2)-Mg(1)-C(32)	127.16 (11)	-
P(1)-C(13)-P(2)	124.15 (17)	124.94 (15)
Mg(1)-N(1)-P(1)	99.61 (12)	-
N(1)-P(1)-C(13)	108.98 (14)	113.42 (9)
N(2)-P(2)-C(13)	111.06 (13)	113.42 (9)
Mg(1)-N(2)-P(2)	101.99 (12)	-

Table 4.01 Selected bond lengths (Å) and angles (°) for 74 and 76

The main interest in preparing the bis(iminophosphorano)methanide methyl magnesium complexes **75** and **76** is to investigate their effectiveness as ethene polymerisation catalysts. Originally we had assumed we would form a magnesium alkyl complex similar to [ZnMe{HC(Ph$_2$P=NSiMe$_3$)$_{2-\kappa^2}$N,N'}], a three coordinate monomer. However, the formation of the dimer is now not so surprising given the tropiminato, β-diketiminate and α-diimine work already reported in chapters 1 and 3. On inspection of the molecular surfaces of **76**, calculated from the crystal structure in ISIS, it is apparent that there is no access for an ethene molecule to react with either of the magnesium centres. Rear side attack of the magnesium from underneath the boat is not favoured, as the approach of the ethene would be hindered by the two phenyl rings, one on each phosphorus atom. The magnesium centres themselves are protected above and below by a combination of the SiMe$_3$ groups and the phenyl groups on the phosphorus atoms that have been pushed forward. The bridging methyl groups add to the inaccessibility of the complex. Figure 4.16 displays the molecular surface of **76** with different orientations.
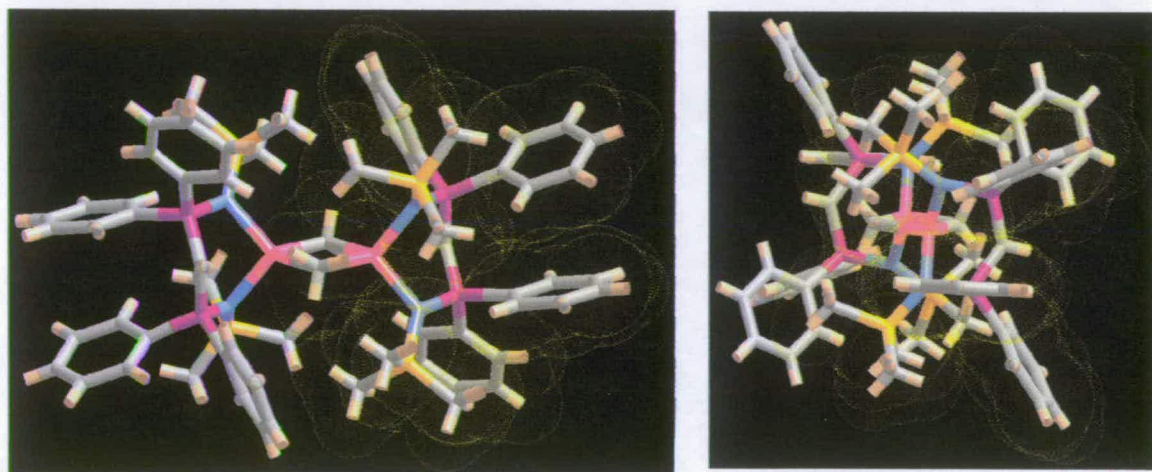

Figure 4.16 Diagrams displaying the molecular structure and surfaces of 76 at different orientations

4.4 Experimental

4.4.1 General Procedures

All the air/moisture sensitive experimental work was performed under N_2 using standard Schlenk techniques on a vacuum line under dry, oxygen free, nitrogen. Some experimental work and characterisations were carried out in a nitrogen filled glove box (Saffron), fitted with oxygen and water scavenging columns. All solvents were dried and deoxygenated before use.

Solvents and reagents where commercially avaiable were bought from Aldrich, Acros or Fischer. With exception of NMR solvents which were purchased from Goss Scientific.Diethyl ether, toluene, hexane, benzene, and THF were all distilled from Na/benzophenone under a nitrogen atmosphere. The NMR solvents were degassed using three freeze-pump-thaw cycles and stored over 4Å molecular sieves.

4.4.2 Instrumentation

Elemental analyses were performed by sealing aluminium capsules containing approx. 1mg of compound under nitrogen in the glove box, and determined using a Perkin Elmer 2400 CHN Analyser. NMR were recorded on a Gemini 200MHz, Bruker 200Mhz, Bruker 250MHz spectometers. IR spectra were obtained on a Perkin Elmer Paragon 1000 FT-IR spectometer as potassium bromide discs or as liquid thin films. . Electron impact (EI) mass spectra were obtained either on a Finnigan MAT 4600 quadrapole spectrometer or on a Kratos MS50TC spectrometer.

$CH_2(PPh_2NSiMe_3)_2$ (74)[1,21]

Bis(diphenylphospino)methanide (4.999 g, 21.72 mmoles) was weighed into a Schlenk tube under N_2, azidotrimethylsilane (15 cm^3, 117.27 mmoles) was added by syringe in the glovebox. The reaction mixture was then heated to reflux under nitrogen at 140°C for 20 hours. The reaction mixture was cooled to 100°C where the excess azide was trapped in vacuum. On cooling to room temperature a white solid formed which was recrystallised from acetonitrile. The product was collected washed with hexane and dried in vacuum (4.111 g, 33%). ^{1}**H NMR** (360.13 MHz, C_6D_6): δ 0.25 (s,18H, Si(CH_3)$_3$), 3.27 (t, J^{P-H}= 13.88 Hz, 2H, PCH_2P), 7.02 (m, 12H, Ar-H), 7.67 (m, 8H, Ar-H). ^{13}**C NMR** (90.55 MHz, C_6D_6): δ 4.31(s, Si(CH_3)$_3$),

37.71 (t, J^{P-C}= 67.27 Hz, CH_2), 128.11 (s, *CH*), 130.61 (s, *CH*), 131.72 (s, *CH*), 136.66 (d, $J^{P-C=}$101.39Hz,) . **^{31}P NMR** (145 MHz, C_6D_6): δ -3.91(s, *P*Ph$_2$).

IR (Nujol mull, cm^{-1}): 1460.1 (s), 1376.3 (s), 1238.7 (s), 1173.1 (s), 1113.4 (s), 1069.4 (s), 1028.1 (s), 997.3 (s), 876.9 (s), 864.8 (s), 846.3 (s), 828.4 (s), 746. 0 (s), 93.5 (s), 650.1 (s), 617.4 (s0, 578.5 (s).

[{CH(PPh₂NSi(CH₃)₃)₂}Mg(CH₃)(THF)](75)

$CH_2(PPh_2NSiMe_3)_2$ (6.149 g, 15.2 mmoles) and $MgMe_2$ (0.830 g, 15.3 mmoles) were weighed together. With stirring THF was added and a pale yellow solution was obtained. The reaction mixture was allowed to stir overnight at room temperature. The solvent was removed in vacuum to produce a fine white powder with stirring. The powder was washed with hexane (150 cm^3) and dried in vacuum to yield a pinky/white powder (4.912 g, 47%). **^{1}H NMR** (360.13 MHz, C_6D_6):

δ -0.45 (s, 3H, (CH_3)Mg);. 0.22 (s, 18H, (CH_3)$_3$Si), 1.29 (br, 4H, (THF)), 1.86 (br, 1H, (*CH*)P); 3.67(br, 4H, THF); 6.94 (t, 8H, *J*=6.88 Hz, ArH); 7.00 (d, 4H, *J* = 7.18 Hz, ArH), 7.55 (t, 8H, *J* = 11.68 Hz, ArH).

^{13}C NMR (90.55 MHz, C_6D_6): δ -11.56 (s, Mg*CH*$_3$); δ 4.19 (s, (CH_3)$_3$Si), 27.45 (t, J^{C-P}= 110.55 Hz, (*CH*)P); 128.17 (s, Ar*CH*); 130.36 (s, Ar*CH*); 131.78(s, Ar*CH*); 137.78 (d, C, J^{C-P}= 97.5 Hz); P*CAr*).

^{31}P NMR (145 MHz, C_6D_6): 24.76 (s, *P*Ph$_2$).

IR (Nujol mull, cm^{-1}): 1455.9 (s), 1374.8 (s), 1302.3 (s), 1240.0 (s), 1169.6 (s), 1153.8 (s), 112.4 (s), 1069.2 (s), 1028.0 (s), 998.8 (s), 967.2 (s), 918.5 (s), 889.3 (s), 864.1 (s), 828.9 (s), 772.4 (s), 740.4 (s), 724.2 (s), 693.5 (s), 653.8 (s), 636.2 (s), 616.5 (s).

[Mg(μ₂-Me){CH(PPh₂NSiMe₃)₂}]₂ (76)

$CH_2(PPh_2NSiMe_3)_2$ (4.000 g, 7.00 mmoles) was dissolved in THF (20 cm^3), and 2M $MgMe_2$ in THF (3.50 cm^3, 7.00 mmoles) added drop wise via syringe at room temperature. A gas evolved, and a yellow solution produced. The reaction mixture was allowed to stir for 1hour. The solvent was removed to produce a white oil, on further vacuum the oil became "foam" like. Once cooled in liquid nitrogen a fine white powder was produced. The product was extracted into toluene (30 cm^3), and

the filtrate collected and concentrated to ~5cm^3 in vacuum, the product started to precipitate at this point and the solution was gently warmed until the solid dissolved. Crystals were obtained from placing the concentrated filtrate at 5°C for 2 weeks. Colourless needles were obtained (2.315 g, 55.3 %). **CHN:** Found C (1) 64.43, (2) 63.49 , H (1) 5.38, (2) 6.20, N (1)4.73, (2) 4.89; $C_{64}H_{84}N_4P_4Si_4Mg_2$ requires

C 64.37, H 7.09, N 4.69. **^{1}H NMR** (360.13 MHz, C_7D_8): δ -0.52 (s (br), 3H, (C*H₃*)Mg);. 0.12 (s (br), 18H, (C*H₃*)₃Si), 1.88 (br, 1H, (C*H*)P); 6.8-7.05 (m, 12H, ArH); 7.41-7.66 (m, 8H, ArH). **^{1}H NMR** (360.13 MHz, C_6D_6):

δ -0.34 (s (br), 3H, (C*H₃*)Mg);. 0.19 (s (br), 18H, (C*H₃*)₃Si), 1.94 (br, 1H, (C*H*)P); 6.89 (td, 8H, Ar*H*); 6.91 (dt, 6H, Ar*H*); 7.47 (td, 8H, Ar*H*).

^{13}C NMR (90.55 MHz, C_7D_8): δ -14.05 (s, Mg*C*H₃); 3.89 (s, (CH₃)₃Si), 26.90 (t, J^{C-P}= 99.93 Hz, (CH)P); 128.28 (s, Ar*C*H); 130.65 (s, Ar*C*H); 131.73 (s, Ar*C*H); 136.39 (d, J^{C-P}=93.0 Hz, P*C*Ar);**^{13}C NMR** (90.55 MHz, C_6D_6):

δ -14.05 (s, Mg*C*H₃); 3.86(s, (CH₃)₃Si), 26.89 (t, J^{C-P}= 99.3Hz, (CH)P); 130.10 (s, *C*H); 137.13 (s, *C*); **^{13}C{^{1}H} NMR** (90.55 MHz, C_6D_6):

δ 26.90 (t, J^{C-P}= 99.5Hz, (*C*H)P); 128.28 (s, *C*H); 130.27 (s, *C*H),131.73 (s, *C*H).

^{31}P NMR (145.78 MHz, C_7D_8): δ 24.44(s);

^{31}P NMR (145.78 MHz, C_6D_6): δ 24.49 (s, *P*Ph₂).

Crystal Data for 76

Data was collected on a SMART diffractometer using a colourless rod of dimensions 0.22 x 0.08 x 0.08 mm using π and ω scans in the range of 4< θ < 53°. Of a total of 21877 reflections collected, 7833 (R_{int} = 0.0391) were independent. The full difference map extrema were 1.119 and –0.708 eÅ^{-3} with a final R of 6.32% for 441 parameters.

Empirical formula	$C_{78}H_{100}Mg_2N_4P_4Si_4$ $[MgMeL]_2.2(C_7H_8)$	$\gamma / °$	90
Formula weight	1378.48	Volume / $Å^3$	3841.3(5)
Crystal system	Monoclinic	Z	2
Space group	$P2_1/c$	Temperature / K	150(2)
a / Å	11.7224(9)	Wavelength / Å	0.71073
b / Å	18.5190(14)	Density calc. / Mg/m^3	1.192
c / Å	18.0199(13)	μ(Mo-Kα) / mm^{-1}	0.221
α / °	90	$R_1[F>4\sigma(F)]$	0.0632
β / °	100.9000(10)	wR_2 (all data)	0.1671

4.5 References

1 Stephan, D.W; *J.Am.Chem.Soc.* **1999**, *121*, 2939-2940.

2 Ong, C.M; Stephan, D.W; *J.Am.Chem.Soc.* **1999**, *121*, 2939-2940.

3 Kasani, A.; Aparna, K; Kamalesh Babu, R.P.; McDonald, R.; Cavell, R.G.; *Angew.Chem.Int.Ed.*, **1999**, *38*, 10, 1483-1484.

4 Kamalesh Babu, R.P.; Aparna, K; McDonald, R.; Cavell, R.G.; *Inorg.Chem.* **2000**, *39*, 4981-4984.

5 Kamalesh Babu, R.P.; Aparna, K; McDonald, R.; Cavell, R.G.; *Organomet.* **2001**, *20*, 1451-1455.

6 Aparna, K.; McDonald, R.; Ferguson, M.; Cavell, R.G.; *Organomet.* **1999**, *18*, 421-423.

7 Aparna, K; McDonald, R.; Cavell, R.G.; *J.Am.Chem.Soc.* **2000**, *122*, 9314-9315.

8 Aparna, K; McDonald, R.; Cavell, R.G.; *Organomet.* **1999**, *18*, 3775-3777.

9 Kamalesh Babu, R.P.; McDonald, R.; Cavell, R.G.; *Chem.Comm.*, **2000**, 481-482.

10 Kamalesh Babu, R.P.; McDonald, R.; Decker, S.A.; Klobukowski, M.; Cavell, R.G.; *Organomet.* **1999**, *18*, 4226-4229.

11 Cavell, R.G.; Kamalesh Babu, R.P.; Aparna, K; McDonald, R.; *J.Am.Chem.Soc.* **1999**, *121*, 5805-5806.

12 Kamalesh Babu, R.P.; McDonald, R.; Cavell, R.G.; *Organomet.* **2000**, *19*, 3462-3465.

13 Aparna, K; McDonald, R.; Cavell, R.G.; *Chem.Comm.* **1999**, 1993-1994.

14 Imhoff, P.; Elsevier., C.J.; *J.Organomet.*Chem. **1989**, *361*, C61-C65.

15 Imhoff, P.; Van Asslet, R.; Elsevier, C.J.; Zoutberg, M.C.; Stam, C.H.; *Inorg.Chim.Acta*, **1991**, *184*, 73-87.

16 Imhoff, P.; Gulpen, J.H.; Vrieze,K.; Smeets, W.J.J.; Speck, A.L.; Elsevier, C.J.; *Inorg.Chim.Acta*, **1995**, *235*, 77-88.

17 Avis, M.W.; Vrieze, K.; Kooijman, H.; Veldman, N.; Spek, A.L.; Elsevier, C.J.; *Inorg.Chem.* **1995**, *34*, 4092-4105.

18 Avis, M.W.; Vrieze, K.; Ernsting, J.M.; Elsevier, C.J.; *Organomet.* **1996**, *15*, 2376-2392.

19 Avis, M.W.; Van der Boom, M.E.; Elsevier, C.J.; Smeets, W.J.J.; Spek, A.L.; *J.Organomet.*Chem. **1997**, *527*, 263-276.

20 Aparna, K.; McDonald, R.; Ferguson, M.; Cavell, R.G.; *J.Chem.*Soc., **2000**, *122*, 726-727.

21 Muller, A.; Mohlen, M.; Neumuller, B.; Faza, N.; Massa, W.; Dehnicke, K.; *Z.Anorg.Allg.Chem.*; **1999**, *625*, 1748-1751.

CHAPTER FIVE ETHENE POLYMERISATION TESTING

This chapter will discuss the polymerisation testing of several compounds prepared by myself, or colleagues as mentioned in earlier chapters. The potential catalysts were activated where required, and in some cases treated with a co-catalyst such as trimethyl aluminium (TMA) or triisobutyl aluminium (TIBA). The ethene polymerisation testing was carried out at either 30 cm^3/ 6 bar or 400 cm^3/ 30 bar. The reactions is observed for the formation of polymer (solid) and is quenched with Methanol. A sample is taken from the reaction mixture and analysed by GCMS to determine whether oligomers have been produced. The solvent is then removed from the reaction mixture by rotary evaporation and the mass of solids determined, to determine if a small amount of polymer invisible to the eye has been produced. The solids are analysed by ^{1}H NMR to determine the presence of any –(CH$_2$)$_2$- or –(CH=CH)- groups.

5.1 General Testing Methods
5.1.1 30 cm^3 Scale Studies

Each reaction was carried out in a Buchi mini autoclave using the following reaction profile:

1) The autoclave was heated to 100 °C in an oven overnight, and placed in the glove box under vacuum to ensure it was dry.

2) The complex of interest was weighed into a sample vial in the glove box.

3) Dry toulene (20 cm^3) was added and the solution stirred for 5-10 mins. The solution was transferred, by washing with additional toluene (10 cm^3), to the autoclave.

4) The autoclave was charged to 6 bar with C$_2$H$_4$ and the solution stirred at room temperature for 30 mins.

5) The complex solution was then heated at 50°C /6 bar for 1h, and then 70°C/6 bar for 1h.

6) The vessels contents were then allowed to cool to room temperature. MeOH was added to quench any reactive species. The following analyses were recorded: NMR, GC and GC/MS. The solvent was removed by rotary evaporation (60°C/70 mBar/1h) and the residue analysed by NMR.
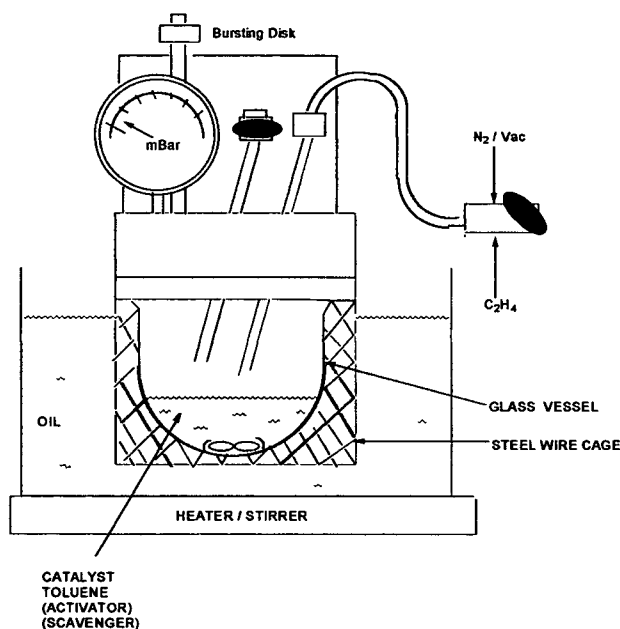
Figure 5.01 Schematic of a Buchi mini autoclave

5.1.2 400 cm^3 Scale Studies (Work by Klaas Von Hebel)

1) A 1 L reactor equipped with turbine stirrer and a steam/water temperature control was heated to 150°C overnight, whilst purging with Nitrogen.

2) The reactor was cooled and then "pickled" at 70 °C using a mixture of TIBA (0.25g) and toluene (200g). The "pickle" mixture was removed and the reactor was charged with a solution of the complex of interest, in dry toluene (10 cm^3) (sometimes containing 1-1.5 mmol of TIBA, depending on reaction).

3) Subsequently toluene (400 cm^3) was added, stirring was started (600 rpm), and the reactor pressurised with ethene (3 bar).

4) The temperature was increased from 25 to 80°C in 5mins, and the ethene pressure was increased to 30 bar.

5) The polymerisation was continued for 105 mins, after which the solution removed from the reactor and analysed for GC-MS.

5.2 Results

A variety of compounds were tested, on both or either the 30 cm³ or 400 cm³ scale (Figure 5.02). The ethene polymerisation/oligomerisation activities of both neutral and charged complexes were investigated. The results of the tests are summarised in Tables 5.01 and 5.02.
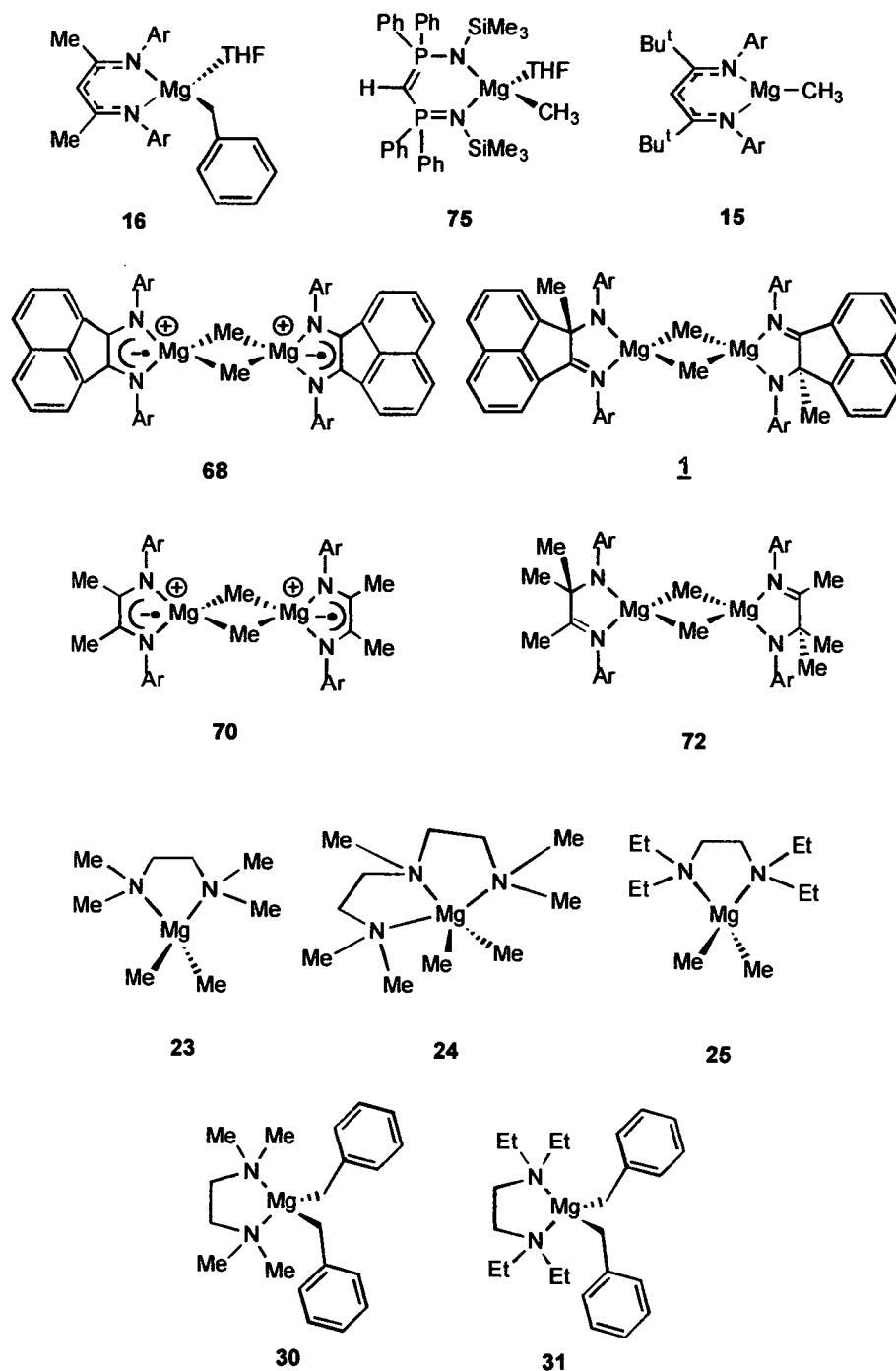

Figure 5.02 Molecular structures of 1,15-16, 23-25, 30-31, 68,70, 72 & 75.

As mentioned in Chapter 3 reaction of α-diimines with magnesium alkyls produce complex reaction mixtures, from which the individual products are difficult to isolate. Therefore, the ethene polymerisation activity of some product mixtures were examined in experiments 4, 5, 22 and 23 (Tables 5.01 and 5.02). However, because **72** could be isolated in crystalline form, in good yield, it was tested in its pure form at 70°C/ 6 bar.

5.3 Discussion

Clearly there is no evidence of either oligomerisation or polymerisation activity of the complexes tested. There is an observed increase in the solids weight (on removal of the solvent), in the final reaction mixture in comparison to the solids originally added in reactions 1-3, 5-6, and 9-10. However, analysis of the solid does not suggest that polymer has been produced.

Comparison of the space-filling models of an active aluminium complex [(Amidinate)AlR]⁺ **2** and the most promising neutral magnesium complex [MgMe{HC[C('Bu)NAr']₂}](**15**) (Ar'=2,6-Diisopropylphenyl) reveals the inactivity of (**15**) can be accounted for by the inaccessibility of the magnesium centre to ethene (Figure 5.03).
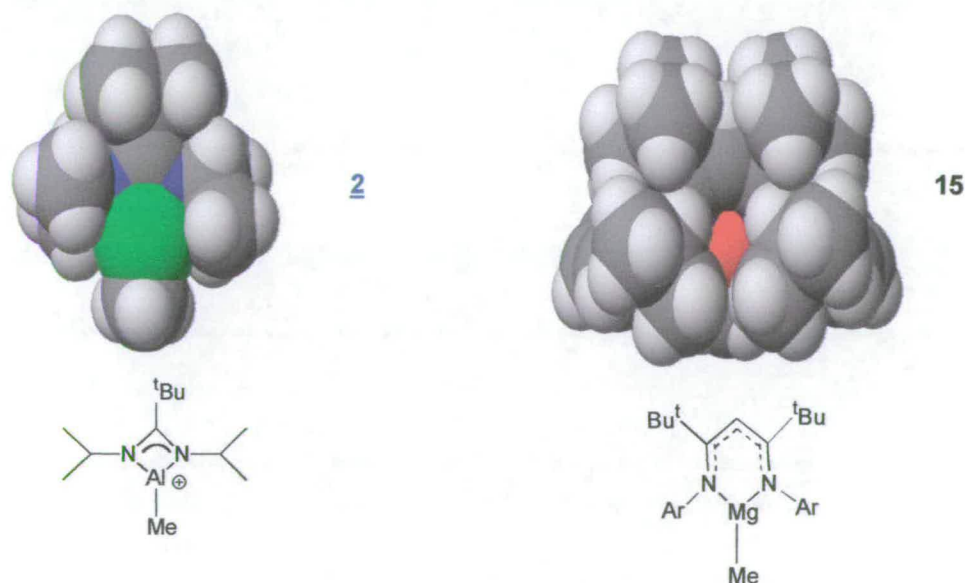

Figure 5.03 Space-filling models of 2 and 15.

Reaction Number	Complex	AMNT μmol	AMNT mg	TIBA mmol	[NHMe$_2$Ph][B(C$_6$F$_5$)$_4$] μmol	[CPh$_3$][B(C$_6$F$_5$)$_4$] μmol	B(C$_6$F$_5$)$_3$ μmol	Polymer Test	GC/MS	Solids g	Solids ^{1}H-NMR
1	16.(toluene)	55	38	0	0	0	0	No polymer	No oligomer	0.223	Ligand
2	75	43.6	30	0	0	0	0	No polymer	No oligomer	0.242	Ligand
3	15	57	30	0	0	0	0	No polymer	No oligomer	0.199	Ligand
4	70 & 72	-	49	0	0	0	0	No polymer	No oligomer	0.025	Ligand
5	68 + A	-	62	0	0	0	0	No polymer	No oligomer	0.671	Ligand
6	72	41	38	0	0	0	0	No polymer	No oligomer	0.048	Ligand
7	25	97	22	0	126	0	0	No polymer	No oligomer	Not Done	Not Done
8	25	158	36	0	0	120	0	No polymer	No oligomer	Not Done	Not Done
9	30	124	40	0	124	0	0	No polymer	No oligomer	0.078	Ligand
10	31	124	47	0	124	0	0	No polymer	No oligomer	0.086	Ligand

Table 5.01 Ethene polymerisation trials of several complexes in the presence of 30 cm^3 toluene at 6 bar of ethene at 70°C

Reaction Number	Complex	AMNT μmol	AMNT mg	TIBA mmol	[NHMe₂Ph][B(C₆F₅)₄] μmol	[CPh₃][B(C₆F₅)₄] μmol	B(C₆F₅)₃ μmol	Polymer Test	GC/MS	Solids g	Solids H-NMR
11	**75**	226	151	0	0	0	0	No polymer	No oligomer	Not Done	Not Done
12	**75**	222	149	1	0	0	0	No polymer	Not Done	Not Done	Not Done
13	**15**	281	152	0	0	0	0	No polymer	Not Done	0.52	Ligand
14	**15**	277	150	1.5	0	0	0	No polymer	No oligomer	0.52	Ligand
15	**16**	217	152	0	0	0	0	No polymer	No oligomer	Not Done	Not Done
16	**24**	131	30	0	138	0	0	No polymer	No oligomer	0.1	Ligand
17	**24**	138	32	0.7	138	0	0	No polymer	Not Done	Not Done	Not Done
18	**24**	141	32	0	0	0	63	No polymer	Not Done	Not Done	Not Done
19	**24**	141	32	0.7	0	0	63	No polymer	Not Done	0.19	Ligand
20	**23**	135	23	0.5	135	0	0	No polymer	No oligomer	0.2	Ligand
21	**23**	135	23	0	135	0	0	No polymer	Not Done	Not Done	Not Done
22	**68 + A**	278	300	0	0	0	0	No polymer	Not Done	Not Done	Not Done
23	**68 + A**	278	300	1.46	0	0	0	No polymer	No oligomer	Not Done	Not Done

Table 5.02 Ethene polymerisation trials of several complexes in the presence of 400 cm³ toluene at 30 bar of ethene at 80°C

It is unfortunate that the catalyst systems prepared and studied in this thesis are inactive to ethene polymerisation but there is evidence as to why each may be inactive in it own right.

The amine based magnesium alkyl systems are far too unstable once activated by boron pentaflurophenyl compounds, and are readily deactivated by C_6F_5 transfer. The diimine based magnesium alkyl systems produce a complex mixture of products that are difficult to isolate from one another. The diimine ligands do not contain sufficient bulk to prevent dimerisation, which in itself will hinder the attack of ethene. In addition, the carbon attoms on the backbone of the ligand are prone to alkylation, rendering the molecule neutral and less attractive to attack by a nucleophile.

The phosphinoimino based magnesium alkyl systems produced are neutral, due to the reduction of the ligand on complexation with $MgMe_2$ and the production of methane gas. The THF adduct **75** was proven to be inactive to ethene. The solvent free neutral dimeric complex **76** although not tested is not expected to be reactive to ethene either. Inspection of the space filling model reveals that the magnesium centre is encapsulated in such a way that an ethene molecule will not be able to approach significantly near the magnesium centre to be able to react.

Although these classes of compounds have been unsuccessful with respect to ethene polymerisation, it does not mean that there are not other possible magnesium based compounds out there that could be active. With the knowledge we have generated through the group (myself, Dr Fabre, Mr Herber and Dr Liddle) a colleague has directed his work to produce a molecule that is self activating through internal charge transfer (Figure 5.04). The compound will avoid activation via boron/pentaflurophenyl based activators and should produce a salt species, in which the magnesium centre is positively charged and stabilised by internal charge separation and resonance effects.
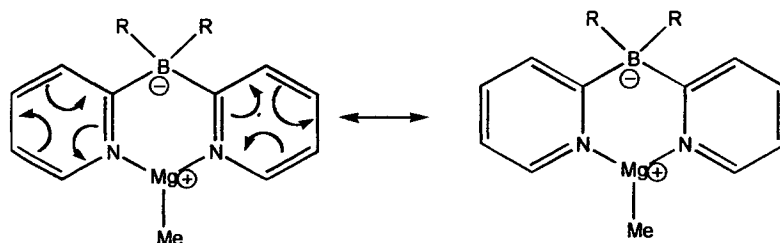

Figure 5.04 Displaying a potential ethene polymerisation catalyst that is internally activated and stabilised by internal charge separation and resonance effects

Compound Numbers

No.	Compound
1	(AlMe$_3$)
2	(Al(^{i}Bu)$_3$)
3	[CPh$_3$][B(C$_6$F$_5$)$_4$]
4	B(C$_6$F$_5$)$_3$
5	[NHMe$_2$Ph][B(C$_6$F$_5$)$_4$]
6	MgMeCl
7	MgMe$_2$
8	[Mg(CH$_2$Ph)$_2$(THF)$_2$]
9	[MgMe{η^2-(^{i}Pr)$_2$ATI}$_2$(THF)]
10	[Mg(μ-Me){η^2-(^{i}Pr)$_2$ATI}]$_2$
11	[Mg(μ-OMe){η^2-(^{i}Pr)$_2$ATI}]$_2$
12	[MgMe{HC[C(Me)NAr']$_2$}(THF)]
13	[Mg(μ-Me){HC[C(Me)NAr']$_2$}]$_2$
14	[MgMe{HC[C(^{t}Bu)NAr']$_2$}(THF)]
15	[MgMe{HC[C(^{t}Bu)NAr']$_2$}] (Ar'=2,6-Diisopropylphenyl)
16	[Mg(CH$_2$Ph){HC[C(Me)NAr']$_2$}(THF)] (Ar'=2,6-Diisopropylphenyl)
17	[Mg(CH$_2$Ph){HC[C(Me)NAr']$_2$}]
18	[Mg(CH$_2$Ph){HC[C(^{t}Bu)NAr']$_2$}(THF)]
19	[Mg(CH$_2$Ph){HC[C(^{t}Bu)NAr']$_2$}] (Ar'=2,6-Diisopropylphenyl).
20	[Mg(^{t}Bu){HC[C(Me) NAr']$_2$}] (Ar'=2,6-Diisopropylphenyl)
21	[HC{C(CH$_3$)NAr'}$_2$Mg(μ-η^2:η^1-OOBz)]$_2$
22	[HC{C(CH$_3$)NAr'}$_2$Mg(μ-OBz)]$_2$
23	[Mg(η^2-TMEDA)Me$_2$]
24	[Mg(η^3-PMDETA)Me$_2$]
25	[Mg(η^2-TEEDA)Me$_2$]
26	[Mg(η^2-TIPEDA)Me$_2$]
27	[N{CH(CH$_3$)$_2$}$_2$CH$_2$]$_2$
28	[Mg(μ-Cl)[η^2-TMEDA)]Me]$_2$
29	[Mg(μ-Cl)[η^2-TMEDA)]Cl]$_2$
30	[Mg(η^2-TMEDA)(CH$_2$Ph)$_2$]
31	[Mg(η^2-TEEDA)(CH$_2$Ph)$_2$]
32	[Mg(η^2-TMEDA)Me{BMe(C$_6$F$_5$)$_3$}]
33	[Mg(η^2-TMEDA)(C$_6$F$_5$)Me]
34	BMe(C$_6$F$_5$)$_2$
35	[Mg(η^2-TMEDA)(C$_6$F$_5$)$_2$]
36	BMe$_2$(C$_6$F$_5$)
37	[Mg(C$_6$F$_5$)Br]

Compound Numbers (Continued)

No.	Compound
38	[Mg(η^2-TEEDA) Me{BMe(C$_6$F$_5$)$_3$}]
39	[Mg(η^2-TEEDA)Me(C$_6$F$_5$)]
40	[Mg(η^2-TEEDA)(C$_6$F$_5$)$_2$]
41	[Mg(η^3-PMDETA)Me][B(C$_6$F$_5$)$_3$Me]
42	[Mg(η^3-PMDETA)Me(C$_6$F$_5$)]
43	[Mg(η^2-TMEDA)(C$_6$F$_5$)(CH$_2$Ph)]
44	[B(CH$_2$Ph)(C$_6$F$_5$)$_3$]$^-$
45	[B(CH$_2$Ph)(C$_6$F$_5$)$_2$]
46	[Mg(η^2-TMEDA)(C$_6$F$_5$)$_2$]
47	[B(CH$_2$Ph)$_2$(C$_6$F$_5$)]
48	[Mg(η^2-TEEDA)(C$_6$F$_5$)(CH$_2$Ph)]
49	[Mg(η^2-TEEDA)(C$_6$F$_5$)$_2$]
50	Mg(η^2-TMEDA)(Me)(NMe$_2$Ph)][B(C$_6$F$_5$)$_4$]
51	[Mg(η^2-TEEDA)Me][B(C$_6$F$_5$)$_4$]
52	NHMe$_2$Ph
53	[Mg(η^3-PMDETA)Me][B(C$_6$F$_5$)$_4$]
54	[Mg(η^2-TMEDA)(CH$_2$Ph)(NMe$_2$Ph)][B(C$_6$F$_5$)$_4$]
55	[Mg(η^2-TEEDA)(CH$_2$Ph)(NMe$_2$Ph)][B(C$_6$F$_5$)$_4$]
56	[Mg(η^2-TMEDA)(CH$_2$Ph)(THF)][B(C$_6$F$_5$)$_4$]
57	[Mg(η^2-TEEDA)(CH$_2$Ph)(THF)][B(C$_6$F$_5$)$_4$]
58	CPh$_3$Me
59	[Mg(η^2-TEEDA)(CH$_2$Ph)][B(C$_6$F$_5$)$_4$]
60	CPh$_3$(CH$_2$Ph)
61	[N(H)Me$_2$CH$_2$CH$_2$NMe$_2$][B(C$_6$F$_5$)$_4$]
62	[(2,6-^{i}Pr$_2$Ph)NCH]$_2$
63	[(2,6-Me$_2$Ph)NCH]$_2$
64	[(2,6-^{i}Pr$_2$Ph)NCMe]$_2$
65	[(2,6-^{i}Pr$_2$Ph)BIAN]
66	[Mg$_{13}$C$_{48.60}$H$_{99.20}$Cl$_{14}$O$_{18.40}$]
67	[Mg(μ_2-OMe){(2,6-^{i}Pr$_2$Ph)BIAN(Me)]
68	[Mg(μ_2-Me){(2,6-^{i}Pr$_2$Ph)BIAN}]$_2$
69	[Mg (μ_2-Me){(2,6-^{i}Pr$_2$Ph)NC(H)}$_2$]$_2$
70	[Mg(μ_2-CH$_3$){(2,6-^{i}Pr$_2$Ph)NCMe}]$_2$
71	[Mg (THF)$_3${(2,6-^{i}Pr$_2$Ph)BIAN}]
72	[Mg(μ_2-Me){(2,6-^{i}Pr$_2$Ph)NC(Me)$_2$C(Me)N(2,6-^{i}Pr$_2$Ph)}]$_2$

Compound Numbers (Continued)

No.	Compound
73	[Mg(μ_2-OH){(2,6-^{i}Pr$_2$Ph)NC(Me)$_2$C(Me)N(2,6-^{i}Pr$_2$Ph)}]$_2$
74	CH$_2$(PPh$_2$NSiMe$_3$)$_2$
75	[Mg(Me){CH(PPH$_2$NSiMe$_3$)$_2$}(THF)]
76	[Mg(μ_2-Me)){CH(PPh$_2$NSiMe$_3$)$_2$}]$_2$